Studies of Low Oxidation State Group 13 Halide, Hydride and Heterocyclic Complexes

by

Marc Kloth

This thesis is presented for the degree of Doctor of Philosophy to the Faculty of Science, Cardiff University, October 2004.

ProQuest LLC
789 East Eisenhower Parkway
P.O. Box 1346
Ann Arbor, MI 48106-1346

Acknowledgements

I would like to express my special thanks to Prof. Cameron Jones for his great supervision, guidance, trust and the unique opportunity he gave me to work on this topic within his research group over the past three years.

Furthermore, I would like to thank Prof. Ulrich Kynast for his support and initiating the idea of a PhD in Cardiff. Thanks are also expressed to Dr. Peter Junk for inviting me to work in his laboratory at Monash University, Melbourne, Australia.

A number of people strongly supported the project, which I would like to acknowledge: Bob (Cardiff) and Marcus (Monash), for being very helpful post-docs; Damien and Charley, for EPR measurements and simulations; Jamie, for theoretical calculations; Rob, Sham and Robin, for their patience training me on the Mass Spec machine; Gaz, for providing me with materials required for my work; Ricky, for repairing my few broken Schlenks; All other technical staff, whose support made my time in the laboratory both efficient and productive.

Reflecting on my time in Cardiff and Melbourne, there are many lasting memories formed by people I have met over the last three years, which have made this time an unforgettable period in my life. Many thanks to Bob, Julia, Matt, Marcus (MC), Mark, Steve, Bresner, Debs, Tom, Aaron, Markus, Rich, Dave, Helga, Alex, Andreas, Dave (Monash), Matze (Monash)... and all the other 'friendly' people in the inorganic chemistry department. Thank you very much for the great time!

An dieser Stelle möchte ich mich herzlichst bei meinen Eltern und insbesondere bei meiner Schwester Simone bedanken, die mir, gemeinsam, durch ihre kontinuierliche Unterstützung das erreichte Ziel erst ermöglicht haben. Bedanken möchte ich mich auch bei meinen Freunden für Unterstützung durch Besuche in Cardiff oder Melbourne und durch ausgiebige Telefonate.

Natalie, I heartily thank you for all the nice things in our life and for your continuous support in the final stage of my PhD.

In Memory of

my Uncle

Heinz Baumeister

***17.1.1942 † 31.3.2004**

Abstract

The work presented in this thesis describes the synthesis, structure and stability of a range of halido, hydrido and heterocyclic complexes of the group 13 elements. The underlying theme is the synthesis of low valent group 13 complexes. The work upon this subject is divided into five chapters.

Chapter 1 provides a general introduction to the members of group 13 and to low oxidation state group 13 halide chemistry. The history of binary group 13 metal trihydride complexes and the reasons behind their inherent instability are also discussed.

Chapter 2 details the use of a stable nucleophilic N-heterocyclic carbene, 1,3-bis(2,6-diisopropylphenyl)imidazol-2-ylidene, (IPr), and nitrogen donor ligands, namely a bulky diazabutadiene (Ar-DAB), Ar = 2,6-$Pr^{i}_{2}C_{6}H_{3}$, quinuclidine and formamidinate, in the formation of group 13 trihalide complexes. A series of metal trihalide complexes have been prepared and characterised, *e.g.* $[InBr_3(L)]$, L = IPr or Ar-DAB, whose reduction reactions with alkali metals did not yield low valent metal—metal bonded group 13 species. In addition, the reactivity of 'GaI' towards pyridine based ligands is described: 'GaI' reacts, for example, with 2,2'-bipyridine (bipy) to give salts of composition $[Ga(bipy)_3][I]_3$, $[\{(bipy)_2Ga\}_2(\mu\text{-}OH)_2]_2[Ga_2I_6][I]_6$ or $[\{(bipy)_2Ga\}_2(\mu\text{-}OH)_2][I]_4$, depending upon the reaction conditions. All new compounds have been crystallographically characterised.

Chapter 3 introduces the reactivity of diazabutadienes (Ar-DAB or Bu^{t}-DAB) towards low oxidation state group 13 iodides which afforded, for example, the paramagnetic compounds, $[\{IGa(Bu^{t}\text{-}DAB)\}_2]$, $[I_2Al(Ar\text{-}DAB)]$ and $[\{ClIn(Ar\text{-}DAB)\}_2]$ which have been characterised by X-ray crystallography and EPR spectroscopy. In addition, the synthesis of the second example of an anionic gallium(I) N-heterocyclic carbene analogue, $[\{(TMEDA)KGa(Ar\text{-}DAB)\}_2]$, is described. This complex displays a Ga···Ga interaction in the solid state which is unprecedented for this complex type.

Chapter 4 lists reactivity studies of a new gallium(I) carbene analogue, $[\{(TMEDA)KGa(Ar\text{-}DAB)\}_2]$, towards main group halide complexes. These studies led to some decomposition products which are paramagnetic and have been studied both crystallographically and by EPR spectroscopy. The reactivity of the gallium carbene analogue towards sources of oxygen has been investigated and the complex, $[\{(\mu\text{-}O)Ga(Ar\text{-}DAB)_2\}_2]^{2-}$, from the reaction with N_2O, has been isolated and structurally characterised. In addition, an

unprecedented π-cyclopentadienyl bridged digallane complex, [{Ga(Ar-DAB)$_2$}$_2${μ-CpK(TMEDA)$_2$}], incorporating the first structurally characterized π–interaction with a Ga(II) center, results from the oxidative coupling of an anionic gallium(I) heterocycle with cyclopentadienyl thallium(I).

Chapter 5 introduces the known hydride chemistry of indium and describes the synthesis of a number of novel group 13 hydride complexes. These include the preparation and characterisation of the first examples of amido indium hydride complexes, one of which has unprecedented thermal stability. In addition, these studies led to the first covalently bonded metal complexes derived from an anionic gallium carbene analogue, one of which, [InH$_2${Ga(Ar-DAB)}$_2$][Li(TMEDA)$_2$], contains the first example of a structurally authenticated In—Ga bond. This chapter also includes the preparation and characterisation of a subvalent pentaindium cluster compound.

Table of Contents

Chapter 3

Reactivity of Diazabutadienes Towards Low Oxidation State Group 13 Iodides and Synthesis of a New Gallium(I) Carbene Analogue

Chapter 4

Reactivity of a New Gallium(I) Carbene Analogue Towards Main Group Halide Complexes

Chapter 5

Synthesis and Characterisation of Novel Group 13 Hydride Complexes

Abbreviations

Å	Angstrom, 1 x 10^{-10} metre
Ad	1-adamantyl
a_{iso}	Hyperfine coupling value
Ar, Ar', Ar*, Ar$^{\#}$	A general aryl substituent
Ar-DAB	N,N'-bis(2,6-diisopropylphenyl)diazabutadiene
bipy	2,2'-bipyridine
br	Broad
Bu^{t}	Tertiary butyl
Bu^{t}-DAB	N,N'-bis(2,6-ditertiarbutyl)diazabutadiene
Bu^{n}	Normal butyl
ca.	Circa
kcal	Kilocalorie (1 kcal = 4.184 kJ)
cm^{-1}	Wavenumber, unit of frequency (= ν/c)
cm^{3}	Cubic centimetre
Cp	Cyclopentadienyl, cyclopentadienide
Cp'	Methylcyclopentadienide
CVD	Chemical Vapour Deposition
Cy	Cyclohexyl
CYCLAM	N,N',N'',N'''-tetramethylcyclam
δ	Chemical shift in NMR (ppm)
d	Doublet
dd	Doublet of doublets
DABCO	1,4-diazabicyclo[2.2.2]octane
dec.	Decomposition temperature
DFT	Density Functional Theory
Dipp	2,6-diisopropylphenyl
DME	1,2-dimethoxyethane
DMSO	Dimethylsulfoxide
E	A general metal or non-metal
EPR	Electron Paramagnetic Resonance

Et_2O	Diethyl ether
$EtIBu^t$	1,2-ethylene-3,3'-di-*tert*-butyldiimidazol-2,2'-diylidene
FTIR	Fourier Transform InfraRed spectroscopy
g_{iso}	Isotropic *g* value
HFiso	Formamidine, $(2,6\text{-}Pr^i_2C_6H_3)NC(H)NH(2,6\text{-}Pr^i_2C_6H_3)$
HOMO	Highest Occupied Molecular Orbital
Hz	Hertz, s^{-1}
IMes	1,3-bis(2,4,5-trimethylphenyl)imidazol-2-ylidene
ipso	ipso-substituent
IPr	1,3-bis(2,6-diisopropylphenyl)imidazol-2-ylidene
IPrH	2-hydro-1,3-bis(2,6-diisopropylphenyl)imidazolium cation
IR	Infrared
$^nJ_{XY}$	Coupling constant between nuclei X and Y, over n bonds, in Hz
kJ	Kilojoule
J	Joule, kg m^2 s^{-2}
L	A general ligand
LICVD	Laser Induced CVD
LUMO	Lowest Unoccupied Molecular Orbital
M	A general metal or Molar (mol dm^{-3})
M^+	Molecular ion
Me	Methyl
m/z	Mass / charge ratio
Mes	Mesityl (2,4,6-trimethylphenyl)
MOVPE	Metal Organic Vapour Phase Expitaxy
MOCVD	Metal Organic CVD
MS(APCI)	Atmospheric Pressure Chemical Ionisation Mass Spectrometry
MS(EI)	Electron Ionisation Mass Spectrometry
m	Multiplet, medium or meta-substituent
m. p.	Melting point
NBO	Natural Bond Orbital
NHC	N-heterocyclic carbene
Np	Neopentyl, *tert*-butylmethyl

NMR	Nuclear Magnetic Resonance spectroscopy
o	ortho-substituent
Ph	Phenyl
Phterpy	2,2`:6`2``-terpyridine
PMDETA	N,N,N`,N``,N``-pentamethyldiethylenetriamine
Pr^i	Isopropyl
p	para-substituent
ppm	Parts per million
py	Pyridine
q	Quartet
quin	Quinuclidine, 1-azabicyclo[2.2.2]octane
R	General organic substituent
s	Singlet or strong
sept	Septet
sh	Sharp
THF	Tetrahydrofuran
TMEDA	N,N,N`,N`-tetramethylethane-1,2-diamine
Tmp	2,2,6,6-tetramethylpiperidine
TRIAZ	1,3,5-trimethylhexahydro-1,3,5-triazine
Trip	2,4,6-triisopropylphenyl
t	Triplet
18-crown-6	1,4,7,10,13,16-hexaoxacyclooctadecane
III/V	Semiconductor material derived from Group 13/15 elements (1:1)
ν	Frequency in Hz
X	A general halide

Chapter 1
General Introduction

1.1 Group 13 Chemistry

Group 13 of the periodic table contains the elements boron, aluminium, gallium, indium and thallium. The ground state of each element exhibits three valence electrons possessing the configuration ns^2np^1. The physical properties of the members of the group vary greatly upon descent of the table.

Boron is the only non-metallic element in the group and is commonly classed as a metalloid. Its physical properties, 'hard' and heat-resistance enable it to act as an electrical insulator. The wide and varying range in the chemistry of boron results from its electron deficiency, due to the four available valence orbitals but only three valence electrons $(2s^2 2p^1)$. This, combined with boron's high electronegativity, encourages the formation of highly localised covalent B—B bonds in its compounds. In many ways boron often appears to have more in common with its horizontal neighbour carbon and diagonal neighbour silicon than the remaining elements of group 13.

The other four elements of group 13 are not comparable with boron, all are soft metals with low melting points, which display high electrical conductivity. Some of the important physical and electronic properties of the group 13 elements are shown in Table 1.

Periodic irregularities of the chemistry of the group 13 elements can be explained by looking into the electronic configurations of the metallic elements. Aluminium possesses the electronic core of the noble gas neon. Gallium and indium, on the other hand, possess the electronic cores of the noble gases argon and krypton, respectively, plus additional filled d^{10} subshells. Thallium has a xenon core plus filled d^{10} and f^{14} subshells. Due to possible different core configurations of these elements, variations in the chemical and physical properties of the group 13 elements can be explained.

A general trend in decreasing ionisation energies can be observed when a group is descended. This occurs because the distance of the valence electrons from the nucleus increases, which compensates for the effect of electronic attraction due to increased effective nuclear charge. On going from boron to aluminium a corresponding decrease in ionisation energy consistent with this trend is seen.[1] The analogous fall in ionisation energies upon

descending from aluminium to gallium does not take place. This difference is caused by the '*d*-block contraction'. This describes the fall in atomic radii after first filling of the *d*-orbitals. The elements gallium to krypton comply with this criterion. The reduction in atomic size increases the effective nuclear charge felt by the valence electrons which makes them harder to remove, this means the ionisation energy increases.[1] The reduced atomic radius also means that the electronegativity of gallium is higher than aluminium according to both the Pauling[1] and Allred-Rochow[2] classifications. The ionisation energy of indium on the other hand, is slightly higher than that of aluminium, but less than gallium, as is its electronegativity. These characteristics come from poor *d*-electron shielding of the extra ten positive charges added to the nuclei.

Table 1

Selected Physical and Chemical Properties of the Group 13 Elements[1-3]

Property	**B**	**Al**	**Ga**	**In**	**Tl**
Atomic Number	5	13	31	49	81
Covalent Radius (Å)	0.81	1.25	1.25	1.50	1.55
Ionisation Energy (kJ mol^{-1}) (1st 3 electrons)	6887	5044	5521	5084	5439
Electronegativity (Pauling)	2.04	1.61	1.81	1.78	2.04
Electronegativity (Allred and Rochow)	2.01	1.47	1.82	1.49	1.44
Melting Point (°C)	2300	660.1	29.8	156.2	302.4

The covalent radii of aluminium and gallium are both 1.25 Å, although indium and thallium have larger radii at 1.50 Å and 1.55 Å, respectively. The reason for the identical covalent radii of aluminium and gallium is because of the reduced shielding that the gallium 3*d*-shell offers its valence electrons, causing them to be held more closely than expected. A similar situation is observed for indium and thallium. The 'lanthanide contraction' arises from

the complete filling of the first set of *f*-orbitals (4*f*). The poor shielding of the effective nuclear charge by the filled 4*f*-shell of thallium induces a minimal increase in atomic radii between the two elements.[2] According to the Pauling scale,[1] this results in an increased electronegativity for thallium relative to its lighter group 13 metal congeners.

Another anomalous feature of group 13 is the low melting points of gallium and indium, especially the melting point of gallium, 29.8 °C.[3] Compared with group 1, where melting points decrease rapidly as the group is descended, these two examples contradict this pattern. The four metallic elements of group 13 have typical close-packed metallic structures with twelve nearest neighbours.[4] Indium shows a slight distortion from this model with four atoms marginally closer,[4] whilst gallium has one neighbouring atom considerably closer (2.45 Å) than the others that occur in pairs at 2.70, 2.73 and 2.79 Å.[4] Therefore, it is unsurprising that gallium melts are thought to include *pseudo*-diatomic Ga—Ga molecules. In this respect the structure of solid gallium shows similarities to the solid state structure of iodine, which contains discrete I_2 units. This typical bond localisation in metalloids may explain the low melting points of gallium and indium.

As the group is descended, a tendency to exhibit the oxidation state +1 rather than +3 increases. The reason for this change is due to the 'inert pair effect'. The *s*-orbital electrons show a gradual reluctance to participate in bonding as the group is descended. The extent of this resistance increases down the group, leading to the chemistry of thallium which features the +1 oxidation state predominately.[5] An explanation is given by the fact that if the required energy to promote the valence *s*-orbital electrons is higher than the energy gained when forming bonds, the *s*-orbital electrons will remain paired. Relativistic effects can also be considered in order to account for the predominance of the +1 oxidation state of the heavier elements. As group 13 is descended the average bond energies decrease, which is illustrated by the group 13 metal trichlorides. They have average bond energies of 242 kJ mol^{-1} for $GaCl_3$, 206 kJ mol^{-1} for $InCl_3$ and 153 kJ mol^{-1} for $TlCl_3$. As suggested, the *s*-electrons are most inert in thallium. This means that the +3 oxidation state is favoured for boron, aluminium and gallium, but the +1 oxidation state commonly occurs for the heavier elements, indium and thallium.

1.2 Low Oxidation State Group 13 Halide Chemistry

The best way to describe the concept of oxidation state is using compounds in which the elements are of considerably different electronegativity which implies molecular orbitals are more closely related to the atomic orbitals of one atom than another. If the difference in electronegativity is small and especially if there are fully delocalised molecular orbitals that are non-bonding, weakly bonding, or anti-bonding, the situation becomes difficult. In complexes containing a halogen, oxygen, or nitrogen σ-bonding ligands, the first case is likely to be found. Ligands supporting low oxidation states are for example, cyanide or phosphorus trifluoride, both outstanding π-accepting ligands.[1] Transition metals, however, mainly underlie this definition of oxidation states and therefore will not be discussed any further here.

The most recent inorganic textbooks describe the +III oxidation state of aluminium and gallium as being the dominant oxidation state of these two metals. The chemistry of low valent compounds of the heavier group 13 elements has made rapid progress only in approximately the last 15 years. Recently there has been a great deal of interest in the chemistry of metastable aluminium(I) and gallium(I) halide complexes, $[\{MX(L)\}_n]$, M = Al or Ga; X = halide; L = Lewis base, which are turning out to be very useful as precursors to a wide range of novel alkyl, silyl and amido low-oxidation state metal complexes and cluster compounds. They have been prepared by the co-condensation of the M(I)-halide with the donor solvent using a specially designed reactor, and several have been crystallographically characterised, for example $[Al_4Br_4(NEt_3)_4]$.[6, 7]

A much more convenient starting material for many low-valent gallium species is Ga_2Cl_4, which exists as a salt, $Ga^+GaCl_4^-$, in the solid as well as in the molten state.[8] By addition of arenes, a series of Ga^+-arene compounds with interesting Ga—π interactions have been prepared.[9] On the other hand genuine gallium(II) species with Ga—Ga bonds are formed by addition of special donor compounds. $Ga_2Cl_4 \cdot 2$dioxane[10] was the first prominent example which was followed by the analogous bromides and by two other examples of donor-stabilized Ga_2I_4 compounds.[11]

Related indium(II) complexes have been known for some time and several have been structurally authenticated, for example $[In_2I_4(PPr^n_3)_2]$.[12]

1.3 Binary Group 13 Metal Hydrides

The beginnings of heavier group 13 metal hydride chemistry (Al – In)[13] occurred with the preparation of an impure binary aluminium hydride species, $[AlH_3]_n$.[5] Several years later, polymeric alane, $[AlH_3]_\infty$, and the trimethylamine adduct of alane, $[AlH_3(NMe_3)]$, were prepared and reported by Stecher and Wiberg.[14] The reaction of $Li[AlH_4]$ with $AlCl_3$ in diethyl ether was found to form the ether adduct, $[AlH_3(Et_2O)]$, in good yield.[15] A simple route to large quantities of alane in THF, by treatment of $Li[AlH_4]$ with sulphuric acid, was reported in 1966.[16] In the past two decades the chemistry of alane has seen a renaissance[17-19] as a direct result of it and its derivates finding applications. These applications are found mainly in microelectronics[20-23] and organic synthesis.[24]

Gallium trihydride, gallane, species have been somewhat ignored, compared with their aluminium counterparts. It was not until the 1960's that any detailed investigation into gallium hydrides was undertaken, when gallane (GaH_3) was reported as a transient species in the gas phase.[25] The first authenticated report of uncoordinated gallane did not occur until 1989 when digallane, Ga_2H_6, was fully characterised in the vapour phase.[26, 27] In the following years gallium hydride chemistry received a great deal of interest, predominantly involving the use of trihydride species as precursor substrates for the deposition of gallium films and semiconductor materials.[19]

The chemistry of indane, InH_3, was reported to have been discovered in 1957 by Wiberg, *et al.*[28] Their report has never been substantiated and therefore should be treated with scepticism. The first successful preparation of solid $[InH_3]_\infty$ and its spectroscopic characterisation, using a new cryogenic method, have now been reported by Andrews, *et al.*[29] In recent times a handful of structurally characterised In—H bond containing complexes have been reported.[30-32] These species have mostly relied upon an ionic makeup to achieve stability. Since 1998, however, Jones, *et al* have reported several structurally authenticated examples of indane complexes.[33] The hydrides of thallium are restricted to a report of $Li[TlH_4]$ and $[TlH_3]_\infty$, which again must be viewed with scepticism given that no characterisation of the materials was presented.[28] Recently published studies of laser-ablated thallium in reaction with pure H_2, manifest the heavy doubts on the synthesis of $Li[TlH_4]$ and $[TlH_3]_\infty$.[29]

It is noteworthy that the majority of research into group 13 trihydrides has centred upon those of boron and aluminium. There is a distinct pattern in thermal stability of hydride complexes as the group is descended. In each case the decomposition temperatures of the three MH_3 species decrease in the order alane > gallane > indane. The trimethylamine adduct of alane decomposes at 87 °C,[17] whilst those of gallane and indane decompose at 25 °C and approximately –30 °C, respectively. It is easy to see that the stability, and therefore scope for investigation, is far greater for alane complexes than gallane and indane complexes. In order to establish legitimate applications for gallane, indane and perhaps even thallane, examples that posses thermal stabilities approaching, if not exceeding, ambient temperatures must be discovered.

1.4 Thermodynamics of Binary Group 13 Metal Trihydrides

The formation of group 13 metal trihydrides is endothermic with respect to the elements in their standard states. With respect to entropy, none of the hydrides of group 13 should be thermodynamically stable at normal temperatures. For group 13 trihydrides to exist there must be a stabilising influence that overcomes these impediments. The unfilled valence shell of the metal involved and the electron rich hydride ligand can give rise to a significant degree of stabilisation when M—H—M bridges are formed.[34]

The weakness of the M—H bond is often stated as the reason for the instability of group 13 metal trihydride complexes. The M—H bonds are weak compared with M—Cl or M—O bonds, although they are stronger than the respective M—C bonds.[34] Group 13 metal alkyl complexes are known to be stable species even though the M—C bond is weaker than the respective M—H bond. Therefore another explanation is required for the instability of group 13 hydrides. The reason is partly kinetic and partly thermodynamic. The hydrides of group 13 have the ability to form M—H—M bridges, which can be a major factor in their decomposition. The decomposition of a discrete molecular hydride can be initiated by homolytic dissociation of an M—H bond, an associative mechanism preceding the concerted elimination of hydrogen which may offer a lower barrier to decomposition.[34] In this way, the formation of intermolecular bridges may actually favour the decomposition of metal hydrides in some cases by offering a lower energy pathway for decomposition to occur. When group

13 metal alkyl species decompose, observations show that the decomposition process occurs by a dissociative mechanism. This is a higher energy pathway than associative mechanisms since the formation of M—C—M bridges is not as favourable as the formation of M—H—M bridges. This observation gives an explanation for group 13 metal alkyls being more stable than group 13 metal trihydrides, even though the M—C bonds are weaker than the corresponding M—H bonds.

1.5 Bonding and Structure in Binary Group 13 Hydrides

The differences in the solid state structures and properties of group 13 complexes can be explained by the electronegativities of the central metal atoms. Using the example of trimethyl group 13 compounds, the trimethyl complex of aluminium exists as a dimer in the solid state[35] whereas those of gallium[36] and indium[37] are monomeric. The lower electronegativity of aluminium results in a greater polarity of the Al—C bonds. This encourages aggregation such as that seen for $[AlMe_3]_2$. The electronegativity of indium is intermediate between those of aluminium and gallium,[1] and thus given that trimethylgallium exists as discrete $[GaMe_3]$ units,[36] an analogous indium species would be expected to exist as either a dimer or a monomer. Observations of trimethylindium show it to have a monomeric solid state structure, though weak intermolecular interactions are seen.[38]

The hydrides of group 13 display a similar trend in their properties as the group is descended. Alane and gallane are both sp^2 hybridised and contain an unoccupied *p*-orbital in their monomeric forms, though their condensed phase structures are different. Alane forms intermolecular bridges to adjacent molecules and exists as a polymeric species in the solid state. Several solid state structures for polymeric alane have been investigated. The commonly accepted structure is that with intermolecular bridges to six adjacent molecules (**1**).[5]

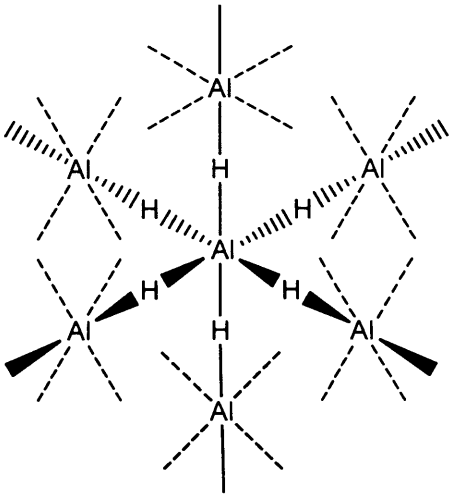

(1)

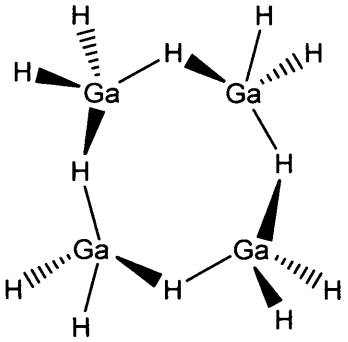

(2)

Gallane exists as a dimer in the gas phase $[GaH_3]_2$, which, once condensed to the solid state, forms the tetrameric species (**2**) in which the gallium centres are four-coordinate.[26, 27] Indane has recently been reported to exist as a polymeric species in the solid state[29] which, considering the intermediate electronegativity of indium and its larger covalent radius compared with those of aluminium and gallium, is to be expected.

The unoccupied *p*-orbital of monomeric group 13 hydrides gives rise to their Lewis acidity. This means they will readily accept a lone pair of electrons from a Lewis base. Due to the electronegativity differences of gallium and aluminium, the acidity of alane is higher than that of gallane. This results in less polar metal-hydrogen bonds, and therefore the gallium centre is more easily electronically satisfied. Consequently, gallane complexes are often four-coordinate around the metal center though at low temperatures unstable five-coordinate examples have been isolated, *e.g.* $[GaH_3(NMe_3)_2]$.[39] In contrast, adducts of alane are often seen to form intermolecular hydride bridges and are commonly five- or six-coordinate. Those few species known for indane are four- or five-coordinate monomers, which display low thermal stability.[33] However, it is likely that the intermediate electronegativity of indium with its increased covalent radius over aluminium and gallium may favour higher coordination numbers in its trihydride complexes.

1.6 References

1. E.A. Keiter J.E. Huheey, R.L. Keiter, *"Inorganic Chemistry, Priciples of Structure and Reactivity"*, fourth edn., Harper Collins College Publishers, New York, 1993.
2. J. Emsley, *"The Elements"*, Oxford University Press, Oxford, 1989.
3. Fluck and Heumann, *"Periodic Table of the Elements"*, VCH, Cambridge, 1991.
4. N.C. Norman, *"Periodicity and the s- and p-Block Elements"*, Oxford University Press, Oxford, 1997.
5. *"Chemistry of Aluminium, Gallium, Indium and Thallium"*, Ed. A.J. Downs, Blackie, Glasgow, 1993.
6. G. Linti, H. Schnöckel, *Coord. Chem. Revs.*, 2000, **206-207**, 285.
7. H. Schnöckel, A. Schnepf, *Adv. Organomet. Chem.*, 2001, **47**, 235.
8. J.W. Akitt, N.N. Greenwood, A. Storr, *J. Chem. Soc.*, 1965, 4410.
9. H. Schmidbaur, *Angew. Chem., Int. Ed. Engl.*, 1985, **24**, 893.
10. J.C. Beamish, R.W.H. Small, I.J. Worrall, *Inorg. Chem.*, 1979, **18**, 220.
11. B. Beagley, S. Godfrey, K. Kelly, S. Kungwankunakorn, C. McAuliffe, R. Pritchard, *Chem. Commun.*, 1996, 2179.
12. S.M. Godfrey, K.J. Kelly, P. Kramkowski, C.A. McAuliffe, R.G. Pritchard, *Chem. Commun.*, 1997, 1001.
13. S. Aldridge, A.J. Downs, *Chem. Rev.*, 2001, **101**, 3305.
14. O. Stecher, E. Wiberg, *Ber.*, 1942, **75(B)**, 2003.
15. A.E. Finholt, A.C. Bond, H.L. Schlesinger, *J. Am. Chem. Soc.*, 1947, **69**, 1199.
16. H.C. Brown, N.M. Yoon, *J. Am. Chem. Soc.*, 1966, **88**, 1464.
17. C. Jones, G.A. Koutsantonis, C.L. Raston, *Polyhedron*, 1993, **12**, 1829.
18. C.L. Raston, *J. Organomet. Chem.*, 1994, **475**, 15.
19. M.G. Gardiner, C.L. Raston, *Coord. Chem. Revs.*, 1997, **166**, 1.
20. T.H. Baum, C.E. Larson, R.L. Jackson, *Appl. Phys. Lett.*, 1989, **55**, 1264.
21. W.L. Gladfelter, D.C. Boyd, K.F. Jensen, *Chem. Mater.*, 1989, **1**, 339.
22. A.T.S. Wee, A.J. Murrell, N.K. Singh, D. O'Hare, J.S. Foord, *J. Chem. Soc., Chem. Commun.*, 1990, 11.
23. L.H. Dubois, B.R. Zegarski, M.E. Gross, R.G. Nuzzo, *Surf. Sci.*, 1991, **244**, 89.
24. H.C. Brown, N.M. Yoon, *J. Am. Chem. Soc.*, 1968, **90**, 2927.
25. P. Breisacher, B. Siegel, *J. Am. Chem. Soc.*, 1965, **87**, 4255.

26. A.J. Downs, M.J. Goode, C.R. Pulham, *J. Am. Chem. Soc.*, 1989, **111**, 1936.
27. A.J. Downs, M.J. Goode, C.R. Pulham, D.W.H. Rankin, H.E. Robertson, *J. Am. Chem. Soc.*, 1991, **113**, 5149.
28. E. Wiberg, O.Z. Dittmann, H. Nöth, M.Z. Schmidt, *Z. Naturforsch. B*, 1957, **12**, 61.
29. L. Andrews, X. Wang, *Angew. Chem., Int. Ed.*, 2004, **43**, 1706.
30. A.G. Avent, C. Eaborn, P.B. Hitchcock, J.D. Smith, A.C. Sullivan, *J. Chem. Soc., Chem. Commun.*, 1986, 988.
31. S. Aldridge, A.J. Downs, S. Parsons, *Chem. Commun.*, 1996, 2055.
32. D.E. Hibbs, M.B. Hursthouse, C. Jones, N.A. Smithies, *Organometallics*, 1998, **17**, 3108.
33. C. Jones, *Chem. Commun.*, 2001, 2293.
34. A.J. Downs, C.R. Pulham, *Chem. Soc. Revs.*, 1994, **23**, 175.
35. R.V. Vranka, E.L. Amma, *J. Am. Chem. Soc.*, 1967, **89**, 3121.
36. N. Muller, A.L. Otermat, *Inorg. Chem.*, 1965, **4**, 296.
37. L. Pauling, A.W.L. Laubengayer, *J. Am. Chem. Soc.*, 1941, **63**, 480.
38. E.L. Amma, R.E. Rundle, *J. Am. Chem. Soc.*, 1958, **80**, 4141.
39. N.N. Greenwood, A. Storr, M.G.H. Wallbridge, *Inorg. Chem.*, 1963, **2**, 1036.

Chapter 2

The Chemistry of N-Heterocyclic Carbene and N-Donor Ligand Complexes of Group 13 Halides

2.1 Introduction

This chapter explores the reactivity of group 13 metal halides towards N-heterocyclic carbene and nitrogen donor ligands.

The preparation of group 13 halide complexes is achieved by using the sterically demanding carbene, 1,3-bis(2,6-diisopropylphenyl)imidazol-2-ylidene, (IPr), as well as several bulky and/or very nucleophilic nitrogen donor ligands, namely a diazabutadiene $[RN=C(H)]_2$, a formamidinate $[(RN)_2CH]^-$ and quinuclidine. Furthermore the preparation of 'GaI' and its reactivity towards pyridine based ligands are described.

2.2 General Introduction to Thermally Stable Carbenes and Group 13 Complexes

For many years carbenes (R_2C:) have been recognised as transient intermediates in organic chemistry.[1] They have found a broad range of applications in synthetic chemistry, not least because of the efforts of Doering in the 1950's[2] and Fischer during the late 1960's.[3] No room temperature stable carbenes had been isolated prior to 1991, however several carbene complexes had been synthesised. During the late 1960's, Öfele[4] and Wanzlick[5] derived several metal-carbene complexes, *e.g.* **1** and **2** (Scheme 1), *via* the reaction of imidazolium salts with precursors containing a metal whose basicity was high enough to deprotonate the precursor salt. No further progress was made on isolating carbenes until 1991 when Arduengo, *et al*[6] succeeded in producing the first crystalline carbene, 1,3-diadamantylimidazol-2-ylidine (**3**). The free carbene was isolated from the deprotonation reaction of 1,3-diadamantylimidazolium chloride. Deprotonation was achieved by addition of one equivalent of sodium hydride and a catalytic amount of DMSO to the hydrochloride salt at room temperature (Scheme 2).

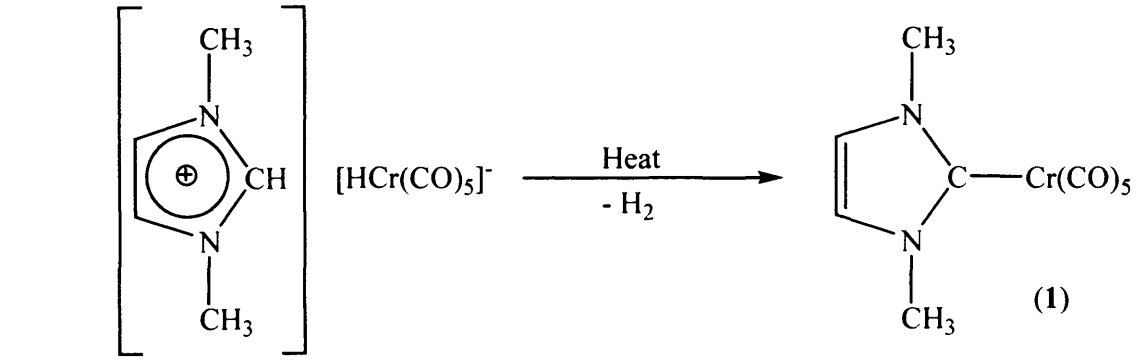

(1)

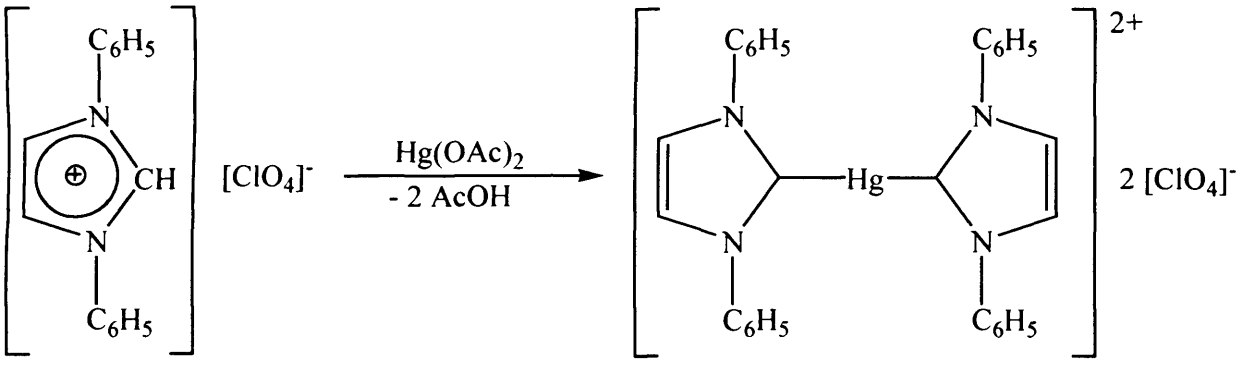

(2)

Scheme 1

The isolation of these stable N-heterocyclic carbenes[6, 7] has led to their use in reactions of fundamental interest.[8, 9] Suffice to say, metal-carbene species are now a significant ingredient in homogeneous catalysis and macromolecular chemistry.[9] It is not unreasonable to suggest that new and exciting applications will be found for these species in the future, especially given the current degree of organometallic research in this area.[8, 9]

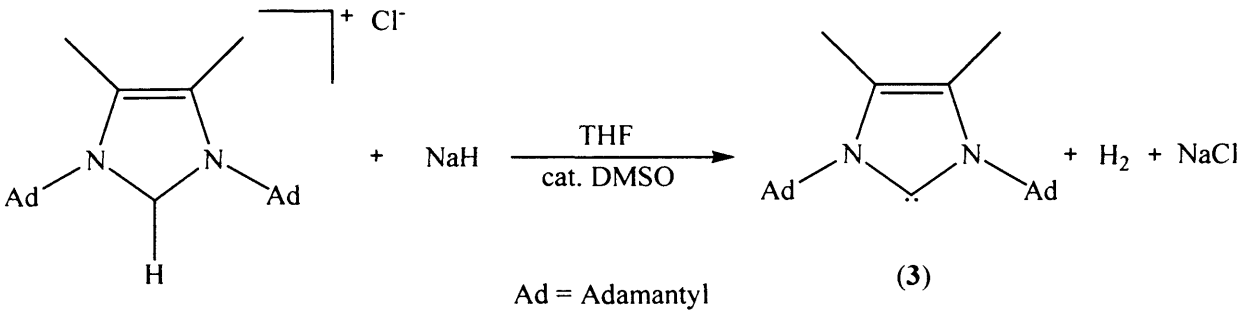

Ad = Adamantyl

(3)

Scheme 2

The use of N-heterocyclic carbenes (NHC) as good σ-donor molecules to stabilise trivalent group 13 compounds was established with the isolation of the first alane adduct of an imidazol-2-ylidene (**4**).[10] The stability of these complexes is demonstrated by the high melting point of **4** (246 °C) without decomposition. In contrast, $[AlH_3(NMe_3)]$ decomposes above 100 °C.[11] The thermal stability of the corresponding gallium and indium compounds, $[MH_3(IMes)]$, M = Ga or In,[12] have also allowed their isolation and characterisation. In addition, the first adducts of a NHC with aluminium (**5**) or gallium (**6**) trihalides have recently been reported by Roesky, *et al.*[13]

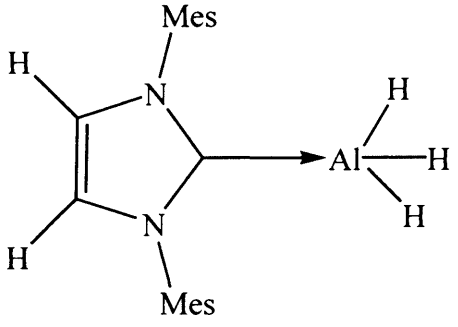

(**4**)

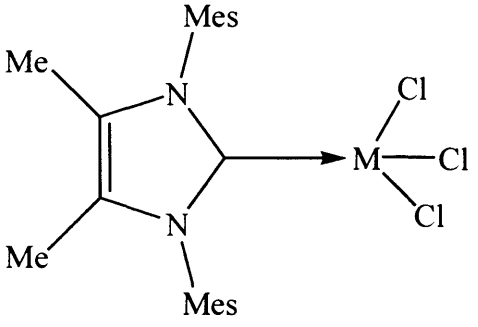

M = Al (**5**) or Ga (**6**)

In contrast, the reaction of a bidentate NHC ligand (EtIBu^t), EtIBu^t = 1,2-ethylene-3,3'-di-*tert*-butyldiimidazol-2,2'-diylidene, with $AlCl_3$ in diethyl ether resulted in formation of an imidazolium salt in moderate yield despite moisture being excluded from the reaction mixture.[14] It is worth noting that, adducts of a phosphanylsilylcarbene with MCl_3 (M = Al (**7**), Ga (**8**), In (**9**)) have been reported and the X-ray crystal structure of **8** was determined.[15]

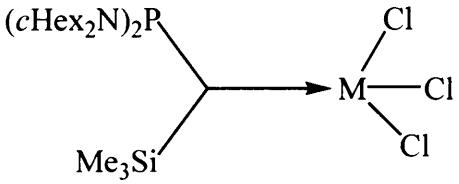

M = Al (**7**), Ga (**8**) or In (**9**)

The co-ordination chemistry of group 13 halides and hydrides with N-heterocyclic carbene ligands has recently been extended by Jones *et al.* They utilised these carbenes as stabilising ligands in the formation of a variety of complexes, *e.g.* the aforementioned $[MH_3(IMes)]$, M = Ga or In,[12] $[MCl_3(IMes)]$, M = In[12] or Tl,[16] $[MH_3\{CN(Pr^i)C_2H_2N(Pr^i)\}]$, M = Al, Ga or In[17] and $[InX_3\{(CN(Pr^i)C_2H_2N(Pr^i)\}_n]$, X = Cl or Br, n = 1 or 2.[18] The stabilising properties of these carbene ligands are perhaps best exemplified by $[InH_3(IMes)]$ (dec. 115 °C) which is by far the most thermally robust InH_3 complex yet reported, a fact which has led to its application in both organic[19] and inorganic synthesis.[20, 21]

2.3 General Introduction to Group 13 Trihalide Chemistry and N-Donor Ligand Group 13 Complexes

The growth of interest in the co-ordination chemistry of the heavier elements of group 13 has been driven to a considerable extent by the developing interest in their co-ordination compounds. In this regard, there is an interesting contrast between boron, which has extensive areas of importance other than co-ordination chemistry, and the heavier metallic elements, which generally do not. A co-ordination compound is simply the product of the association of a base with an acid, using the Lewis definitions of acid and base to identify molecules that can accept or donate a pair of electrons. MX_3 (M = Al, Ga or In; X = halide) compounds are readily available electron-pair acceptors, and ligands containing N, P, O or S atoms are electron-pair donators.[22]

There has been a large number of reported adducts of AlX_3 (X = Cl, Br or I) with nitrogen donor molecules. The simplest route to these various adducts is by direct addition of the ligand to a solution of AlX_3 in a weak donor-solvent, such as Et_2O (Scheme 3).

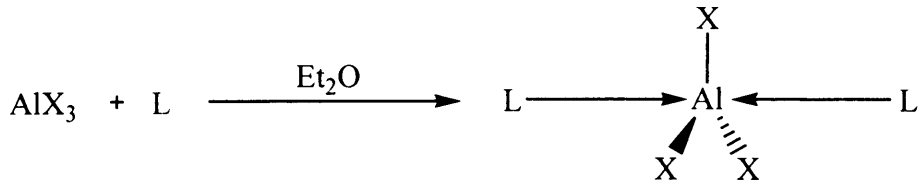

L = nitrogen donor ligand
X = halide

Scheme 3

In addition to adducts of amines, similar compounds are known with other nitrogen donors, and with phosphorus, arsenic, antimony and bismuth species, all with the metal in the +3 oxidation state.[22] With pyridine (py), for example, structural investigations show that $[AlCl_3(py)]$ is a simple 1:1 molecular adduct, whilst $[AlCl_3(py)_2]$ exists as $[trans\text{-}AlCl_2(py)_4]^+[AlCl_4]^-$, and $[AlCl_3(py)_3]$ exists as the neutral *mer*-isomer with pseudo-octahedral stereochemistry.[23]

The extensive chemistry of aluminium-nitrogen compounds and their gallium and indium counterparts includes that of amides, $[M(NH_2)_3]$, $[MX(NH_2)_2]$ and $[MX_2NH_2]$, (M = Al, Ga or In) and the corresponding species incorporating the organoamido substituents, –NHR and $-NR_2$. Also to be considered are imides and organoimido-derivatives containing the groups -NH and –NR–, respectively, together with a few hydrazide and methyleneamide (ketimide) complexes, *e.g.* $[M(N{=}CR_2)_3]$, (M = Al, Ga or In).[22] Dialkylamido compounds are readily accessible, and are easier to handle than the simple amide analogues. For example, treatment of $Li[AlH_4]$ with Me_2NH gives $Li[Al(NMe_2)_4]$, while the reaction between the aluminium and the amine produces $[Al(NMe_2)_3]$. This compound and the gallium analogue are dimeric in the solid state with four-membered M_2N_2 rings.[24] Compounds with more bulky ligands, such as $[Al\{N(SiMe_3)_2\}_3]$, are three co-ordinate and planar. A similar situation pertains to gallium systems.

Neutral ligands containing N, P, O or S donor atoms also show a rich variety of co-ordination complexes with indium(III) halides.[22] Depending on the stoichiometry employed, many geometries have been observed in the solid state, *e.g.* $[InI_3(PHBu^t_2)]$ (**10**) is distorted tetrahedral, $[InCl_3(PMe_3)_2]$ (**11**) is trigonal bipyramidal,[25] whilst both *fac* and *mer* isomers of $[InCl_3(OPMe_3)_3]$ have been isolated.[26] There is also the possibility of ionic complexes being formed, as in $[InI_2(DMSO)_4][InI_4]$ (DMSO = dimethyl sulfoxide).[27]

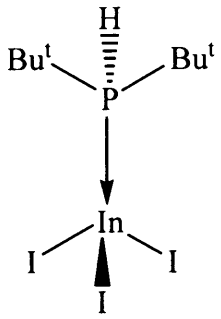

(10)

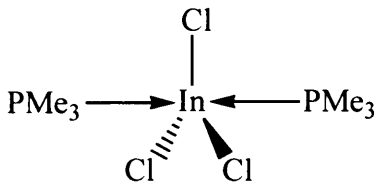

(11)

2.4 Preparation and Reactivity of 'GaI'

In the past five years there has been much interest in the chemistry of metastable aluminium(I) and gallium(I) halide complexes, as already described in section 1.2. An alternative to these halide complexes, whose synthesis requires a specialised apparatus, is available with 'GaI' which has been reported by Green *et al.*[28] It is simply formed by sonicating gallium metal with 0.5 equivalents of I_2. It is worth noting that the formulation of 'GaI' is unknown but has been proposed to be $[Ga]_2^+[Ga_2I_6]^{2-}$ based on Raman spectroscopic studies.[29] Its reactivity has indicated that it can be used as a source of gallium(I), *e.g.* 'GaI' + RI $\rightarrow$ $RGaI_2$, (*e.g.* R = $[Fe(\eta\text{-}C_5H_5)(CO)_2]$ or $[Mo(\eta\text{-}C_5H_4Me)(CO)_3]$).[28] Jones, *et al* have shown that 'GaI' reacts with primary and secondary amines or secondary phosphines to give a variety of gallium(II) iodide complexes of the type $[Ga_2I_4(L)_2]$ (L = NR_2H, NRH_2, PR_2H) *via* disproportionation reactions.[30] It is noteworthy that others have seen similar reactivity of gallium subhalides with tertiary amines,[31] phosphines[32] and arsines,[33] to give gallium (I) and (II) iodide complexes, *e.g.* $[Ga_2I_4(NEt_3)_2]$,[31] $[Ga_3I_5(PEt_3)_3]$[32] and $[Ga_2I_4(AsEt_3)_2]$.[33]

2.5 Research Proposal

As evidenced by even the most recent inorganic textbooks, the +III oxidation state is still being taught as the dominant, if not only, oxidation state of aluminium and gallium in its complexes. It was only in the last decade of the past millennium that the chemistry of low valent compounds of the heavier group 13 elements made rapid progress. Driven by the fascination with metal—metal bonded species, a series of new cluster compounds of these elements has been synthesised and characterised. In the meantime, a structural variety has been reached which has in many cases no analogies by other elements.[34]

The aim of this study was the preparation of a number of N-heterocyclic carbene and N-donor ligand complexes of several group 13 trihalide fragments and their crystallographic and spectroscopic characterisation. Furthermore it was the intention to reduce these group 13 trihalide complexes with alkali metals, *e.g.* Na or K, to form metal—metal bonded species or cluster compounds.

A further objective of this work was the investigation of the reactivity of several pyridine type ligands towards 'GaI' in the hope of preparing new complexes that could be used as precursors to low valent group 13 metal compounds or cluster compounds.

2.6 Results and Discussion

2.6.1 Carbene complexes of group 13 halides

The bulky 2,6-diisopropylphenyl substituted carbene (IPr) has been used to prepare a complex of indium tribromide. An initial reaction of IPr with $InBr_3$ in Et_2O did not give the expected 1:1 adduct, $[InBr_3(IPr)]$ (**12**), but instead the imidizolium salt $[IPrH][InBr_4]$, **13**, (Scheme 4) which has been structurally characterised, Figure 1.

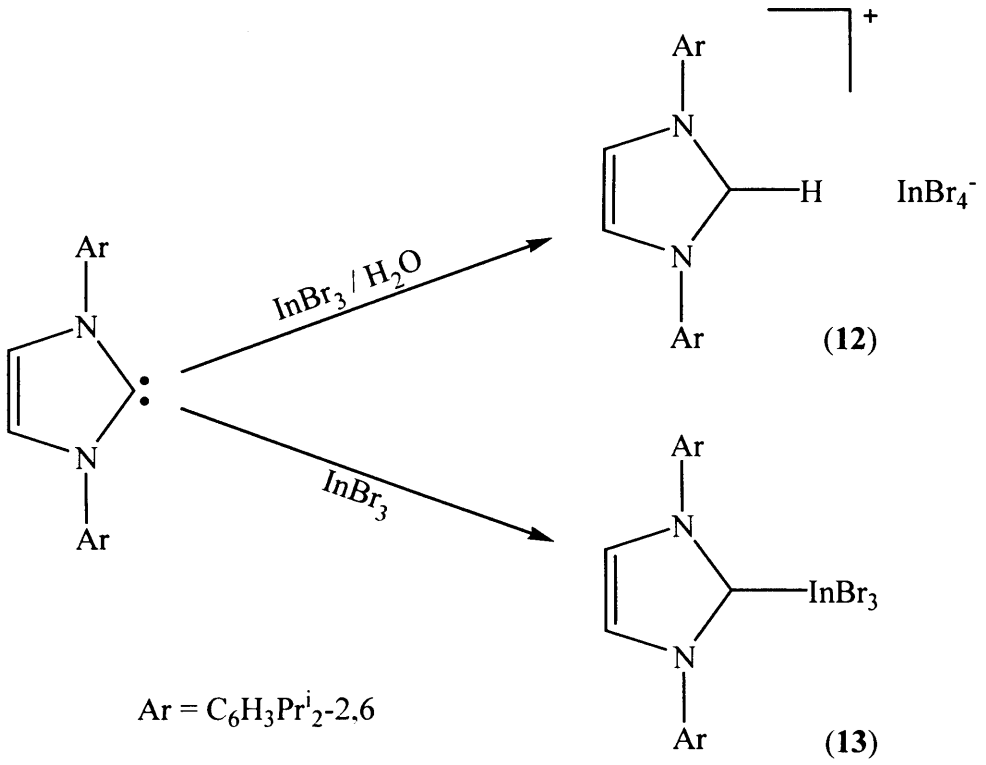

Scheme 4

From previous work in the Jones group on carbene—InX_3 (X = Cl, Br) compounds in which the formation of similar imidazolium compounds has been observed,[18, 35] it is thought that **12** probably arises from a trace of water in the $InBr_3$ starting material which reacts with the carbene to give **12** and '$InBr_2OH$' as the reaction by-product. The structure of **12** contains two crystallographically independent molecules in the asymmetric unit which display very similar geometries so data for only one will be discussed here. The tetrahedral $InBr_4^-$ anion has no interaction with the cation and the metric parameters of the imidazolium ring indicate a

delocalised system, [N—C—N angle of **12** 108.0(7)°]. The ^{1}H-NMR spectrum clearly shows the imidazolium proton of the N—C—N fragment resonating at δ 8.42 ppm.

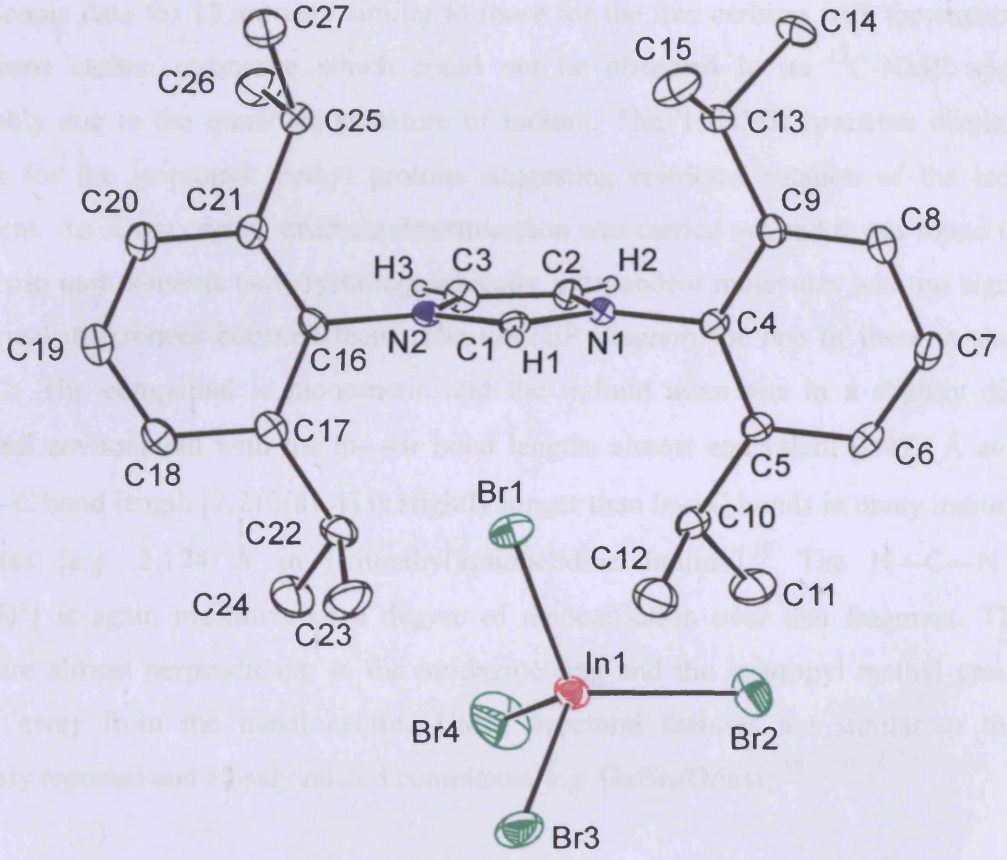

Figure 1 Molecular structure of [IPrH][$InBr_4$] (**12**)

Selected bond lengths (Å) and angles (°): C(1)—N(1) 1.329(11), N(1)—C(2) 1.367(11), N(1)—C(4) 1.467(11), C(2)—C(3) 1.361(13), N(2)—C(1) 1.339(10), N(2)—C(3) 1.374(11), N(2)—C(16) 1.457(11), In(1)—Br(1) 2.4995(16), In(1)—Br(2) 2.4862(16), In(1)—Br(3) 2.4699(17), In(1)—Br(4) 2.4814(19), N(1)—C(1)—N(2) 108.0(7), C(1)—N(2)—C(3) 108.9(7), C(1)—N(2)—C(16) 125.3(7), C(1)—N(1)—C(2) 109.3(7), C(1)—N(1)—C(4) 123.7(7), Br(1)—In(1)—Br(2) 111.16(6), Br(2)—In(1)—Br(4) 107.27(9), Br(4)—In(1)—Br(3) 108.55(9), Br(3)—In(1)—Br(1) 107.97(6).

The reaction was repeated with carefully resublimed $InBr_3$ and the 1:1 adduct, [$InBr_3$(IPr)] (**13**), was isolated in low yield (Scheme 4). The analogous 2:1 reaction of IPr with $InBr_3$ also gave (**13**). The formation of compound **13** in the 2:1 reaction is presumably favoured due to the steric bulk of the ligand IPr, which prevents the formation of an 2:1 adduct and the nucleophilic IPr ligand electronically satisfying the metal centre. The spectroscopic data for **13** are very similar to those for the free carbene with the exception of the carbene carbon resonance which could not be observed in its ^{13}C-NMR spectrum, presumably due to the quadrupolar nature of indium. The ^{1}H-NMR spectrum displays two doublets for the isopropyl methyl protons suggesting restricted rotation of the isopropyl substituent. An X-ray crystal structure determination was carried out and it was found that the asymmetric unit contains two crystallographically independent molecules with no significant geometrical differences between them. The ORTEP diagram for one of these is shown in Figure 2. The compound is monomeric and the indium atom sits in a slightly distorted tetrahedral envitonment with the In—Br bond lengths almost equivalent [2.497 Å average]. The In—C bond length [2.212(8) Å] is slightly longer than In—C bonds in many indium alkyl complexes [*e.g.* 2.174 Å in (trimethyl)quinuclidine indium].[36] The N—C—N angle [106.5(7)°] is again indicative of a degree of delocalisation over that fragment. The aryl groups are almost perpendicular to the imidazole ring and the isopropyl methyl groups are directed away from the metal centre. These structural features are similar to those in previously reported and closely related complexes, *e.g.* [$InBr_3$(IMes)].[37]

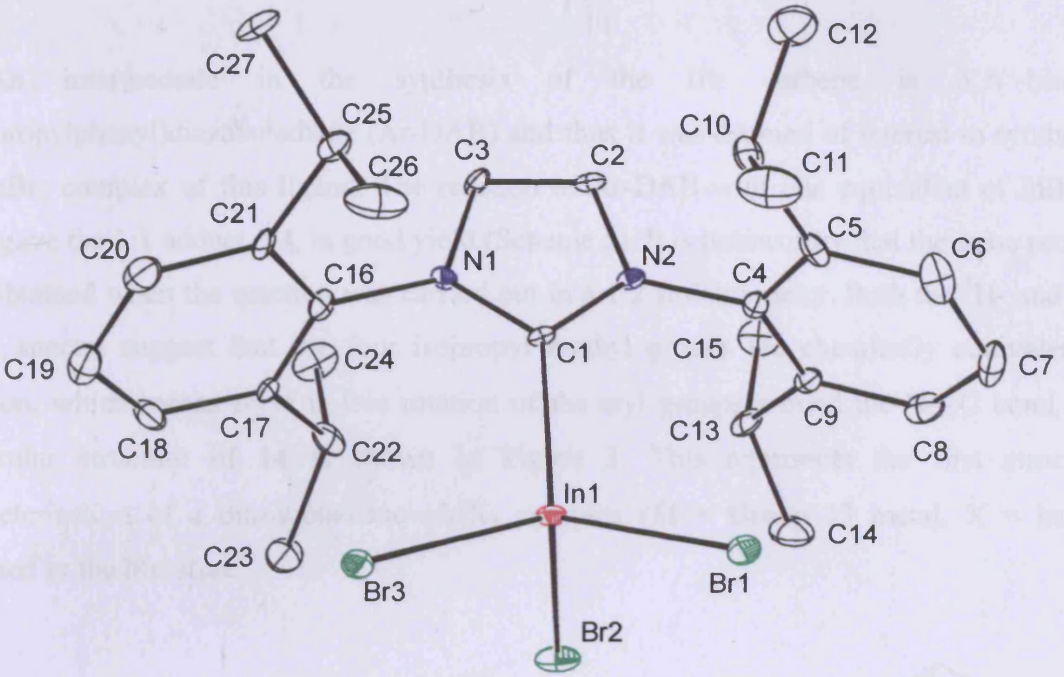

Figure 2 Molecular structure of [$InBr_3$(IPr)] (**13**)

Selected bond lengths (Å) and angles (°): C(1)—In(1) 2.212(8), C(1)—N(1) 1.331(12), N(1)—C(3) 1.407(12), N(1)—C(16) 1.449(13), C(2)—C(3) 1.320(13), N(2)—C(2) 1.397(11), N(2)—C(1) 1.322(12), N(2)—C(4) 1.462(13), In(1)—Br(1) 2.4935(14), In(1)—Br(2) 2.5000(12), In(1)—Br(3) 2.4999(13), N(1)—C(1)—N(2) 106.5(7), C(1)—N(2)—C(2) 109.8(8), C(1)—N(2)—C(4) 124.6(7), C(1)—N(1)—C(3) 110.3(8), C(1)—N(1)—C(16) 126.4(8), Br(1)—In(1)—Br(2) 107.43(5), Br(2)—In(1)—Br(3) 107.92(5), Br(3)—In(1)—Br(1) 107.34(4), C(1)—In(1)—Br(1) 113.6(3), C(1)—In(1)—Br(2) 108.1(2), C(1)—In(1)—Br(3) 112.2(3).

2.6.2 Nitrogen donor ligand complexes of group 13 halides

An intermediate in the synthesis of the IPr carbene is *N,N'*-bis(2,6-diisopropylphenyl)diazabutadiene (Ar-DAB) and thus it was deemed of interest to synthesise the $InBr_3$ complex of this ligand. The reaction of Ar-DAB with one equivalent of $InBr_3$ in Et_2O gave the 1:1 adduct, **14**, in good yield (Scheme 5). It is noteworthy that the same product was obtained when the reaction was carried out in a 1:2 stoichiometry. Both the ^1H- and ^{13}C-NMR spectra suggest that the four isopropyl methyl groups are chemically equivalent in solution, which means there is free rotation of the aryl groups around the N—C bond. The molecular structure of **14** is shown in Figure 3. This represents the first structural characterisation of a diazabutadiene—MX_3 complex (M = Group 13 metal, X = halide) reported in the literature.

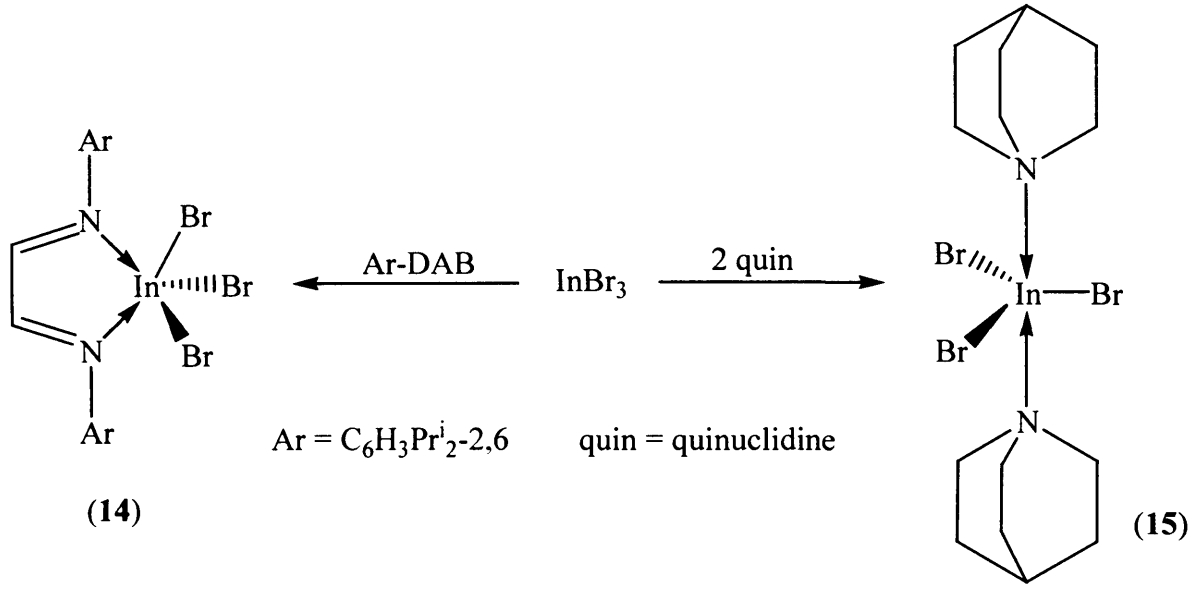

(14) **(15)**

Scheme 5

The compound crystallises in the chiral space group *P*1 with four crystallographically independent molecules in the asymmetric unit. The geometries of these are significantly different, ranging from distorted square based pyramidal to distorted trigonal pyramidal. Despite these differences, comment will only be made on one of the molecules here. It is interesting, in light of these solid state geometrical differences, that in solution all the methyl groups of **14** are chemical equivalent which strongly suggests that there is a fluxional process occurring, perhaps involving the decomplexation/complexation of the DAB molecule from

the $InBr_3$ unit. Cooling solutions of **14** to –50 °C did not lead to a resolution of the spectrum and all resonances broadened only slightly, presumably because the fluxional process is rapid even at this temperature.

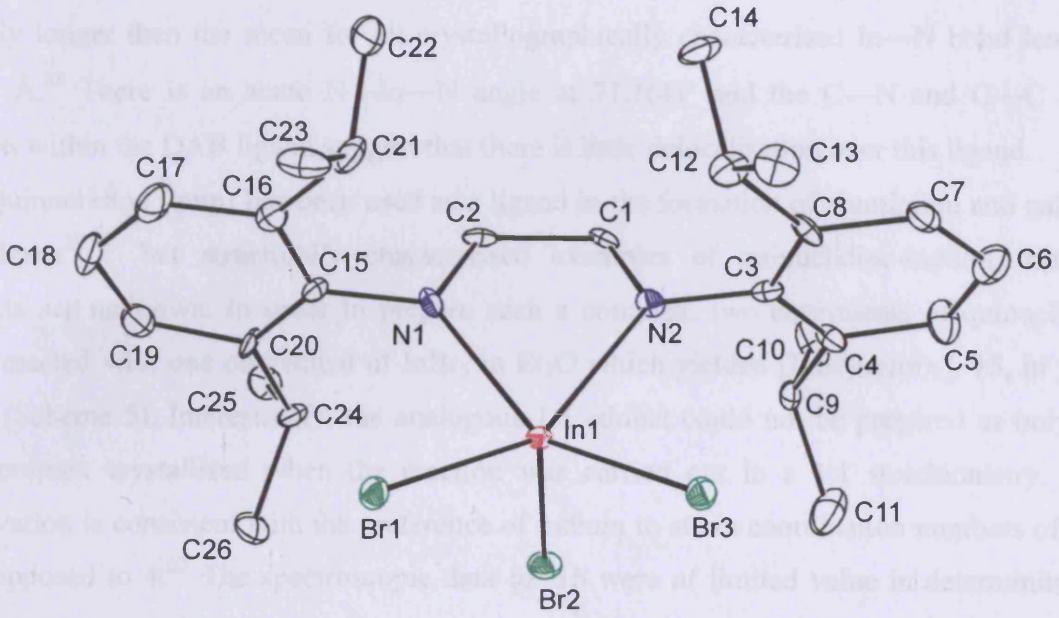

Figure 3 Molecular structure of [$InBr_3$(Ar-DAB)] (**14**)

Selected bond lengths (Å) and angles (°): In(1)—N(1) 2.332(14), N(1)—C(2) 1.27(2), N(1)—C(15) 1.45(2), C(1)—C(2) 1.57(2), N(2)—C(1) 1.24(2), N(2)—C(3) 1.46(2), In(1)—N(2) 2.314(12), In(1)—Br(1) 2.532(2), In(1)—Br(2) 2.505(2), In(1)—Br(3) 2.539(2), N(1)—In(1)—N(2) 71.1(4), N(1)—In(1)—Br(1) 88.8(3), Br(1)—In(1)—Br(3) 95.37(7), Br(3)—In(1)—N(2) 89.4(3), Br(1)—In(1)—Br(2) 108.98(8), Br(3)—In(1)—Br(2) 107.34(8), N(1)—In(1)—Br(2) 101.5(3), N(2)—In(1)—Br(2) 100.0(3).

The chirality of the crystal structure arises from an 'end to end' packing of molecules of **14** which gives rise to an infinite helical chain. The geometry around In(1) is distorted square based pyramidal with the two Br ligands *trans* to the nitrogen centres and at similar distance from the indium atom [In(1)—Br(1) 2.532(2) Å and In(1)—Br(3) 2.539(2) Å] with one closer apical Br ligand [In(1)—Br(2) 2.505(2) Å]. The In—N bond lengths are comparable but slightly longer than the mean for all crystallographically characterised In—N bond lengths, 2.294 Å.[38] There is an acute N—In—N angle at 71.1(4)° and the C—N and C—C bond lengths within the DAB ligand suggest that there is little delocalisation over this ligand.

Quinuclidine (quin) has been used as a ligand in the formation of aluminium and gallium complexes[39, 40] but structurally characterised examples of quinuclidine-indium trihalide adducts are unknown. In order to prepare such a complex, two equivalents of quinuclidine were reacted with one equivalent of $InBr_3$ in Et_2O which yielded $[InBr_3(quin)_2]$, **15**, in good yield (Scheme 5). Interestingly, the analogous 1:1 adduct could not be prepared as only the 2:1 complex crystallised when the reaction was carried out in a 1:1 stoichiometry. This observation is consistent with the preference of indium to attain coordination numbers of 5 or 6 as opposed to 4.[22] The spectroscopic data for **15** were of limited value in determining its structure as they closely resemble those for the free quin ligand. As a result an X-ray structural analysis was carried out and the molecular structure of **15** is shown in Figure 4. The complex is trigonal bipyramidal with the bromide ligands in the equatorial sites and the amine ligands in the axial positions. A similar arrangement has been seen in $[GaHCl_2(quin)_2]$[39] and $[AlClH_2(quin)_2]$.[40] Both the In—Br [2.5959 Å average] and In—N bond lengths [2.364(3) Å] are unexceptional being close to those in related complexes, *e.g.* $[InBr_3(trimethyltriazacyclononane)]$.[41]

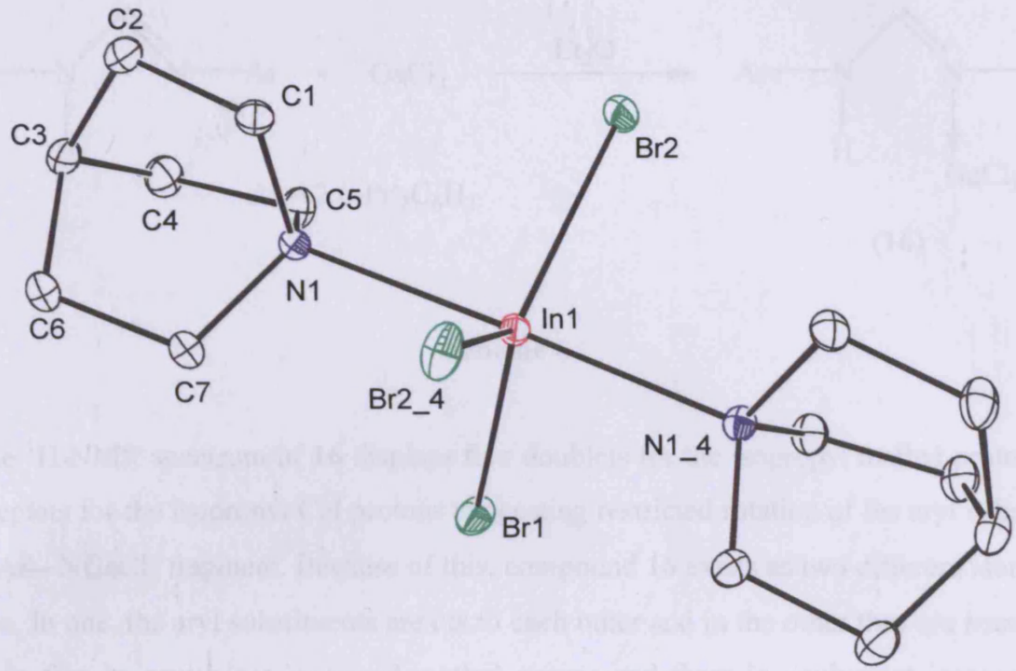

Figure 4 Molecular structure of $[InBr_3(quin)_2]$ (**15**)

Selected bond lengths (Å) and angles (°): In(1)—Br(1) 2.5271(8), In(1)—Br(2) 2.5254(5), In(1)—N(1) 2.364(3), N(1)—In(1)—N(1_4) 178.40(14), Br(2)—In(1)—Br(2_4) 117.86(3), Br(1)—In(1)—Br(2) 121.07(2).

Considering the increasing importance of amidine complexes of the main group elements,[42] the bulky formamidine ligand $(2,6\text{-}Pr^i_2C_6H_3)NC(H)NH(2,6\text{-}Pr^i_2C_6H_3)$, HFiso, was reacted with $GaCl_3$ in Et_2O to yield the crystalline 1:1 adduct, **16**, in good yield (Scheme 6). The 1:1 reaction of the lithiated form of the formamidine ligand, LiFiso, with $GaCl_3$ yielded the same product, **16**. It was thought that compound **16** in this reaction probably arises from a trace of water in the solvent used (THF). However, carefully repeating this reaction with freshly distilled THF did not give a different product, but compound **16**. It is unknown why this occurs.

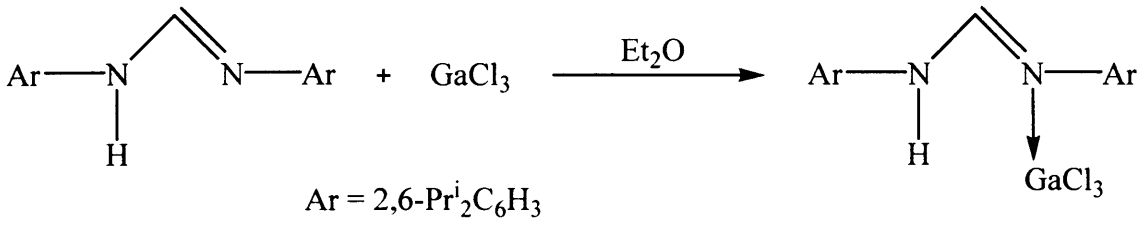

Ar = 2,6-$Pr^i_2C_6H_3$

(16)

Scheme 6

The ^{1}H-NMR spectrum of **16** displays five doublets for the isopropyl methyl protons and three septets for the isopropyl CH protons suggesting restricted rotation of the aryl substituent of the Ar—$NGaCl_3$ fragment. Because of this, compound **16** exists as two different isomers in solution. In one, the aryl substituents are *cis* to each other and in the other they are *trans*. This results in five in equivalent isopropyl methyl groups and three in equivalent isopropyl CH protons for the two isomers, thus explaining the observed spectrum. The N—H protons for the two isomers have been observed in the ^{1}H-NMR spectrum at δ = 8.67 and 8.71 ppm. An X-ray crystal structure determination was carried out, the results which are shown in Figure 5.

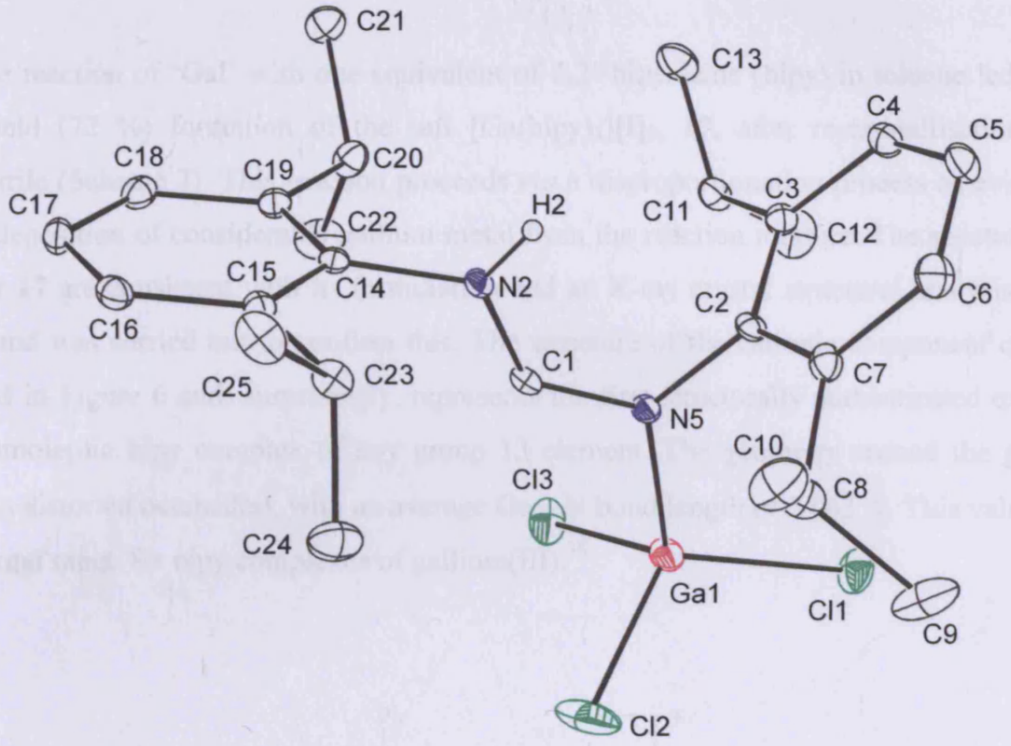

Figure 5 Molecular structure of [$GaCl_3$(HFiso)] (**16**)

Selected bond lengths (Å) and angles (°): N(5)—Ga(1) 1.941(5), C(1)—N(5) 1.307(13), C(1)—N(2) 1.309(2), N(5)—C(2) 1.452(7), N(2)—C(14) 1.455(4), N(2)—H(2) 0.841(1), Ga(1)—Cl(1) 2.140(3), Ga(1)—Cl(2) 2.168(4), Ga(1)—Cl(3) 2.168(4), N(2)—C(1)—N(5) 128.6(0), C(1)—N(5)—C(2) 118.8(5), C(1)—N(2)—C(14) 120.4(7), Cl(1)—Ga(1)—Cl(2) 114.7(5), Cl(2)—Ga(1)—Cl(3) 107.3(0), Cl(3)—Ga(1)—Cl(1) 114.5(7), N(5)—Ga(1)—Cl(1) 109.1(8), N(5)—Ga(1)—Cl(2) 104.5(1), N(5)—Ga(1)—Cl(3) 105.6(9).

Treatment of the prepared group 13 halide complexes, **12-16**, with either Na or K metal in THF did not yield the expected low valent metal—metal bonded group 13 species but instead significant decomposition was observed and the free ligands were isolated. Investigations of the oxidation/reduction potentials of the central metal ions in these complexes by using cyclic voltammetry did not lead to any useful information for the intended reductions.

2.6.3 Reactivity of 'GaI' towards pyridine based ligands

The reaction of 'GaI' with one equivalent of 2,2'-bipyridine (bipy) in toluene led to the high yield (72 %) formation of the salt $[Ga(bipy)_3][I]_3$, **17**, after re-crystallisation from acetonitrile (Scheme 7). This reaction proceeds *via* a disproportionation process as evidenced by the deposition of considerable gallium metal from the reaction mixture. The spectroscopic data for **17** are consistent with its formulation and an X-ray crystal structural analysis of the compound was carried out to confirm this. The structure of the cationic component of **17** is depicted in Figure 6 and, surprisingly, represents the first structurally authenticated example of a homoleptic bipy complex of any group 13 element. The geometry around the gallium centre is distorted octahedral, with an average Ga—N bond length of 2.063 Å. This value is in the normal range for bipy complexes of gallium(III).[38]

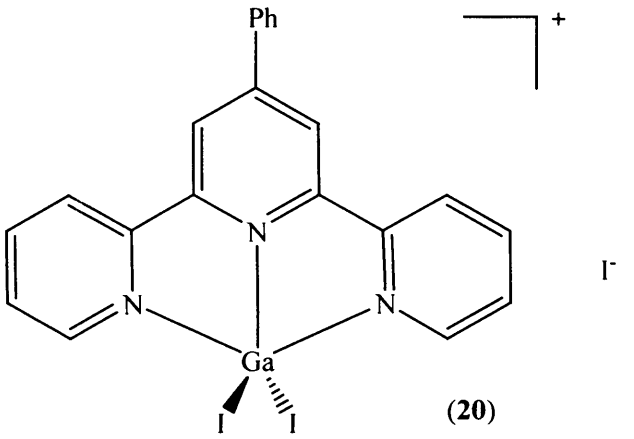

(20)

iii

$[Ga(bipy)_3][I]_3$ **(17)** ← i — 'GaI' — ii → $[\{(bipy)_2Ga\}_2(\mu\text{-}OH)_2]_2[Ga_2I_6][I]_6$ **(18)** and $[\{(bipy)_2Ga\}_2(\mu\text{-}OH)_2][I]_4$ **(19)**

Scheme 7 Reagents and conditions: i, bipy, toluene, -Ga; ii, bipy/H_2O, toluene, -Ga; iii, Phterpy, toluene, -Ga.

The three iodide anions do not display any short contacts with the cation or themselves. It is noteworthy that the complex crystallises in the chiral space group, $Pna2_1$, and in the crystal selected for the X-ray experiment the cation exists as its Λ–enantiomer.

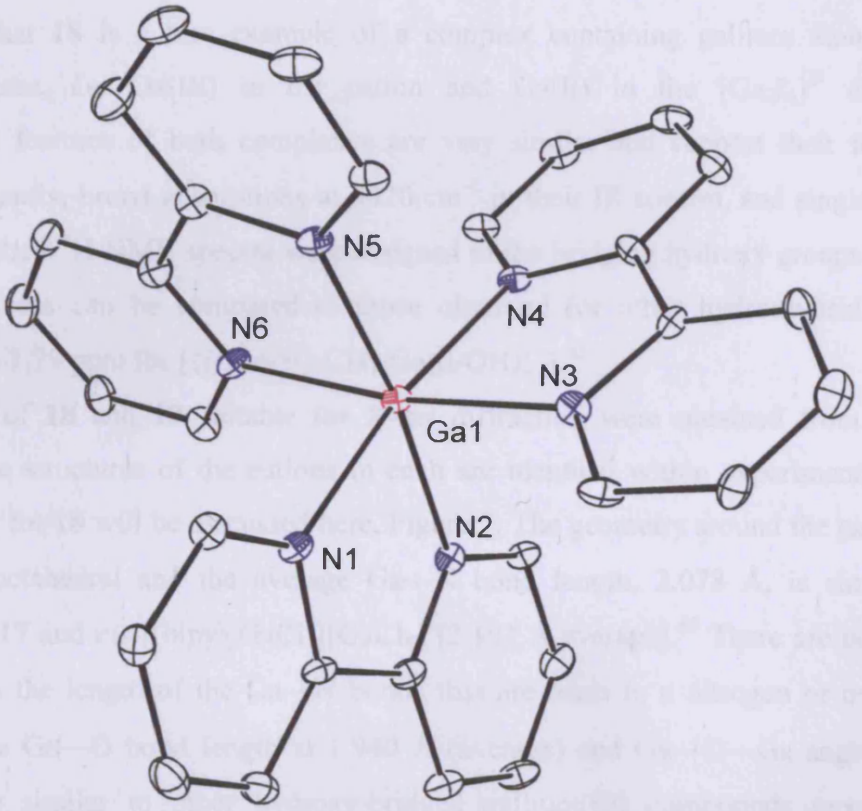

Figure 6 Structure of the cationic component of $[Ga(bipy)_3][I]_3$ (**17**)

Selected bond lengths (Å) and angles (°): Ga(1)—N(1) 2.070(6), Ga(1)—N(2) 2.056(5), Ga(1)—N(3) 2.062(6), Ga(1)—N(4) 2.053(6), Ga(1)—N(5) 2.071(5), Ga(1)—N(6) 2.069(6), N(1)—Ga(1)—N(2) 80.1(2), N(1)—Ga(1)—N(3) 93.92(19), N(1)—Ga(1)—N(4) 171.4(2), N(1)—Ga(1)—N(5) 93.7(2), N(1)—Ga(1)—N(6) 91.5(2), N(2)—Ga(1)—N(3) 91.3(2), N(2)—Ga(1)—N(4) 94.2(2), N(2)—Ga(1)—N(5) 172.3(3), N(2)—Ga(1)—N(6) 95.6(2), N(3)—Ga(1)—N(4) 79.8(2), N(3)—Ga(1)—N(5) 93.8(2), N(3)—Ga(1)—N(6) 171.9(2), N(4)—Ga(1)—N(5) 92.4(2), N(4)—Ga(1)—N(6) 95.4(2), N(5)—Ga(1)—N(6) 79.9(2).

In the first attempted preparation of **17**, two salts containing hydroxy-bridged digallium(III) tetracations, *viz.* $[\{(bipy)_2Ga\}_2(\mu\text{-}OH)_2]_2[Ga_2I_6][I]_2$, **18**, and $[\{(bipy)_2Ga\}_2(\mu\text{-}OH)_2][I]_4$, **19**, were formed in low yields as yellow crystalline solids which were manually separated from orange **17**. Both compounds presumably form as a result of hydrolysis arising from contamination of the solvent or bipy starting material with water (Scheme 7). It is noteworthy that **18** is a rare example of a complex containing gallium atoms in mixed oxidation states, *i.e.* Ga(III) in the cation and Ga(II) in the $[Ga_2I_6]^{2-}$ dianion. The spectroscopic features of both complexes are very similar and support their formulations. Most significantly, broad absorptions at 3420 cm^{-1} in their IR spectra, and singlet peaks at δ 2.05 ppm in their ^{1}H-NMR spectra were assigned to the bridging hydroxy groups. The proton NMR resonances can be compared to those observed for other hydroxy-bridged gallium dimers, *e.g.* δ 1.79 ppm for $[\{[(Me_3Si)_2CH]_2Ga(\mu\text{-}OH)\}_2]$.[43]

Crystals of **18** and **19** suitable for X-ray diffraction were obtained from acetonitrile solutions. The structures of the cations in each are identical within experimental error and thus only that for **18** will be discussed here, Figure 7. The geometry around the gallium atoms is distorted octahedral and the average Ga—N bond length, 2.078 Å, is similar to that observed for **17** and *cis*-$[(bipy)_2GaCl_2][GaCl_4]$ [2.103 Å average].[44] There are no significant differences in the length of the Ga—N bonds that are *trans* to a nitrogen or oxygen atom. Moreover, the Ga—O bond length at 1.940 Å (average) and Ga—O—Ga angles at 102.9° (average) are similar to other hydroxy-bridged gallium(III) compounds reported in the literature, *e.g.* 1.949(2) Å and 99.6(1)° respectively for $[\{(Mes)_2Ga\}_2(\mu\text{-}OH)_2]$.[45] The metric parameters for the $[Ga_2I_6]^{2-}$ counter ion, Figure 8, are almost identical to those seen for $[PPh_3H][Ga_2I_6]$.[46] It is interesting to note that a Raman spectroscopic study has suggested that the 'GaI' starting material used in the formation of **18** exists as $[Ga]_2^+[Ga_2I_6]^{2-}$ and thus contains this dianion.[29]

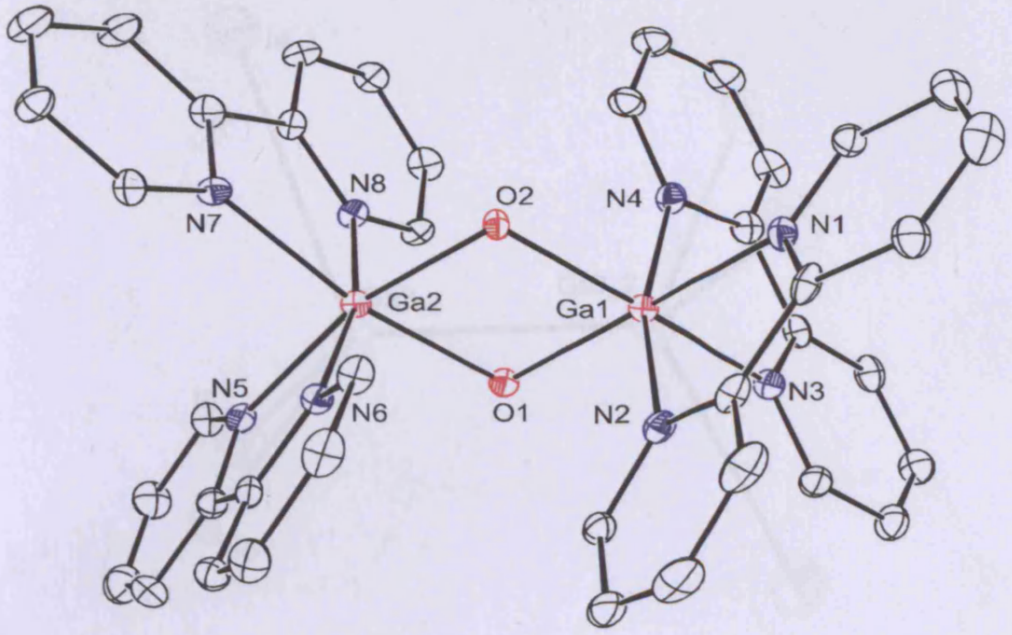

Figure 7 Structure of the cationic component of $[\{(bipy)_2Ga\}_2\text{-}(\mu\text{-}OH)_2]_2[Ga_2I_6][I]_2$ (**18**)

Selected bond lengths (Å) and angles (°): Ga(1)—O(1) 1.942(5), Ga(1)—O(2) 1.941(5), Ga(2)—O(1) 1.942(5), Ga(2)—O(2) 1.937(5), Ga(1)—N(1) 2.071(6), Ga(1)—N(2) 2.094(6), Ga(1)—N(3) 2.066(6), Ga(1)—N(4) 2.085(7), Ga(2)—N(5) 2.070(6), Ga(2)—N(6) 2.075(6), Ga(2)—N(7) 2.078(6), Ga(2)—N(8) 2.088(6), O(1)—Ga(1)—O(2) 77.0(2), O(1)—Ga(1)—N(1) 166.4(2), O(1)—Ga(1)—N(2) 91.5(2), O(1)—Ga(1)—N(3) 93.4(2), O(1)—Ga(1)—N(4) 99.5(2), O(1)—Ga(2)—N(5) 91.7(2), O(1)—Ga(2)—N(6) 92.7(2), O(1)—Ga(2)—N(7) 169.2(2), O(1)—Ga(2)—N(8) 93.8(2), O(2)—Ga(1)—N(1) 95.8(2), O(2)—Ga(1)—N(2) 98.4(2), O(2)—Ga(1)—N(3) 164.1(2), O(2)—Ga(1)—N(4) 90.3(2), O(2)—Ga(2)—N(5) 165.1(2), O(2)—Ga(2)—N(6) 92.7(2), O(2)—Ga(2)—N(7) 95.7(2), O(2)—Ga(2)—N(8) 95.8(2), Ga(1)—O(1)—Ga(2) 102.8(2), Ga(1)—O(2)—Ga(2) 103.0(2).

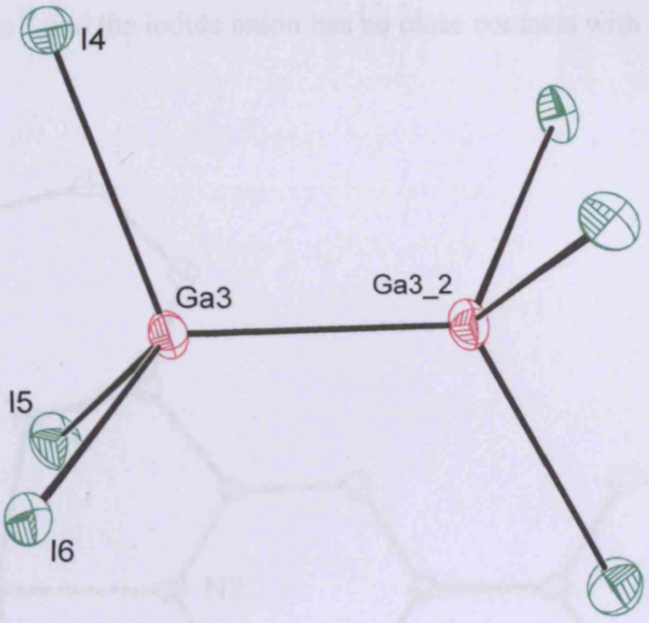

Figure 8 Structure of the anionic component of $[\{(bipy)_2Ga\}_2\text{-}(\mu\text{-}OH)_2]_2[Ga_2I_6][I]_2$ (**18**)

Selected bond lengths (Å) and angles (°): Ga(3)—Ga(3_2) 2.418(5), Ga(3)—I(4) 2.624(4), Ga(3)—I(5) 2.584(7), Ga(3)—I(6) 2.612(3), I(4)—Ga(3)—I(5) 106.4(6), I(4)—Ga(3)—I(6) 104.9(8), I(5)—Ga(3)—I(6) 107.3(9).

For sake of comparison, the 1:1 reaction of the tridentate 4'-phenyl-2,2':6',2''-terpyridine (Phterpy) ligand with 'GaI' in toluene was carried out and this gave rise to a yellow precipitate. On re-crystallisation of this precipitate from acetonitrile the salt $[GaI_2(Phterpy)][I]$, **20**, could be isolated in a high yield (87 %) (Scheme 7). Due to its poor solubility in common organic solvents, little meaningful spectroscopic data could be obtained on the complex and so crystals suitable for X-ray diffraction were grown from acetonitrile in order to determine its structure, the cationic component of which is depicted in Figure 9. The geometry around the gallium atom is distorted trigonal bipyramidal, with N(1) and N(3) taking up the axial positions [N(1)—Ga(1)—N(3) 154.6(2)°]. As would be expected, the two axial Ga—N bonds are longer [2.104 Å average] than the equatorial bond, [Ga(1)—N(2) 2.007(5) Å], though the average length for all three [2.071 Å] is close to that observed for

neutral [$GaCl_3$(terpy)] [2.086 Å average][47] and complexes **17-19**. The Ga—I bond distances are in the normal range[38] and the iodide anion has no close contacts with the cation.

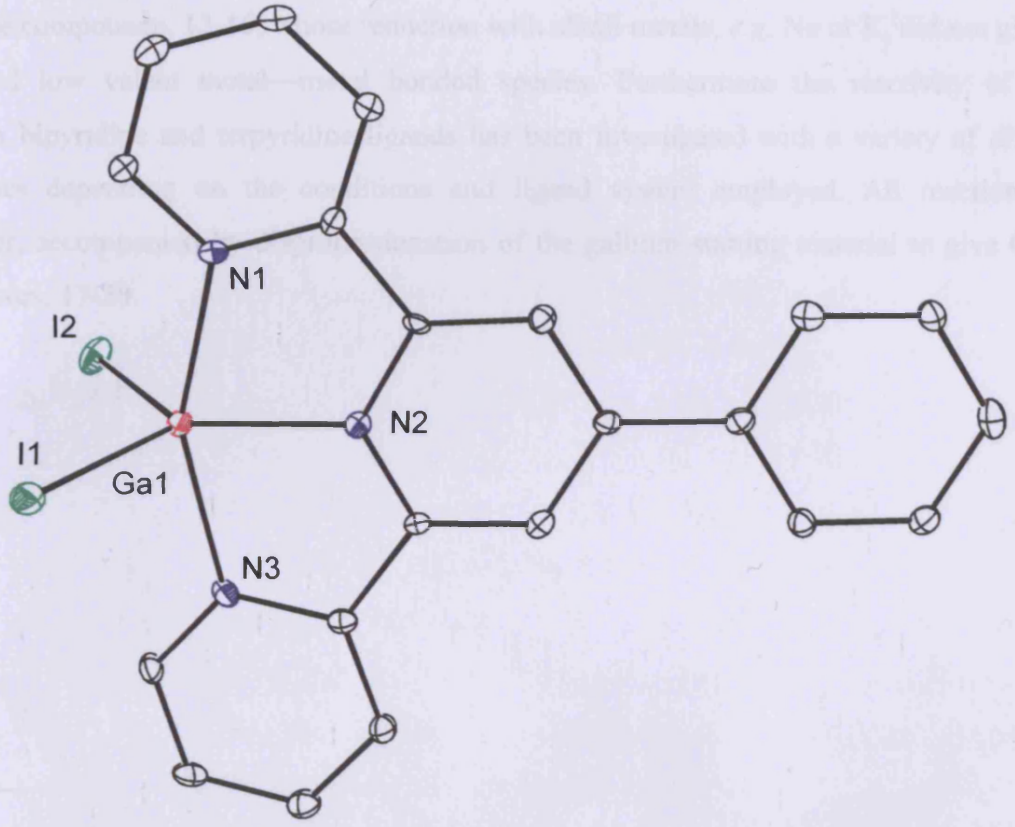

Figure 9 Structure of the cationic component of [GaI_2(Phterpy)][I] (**20**)

Selected bond lengths (Å) and angles (°): Ga(1)—I(1) 2.5389(11), Ga(1)—I(2) 2.5144(12), Ga(1)—N(1) 2.087(5), Ga(1)—N(2) 2.007(5), Ga(1)—N(3) 2.121(5), N(1)—Ga(1)—N(2) 77.4(2), N(1)—Ga(1)—N(3) 154.6(2), N(1)—Ga(1)—I(1) 97.08(15), N(1)—Ga(1)—I(2) 96.75(15), N(2)—Ga(1)—N(3) 77.3(2), N(2)—Ga(1)—I(1) 122.34(15), N(2)—Ga(1)—I(2) 120.29(15), N(3)—Ga(1)—I(1) 95.11(15), N(3)—Ga(1)—I(2) 97.32(15), I(1)—Ga(1)—I(2) 117.37(4).

2.7 Conclusions

In conclusion, this chapter describes some co-ordination chemistry of group 13 halides. A very bulky carbene and several nitrogen donor ligands have been used to prepare group 13 trihalide compounds, **12-16**, whose reduction with alkali metals, *e.g.* Na or K, did not give the expected low valent metal—metal bonded species. Furthermore the reactivity of 'GaI' towards bipyridine and terpyridine ligands has been investigated with a variety of different outcomes depending on the conditions and ligand system employed. All reactions are, however, accompanied by disproportionation of the gallium starting material to give Ga(III) complexes, **17-20**.

2.8 Experimental

For general experimental procedures, refer to appendix 1. $InBr_3$, $GaCl_3$ and quinuclidine were purchased from Aldrich and $InBr_3$ was resublimed before use. 'GaI' was synthesised by a modification of the literature method,[28] as were the ligands IPr,[48] Ar-DAB[48] and HFiso.[49] Bipy and Phterpy were obtained commercially and re-crystallised from CH_3CN prior to use.

[IPrH][InBr4].$(Et_2O)_{0.5}$ (12)

To a solution of IPr (0.54 g, 1.40 mmol) in Et_2O (10 cm^3) was added a solution of $InBr_3$ (0.50 g, 1.40 mmol) in Et_2O (10 cm^3). After stirring for 2 hrs the solution was concentrated and cooled to –35 °C to yield colourless crystals of **12** (0.11 g, 9 %); m. p. 187 – 189 °C (dec.); ^1H NMR (400 MHz, C_6D_6, 298 K) δ 1.15 (d, 12 H, $^3J_{HH}$ = 7.0 Hz, CH_3), 1.26 (d, 12 H, $^3J_{HH}$ = 7.0 Hz, CH_3), 2.38 (sept, 4 H, $^3J_{HH}$ = 7.0 Hz, CH), 7.86 (s, 2 H, NCH), 7.30 (d, 4 H, $^3J_{HH}$ = 8.0 Hz, m-ArH), 7.51 (t, 2 H, $^3J_{HH}$ = 8.0 Hz, p-ArH), 8.42 (s, 1 H, NCHN); ^{13}C NMR (100.6 MHz, C_6D_6, 298 K) δ 23.1 (CH_3), 26.1 (CH_3), 29.1 (CH), 124.8 (p-ArC), 126.6 (m-ArC), 131.9 (o-ArC), 136.5 (ipso-ArC), 145.0 (NCN), 145.3 (NC); IR ν/cm^{-1} (Nujol): 1594 m, 1328 m, 1212 m, 1117 m, 1062 m, 800 w; MS(APCI) m/z (%): 388 [IPr^+, 100]; $C_{29}H_{42}Br_4InN_2O_{0.5}$ requires C 40.45, H 4.92, N 3.25 %; found C 41.69, H 4.77, N 3.45 %.

[$InBr_3$(IPr)] (13)

To a solution of IPr (0.54 g, 1.40 mmol) in Et_2O (10 cm^3) was added a solution of freshly sublimed $InBr_3$ (0.50 g, 1.40 mmol) in Et_2O (10 cm^3). After stirring for 2 hrs the solution was concentrated and cooled to –35 °C to yield colourless crystals of **13** (0.11 g, 11 %); m. p. 187 °C; ^1H NMR (400 MHz, C_6D_6, 298 K) δ 1.10 (d, 12 H, $^3J_{HH}$ = 7.0 Hz, CH_3), 1.35 (d, 12 H, $^3J_{HH}$ = 7.0 Hz, CH_3), 2.48 (sept, 4 H, $^3J_{HH}$ = 7.0 Hz, CH), 7.86 (s, 2 H, NCH), δ 7.31 (d, 4 H, $^3J_{HH}$ = 8.0 Hz, m-ArH), 7.57 (t, 2 H, $^3J_{HH}$ = 8.0 Hz, p-ArH); ^{13}C NMR (100.6 MHz, C_6D_6, 298 K) δ 24.1 (CH_3), 24.8 (CH_3), 29.3 (CH), 125.1 (p-ArC), 126.7 (m-ArC), 129.4 (o-ArC), 132.7 (ipso-ArC), 145.0 (NC); IR ν/cm^{-1} (Nujol): 1568 m, 1328 m, 1257 m, 1117 m, 1062 m; MS(APCI) m/z (%): 663 [M-Br^+, 41], 388 [IPr^+, 100].

[$InBr_3$(Ar-DAB)].(Et_2O)$_{0.5}$ (14)

To a solution of Ar-DAB (0.53 g, 1.40 mmol) in Et_2O (10 cm^3) was added a solution of $InBr_3$ (0.50 g, 1.40 mmol) in Et_2O (10 cm^3). This was stirred for 2 hrs to give a deep red solution, which was filtered, concentrated and cooled to –35 °C to yield red crystals of **14** (0.16 g, 31 % on ether free sample): m. p. 178 – 180 °C; ^{1}H NMR (400 MHz, C_6D_6, 298 K) δ 1.28 (d, 24 H, $^3J_{HH}$ = 7.0 Hz, CH_3), 3.25 (sept, 2 H, $^3J_{HH}$ = 7.0 Hz, CH), 7.16 (d, 4 H, $^3J_{HH}$ = 7.0 Hz, m-ArH), 7.18 (t, 2 H, $^3J_{HH}$ = 7.0 Hz, p-ArH), 8.45 (s, 2 H, NCH); ^{13}C NMR (100.6 MHz, C_6D_6, 298 K) δ 23.5 (CH_3), 28.9 (CH), 124.0 (m-ArC), 124.5 (p-ArC), 138.8 (o-ArC), 146.4 (ipso-ArC), 163.6 (NC); IR ν/cm^{-1} (Nujol): 1654 m, 1594 m, 1172 m, 1107 m, 936 m; MS(APCI) m/z (%): 649 [M-Br^+, 2], 376 [Ar-DAB^+, 5], 333 [Ar-DAB-Pr^{i+}, 100]; $C_{26}H_{36}Br_3N_2In$ requires C 42.71, H 4.96, N 3.83 %; found C 41.51, C 4.98, N 3.55 %.

[$InBr_3$(quin)$_2$] (15)

To a solution of quinuclidine (0.31 g, 2.80 mmol) in Et_2O (10 cm^3) was added a solution of $InBr_3$ (0.50 g, 1.40 mmol) in Et_2O (10 cm^3). The reaction was stirred for 2 hrs to give a white precipitate, which was isolated by filtration and extracted into toluene (2 x 20 cm^3). Concentrating and cooling to –35 °C gave colourless crystals of **15** (0.67 g, 83 %); m. p. 178 – 180 °C; ^{1}H NMR (400 MHz, $CDCl_3$, 298 K) δ 1.88 (br m, 12 H, CH_2), 2.17 (br m, 2 H, CH), 3.24 (br m, 12 H, CH_2N); ^{13}C NMR (100.6 MHz, $CDCl_3$, 298 K) δ 19.6 (CH), 23.1 (CH_2), 46.8 (NCH_2); IR ν/cm^{-1} (Nujol): 1323 m, 1281 w, 1258 w, 1044 m, 979 m, 771 m; MS(APCI) m/z (%): 385 [M-Br^+, 13], 274 [$InBr_2^+$, 21], 112 [$quin^+$, 100].

[$GaCl_3$(HFiso)] (16)

To a solution of $GaCl_3$ (0.25 g, 1.37 mmol) in Et_2O (10 cm^3) at –78 °C was added a solution of HFiso (0.50 g, 1.37 mmol) in Et_2O (10 cm^3). The resulting solution was allowed to warm to 25 °C, filtered and solvent removed under vacuum. The residue was extracted into toluene (8 cm^3) and cooling to –35 °C yielded colourless crystals of **16** (0.48 g, 65 %); m. p. 158 – 160 °C; ^{1}H NMR (300 MHz, C_6D_6, 298 K) δ 1.05 (d, 6 H, $^3J_{HH}$ = 6.9 Hz, CH_3), 1.13 (d, 24 H, $^3J_{HH}$ = 6.8 Hz, CH_3), 1.23 (d, 6 H, $^3J_{HH}$ = 6.7 Hz, CH_3), 1.44 (d, 6 H, $^3J_{HH}$ = 6.9 Hz, CH_3), 1.52 (d, 6 H, $^3J_{HH}$ = 6.7 Hz, CH_3), 3.22 (sept, 2 H, $^3J_{HH}$ = 6.8 Hz, CH), 3.27 (sept, 4 H, $^3J_{HH}$ = 6.8 Hz, CH), 3.36 (sept, 2 H, $^3J_{HH}$ = 6.8 Hz, CH), 7.07 (m, 12 H, Ar-H), 7.83 (s, 1 H, NC(H)N), 7.87 (s, 1 H, NC(H)N), 8.67 (s, 1 H, NH), 8.71 (s, 1 H, NH); ^{13}C NMR (100.6 MHz, C_6D_6,

298 K) δ 22.3 (CH_3), 22.7 (CH_3), 23.1 (CH_3), 23.5 (CH_3), 23.9 (CH_3), 27.1 (CH), 27.4 (CH), 27.9 (CH), 122.6, 122.9, 124.1, 127.5 (ArC), 146.2 (NCN); IR ν/cm^{-1} (Nujol): 3313 s, 1586 m, 1327 s, 1175 s, 1058 s, 806 s; MS(APCI) m/z (%): 366 [$HFisoH^+$, 100], 541 [MH^+, 5].

$[Ga(bipy)_3][I]_3$ (17)

To a suspension of 'GaI' (5.80 mmol) in toluene (15 cm^3) was added a solution of 2,2'-bipyridine (0.90 g, 5.80 mmol) in toluene (15 cm^3) at –78 °C over 5 min. The resulting suspension was warmed to room temperature and stirred overnight to yield a yellow-orange precipitate. Volatiles were removed *in vacuo* and the residue extracted with CH_3CN (30 cm^3) and filtered. Cooling of the filtrate to –30 °C overnight yielded orange crystals of **17** (1.28 g, 72 %) m. p. 261 °C; ^1H NMR (400 MHz, CD_3CN, 298 K) δ 7.51 (m, 6 H, C5H), 7.81 (m, 6 H, C4H), 8.41 (m, 6 H, C3H), 8.51 (m, 6 H, C6H); ^{13}C NMR (100.6 MHz, CD_3CN, 298 K) δ 125.8 (C3), 128.7 (C5), 142.6 (C4), 146.7 (C6), 147.5 (C2); IR ν/cm^{-1} (Nujol): 1602 s, 1319 s, 1260 s, 1102 s, 801 s; MS(APCI) m/z (%): 157 [$bipyH^+$, 100].

$[\{(bipy)_2Ga\}_2\text{-}(\mu\text{-}OH)_2]_2[Ga_2I_6][I]_2$ (18) and $[\{(bipy)_2Ga\}_2\text{-}(\mu\text{-}OH)_2][I]_4$ (19)

In an attempted preparation of **17** in which the reaction solvent was contaminated with water, the hydrolysis products, **18** (m. p. 140 – 142 °C dec.) and **19** (m. p. 146 – 148 °C dec.) were formed in low yield (*ca.* 20 % as a mixture). Manual separation of **18** and **19** was achieved based on crystal morphology and the spectroscopic data for each were found to be indistinguishable. ^1H NMR (400 MHz, CD_3CN, 298 K) δ 2.05 (br, 2 H, OH), 7.40 (m, 4 H, C5H), 7.48 (m, 4 H, C5'H), 8.26 (m, 4 H, C4H), 8.42 (m, 4 H, C4'H), 8.53 (m, 4 H, C3H), 8.64 (m, 4 H, C3'H), 8.76 (m, 4 H, C6H), 8.83 (m, 4 H, C6'H); ^{13}C NMR (100.6 MHz, CD_3CN, 298 K) δ 124.3 (C3), 124.8 (C3'), 128.9 (C5), 129.0 ($C5_5$), 144.1 (C4), 145.0 (C4'), 145.8 (C6), 146.4 (C6'), 147.2 (C2), 147.6 (C2'); IR ν/cm^{-1} (Nujol): 3420 br, 1600 s, 1312 s, 1156 s, 1026 s, 774 s; MS(APCI) m/z (%): 469 [$(bipy)_2Ga_2OH^+$, 100].

[GaI_2(Phterpy)][I] (20)

To a suspension of 'GaI' (1.30 mmol) in toluene (15 cm^3) was added a solution of Phterpy (0.40g, 1.30 mmol) in toluene (15 cm^3) at –78 °C. The resulting suspension was warmed to room temperature and stirred overnight to yield a yellow precipitate. Volatiles were removed *in vacuo* and the residue extracted with CH_3CN (30 cm^3) then filtered. Cooling to –30 °C overnight yielded yellow crystals of **20** (0.28 g, 87 %); m. p. 172 °C (dec.); ^1H NMR (400 MHz, CD_3CN, 298 K) δ 7.67 (m, 3 H, o-/p-PhH), 8.01 (m, 2 H, C5H), 8.10 (m, 2 H, m-PhH), 8.46 (m, 2 H, C4H), 8.72 (m, 2 H, C3H), 8.94 (s, 2 H, C3′H, C5′H), 8.97 (m, 2 H, C6H); IR ν/cm^{-1} (Nujol): 1618 s, 1259 s, 1095 s, 1022 s, 800 s; MS(ESI) m/z (%): 310 [$PhterpyH^+$, 100].

2.9 References

1. *"Carbene Chemistry"*, second edn., W. Kirmse Ed., New York Academic Press, 1971.
2. W.v.E. Doering, A.K. Hoffmann, *J. Am. Chem. Soc.*, 1954, **76**, 6162.
3. E.O. Fischer, A. Maasböl, *Angew. Chem., Int. Ed. Engl.*, 1964, **3**, 580.
4. K. Öfele, *J. Organomet. Chem.*, 1968, **12**, P 42.
5. H.J. Schönherr, W. Wanzlick, *Angew. Chem., Int. Ed. Engl.*, 1968, **7**, 141.
6. A.J. Arduengo III, R.L. Harlow, M.Kline, *J. Am. Chem. Soc.*, 1991, **113**, 361.
7. A.J. Arduengo III, H.V.R. Dias, R.L. Harlow, M. Kline, *J. Am. Chem. Soc.*, 1992, **114**, 5530.
8. D. Bourissou, O. Guerret, F.P. Gabbai, G. Bertrand, *Chem. Rev.*, 2000, **100**, 39.
9. W.A. Herrmann, *Angew. Chem., Int. Ed.*, 2002, **41**, 1290.
10. A.J. Arduengo III, H.V.R. Dias, J.C. Calabrese, F. Davidson, *J. Am. Chem. Soc.*, 1992, **114**, 9724.
11. C.L. Raston, *J. Organomet. Chem.*, 1994, **475**, 15.
12. C.D. Abernathy, M.L. Cole, C. Jones, *Organometallics*, 2000, **19**, 4852.
13. A. Stasch, S. Singh, H. Roesky, M. Noltemeyer, H.G. Schmidt, *Eur. J. Inorg. Chem.*, 2004, 4052.
14. R.J. Baker, M.L. Cole, C. Jones, M.E. Mahon, *J. Chem. Soc., Dalton Trans.*, 2002, 1992.
15. A.H. Cowley, F.P. Gabbai, C.J. Carrano, L.M. Mokry, M.R. Bond, G. Bertrand, *Angew. Chem., Int. Ed. Engl.*, 1994, **33**, 578.
16. M.L. Cole, A.J. Davies, C. Jones, *J. Chem. Soc., Dalton Trans.*, 2001, 2451.
17. M.D. Francis, D.E. Hibbs, M.B. Hursthouse, C. Jones, N.A. Smithies, *J. Chem. Soc., Dalton Trans.*, 1998, 3249.
18. S.J. Black, D.E. Hibbs, M.B. Hursthouse, C. Jones, K.M.A. Malik, N.A. Smithies, *J. Chem. Soc., Dalton Trans.*, 1997, 4313.
19. C.D. Abernathy, M.L. Cole, A.J. Davies, C. Jones, *Tett. Lett.*, 2000, **41**, 7567.
20. C. Jones, *Chem. Commun.*, 2001, 2293.
21. C.D. Abernathy, R.J. Baker, M.L. Cole, A.J. Davies, C. Jones, *Transition Met. Chem.*, 2003, **28**, 296.
22. *"Chemistry of Aluminium, Gallium, Indium and Thallium"*, Ed. A.J. Downs, Blackie, Glasgow, 1993.

23. P. Pullmann, K. Hensen, J.W. Bats, *Z. Naturforsch., Teil B*, 1982, **37**, 1312.
24. K.M. Waggoner, M.M. Olmstead, P.P. Power, *Polyhedron*, 1990, **9**, 257.
25. N.W. Alcock, I.A. Degan, O.W. Howarth, M.G.H. Wallbridge, *J. Chem. Soc., Dalton Trans.*, 1992, 2775.
26. W.T. Robinson, C.J. Wilkins, Z. Zeying, *J. Chem. Soc., Dalton Trans.*, 1990, 219.
27. F.W.B. Einstein, D.G. Tuck, *J. Chem. Soc., Chem. Commun.*, 1970, 1182.
28. M.L.H. Green, P. Mountford, G.J. Smout, S.R. Speel, *Polyhedron*, 1990, **9**, 2763.
29. M. Kehrwald, W. Köstler, G. Linti, T. Blank, N. Wilberg, *Organometallics*, 2001, **20**, 860.
30. R.J. Baker, H. Bettentrup, C. Jones, *Eur. J. Inorg. Chem.*, 2003, 2446.
31. C.U. Doriat, M. Friesen, E. Baum, A. Ecker, H. Schnöckel, *Angew. Chem., Int. Ed.*, 1997, **36**, 1969.
32. A. Schnepf, C.U. Doriat, E. Möllhausen, H. Schnöckel, *Chem. Commun.*, 1997, 2111.
33. B. Beagley, S. Godfrey, K. Kelly, S. Kungwankunakorn, C. McAuliffe, R. Pritchard, *Chem. Commun.*, 1996, 2179.
34. A. Schnepf, H. Schnöckel, *Angew. Chem., Int. Ed.*, 2002, **41**, 3532.
35. D.E. Hibbs, M.B. Hursthouse, C. Jones, N.A. Smithies, *Main Group Chem.*, 1998, **2**, 293.
36. J.L. Atwood, S.G. Bott, N.C. Means, C.M. Means, *Inorg. Chem.*, 1987, **26**, 1466.
37. R.J. Baker, A.J. Davies, C. Jones, M. Kloth, *J. Organomet. Chem.*, 2002, **656**, 203.
38. Value obtained from a survey of the Cambridge Crystallographic Database.
39. B. Luo, V.G. Young, Jr. and W.L. Gladfelter, *Chem. Commun.*, 1999, 123.
40. C. Jones, P.C. Junk, M.L. Cole, *Main Group Chem.*, 2001, **24**, 249.
41. G.R. Willey, D.R. Aris, J.V. Haslop, W. Errington, *Polyhedron*, 2001, **20**, 423.
42. M.L. Cole, P.C. Junk, *J. Organomet. Chem.*, 2003, **666**, 55.
43. W. Uhl, I. Hahn, M. Koch, M. Layh, *Inorg. Chim. Acta.*, 1996, **249**, 33.
44. R. Restivo, G.J. Palenik, *J. Chem. Soc., Dalton Trans.*, 1972, 341.
45. J. Storre, A. Klamp, H.W. Roesky, H.G. Schmidt, M. Noltemeyer, R. Fleischer, D. Stalke, *J. Am. Chem. Soc.*, 1996, **118**, 1380.
46. M.A. Khan, D.G. Tuck, M.J. Taylor, D.A. Rogers, *J. Crystallogr. Spectrosc. Res.*, 1986, **16**, 895.
47. G. Beran, A.J. Carty, H.A. Patel, G.J. Palenik, *J. Chem. Soc., Chem. Commun.*, 1970, 222.

48. L. Jafarpour, E.D. Stevens, S.P. Nolan, *J. Organomet. Chem.*, 2000, **606**, 49.

49. R.M. Roberts, *J. Org. Chem.*, 1949, **14**, 277.

involved. These compounds are also accessible *via* metathesis reactions involving 'GaI' or reduction of metal(III) complexes, RMX_2.[2] In their monomeric state, group 13 diyls, :MR, have *sp*-hybridised metal centres with a singlet lone pair of electrons and two empty *p*-orbitals. As a result, they have the potential to act as strong σ-donor ligands by utilising their lone-pair, whilst their empty *p*-orbitals could possibly participate in π-back-bonding from suitable filled transition metal *d*-orbitals. In this respect, group 13 diyls could be thought of as analogues of CO or acyclic carbenes. In practice, these compounds have been employed as both terminal and bridging ligands in a wide variety of transition and main group metal complexes.[3, 2] The degree of back-bonding in these complexes has been a controversial issue, perhaps best exemplified by the iron—gallium diyl complex, $[(Ar^*Ga)Fe(CO)_4]$, **1**, Ar* = 2,6-(2,4,6-$Pr^i_3C_6H_2)_2C_6H_3$, which has alternately been described as containing an iron—gallium triple[4] or single bond.[5]

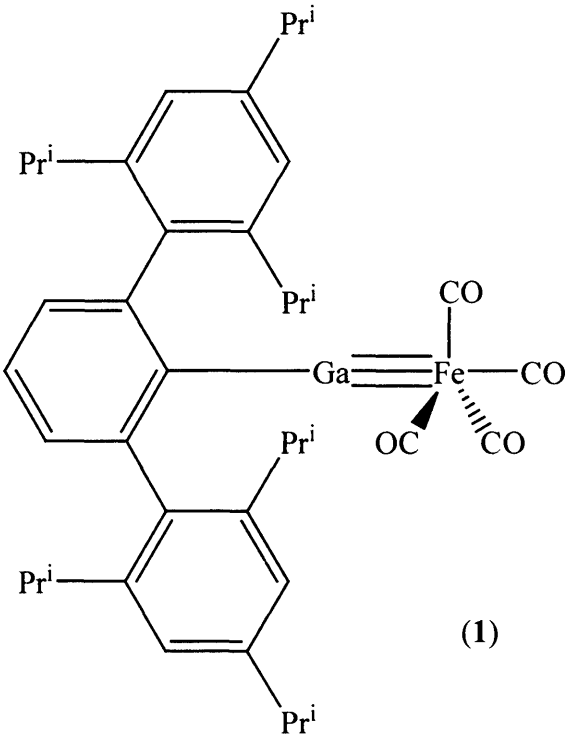

(1)

Numerous theoretical studies on this and related complexes have since been carried out and it is now generally accepted that the degree of metal—metal back-bonding is minimal due to the relatively high energy of the group 13 metal *p*-orbitals.[6, 7] This is, however, not always the case as in homoleptic complexes, *e.g.* $[Ni\{GaC(SiMe_3)_3\}_4]$, where the diyl ligand does not

compete with other ligands for π-electron density, significant π-back-bonding has been calculated.[8]

3.3 Group 13 Metal(I) Carbene Analogues and Their Use as Ligands

The isolation of stable carbenes based on imidazolium heterocycles (N-heterocyclic carbenes, NHCs) has attracted much attention over the last decades. Like group 13 diyls, the NHC class of ligand, **2**, E = C, have singlet lone pairs and act as strong σ-donors towards a wide range of s, p and d-block metal fragments.[9-11] In NHC-transition metal complexes, the *p*-orbital at the carbene centre is not thought to engage in π-bonding with filled metal *d*-orbitals to any extent. This arises from a significant overlap of the nitrogen *p*-orbital lone pairs with the carbene *p*-orbital. The electronic and steric properties of NHCs have lent them to a variety of applications in synthesis and catalysis where they are often thought of as phosphine mimics. Considerable attention has also been paid to the heavier group 14 analogues of NHCs, **2**, E = Si, Ge or Sn, which in the case of the silicon and germanium heterocycles, have been used as ligands in the formation of an ever increasing number of complexes.[12, 13] In addition, several valence isoelectronic, cationic phosphorus and arsenic analogues of NHCs, **2**, E = P or As, have been reported.[14, 15] A small number of complexes derived from the cyclic phosphenium cations have come forward[16, 17] but no cyclic arsenium complexes have been structurally characterised to date. However, an anionic group 13 heterocycle, **2**, E = Ga, R = Bu^t, was only synthesised very recently.[18] Related to these compounds were the syntheses of the neutral 6-membered aluminium and gallium heterocycles, and their isoelectronic Ge analogue, **3**, E = Al, Ga or Ge.

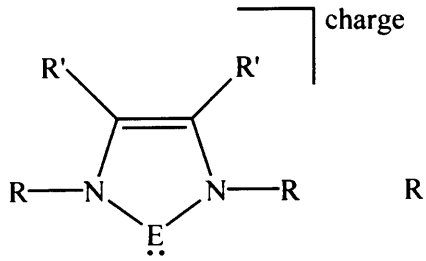

(2)

R and R' = alkyl, aryl or H

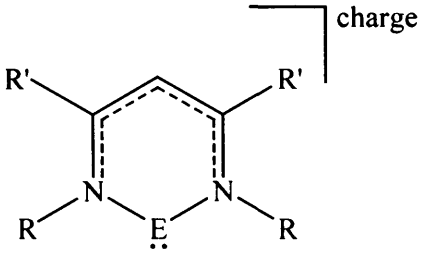

(3)

E = group 13 element, charge = -1
E = group 14 element, charge = 0
E = group 15 element, charge = +1

E = Al, Ga, In, charge = 0
E = Ge, charge = +1

3.3.1 Theoretical treatment of free group 13(I) heterocycles

Two papers regarding the structure and bonding of group 13 heterocycles valence isoelectronic to NHCs have appeared. Schoeller and his group has carried out DFT calculations on $[E\{N(H)C(H)\}_2]^-$, **4**, where E = B, Al, Ga and In.[19] In general, the stability of NHCs is dependent on the singlet-triplet energy separation whilst the anionic group 13 systems have an additional factor in that the electron affinity has to be large for stable anions to exist. It was found that the singlet-triplet energy gap was sizeable, indicating that the ground state is singlet for B - In. Additionally, the electron affinity (*i.e.* the tendency for the heterocycle to retain its negative charge) is much higher for the heavier homologues compared to boron. A further calculation focussed on the 1,2-hydrogen shifted structure whereby one of the hydrogens on the nitrogen has migrated to E. For E = B the hydrogen shifted structure has the lowest energy, whilst heterocycles with E = Al or Ga were higher in energy compared to the carbenic structure. Finally, the electron distribution within the heterocycles was analysed using NBO calculations. These showed that for boron there is a non-bonding *sp*-type lone pair at the element whilst for Al and Ga this becomes less directional and there is increasing *p*-electron density at the nitrogens. The E—N bond order is almost 1 for boron but almost 1/2 for Al, Ga and In. These calculations suggest that for E = Al - In the structure can be formulated as a donor-acceptor interaction of E^+ and a chelating diamido unit, which is due to the electropositive elements releasing their formal negative charge to the more electronegative nitrogen atoms.

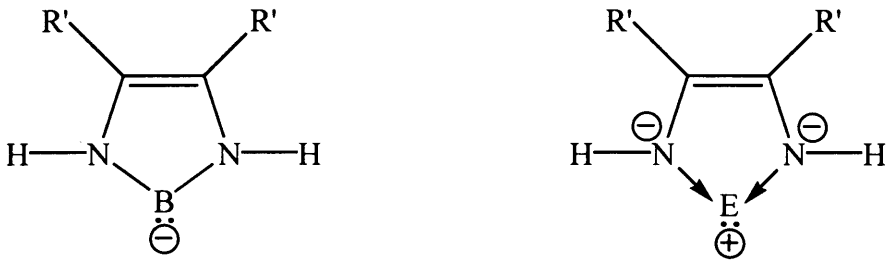

(4)

E = Al, Ga or In

Similar results have been obtained using *ab initio* calculations on the borane and alane anions.[20] Whilst the calculated geometries match those of Schoeller *et al*, these results also include a treatment of the stabilising effect of delocalisation onto the diazabutadiene backbone. It was found that there is appreciable aromatic stabilisation, with E = B having a greater aromatic ring current than E = Al. However, normal N-heterocyclic carbenes have more aromatic stabilisation, at the same level of theory. Finally, a molecular orbital treatment found that the empty orbital on boron is fully incorporated into the delocalised π system, whereas for Al there is little overlap and the HOMOs of both the B and Al are the lone pair at the group 13 centre.

In an extension to their work, the group of Schoeller has investigated the stabilisation of anionic group 13 and neutral group 14 carbene analogues using the diphosphabutadiene ligand (HPCH=CHPH).[21] Using the same methodology as for the diazabutadiene ligand systems, it was found that the P—E bond in $[E\{P(H)C(H)\}_2]^{-1 \text{ or } 0}$, E = group 13 or 14 element, becomes more covalent due to the lower electronegativity of phosphorus compared to nitrogen. For the group 13 homologues, the singlet ground state is stabilised more by the lighter elements, and the electron affinities are larger than those calculated for the DAB ligand. Therefore, compounds of this type should experimentally be accessible but no examples are known yet.

The neutral 6-membered group 13(I) heterocycles $[\{HC(CHNH)_2\}E]$ (E = B, Al, Ga, In) have also been the subject of DFT calculations[22]. Their calculated geometries compare favourably with those of the experimental Al and Ga heterocycles. Also found is that for E = Al – In, the metal carries a partial positive charge and the N—E bonds have a substantial ionic character, whilst when E = B the boron carries a negative charge and has much more covalent B—N bonds. Electron Localisation Function calculations were also carried out to visualise

the lone pair on the group 13 centre, and these showed that there are indeed directional electron pairs on all the group 13 centres and also that the N—E bonds are polar for E = Al - In. The triplet-singlet energy gaps have been calculated and for boron the states are energetically close but for the higher homologues the gap is substantial (*ca.* 150 kJ mol^{-1}). From these calculations it was concluded that for E = Al – In, the best representation is a donor-acceptor structure between a anionic chelating ligand and a positively charged group 13 element in the +1 oxidation state. For the boron example, a diradical species is the best description with a B(II) centre, which implies that it would be too reactive to synthesise and isolate. This is in contrast to the results obtained on the anionic 5-membered heterocycles.

Finally, the reactivity of these compounds towards electron donating NH_3 and electron accepting BF_3 was investigated. It was found that for E = Al – In, the group 13 centre acts as a Lewis acid if the NH_3 approaches from above the plane, whilst a rearrangement occurs for boron. All compounds form compounds with BF_3 in the plane of the heterocyclic system, as expected. However, due to the increased *s*-character of the lone pair on descending the group, the Lewis base character at the metal is reduced and for Ga and especially indium the E—B donor-acceptor bond is much weaker.

The synthesis of $[:Ge\{N(Ar)C(Me)\}_2CH]^+$ has been reported. This is isoelectronic with the neutral gallium heterocycle and thus of relevance.[23] This compound was the subject of Hartree-Fock and DFT calculations, and the results showed that the HOMO is π-bonding with respect to the Ge—N and C—C, and antibonding with respect to the C—N bond. The lone pair is in the HOMO-1 orbital, whilst the LUMO includes the Ge 4*p* orbital. This is the same ordering of molecular orbitals found for the anionic 5-membered gallium carbene analogue, and suggests that both heterocycles should show similar bonding in their complexes.

3.3.2 Synthesis of anionic 5-membered group 13(I) heterocycles

The first and only report of the synthesis of an anionic gallium carbene analogue, prior to our work, appeared from the group of Schmidbaur as recently as 1999.[18] The synthesis is shown in Scheme 1.

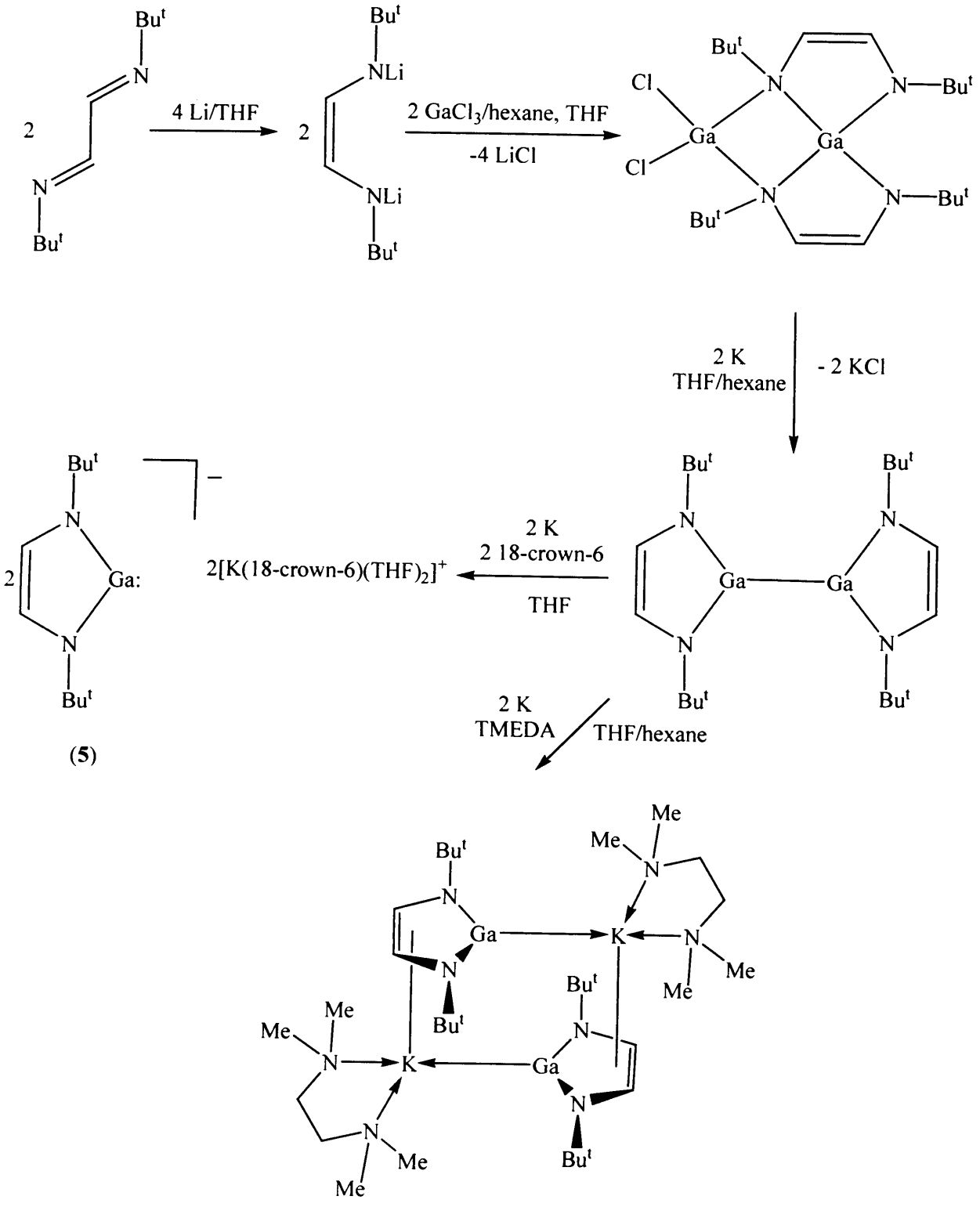
4 Li/THF
2 GaCl3/hexane, THF
-4 LiCl
2 K
THF/hexane
- 2 KCl
2 K
2 18-crown-6
THF
2[K(18-crown-6)(THF)2]+
2 K
TMEDA
THF/hexane

(5)

(6)

Scheme 1

Treatment of the dilithiated diazabutadiene ligand with $GaCl_3$ gives a chlorogalla-imidazole which can be reduced stepwise over 5 days with potassium and a crown ether to give the anionic heterocycle **5** in poor yield (3 %). If the reduction is carried out in the presence of TMEDA as a chelating agent, complex **6** can be isolated in 18 % yield after 14 days.[24] Both compounds were structurally characterised and compound **5** shows no cation-anion contacts, *i.e.* it contains a discrete 2 co-ordinate gallium centre where the oxidation state of the metal is +1. The heterocycle is virtually planar with a N—Ga—N angle of 81.8(3)°, Ga—N bond length of 1.985(6) Å and C—C bond length of 1.380(6) Å. These metric parameters compare favourably with those calculated for both $[\{(H)C(Bu^t)N\}_2Ga]^-$ and $[\{(H)C(H)N\}_2Ga]^-$ [19] (Ga—N 2.041, 1.983 Å; N—C 1.390, 1.388 Å; C—C 1.368, 1.368 Å, respectively). Moreover, the experimentally determined values suggest partial ring delocalisation so that aromaticity effects are small but not negligible, as predicted by previous theory.[20] Complex **6** was shown to be dimeric in the solid state and can be considered as consisting of monomeric units which comprise a gallium 'carbene' heterocycle η^5-co-ordinated to a K(TMEDA) fragment. An intermolecular interaction of the gallium lone pairs with two potassiums aggregates these monomeric units into centrosymmetric dimers. The dimensions within the heterocycle are similar to those found in compound **5**, whilst the Ga—K bond lengths are 3.468(1) Å for the intramolecular η^5-K interaction and 3.438(1) Å for the intermolecular contact. A line connecting the ring plane of the C_2N_2Ga and K forms an angle of only 20.8° indicating that the lone pair of electrons at the gallium atom is orientated towards the potassium counterion. Other than this complex, there is no known co-ordination chemistry derived from the anionic heterocycle, **5**.

3.3.3 Synthesis of neutral 6-membered group 13(I) heterocycles

The synthesis of neutral 6-memebred aluminium(I)[25], gallium(I)[26] and indium(I)[27] heterocycles derived from the β-diketiminate ligand $HC(CMeNAr)_2^-$ (Ar = 2,6-diisopropylphenyl) have been reported and their synthesis is shown in Scheme 2.

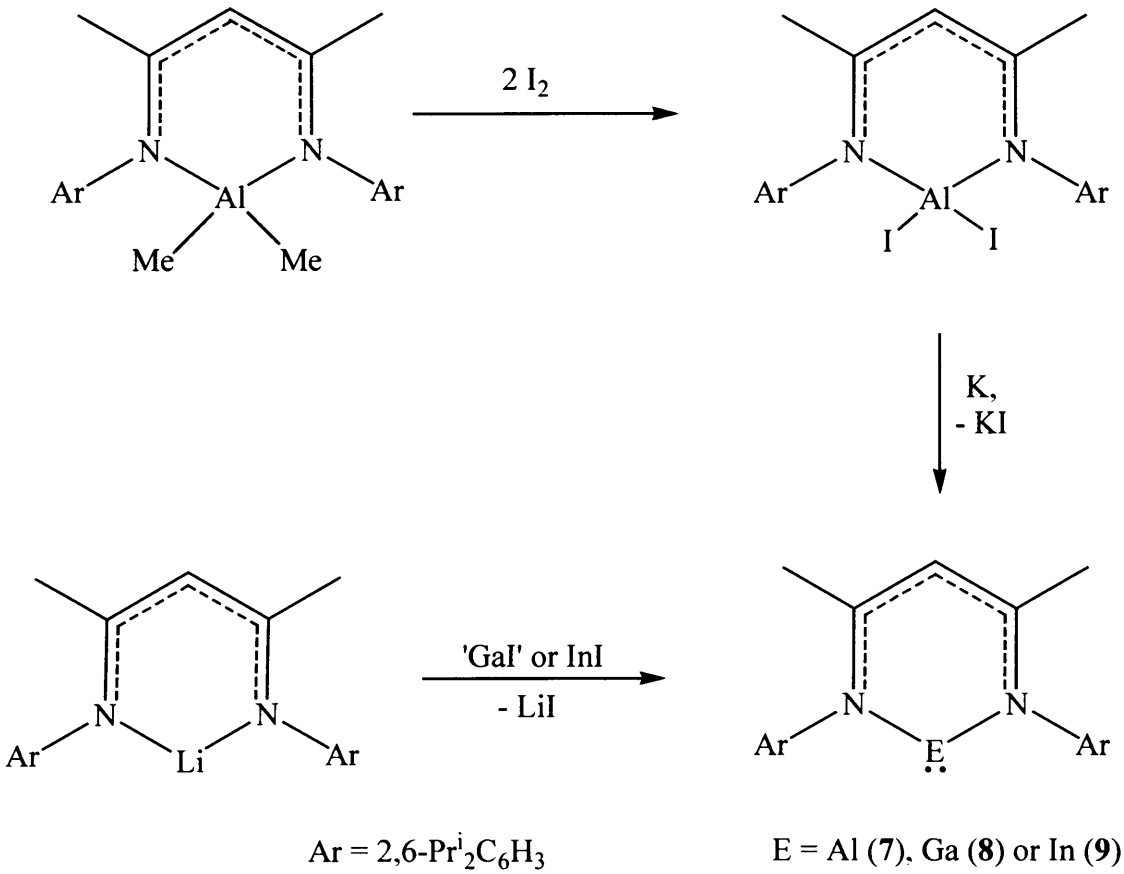

Scheme 2

Reaction of [{HC(CMeNAr)$_2$}AlMe$_2$] with I_2 gives the corresponding diiodide in good yield. This can be reduced with potassium over 3 days to give **7** in 21% yield. A crystal structure determination shows well-separated monomeric units with the first example of a two co-ordinate aluminium centre. The Al—N bond length [1.957(2) Å] is longer and the N—Al—N angle [89.86(8)°] is more acute than seen in the parent complex [{HC(CMeNAr)$_2$}AlMe$_2$] [1.922 Å average and 96.18(9)°, respectively]. This can be explained by the larger covalent radius of the Al(I) centre in **7**, two 3*p*-orbitals of which are involved in bonding to the two nitrogen atoms, leaving a non-bonded lone pair of electrons at the aluminium centre. This bonding view has been confirmed by *ab initio* calculations. Analysis of the Laplacian of electronic density in the plane of the ligand shows clearly the presence of a lone pair localised on the metal and outside the heterocycle in a quasi-trigonal-planar geometry. The authors argue that the electrons originating from an s^2 configuration of the Al^I centre are stereochemically active, leading to an *sp*-like hybrid. The aluminium atom

can be considered as acting as both a Lewis acid in its interaction with the nitrogen atoms of the ligand and potentially as a Lewis base with its lone pair of electrons.

The synthesis of both, the gallium, **8**, (39 %) and the indium, **9**, (36 %, photolabile) ring systems involve salt elimination reactions between the β-diketiminate anion and the appropriate metal(I) iodide (Scheme 2). It is noteworthy that a previous attempt to prepare **9**, by this method but using InCl was not successful.[28] In contrast to the aluminium congener which decomposes above 150 °C, **8** is much more stable and decomposes at 202 - 204 °C. The molecular structure of **8** shows it to be isostructural to **7**. The Ga—N bond lengths [2.054(2) Å average] are longer than those commonly observed in three co-ordinate trivalent complexes and the N—Ga—N angle is nearly perpendicular [87.56(6)°], indicating that the bonding situation can be considered as a Ga^+ ion chelated by a monoanionic $[(NArCMe)_2CH]^-$ ligand. DFT calculations on a model compound show that the HOMO corresponds to the gallium lone pair, whilst the unoccupied *p* orbital is the LUMO +1. The energy difference between these orbitals is calculated to be *ca.* 110 kcal mol^{-1} indicating that this complex will be a good σ donor but poor π acceptor. Calculations on the aluminum analogue show that the HOMO-LUMO+1 separation is *ca.* 12 kcal mol^{-1} less than the gallium species which is due primarily to the higher energy of the aluminium lone pair.[29]

3.3.4 Reactions of neutral 6-membered group 13(I) carbene analogues with transition metal precursors

The only reaction reported for the 6 membered neutral carbene analogues is that of $[Ga\{N(Ar)C(Me)\}_2CH]$ with $Fe(CO)_5$ to form the compound $[Fe(CO)_4\{Ga[N(Ar)C(Me)]_2CH\}]$, **10**.[30] The isolation of this neutral species enabled the influence of the co-ordination of the gallium to be examined. Not surprisingly, it has been found that the Fe—Ga bond in **10** is longer than in related gallium diyl complexes containing 2 co-ordinate Ga centres.[4] The Ga—N bond lengths in **10** shorten on complexation with respect to the free heterocycle, due to loss of electron density from gallium giving a greater δ+ charge at Ga and hence more ionic Ga—N bonds. Moreover, the CO stretching frequencies of this compound suggest negligible π back-bonding between the Fe and Ga centres.

3.3.5 Reactions of neutral group 13(I) carbene analogues with main group metal precursors

Whilst there has been only one reported example of a transition metal complex derived from the neutral 6-membered carbene analogues, their main group chemistry has been more extensively investigated. The only example of a group 13 compound of the neutral gallium carbene analogue **8** is its donor-acceptor complex with $B(C_6F_5)_3$, **11**.[31] This compound has been used to gauge the strength of the donor-acceptor interactions in other low valent group 13 donor compounds, by comparing degrees of distortion from trigonal planar to tetrahedral geometries at the boron centres. The results obtained from this study show that the order of increasing Lewis basicity is Cp*Ga < $GaAr^{\#}$ < Cp*Al < Ar'GaGaAr' ≈ GaAr* < **8** ($Ar^{\#}$ = C_6H_3-2,6-(Bu^tDipp)$_2$; Ar' = C_6H_3-2,6-$Dipp_2$; Ar* = C_6H_3-2,6-$Trip_2$; Dipp = 2,6-diisopropylphenyl; Trip = 2,4,6-triisopropylphenyl). The carbene analogue **8** is presumably a better Lewis base due to the increased electron density at the gallium centre provided by the ligand and the increased co-ordination number at the metal centre.[30] An additional structural feature of **11** is the considerable shortening of the Ga—N bonds compared to **8** [1.942(6) Å and 2.054(2) Å average], again due to loss of charge from the gallium centre. There are no NHC carbene analogues to compare to this but the silicon analogue $[(F_5C_6)_3B\leftarrow Si\{N(Bu^t)C(H)\}_2]$ is known, though not structurally characterised.[32]

The reactivity of **7** towards alkynes was investigated, as reactive NHCs are known to undergo [2+1] cycloadditions with alkynes. Surprisingly, compound **7** has been found to be unreactive towards [2+1] cycloadditions with alkynes but the aluminacyclopropenes expected from these reactions, $[\{C(R)=C(R)\}Al\{[N(Ar)C(Me)]_2CH\}]$, R = $SiMe_3$, Ph *etc.*, can alternatively be prepared in one pot potassium reductions of mixtures of an appropriate alkyne and $[I_2Al\{[N(Ar)C(Me)]_2CH\}]$.[33] It is belived that the aluminacyclopropenes are not formed *via* an *in situ* formation of the Al(I) heterocycle, **7**, but instead a radical process is involved. The aluminacyclopropenes are currently finding synthetic utility in a number of reactions.[34]

One of the interesting applications of these group 13 carbene analogues is that given their steric bulk and good donor ability they could be used as precursors to compounds containing multiple bonds to the group 13 centre. This has been exemplified by the reactions of both **7** and **8** with azides (Scheme 3).

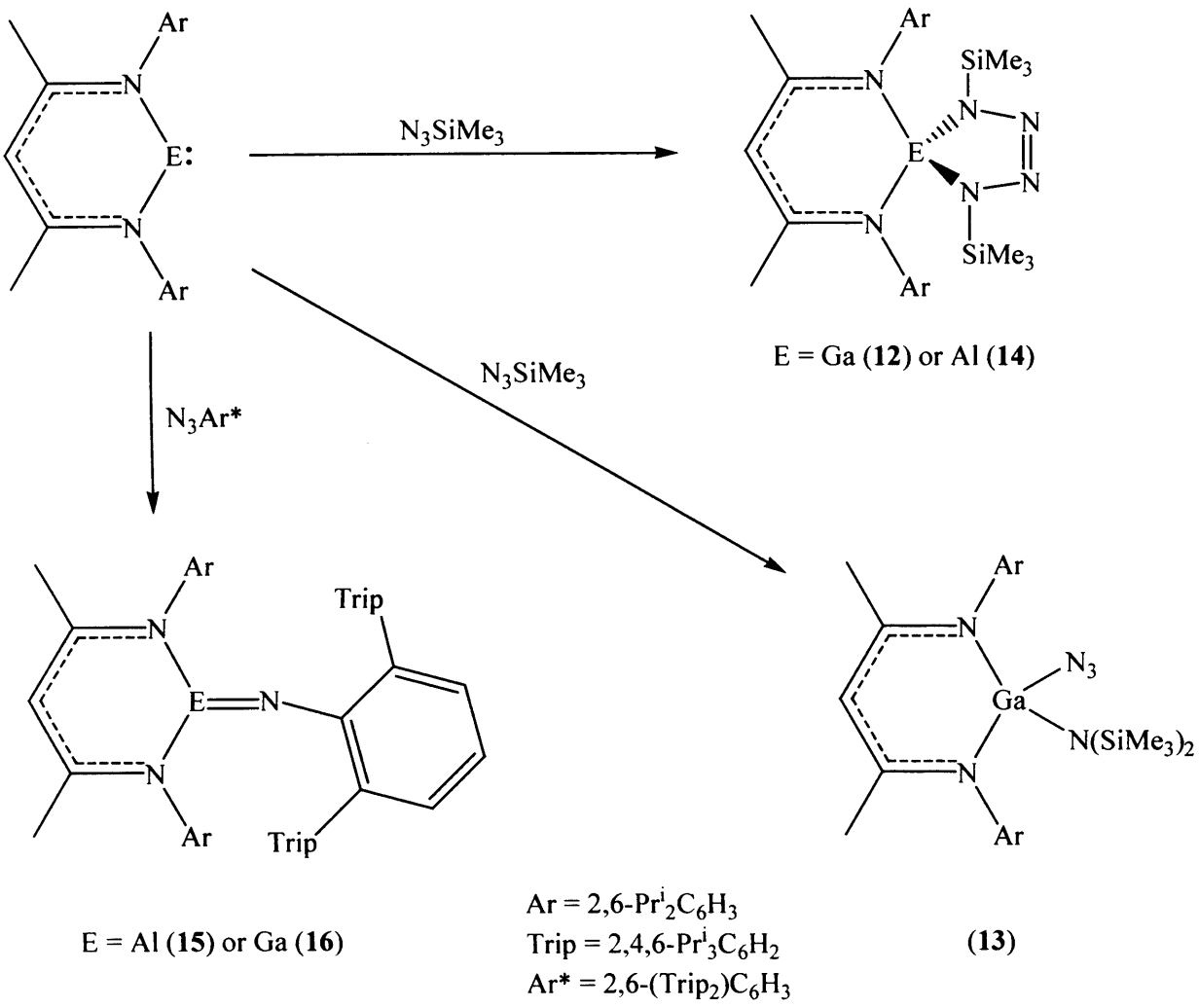

Scheme 3

Compound **8** reacts with Me_3SiN_3 in a 1:2 ratio to give a tetrazole (**12**) or amide/azide adduct (**13**) in 19 % and 54 % yields respectively, presumably *via* an imide intermediate.[35] When **7** is treated with Me_3SiN_3 the analogous tetrazole (**14**) is also isolated (58 %).[34] However, the first monomeric imide of the heavier group 13 elements was isolated by treatment of **7** or **8** with the very bulky azide, N_3-Ar*.[36] Compounds **12** and **14** are the first structurally characterised examples of cyclic tetrazoles. They both feature planar EN_4 rings and the E—N bond lengths in the tetrazole fragment are shorter than the E—N bonds in **7** and **8**. The isolation of tetrazole-amide/azide isomers is unique and can be rationalised by the steric protection afforded by the β-diketiminate ligand which prevents dimerisation of the Ga=N intermediate, but allows further reactivity with the much less hindered N_3SiMe_3. The

preference for the amide/azide isomer in gallium chemistry contrasts with that of aluminium where only the tetrazole isomer has been observed. The monomeric imides **15** and **16** were isolated in 52 % and 74 % yield respectively. ^{1}H- and ^{13}C-NMR spectroscopy show that there is restricted rotation around the Ga—N bond, indicating a Ga—N π bond from overlap of gallium and nitrogen *p* orbitals. Only **16** has been structurally characterised and the structural features confirm multiple bonding between Ga and N. The Ga—N imide bond length is shorter than any other Ga—N bond and the imide nitrogen has a bent geometry consistent with a stereochemically active lone pair. To further examine the multiple bond nature in this compound, restricted Hartree-Fock calculations were performed on the model complex, [HN=Ga{[N(H)C(H)]$_2$CH}]. The calculated optimum Ga—N imido nitrogen bond length compares very favourably to that observed in the structure of **16** whilst the energy difference between planar and perpendicular Ga—N—H orientations both support the view of the presence of a weak π-bond. Therefore, the calculations and structural studies point towards a strong σ-donation by the gallium to the nitrogen and weaker π back donation from nitrogen to gallium. It should also be noted that the silicon carbene, [:Si{N(Bu^{t})C(H)}$_2$], reacts with organic azides in a similar manner and related azide/amide and tetrazole complexes have been isolated.[37, 38]

The isolation of aluminium and gallium carbene analogues acting as good σ-donor ligands is unusual in group 13 chemistry, where these metals more commonly act as Lewis acids in their complexes. Similarly, there have been examples of typical Lewis bases (*e.g.* phosphines[39] or amines[40]) being observed to demonstrate Lewis acceptor behaviour. The combination of these two compound types has been investigated and an example of a co-ordination chemistry Umpolung has been established in the reaction of **8** with [Ph$_3$P—PPh$_2$][SO$_3$CF$_3$] to give **17** in 69 % yield (Scheme 4).[39] In this example, the Ga—N bond lengths are slightly shorter compared to **8**. The other structural feature of note is the Ga—O bond length which is significantly shorter than the P—O distance, thus indicating a preference for Ga—O covalency and avoiding co-ordinative unsaturation at the gallium, *i.e.* not an ion separate salt.

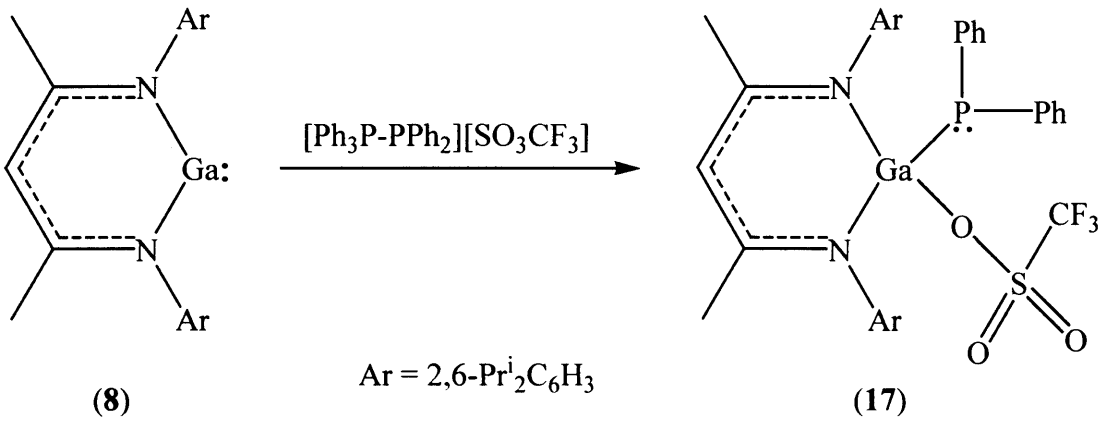

(8) Ar = 2,6-$Pr^i_2C_6H_3$ (17)

Scheme 4

The reactivity of **8** towards N_2O or S_8 has also been investigated. In both reactions dimeric compounds with Ga_2O_2 or Ga_2S_2 cores were isolated and structurally characterised (Scheme 5).[41] For the sulfur example, the Ga—S bonds are normal for single bonded interactions. The Ga—S—Ga angle is more acute compared to the Ga—O—Ga angle, which is due to the relative reluctance of the sulfur atom to hybridise in its complexes.

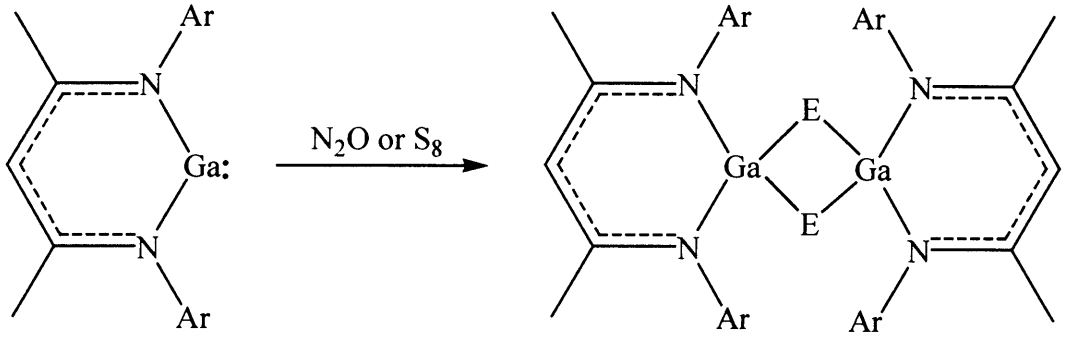

(8) Ar = 2,6-$Pr^i_2C_6H_3$
E = O or S

Scheme 5

3.4 Research Proposal

Much interest has been paid to diazabutadiene-group 13 complexes over the last 15 years and many complex types have arisen from this work. Some of the more interesting compounds that have come forward are the paramagnetic gallium(III) complex, [(Bu^t-DAB)$_2$Ga],[42] the diamagnetic gallium(II) complex, [{(Bu^t-DAB)Ga}$_2$],[18] the gallium(II) complex, [{(Ar-DAB)Ga}$_2$],[43] and the remarkable anionic gallium(I) heterocycle, **5**,[18] which is a valence isoelectronic N-heterocyclic carbene (NHC) analogue. This anion has been obtained in an uncoordinated state (*i.e.* there is no Ga:→K co-ordination) as its potassium salt, [:Ga{N(Bu^t)C_2H_2N(Bu^t)}][K(18-crown-6)(THF)$_2$],[18] and as a dimeric potassium complex, **6**.[24]

One aim of the current work was to attempt the formation of indium analogues of **5**. In this respect, the first example of a two co-ordinate, neutral, 6-membered indium(I) singlet carbene analogue has recently been reported in the literature.[27] Another aim of this study was the investigation of the reactivity of diazabutadienes towards 'GaI' and AlI_3/Al mixtures, and the attempted preparation of a new anionic gallium(I) and aluminium(I) NHC analogues. If this could be achieved it was proposed in later studies to investigate the co-ordination chemistry of the anionic group 13 carbene analogues and compare it to both NHCs, group 13 diyls, :MR, and neutral 6-membered group 13 metal(I) heterocycles.

3.5 Results and Discussion

3.5.1 Reactivity of indium(I) halides toward diazabutadienes

The 3:2 reaction of Ar-DAB [$(ArN{=}CH)_2$, Ar = 2,6-$Pr^i_2C_6H_3$] with InCl afforded the paramagnetic In(II) complex, **18** (decomp. 84 – 87 °C) in low yield (12 %) after crystallisation from DME (Scheme 6). Presumably, the compound is formed by a mechanism involving [$^{\bullet}$InCl(Ar-DAB$^{\bullet}$)] as intermediate, where the Ar-DAB ligand is singly reduced by the metal centre prior to dimer formation. Interestingly, significant indium metal deposition was seen in the reaction that gave **18** but this does not arise from the disproportionation of this compound as it is indefinitely stable in solution at room temperature.

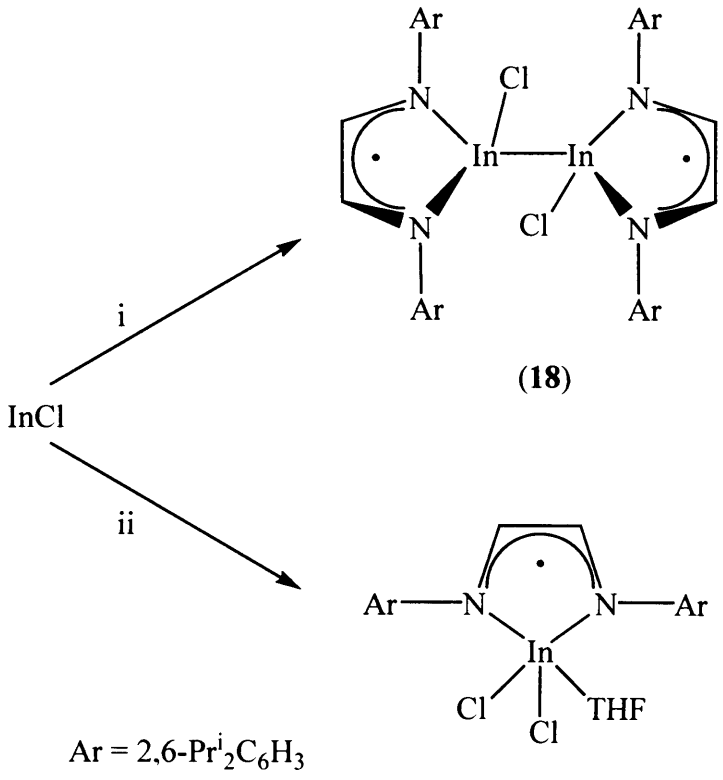

Scheme 6 Reagents and conditions: i, Ar-DAB, DME; ii, Ar-DABLi$_2$, THF, -LiCl, -In.

It is worth noting here that **18** is notionally related to the gallium(II) complex, [{(Bu^t-DAB)Ga}$_2$],[18] though that compound is halide free, diamagnetic and possesses doubly reduced diazabutadiene ligands.

The paramagnetic nature of **18** meant only the NMR spectroscopic data corresponding to a molecule of Ar-DAB that co-crystallises with **18** could be observed. The Raman spectrum of **18**, however, displays a band at 179 cm^{-1}, which is consistent with previously reported In—In stretching modes in compounds of the type [$In_2X_2(L)_2$], X = Br or Cl.[44] The X-band EPR spectrum of **18** was obtained and satisfactorily simulated (Figure 1) using an isotropic g value of g_{iso} = 2.0012, and hyperfine splittings to two equivalent proton (a_{iso} = 0.5 mT) and nitrogen (a_{iso} = 0.5 mT) centres. These g and a_{iso} values are comparable to those reported for similar diazabutadiene anion radicals.[45] In addition, a splitting arising from an electron interaction with the In nucleus was observed [a_{iso} = 2.62 mT for ^{115}In (95.7 % abundant) and a_{iso} = 2.61 mT for ^{113}In (4.3 % abundant)].

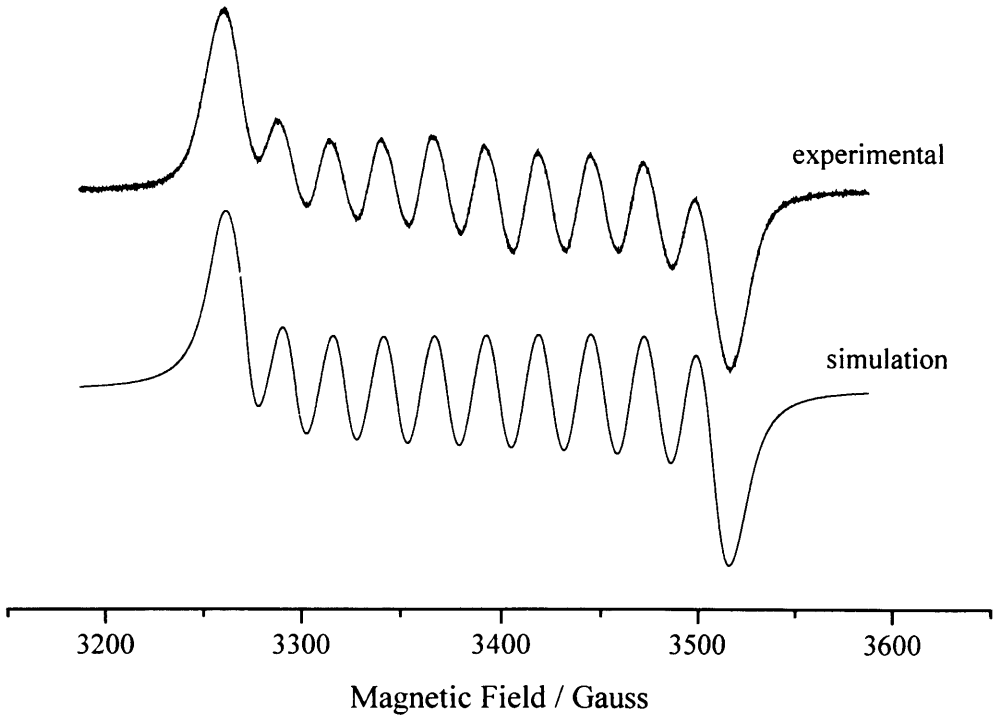

Figure 1 X-band EPR spectrum and computer simulation of [{(Ar-DAB$^•$)InCl}$_2$] (**18**) in DME at 298 K.

The magnitude of these splittings confirms that the unpaired electron is largely delocalised over the NCCN fragment with negligible spin density (0.36 %) on the indium centre and therefore it can be concluded that the oxidation state of the indium centres is +2.

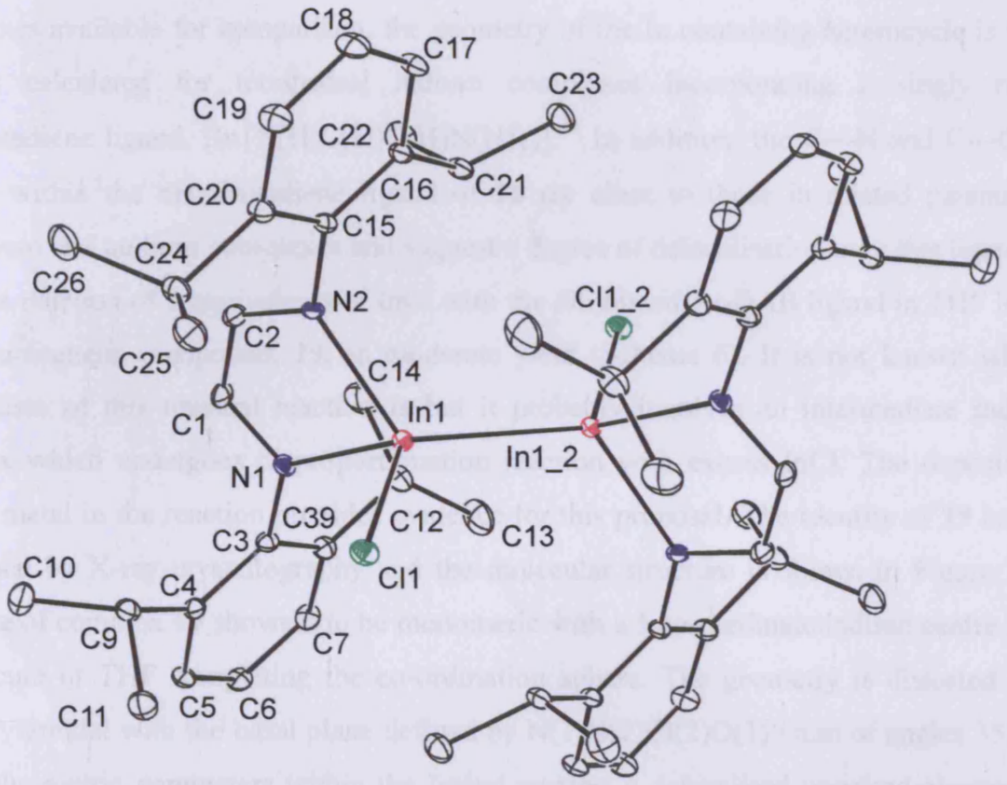

Figure 2 Molecular structure of [{(Ar-DAB$^{\bullet}$)InCl}$_2$] (**18**)

Selected bond lengths (Å) and angles (°): In(1)—N(1) 2.167(2), In(1)—N(2) 2.169(3), In(1)—Cl(1) 2.4094(9), In(1)—In(1_2) 2.7280(9), N(1)—C(1) 1.317(4), N(1)—C(3) 1.442(4), N(2)—C(2) 1.329(4), N(2)—C(15) 1.447(3), N(1)—In(1)—N(2) 78.71(9), N(1)—In(1)—Cl(1) 104.18(7), N(2)—In(1)—Cl(1) 103.98(7), N(1)—In(1)—In(1_2) 121.30(7), N(2)—In(1)—In(1_2) 122.18(7), Cl(1)—In(1)—In(1_2) 118.79(3), C(1)—N(1)—In(1) 110.50(19), C(2)—N(2)—In(1) 109.98(19), N(1)—C(1)—C(2) 120.4(3), N(2)—C(2)—C(1) 120.4(3).

The molecular structure of **18** is shown in Figure 2. Compound **18** co-crystallises with a molecule of Ar-DAB that has no interaction with it. Its structure possesses distorted tetrahedral indium centres with an In—In distance of 2.7280(9) Å, which is close to those in related compounds, *e.g.* 2.745 Å in $[In_2I_4(PPr^i_3)_2]$,[46] and the In—Cl distances are in the normal range. Although there are no structurally characterised diazabutadiene-indium complexes available for comparison, the geometry of the In containing heterocycle is similar to that calculated for tetrahedral indium complexes incorporating a singly reduced diazabutadiene ligand, $[In\{N(H)C(H)C(H)N(H)\}_2]$.[47] In addition, the C—N and C—C bond lengths within the diazabutadiene ligand of **18** are close to those in related paramagnetic aluminium and gallium complexes and suggest a degree of delocalisation over this ligand.[47]

The reaction of 2 equivalents of InCl with the dilithiated Ar-DAB ligand in THF leads to the paramagnetic compound, **19**, in moderate yield (Scheme 6). It is not known what the mechanism of this unusual reaction is but it probably involves an intermediate indium(I) complex which undergoes disproportionation reaction with excess InCl. The deposition of indium metal in the reaction provides evidence for this proposal. The identity of **19** has been confirmed by X-ray crystallography and the molecular structure is shown in Figure 3. The structure of complex **19** shows it to be monomeric with a 5 co-cordinate indium centre having a molecule of THF completing the co-ordination sphere. The geometry is distorted square based pyramidal with the basal plane defined by N(1)N(2)Cl(2)O(1) (sum of angles 352.56°), whilst the metric parameters within the ligand suggest a delocalised unpaired electron. The In—N bond lengths of 2.193 Å (average) are shorter than that seen in the complex $[InBr_3$(Ar-DAB)] (Chapter 2), [2.323(13) Å average], but similar to that seen in **18** [2.168(2) Å average], in line with expectations.

Again, the paramagnetic nature of **19** meant no meaningful NMR spectroscopic data could be obtained for this compound. The X-band EPR spectrum of **19** was obtained and simulated using an isotropic g value of g_{iso} = 2.0012, and hyperfine splittings to two equivalent proton (a_{iso} = 0.5 mT) and nitrogen (a_{iso} = 0.5 mT) centres. These g and a_{iso} values are comparable to those for complex **18**. The X-band EPR spectrum and the computer simulation of **19** are very similar to that of compound **18** and are shown in Figure 4. In addition, a splitting arising from an electron interaction with the In nucleus was also observed [a_{iso} = 2.61 mT for ^{115}In and a_{iso} = 2.61 mT for ^{113}In]. In both complexes, **18** and **19**, the g values are close to free spin, indicating the organic nature of the radical.

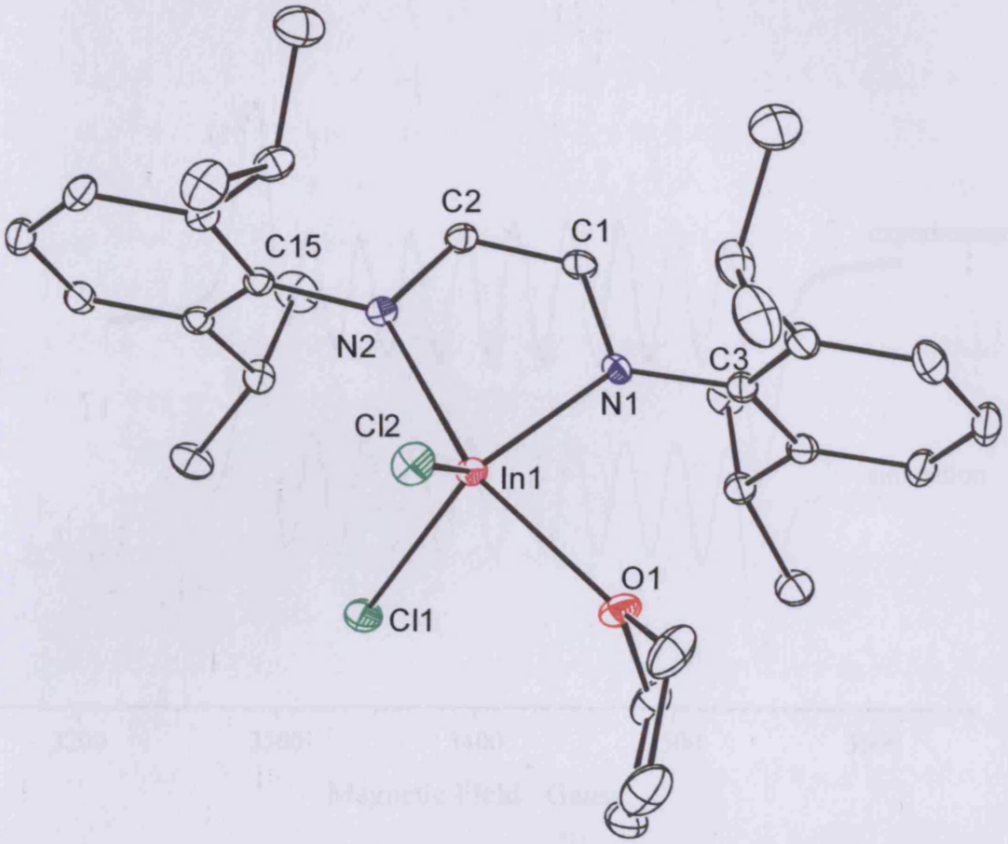

Figure 3 Molecular structure of $[InCl_2(THF)(Ar\text{-}DAB^{\bullet})]$ (**19**)

Selected bond lengths (Å) and angles (°): In(1)—N(1) 2.157(4), In(1)—N(2) 2.230(4), In(1)—O(1) 2.290(4), In(1)—Cl(1) 2.3646(15), In(1)—Cl(2) 2.3627(17), N(1)—C(1) 1.341(7), C(1)—C(2) 1.384(8), N(2)—C(2) 1.321(7), N(1)—In(1)—N(2) 77.01(16), N(1)—In(1)—O(1) 83.41(16), N(1)—In(1)—Cl(1) 127.39(12), N(1)—In(1)—Cl(2) 120.68(12), N(2)—In(1)—O(1) 160.25(15), N(2)—In(1)—Cl(1) 99.78(12), N(2)—In(1)—Cl(2) 101.47(12), Cl(1)—In(1)—Cl(2) 111.50(6), Cl(1)—In(1)—O(1) 88.98(12), Cl(2)—In(1)—O(1) 90.67(11).

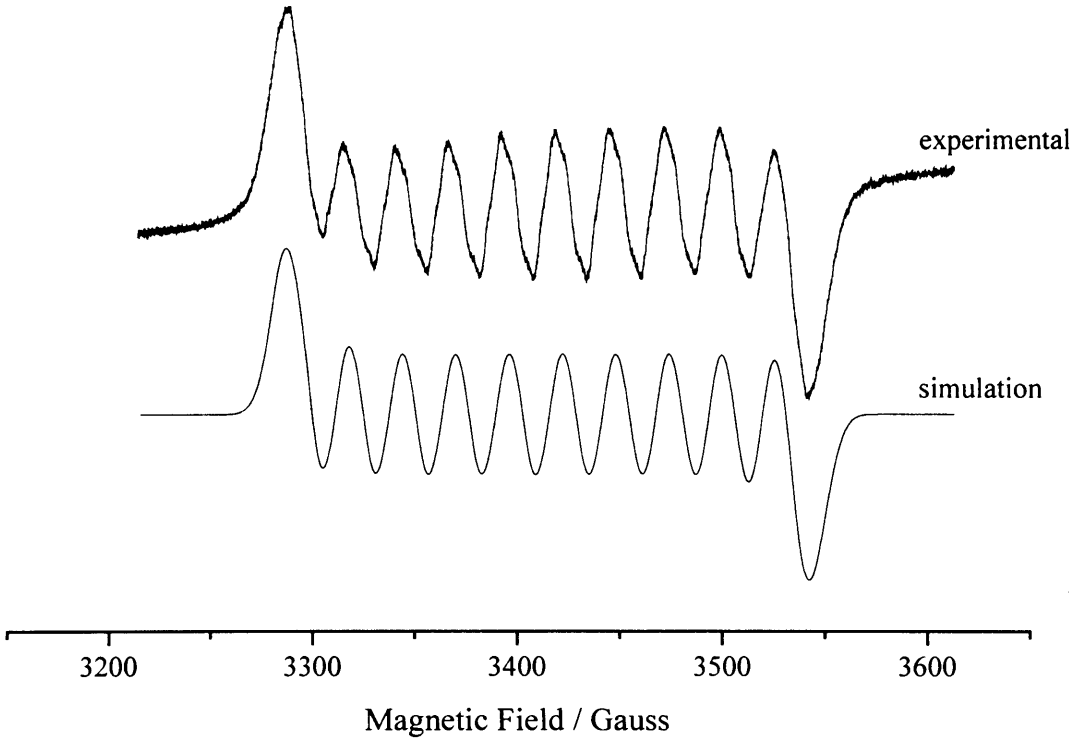

Figure 4 X-band EPR spectrum and computer simulation of $[InCl_2(THF)(Ar\text{-}DAB^{\bullet})]$ (**19**) in DME at 298 K.

Attempts were made to reduce **18** and **19** to yield an anionic indium(I) carbene analogue related to **5**, using alkali metals, *e.g.* Na or K, in THF. However, only decomposition products were isolated.

3.5.2 Reactivity of 'GaI' and AlI_3/Al toward diazabutadienes

Considering the unexpected formation of **18** from the reaction of Ar-DAB with InCl it was decided to investigate the analogous reactions of diazabutadienes with 'GaI'. When the reaction of 'GaI' with Ar-DAB was carried out in a 2:1 stoichiometry in toluene at low temperature, gallium metal deposition occurred and a deep red solution resulted which upon work-up afforded a high yield (> 90 %) of the paramagnetic gallium(III) complex, **20** (Scheme 7). Since carrying out this work Jutzi *et al* have reported[43] a similar preparation of this compound, the spectroscopic and crystallographic data for which were found to be identical to **20**. The formation of **20** contrasts with the analogous reaction that gave **18**. Despite this, the yield of **18** was low (12 %) and considerable indium deposition was seen in this reaction which presumably arose from the formation of an indium analogue of **20** as the major product in that reaction, *i.e.* **19**.

Compound **20** crystallises in the space group *Pnma* (Figure 5). The molecular structure is symmetric with respect to a mirror plane through the gallium and two iodine atoms. The gallium iodine distances are normal at 2.5189 Å (average) and the GaN_2C_2 fragment is planar within experimental error. The nitrogen atoms adopt slightly distorted trigonal planar geometries, whilst the gallium atom has a distorted tetrahedral geometry. The bond lengths within the Ar-DAB fragment are comparable to those found for the singly reduced DAB unit in $[(Bu^t\text{-DAB})_2Ga]$.[42]

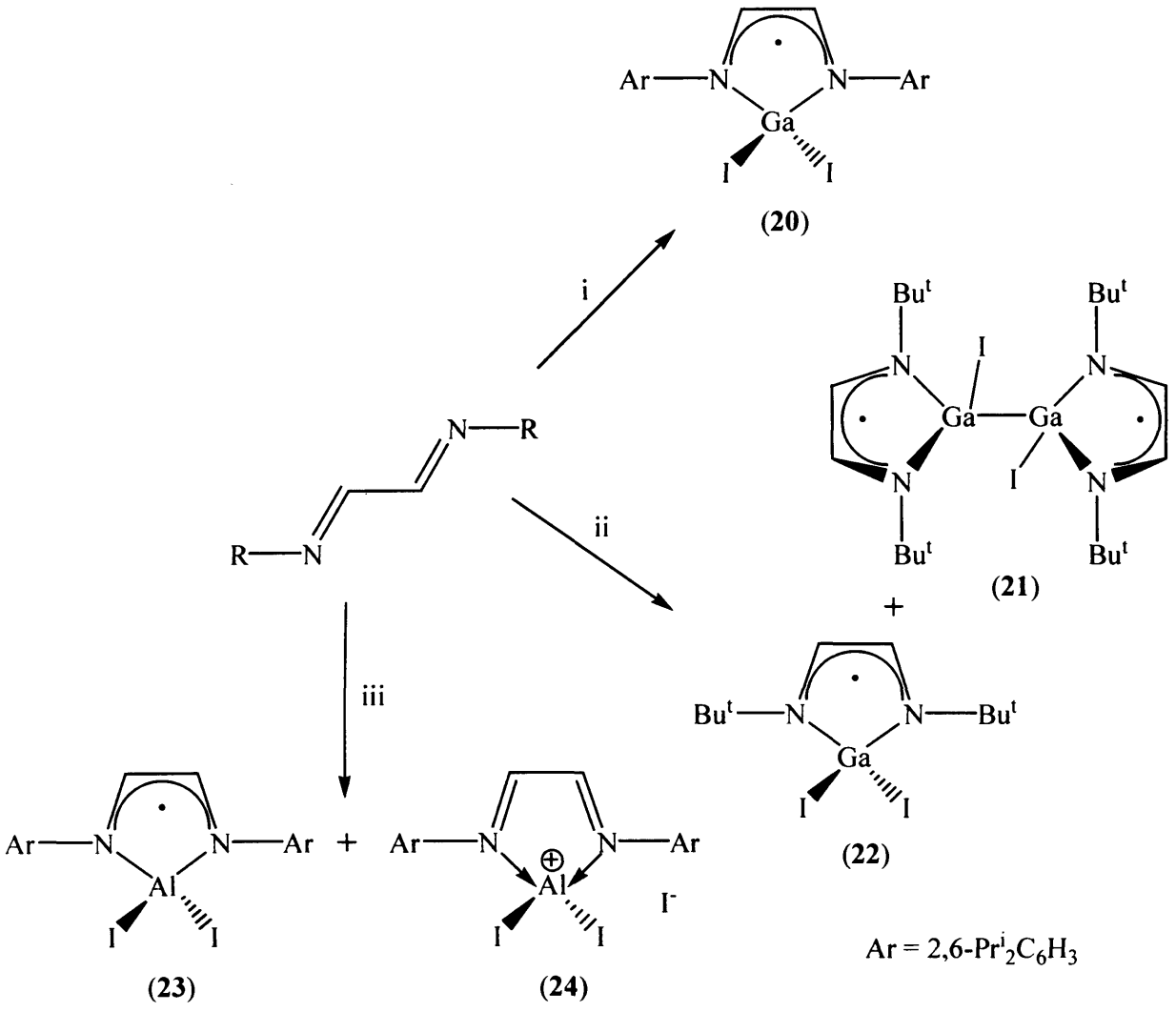

Scheme 7 Reagents and conditions: i, 'GaI', -Ga, toluene, R = Ar; ii, 'GaI', -Ga, toluene, R = Bu^t; iii, AlI_3/Al, toluene, R = Ar.

The paramagnetic nature of **20** meant no meaningful NMR spectroscopic data could be obtained for the compound. The room temperature X-band EPR spectrum of **20** was obtained and the isotropic g value measured to be g_{iso} = 2.0038. The spectrum was found to not be resolved due to overlapping couplings of the unpaired electron with ^{1}H, ^{14}N, ^{69}Ga, ^{71}Ga and ^{127}I nuclei.

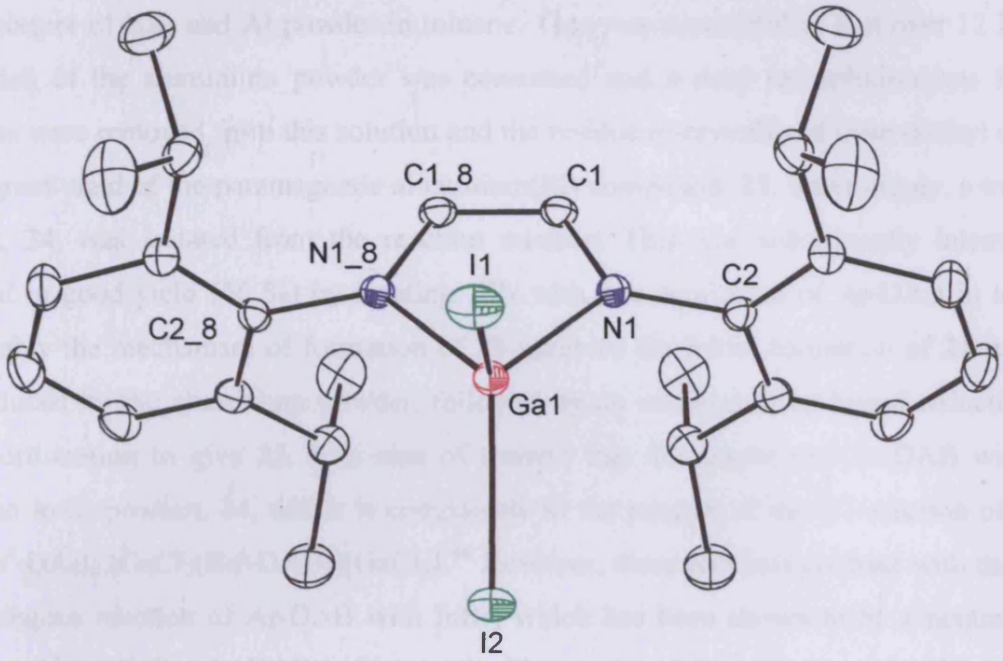

Figure 5 Molecular structure of [GaI_2(Ar-DAB$^{\bullet}$)] (**20**)

Selected bond lengths (Å) and angles (°): Ga(1)—I(1) 2.535(55), Ga(1)—I(2) 2.496(45), Ga(1)—N(1) 1.944(32), N(1)—C(1) 1.335(74), C(1)—C(1_8) 1.380(21), N(1)—Ga(1)—N(1_8) 85.76(56), N(1)—Ga(1)—I(1) 111.70(2), N(1)—Ga(1)—I(2) 116.80(7), I(1)—Ga(1)—N(2) 111.61(3), C(1)—N(1)—Ga(1) 108.32(6), N(1)—C(1)—C(1_8) 118.30(2).

In contrast to the reactions that gave **18** and **20**, the 1:1 or 1:2 reactions of Bu^t-DAB, [(Bu^{t}N=CH)$_2$], with 'GaI' in toluene yielded predominantly the dimeric complex, **21**, but also small amounts of the monomeric species, **22**. It is interesting that the dimeric gallium(II) species is the major product in this reaction whereas in the analogous Ar-DAB reaction the monomeric gallium(III) compound, **20**, is in the majority. An explanation for this behaviour may be given by the steric differences between the two diazabutadiene ligands. When the presumed intermediate, [$^{\bullet}$GaI(R-DAB$^{\bullet}$)], is formed, it dimerises with small R-groups but for larger R-groups (R = Bu^t or 2,6-Pr$^i_2$C$_6$H$_3$) disproportionation is favoured which leads to a monomeric species.

An attempt was made to prepare the aluminium analogue of **20** by reacting Ar-DAB with a 1:2 mixture of AlI_3 and Al powder in toluene. This was successful in that over 12 hours a proportion of the aluminium powder was consumed and a deep red solution was formed. Volatiles were removed from this solution and the residue re-crystallised from diethyl ether to give a good yield of the paramagnetic aluminium(III) compound, **23**. Interestingly, a trace by-product, **24**, was isolated from the reaction mixture. This was subsequently intentionally prepared in good yield (66 %) by reacting AlI_3 with one equivalent of Ar-DAB in toluene. Presumably the mechanism of formation of **23** involves the initial formation of **24** which is then reduced by the aluminium powder, followed by an intramolecular ligand reduction and disproportionation to give **23**. It is also of interest that the reaction of Ar-DAB with AlI_3 yields an ionic product, **24**, which is comparable to the product of the 2:1 reaction of $GaCl_3$ with Bu^t-DAB, $[GaCl_2(Bu^t\text{-DAB})][GaCl_4]$.[48] However, these products contrast with that from the analogous reaction of Ar-DAB with $InBr_3$ which has been shown to be a neutral 5 co-ordinate adduct, $[InBr_3(Ar\text{-DAB})]$ (Chapter 2). The results of these reactions are also different to that from the reaction of BCl_3 with Ar-DAB which leads to chloroboration of the diimine and formation of [BCl{ArNC(H)(Cl)C(H)(Cl)NAr}].[49]

No meaningful NMR data could be obtained on compounds **21-23** due to their paramagnetic nature but all other spectroscopic data pointed towards their formulations. The ionic compound, **24**, is not paramagnetic but its ^{1}H-NMR spectrum showed significantly broadened signals. It is thought, that this is due to an exchange of iodide ligands at the aluminium centre on the NMR time scale which could proceed *via* a 5 co-ordinate neutral intermediate, $[AlI_3(Ar\text{-DAB})]$. This proposal seems feasible in light of the fact that the indium analogue of this compound, $[InBr_3(Ar\text{-DAB})]$, is neutral and 5 co-ordinate in the solid state (Chapter 2). The ^{1}H-NMR spectrum of **24** could not be resolved when solutions of the compound were heated to 70 °C or cooled to 0 °C. Further cooling of solutions of **24** led to significant precipitation of the compound. Despite the broadening of the signals in the ^{1}H-NMR spectrum of **24** the data suggest that the Ar-DAB ligand is acting as a localised Lewis base because the protons on the diimine backbone of the ligand resonate near those of the free ligand and the neutral indium compound, $[InBr_3(Ar\text{-DAB})]$, but significantly downfield from the imine protons in related systems incorporating reduced diazabutadiene ligands, *e.g.* $[\{(Bu^t\text{-DAB})Ga\}_2]$[18], **5** and **6**.

Table 1 Isotropic *g* and hyperfine coupling values for complexes **20**, **21**, **22**, **23**, obtained from simulation of their room temperature EPR spectra.

Complex	g_{iso}	M[a]	^{1}H[b]	^{14}N[b]	^{127}I[c]
20	2.0036	^{69}Ga & ^{71}Ga ~ 2.5	~ 0.5	~ 0.5	
21	2.00385	^{69}Ga = 0.12 ^{71}Ga = 0.155	0.14	0.84	0.13
22	2.0038	^{69}Ga = 0.13 ^{71}Ga = 0.165	0.14	0.862	0.13
23	2.0038	^{27}Al = 0.285	0.595	0.675	0.038

All isotropic hyperfine couplings in mT. [a] M refers to gallium or aluminium. [b] ^{1}H refers to two equivalent imine protons and ^{14}N refers to the two equivalent nitrogen nuclei. [c] Two equivalent iodine nuclei simulated in **21** and **23**, but only one in **22**.

The EPR spectra of **21-23** were recorded at X-band frequencies. The spectrum and associated computer simulation for **21** are shown in Figure 6. This spectrum was particularly well resolved, allowing accurate spin Hamiltonian parameters to be obtained (Table 1). Similar spin Hamiltonian parameters were used to simulate the spectrum of **22** (with only one interacting ^{127}I nucleus) indicating the similarity of the radical fragment in both cases. In both gallium complexes, **21** and **22**, the spin density on the $^{69, 71}Ga$ nuclei was very small (0.03 %) and negligible on the ^{127}I nuclei (0.008 %). Nevertheless, without this contribution from the ^{127}I nuclei an accurate simulation could not be obtained. The hyperfine couplings to the imine protons (0.14 mT) and nitrogen nuclei (*ca.* 0.85 mT) of **21** and **22** were found to be different compared to the aluminium complex, **23**, and the previously discussed complex, **18**, where a_{iso} values close to 0.5 mT were observed (see Table 1). The spectrum and computer simulation for **23** is shown in Figure 7. It is noteworthy that compound **20** shows similar couplings of *ca.* 0.50 mT and *ca.* 0.50 mT for the protons and nitrogen nuclei respectively. Therefore, it seems that the presence of the *tert*-butyl groups in **21** and **22** have a significantly different influence on the spin density around the imine protons and nitrogen nuclei, compared to the influence on the aryl groups in **18**, **20** and **23**. This influence by the *tert*-butyl groups on the electron spin density is also manifested in the hyperfine couplings to the metal

centres, which was found to be 0.03 % in **21** and **22**, but *ca.* 0.3 % in **18** and **23**. *Tert*-butyl groups, however, are more electron donating than aryl groups and this may explain the different observations in the EPR measurements. In all complexes, **20-23**, the *g* values are close to free spin, indicating the essentially organic nature of the radical.

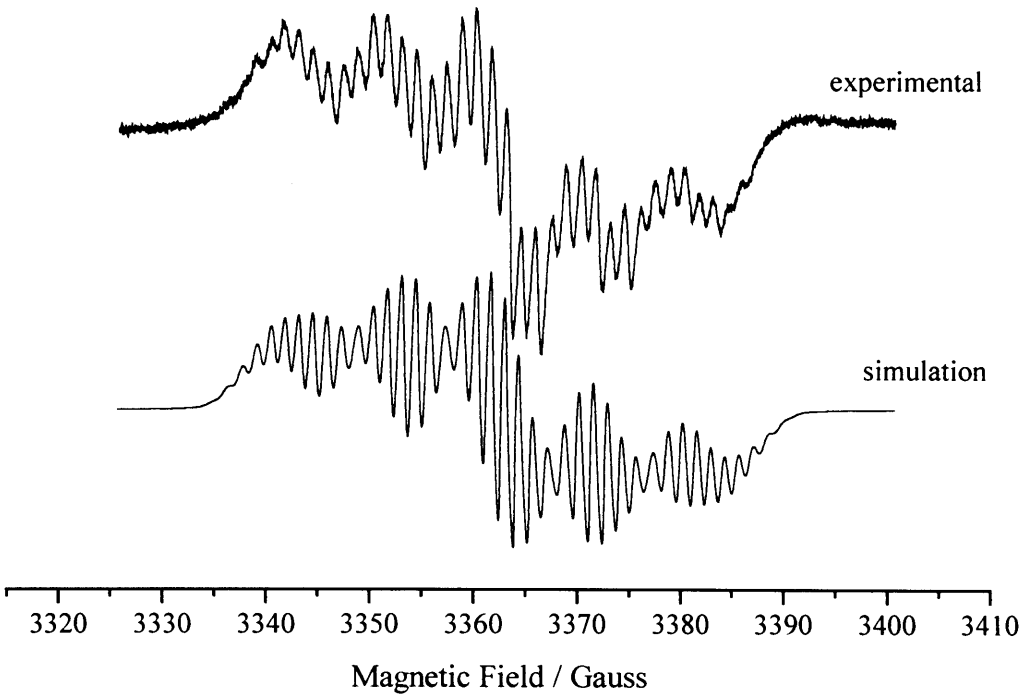

Figure 6 X-band EPR spectrum and computer simulation of [{(Bu^t-DAB$^\bullet$)GaI}$_2$] (**21**) in CD_2Cl_2/C_7D_8 (50 : 50) at 298 K.

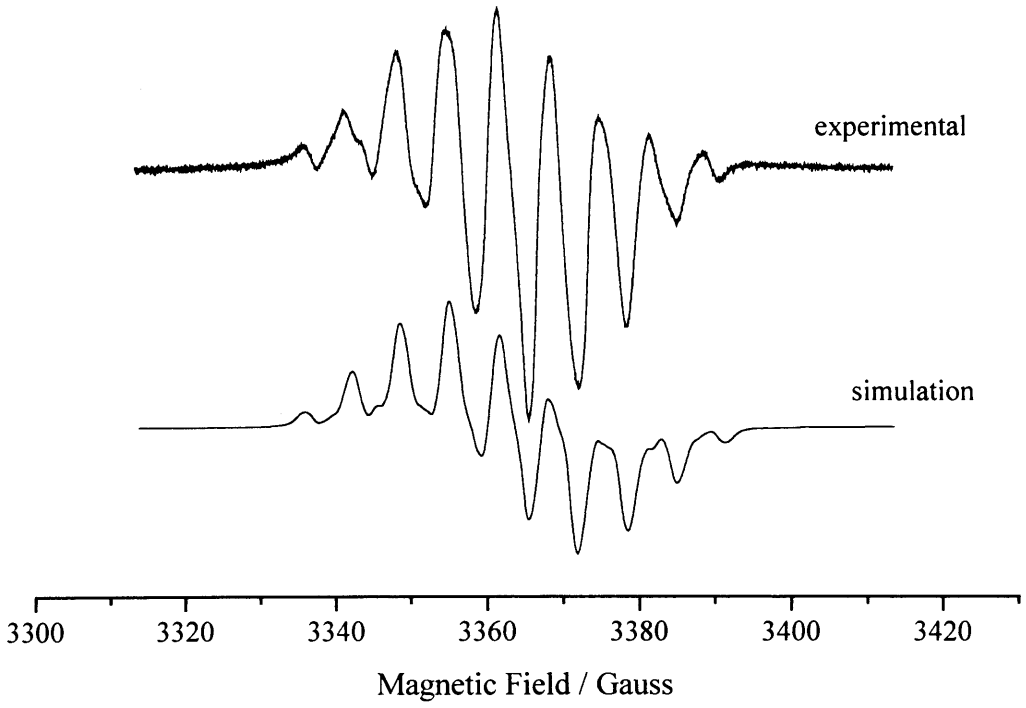

Figure 7 X-band EPR spectrum and computer simulation of [(Ar-DAB$^{\bullet}$)AlI_2] (**23**) in CD_2Cl_2/C_7D_8 (50 : 50) at 298 K.

The X-ray crystal structures of all compounds **21-24** were obtained and are depicted in Figures 8-11. The dimeric gallium compound, **21**, is closely related to **18** and as in that compound the bond lengths within the diazabutadiene framework show the ligand to be delocalised. The gallium centres possess distorted tetrahedral geometries and the N—Ga bond lengths and the N—Ga—N angles are close to those in **20**. Similarly, the Ga—Ga distance of 2.4232(7) Å compares well with the metal—metal interaction in related diazabutadiene complexes, e.g. [{(Bu^t-DAB)Ga}$_2$][18] [2.333(1) Å].

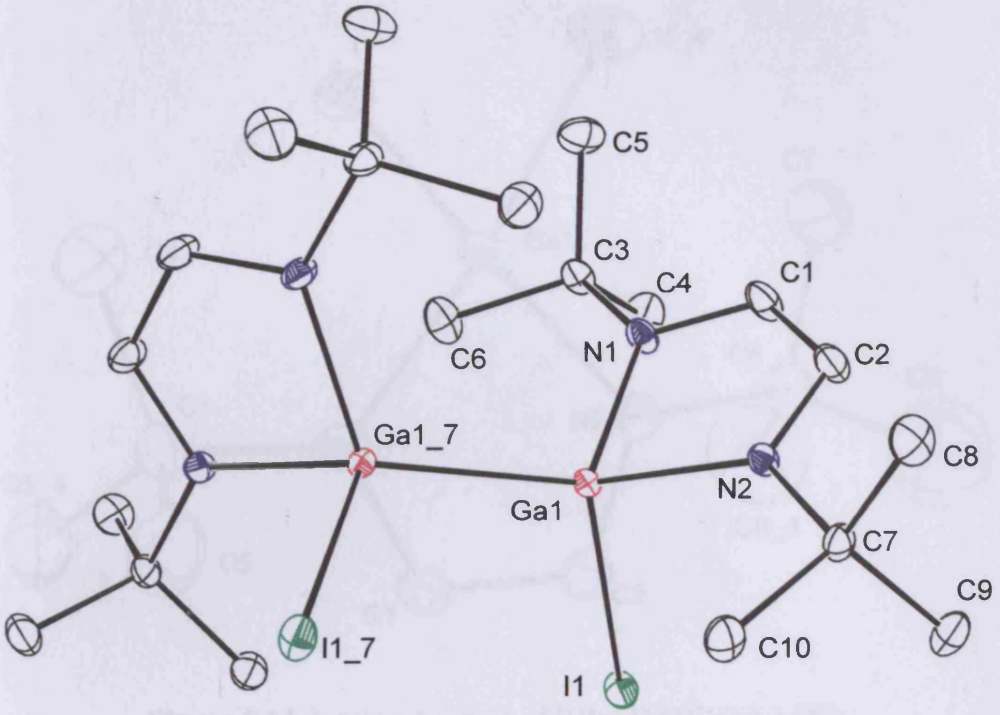

Figure 8 Molecular structure of [{(Bu^t-DAB$^\bullet$)GaI}$_2$] (**21**)

Selected bond lengths (Å) and angles (°): Ga(1)—Ga(1_7) 2.4232(7), Ga(1)—I(1) 2.6169(5), Ga(1)—N(2) 1.958(3), Ga(1)—N(1) 1.966(3), N(1)—C(1) 1.322(4), N(2)—C(2) 1.333(4), C(1)—C(2) 1.395(5), N(2)—Ga(1)—N(1) 85.23(11), N(2)—Ga(1)—Ga(1_7) 124.87(8), N(1)—Ga(1)—Ga(1_7) 116.26(9), N(2)—Ga(1)—I(1) 103.47(8), N(1)—Ga(1)—I(1) 107.33(9), I(1)—Ga(1)—Ga(1_7) 115.153(14), C(1)—N(1)—Ga(1) 108.8(2), C(2)—N(2)—Ga(1) 109.0(2), N(1)—C(2)—C(2) 118.7(3), N(2)—C(2)—C(1) 118.0(3).

Compound **22** is similar to **20** in that it is monomeric and its gallium centre has a distorted tetrahedral geometry. The Ga—N bond lengths [1.930 Å average] are close to those in **20** [1.9449(10) Å], as are the backbone C—N and C—C distances [**22**: 1.336 Å average, 1.450(11) Å; **20**: 1.3386(15) Å, 1.406(2) Å]. Both sets of values are comparable to those observed in the singly reduced Bu^t-DAB ligand in the related Ga(III) compound, [(Bu^t-DAB)$_2$Ga],[42] and are strongly suggestive of delocalised diazabutadiene ligand systems.

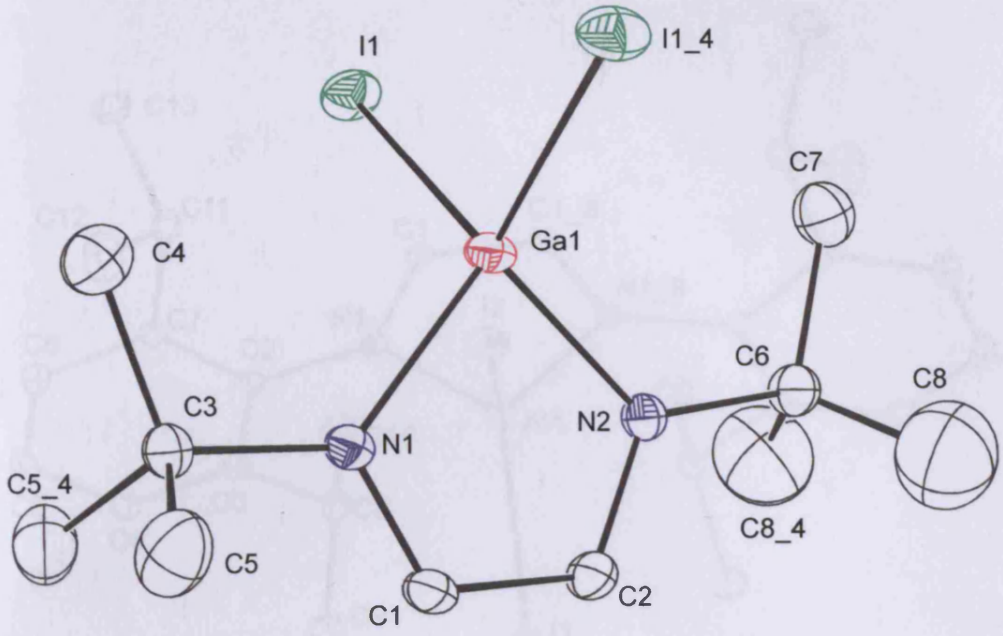

Figure 9 Molecular structure of [(Bu^t-DAB$^•$)GaI_2] (**22**)

Selected bond lengths (Å) and angles (°): I(1)—Ga(1) 2.5312(7), Ga(1)—N(2) 1.896(6), Ga(1)—N(1) 1.965(6), N(1)—C(1) 1.316(10), N(2)—C(2) 1.357(10), C(1)—C(2) 1.450(11), N(1)—Ga(1)—N(2) 87.1(3), N(2)—Ga(1)—I(1) 115.89(8), N(1)—Ga(1)—I(1) 113.66(9), I(1)—Ga(1)—I(1_4) 109.33(4), C(1)—N(1)—Ga(1) 108.3(5), C(2)—N(2)—Ga(1) 110.8(5), N(1)—C(1)—C(2) 118.6(7), N(2)—C(2)—C(1) 115.2(7).

The paramagnetic aluminium(III) compound, **23**, is isomorphous to **20** and both compounds have similar geometries and bond lengths about their metal centres, which is not surprising given the almost equivalent covalent radii for the two metals involved.[50] In addition, the bond lengths within the diazabutadiene ligand in **23** are indicative of a similar degree of delocalisation as possessed by **20**. There appears to be more localised N—C and C—C bonds for the Ar-DAB ligand in the cation **24** compared to **23**, despite their structural similarities. This is evidenced by the shorter N—C and longer C—C and Al—N distances in the former which is consistent with its formulation as a diamagnetic Ar-DAB adduct of the AlI_2^+ cation.

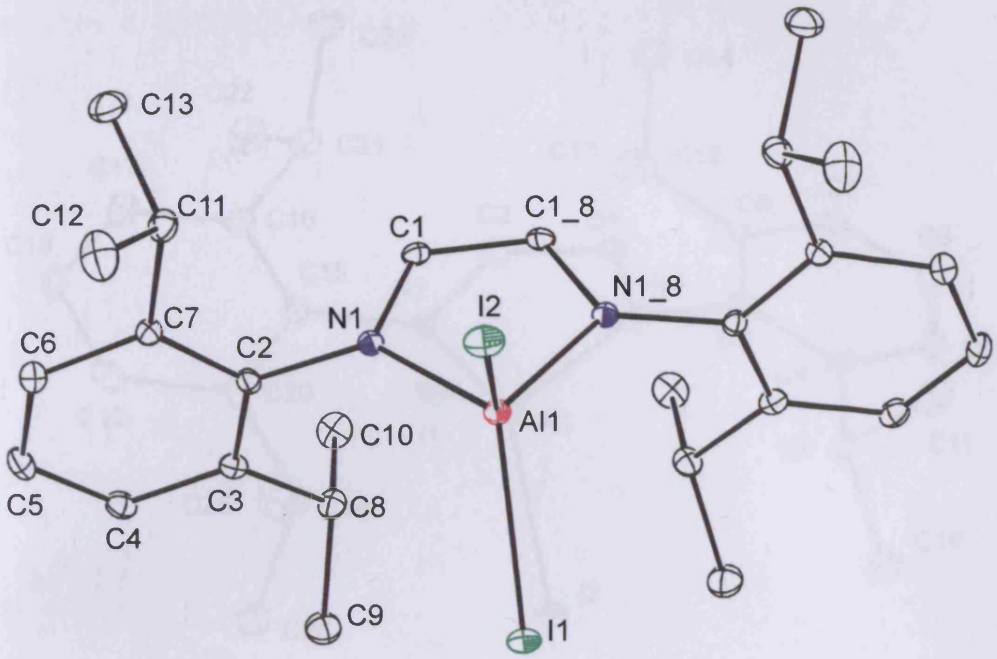

Figure 10 Molecular structure of [(Ar-DAB$^{\bullet}$)AlI$_2$] (**23**)

Selected bond lengths (Å) and angles (°): Al(1)—I(1) 2.4957(11), Al(1)—I(2) 2.5318(11), Al(1)—N(1) 1.889(2), N(1)—C(1) 1.337(3), C(1)—C(1_8) 1.409(5), N(1)—Al(1)—N(1_8) 87.42(13), N(1)—Al(1)—I(1) 116.50(7), N(1)—Al(1)—I(2) 111.93(7), I(1)—Al(1)—I(2) 110.78(4), C(1)—N(1)—Al(1) 108.93(17), N(1)—C(1)—C(1_8) 116.71(14).

Compounds **20** and **23** seemed to be ideally suited as precursors to the group 13 valence isoelectronic NHC analogues, [:M(Ar-DAB)]$^-$, M = Ga or Al, *via* reduction reactions. To date the only known example of such an anion is **5** which is prepared in a multi-step low yield synthesis (see **3.3.2**). Unfortunately the reduction of **23** with an excess of potassium metal in THF did not lead to the Al(I) carbene analogue. In all reduction attempts decomposition products which included the free Ar-DAB ligand and elemental aluminium were observed.

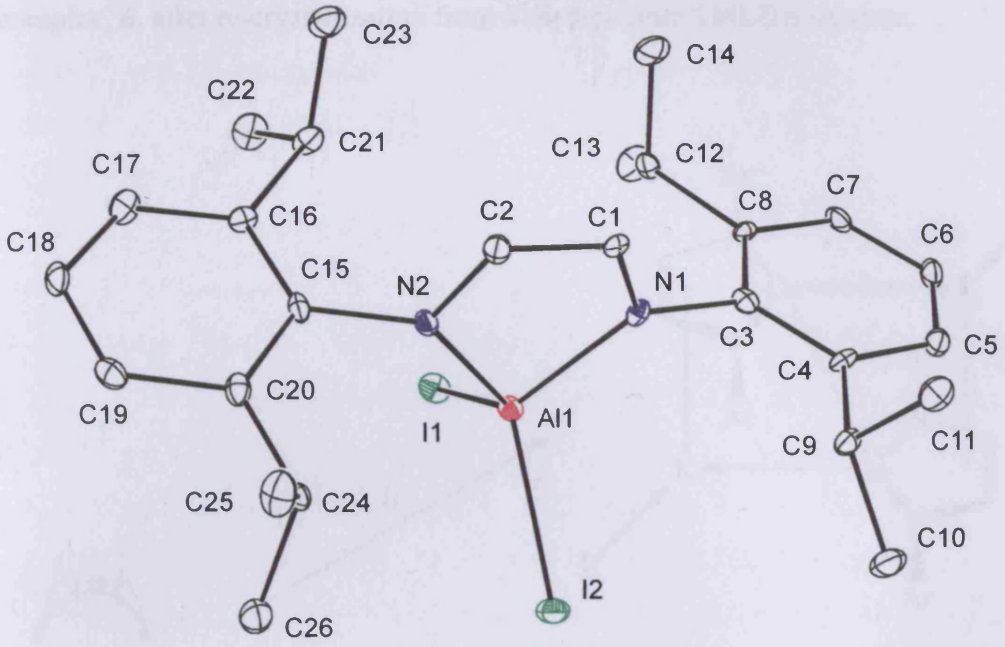

Figure 11 Structure of the cationic component of [(Ar-DAB)AlI_2]I (**24**)

Selected bond lengths (Å) and angles (°): Al(1)—I(1) 2.491(3), Al(1)—I(2) 2.487(3), Al(1)—N(2) 1.903(8), Al(1)—N(1) 1.933(8), N(1)—C(1) 1.289(11), N(2)—C(2) 1.325(12), C(1)—C(2) 1.442(13), N(2)—Al(1)—N(1) 85.7(3), N(2)—Al(1)—I(2) 116.4(3), N(1)—Al(1)—I(2) 110.7(2), N(2)—Al(1)—I(1) 112.8(3), N(1)—Al(1)—I(1) 116.8(3), I(2)—Al(1)—I(1) 112.12(11), C(1)—N(1)—Al(1) 109.9(6), C(2)—N(2)—Al(1) 110.7(6), N(1)—C(1)—C(2) 117.7(8), N(2)—C(2)—C(1) 115.4(9).

3.5.3 Preparation of a new anionic gallium(I) carbene analogue

The analogous reduction of **20**, using potassium metal in THF, was however, more successful than the reduction reactions of **18**, **19** and **23**. After 8 hours reaction time at room temperature and subsequent re-crystallisation from hexane the new gallium(I) carbene analougue, **25**, was formed in good yield (Scheme 8). Unfortunately, the quality of the crystals of **25** were not suitable for X-ray crystallographic studies. Re-crystallisation of **25** from diethyl ether gave **26**, also in a high yield. In a similar fashion the reduction of the

dimeric gallium(II) compound, **21**, with an excess of potassium led to a high yield of the known complex, **6**, after re-crystallisation from a diethyl ether/TMEDA mixture.

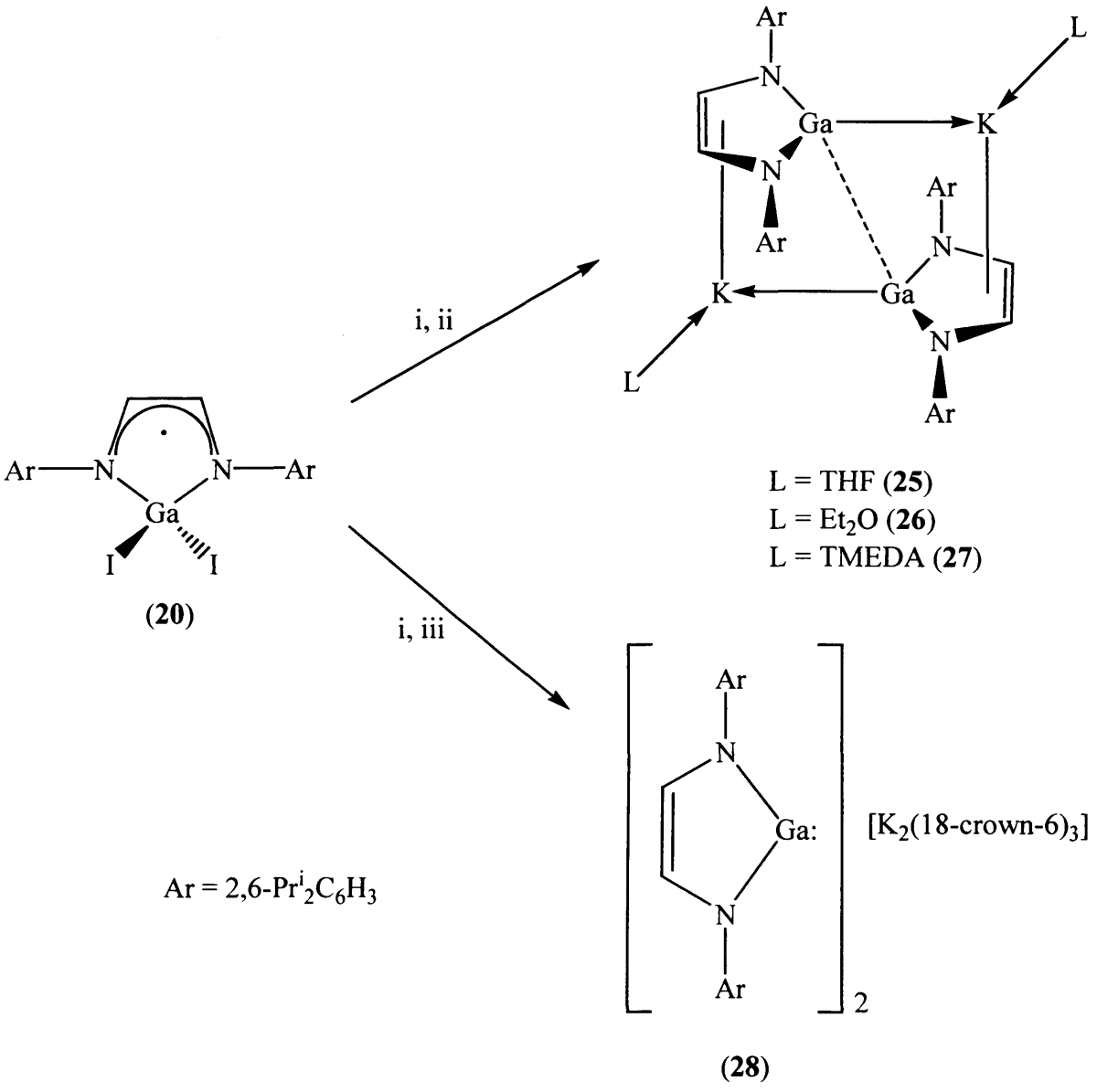

Scheme 8 Reagents and conditions: i, K, -KI, THF; ii, hexane, Et_2O or TMEDA/Et_2O; iii, 18-crown-6.

The spectroscopic data for **25** and **26** are consistent with their proposed structures and are indicative of a 1:1 ratio of potassium and co-ordinated THF or Et_2O, respectively. As in the case of **5** the ^1H and ^{13}C resonances for the olefinic fragment of the Ar-DAB backbone are significantly shifted to higher field relative to those for the free ligand, as would be expected in a reduced anionic system.

The molecular structure of **26** is depicted in Figure 12. This shows the molecule to be dimeric and to sit on a centre of inversion. It can be considered as consisting of monomeric units which comprise a gallium 'carbene' heterocycle η^5-co-ordinated to a $K(Et_2O)$ fragment. Dimerisation of these fragments occurs *via* intermolecular interactions of gallium lone pairs with two potassium centres. At first glance this seems to be a very similar arrangement to that seen for **6**. The geometries of the essentially planar gallium heterocycles in **6** and **26** are similar and close to that predicted by theoretical studies for the model heterocycle, $[:Ga\{N(H)C(H)C(H)N(H)\}]^-$.[19] In addition, the Ga→K distances in **6** [3.438(1) Å] and **26** [3.4223(10) Å], and the η^5-interactions from the heterocycles to the gallium centres are comparable [Ga→K 3.4681(5) Å **6**, 3.3784(13) Å **26**; K—N average 2.889 Å **6**, 2.962 Å **26**; K—C average 2.999 Å **6**, 2.997 Å **26**]. Despite these similarities there are also significant differences between **6** and **26**. For example, in **6** the Ga→K bond forms an angle of 20.8° with the C_2N_2Ga ring plane whereas in **26** this angle is only 3.4°. This in turn means that the distances between the Ga centres in **6** is 4.21 Å and the heterocycle centroid—Ga—Ga angle is 106.0° whereas in **26** the same angle is 119.2° and the Ga—Ga distance is only 2.8640(13) Å. Although the difference in these Ga—Ga distances is almost 1.4 Å, the shorter interaction is still longer than normally seen for Ga—Ga single bonds, *e.g.* 2.541(1) Å in $[(tmp)_2Ga—Ga(tmp)_2]$, tmp = 2,2,6,6-tetramethylpiperidine,[51] but not markedly so, especially considering the expected larger covalent radius of the Ga(I) centre in **26** relative to the Ga(II) centres in $[(tmp)_2Ga—Ga(tmp)_2]$ and other related dimers. This could mean that in **26** the two anionic gallium centres are held together, not only by an electrostatic attraction to the potassium cations but perhaps also by partial interaction of electron density from the lone pair on each gallium centre with the *p*-orbital on the other. If this were the case it is only a weak interaction and it is not known why it does not occur in **6**, which should be more open to an approach of the two gallium centres, at least on steric grounds.

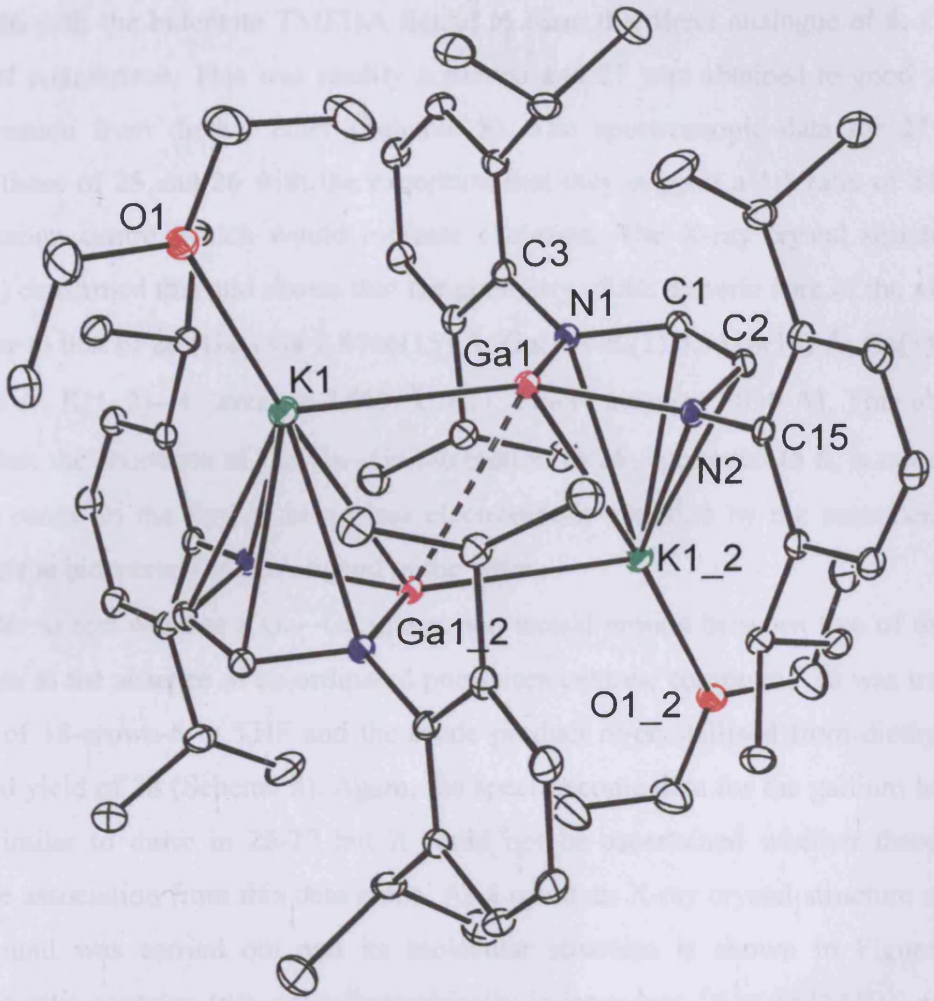

Figure 12 Molecular structure of [{(Et_2O)KGa(Ar-DAB)}$_2$] (**26**)

Selected bond lengths (Å) and angles (°): Ga(1)—Ga(1_2) 2.8640(13), Ga(1)—N(1) 2.005(2), Ga(1)—N(2) 2.009(2), Ga(1)—K(1_2) 3.3784(13), Ga(1)—K(1) 3.4223(10), K(1)—O(1) 2.718(2), K(1)—N(1_2) 2.936(3), K(1)—C(1_2) 2.977(3), K(1)—N(2_1) 2.987(2), K(1)—C(2_1) 2.997(3), K(1)—Ga(1_2) 3.3784(13), C(1)—C(2) 1.356(4), N(1)—Ga(1)—N(2) 81.88(9), N(1)—Ga(1)—Ga(1_2) 107.95(7), N(2)—Ga(1)—Ga(1_2) 109.68(7), N(1)—Ga(1)—K(1) 138.96(6), N(2)—Ga(1)—K(1) 139.15(6), Ga(1)—N(1)—C(1) 111.05(17), C(2)—N(2)—Ga(1) 110.65(16), N(1)—C(1)—C(2) 116.8(2), N(2)—C(2)—C(1) 117.3(2).

It was thought of sufficient worth to attempt the replacement of the co-ordinated Et_2O ligand of **26** with the bidentate TMEDA ligand to form the direct analogue of **6**, *i.e.* **27**, for purposes of comparison. This was readily achieved and **27** was obtained in good yield after re-crystallisation from diethyl ether (Scheme 8). The spectroscopic data for **27** are very similar to those of **25** and **26** with the exception that they suggest a 1:1 ratio of TMEDA to each potassium centre, which would indicate chelation. The X-ray crystal structure of **27** (Figure 13) confirmed this and shows that the geometry of the dimeric core of the molecule is very similar to that of **26** [Ga—Ga 2.8746(15) Å; Ga(1)—K(1) 3.5318(18) Å; Ga(1)—K(1_2) 3.4620(16) Å; K(1_2)—C average 3.013 Å; K(1_2)—N average 3.030 Å]. This observation confirms that the shortness of the Ga···Ga interaction in **26**, compared to **6**, is not due to the potassium centre in the former being less electronically satisfied by the monodentate ether ligand than the bidentate TMEDA ligand in the latter.

In order to test whether a Ga···Ga interaction would remain between two of the gallium heterocycles in the absence of co-ordinated potassium centres, compound **26** was treated with an excess of 18-crown-6 in THF and the crude product re-crystallised from diethyl ether to give a good yield of **28** (Scheme 8). Again, the spectroscopic data for the gallium heterocycle are very similar to those in **25-27** but it could not be ascertained whether there was any heterocycle association from this data alone. As a result an X-ray crystal structure analysis of the compound was carried out and its molecular structure is shown in Figure 14. The asymmetric unit contains two crystallographically independent [:Ga(Ar-DAB)]$^-$ anions and two K(18-crown-6)$_{1.5}$ cations, the latter of which are generated into dicationic units, [(18-crown-6)K(μ-18-crown-6)K(18-crown-6)]$^{2+}$, by inversion centres. One of these is shown in Figure 14(b) and it is clear that the terminal 18-crown-6 ligands are η^6-co-ordinated to a potassium centre whilst the bridging crown is η^2-co-ordinated to both K centres. There are no contacts between [:Ga(Ar-DAB)]$^-$ anions which strongly suggests that the Ga···Ga interactions in **26** and **27** are weak and will not persist in the absence of the coulombic assistance provided by the partially solvated potassium ions. The GaN_2C_2 five membered rings of both [:Ga(Ar-DAB)]$^-$ anions are positionally disordered over two sites in an 80 : 20 ratio. This disorder was successfully modelled and the geometries of the two major occupancy sets are similar so only one is shown in Figure 14(a).

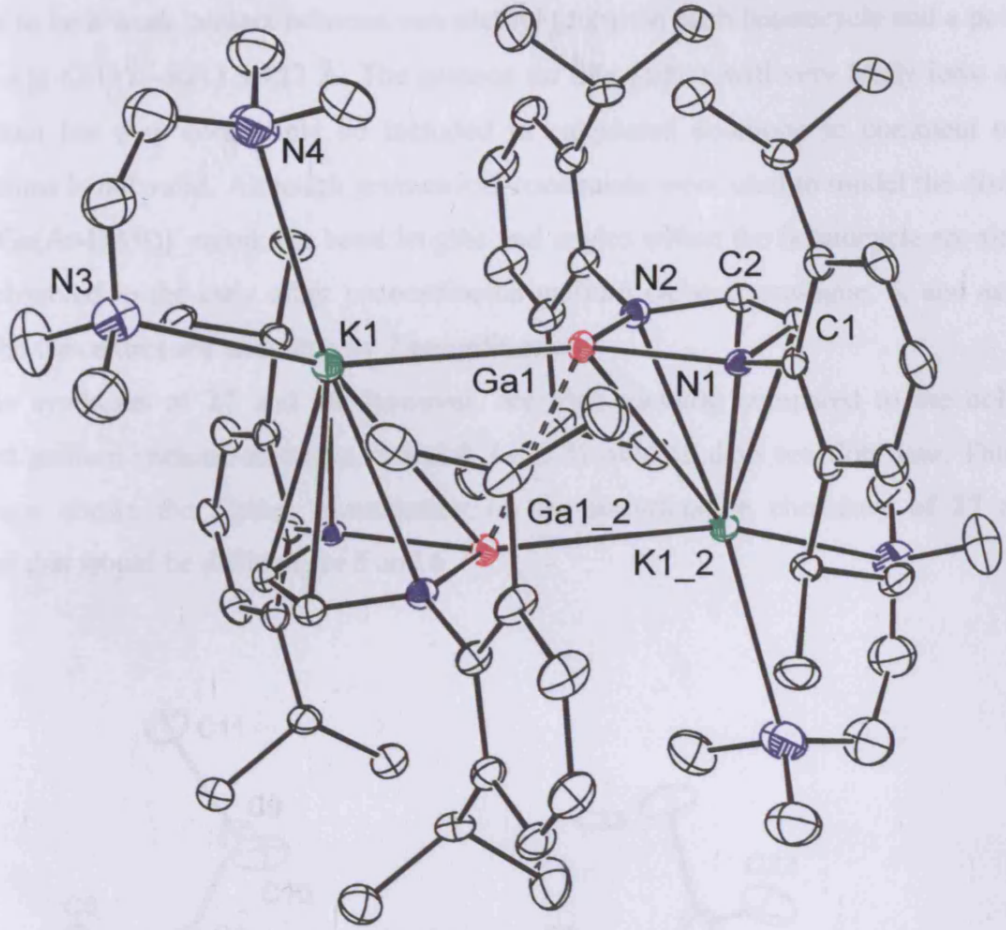

Figure 13 Molecular structure of [{(TMEDA)KGa(Ar-DAB)}$_2$] (**27**)

Selected bond lengths (Å) and angles (°): Ga(1)—Ga(1_2) 2.8746(15), Ga(1)—N(1) 2.014(4), Ga(1)—N(2) 2.011(4), Ga(1)—K(1_2) 3.4620(16), Ga(1)—K(1) 3.5318(18), K(1)—N(3) 2.996(6), K(1)—N(4) 3.055(7), K(1)—N(1_2) 3.027(4), K(1)—C(1_2) 3.009(5), K(1)—N(2_1) 3.034(4), K(1)—C(2_1) 3.016(5), K(1)—Ga(1_2) 3.4620(16), C(1)—C(2) 1.350(6), N(1)—Ga(1)—N(2) 82.05(15), N(1)—Ga(1)—Ga(1_2) 109.79(12), N(2)—Ga(1)—Ga(1_2) 109.79(12), N(1)—Ga(1)—K(1) 138.84(10), N(2)—Ga(1)—K(1) 139.09(11), Ga(1)—N(1)—C(1) 110.4(3), C(2)—N(2)—Ga(1) 110.4(3), N(1)—C(1)—C(2) 117.2(4), N(2)—C(2)—C(1) 118.0(4).

Although, the [:Ga(Ar-DAB)]$^-$ units do not have an interaction with each other, there appears to be a weak contact between one methyl group on each heterocycle and a potassium centre, *e.g.* C(11)—K(1) 3.432 Å. The protons on this carbon will very likely have a closer interaction but they could only be included in calculated positions so comment on such interactions is not valid. Although geometrical constraints were used to model the disorder in each [:Ga(Ar-DAB)]$^-$ anion, the bond lengths and angles within the heterocycle are similar to those observed in the only other uncoordinated gallium carbene analogue, **5**, and as in that anion the Ga centres are undoubtedly 2 co-ordinate.

The syntheses of **27** and **28**, however, are high yielding compared to the only other reported gallium carbene analogue, **5** and **6**, *i.e.* 3 % over 10 days reaction time. This major difference allows the further examination of the co-ordination chemistry of **27** and **28**, whereas this would be difficult for **5** and **6**.

(a)

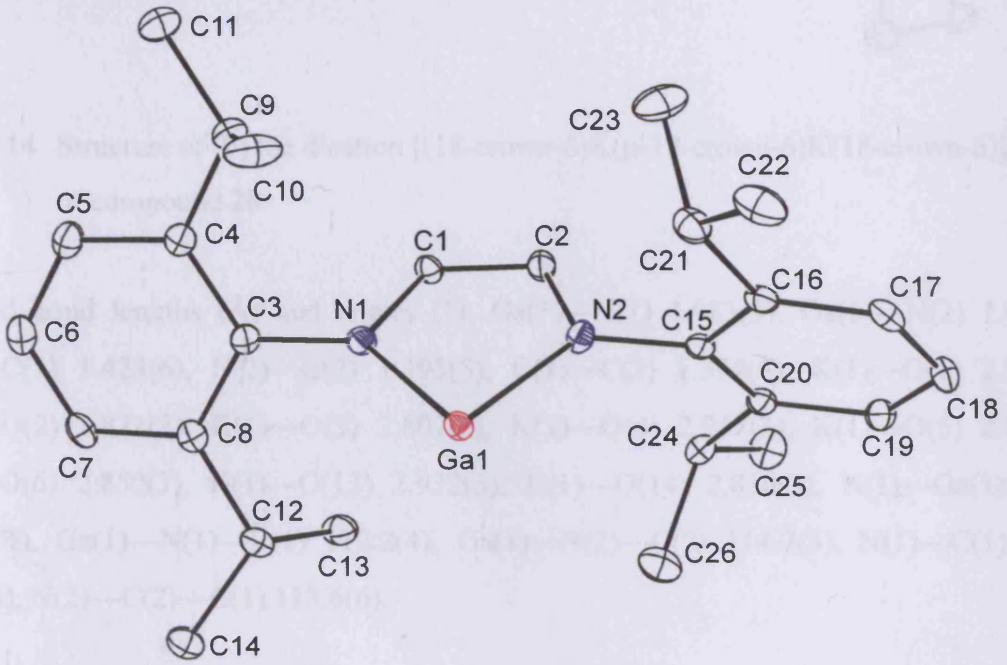

Figure 14 Structure of (a) the anion [:Ga(Ar-DAB)]$^-$ of compound **28**

(b)

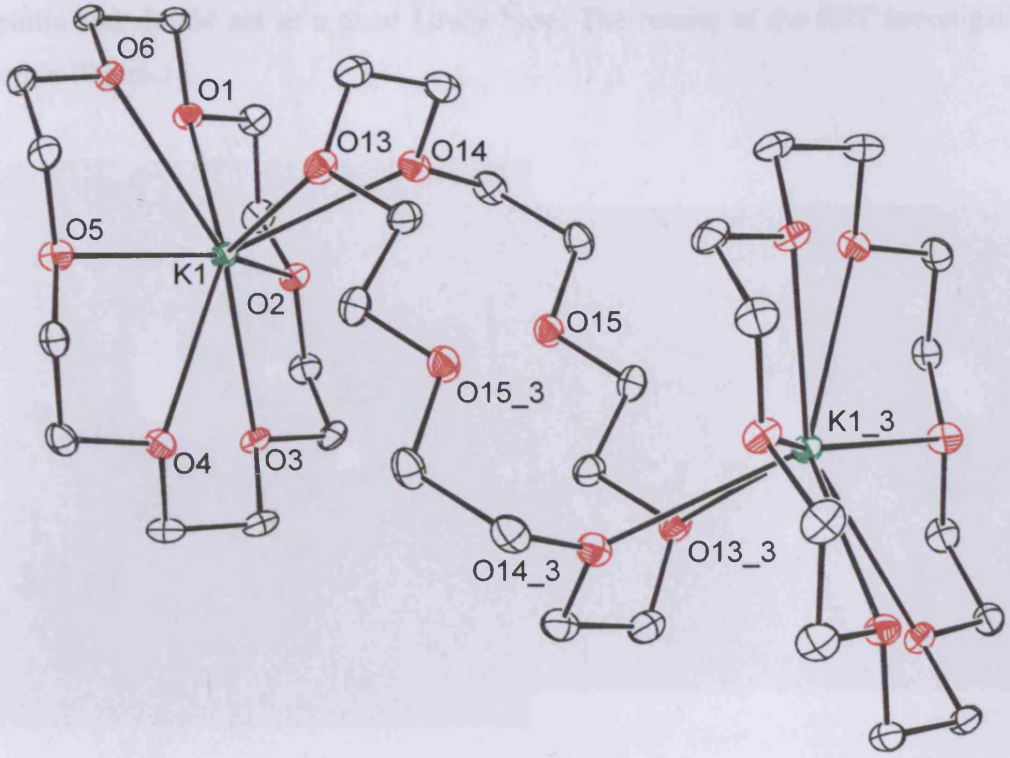

Figure 14 Structure of (b) the dication $[(18\text{-crown-6})K(\mu\text{-}18\text{-crown-6})K(18\text{-crown-6})]^{2+}$ of compound **28**

Selected bond lengths (Å) and angles (°): Ga(1)—N(1) 1.983(3), Ga(1)—N(2) 1.956(3), N(1)—C(1) 1.423(6), N(2)—C(2) 1.395(5), C(1)—C(2) 1.374(6), K(1)—O(1) 2.875(3), K(1)—O(2) 2.871(3), K(1)—O(3) 2.807(3), K(1)—O(4) 2.957(3), K(1)—O(5) 2.859(3), K(1)—O(6) 2.850(3), K(1)—O(13) 2.932(3), K(1)—O(14) 2.816(3), N(1)—Ga(1)—N(2) 83.02(11), Ga(1)—N(1)—C(1) 110.2(4), Ga(1)—N(2)—C(2) 114.7(3), N(1)—C(1)—C(2) 118.5(6), N(2)—C(2)—C(1) 113.6(6).

In collaboration with Dr. Jamie Platts at Cardiff University, the electronic structure of a model of the free carbene analogue, **28**, has been investigated by DFT calculations, and it was found that the LUMO has high gallium *p*-orbital character, whilst the HOMO is associated with the in phase C—C interaction and in phase N—Ga interactions. The HOMO-1 is only slightly lower in energy and corresponds to the lone pair on the gallium centre, which is

effectively *sp*-hybridised and suggests that the gallium carbene analogue, **28**, should be very nucleophilic and should act as a good Lewis base. The results of the DFT investigation are displayed in Figure 15.

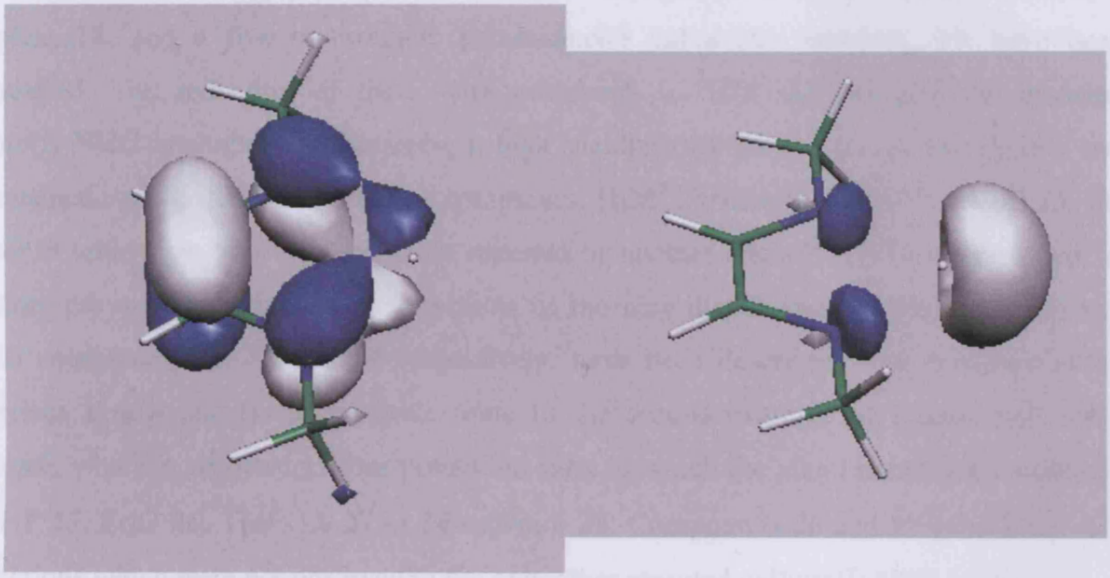

HOMO (176.56 kJ mol^{-1})

HOMO-1 (50.86 kJ mol^{-1})

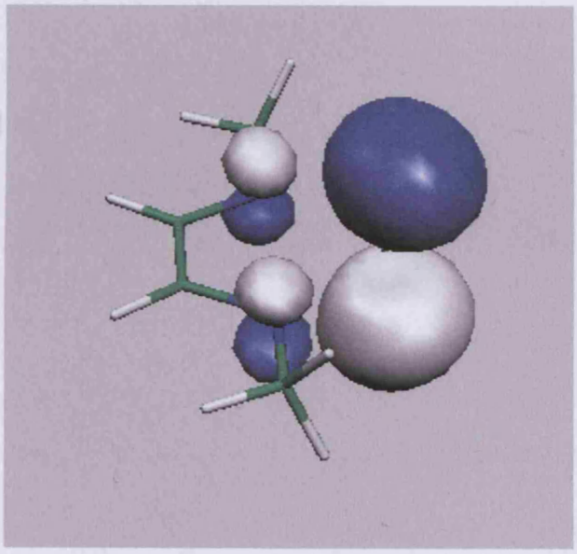

LUMO (375.24 kJ mol^{-1})

Figure 15 DFT calculated structure and frontier orbitals of $[Ga:\{N(Me)C(H)\}_2]^-$

3.6 Conclusions

In conclusion, this chapter describes the chemistry of low valent group 13 halides in reaction with diazabutadiene ligands. The first example of a diazabutadiene indium(II) complex, **18**, and a five co-ordinate, paramagnetic indium(III) complex, **19**, have been synthesised. The reduction of these with potassium in THF did not give the intended indium(I) NHC analogue. Furthermore, a high yielding synthetic route to monomeric and paramagnetic group 13 diazabutadiene complexes, $[I_2M^{III}(Ar\text{-}DAB)]$, M = Ga **20**, Al **23**, the former of which has been independently reported by another group,[43] has been developed. In addition, the syntheses and characterisations of the new diazabutadiene-Ga(II), Ga(III) and Al(III) complexes, **21**, **22** and **24** respectively, have been described. The reduction of **20** comprises a new and facile synthetic route to the second example of a gallium(I) NHC analogue, which is reported as four potassium salts in which the alkali metal is co-ordinated by THF **25**, Et_2O **26**, TMEDA **27** or 18-crown-6 **28**. Compounds **26** and **27** exhibit Ga···Ga interactions which were not observed in the only other reported gallium(I) NHC analogue.

3.7 Experimental

For general experimental procedures, refer to appendix 1. $AlCl_3$, InCl, potassium and sodium were purchased from Aldrich and $AlCl_3$ was resublimed before use. 'GaI' was synthesised by a modification of the literature method,[52] as were the ligands Ar-DAB[53] and Bu^t-DAB[54] and **20** was prepared by a variation of the published method.[43] Meaningful NMR spectra for **18-23** could not be obtained due to their paramagnetic nature. A useful ^{13}C-NMR spectrum of **24** could not be obtained due to the fluxional nature of the compound in solution. The EPR spectra were recorded at room temperature on an X-band Bruker ESP 300e series spectrometer operating at 12.5 kHz field modulation in a Bruker EN801 cavity. The spectra were obtained with a 2.5 mW power source. The *g* values were obtained using a Bruker ER035 gaussmeter calibrated using the perylene radical cation in concentrated H_2SO_4 (g = 2.002569). Computer simulations were performed using the SIMFONIA Bruker software.[55]

[{(Ar-DAB$^\bullet$)InCl}$_2$] (18)

To a suspension of InCl (0.50 g, 3.30 mmol) in DME (15 cm^3) was added a solution of Ar-DAB (1.86 g, 5.50 mmol) in DME (15 cm^3) at –50 °C. The suspension was warmed to room temperature and stirred for 4 hours to yield a deep red solution and a precipitate of indium metal. This suspension was filtered and the filtrate cooled to –30 °C to yield red crystals of **18** (0.274 g, 12 %); m. p. 84 – 87 °C (dec.); IR ν/cm^{-1} (Nujol): 1618 m, 1449 m, 1372 m, 1326 m, 1250 s, 1101 m, 819 m; MS(APCI) m/z (%): 377 [Ar-DABH$^+$, 100]. Reproducible microanalyses on the compound could not be obtained due to its extreme air sensitivity.

[InCl$_2$(THF)(Ar-DAB$^\bullet$)] (19)

To a solution of Ar-DAB (0.5 g, 1.33 mmol) in Et_2O/THF (10 cm^3 / 5 cm^3) was added a suspension of Li-powder (0.1 g, 14.0 mmol) in Et_2O (15 cm^3) at –78 °C. The suspension was warmed to room temperature and stirred for 3 hours to yield a orange solution. Filtration yielded a clear, red solution of [(Ar-DAB)Li$_2$]. To this, a suspension of InCl (0.40 g, 2.66 mmol) in Et_2O (15 cm^3) was added at –78 °C. The resulting solution was warmed to room temperature and stirred over-night after which a precipitate of indium metal was observed. The solution was filtered, volatiles removed *in vacuo* and the residue extracted into Et_2O (10

cm^3). Cooling to –30 °C yielded red crystals of **19** (0.54 g, 64 %); m. p. 142 °C (dec.); IR ν/cm^{-1} (Nujol): 1625 s, 1260 s, 1098 s, 800 s, 760 s,; MS(APCI) m/z (%): 377 [Ar-DABH$^+$, 100]. Reproducible microanalyses on the compound could not be obtained due to its extreme air sensitivity.

[GaI_2(Ar-DAB$^\bullet$)] (20)

To a suspension of Ga metal (0.33 g, 4.70 mmol) in toluene (15 cm^3) was added I_2 (0.60 g, 2.35 mmol) at 25 °C. The mixture was sonicated until the solution had become colourless and a pale green precipitate was produced. To this suspension was added a solution of Ar-DAB (1.77g, 4.70 mmol) in toluene (15 cm^3) and the resulting suspension stirred overnight to yield a red solution. This was filtered, concentrated to *ca.* 10 cm^3 and placed at –30 °C overnight to yield red crystals of **20** (0.85 g, 52 %); m. p. 225 – 227 °C; IR ν/cm^{-1} (Nujol): 1926 m, 1864 m, 1824 s, 1583 s, 1255 s, 938 s; MS(APCI) m/z (%): 578 [M$^+$-I, 100], 445 [M$^+$-2I, 3]; $C_{26}H_{36}N_2GaI_2$ requires C 44.60, H 5.18, N 4.25 %; found C 44.41, H 5.23, N 3.88 %.

[{(Bu^t-DAB$^\bullet$)GaI}$_2$] (21) and [(Bu^t-DAB$^\bullet$)GaI_2] (22)

To a suspension of Ga metal (0.24 g, 3.40 mmol) in toluene (15 cm^3) was added I_2 (0.43 g, 1.70 mmol) at 25 °C. The mixture was sonicated until the solution had become colourless and a pale green precipitate was produced. To this suspension was added a solution of Bu^t-DAB (0.59 g, 3.40 mmol) in toluene (15 cm^3) and the resulting suspension stirred for 4 hours to yield a red solution. This was filtered, whereupon volatiles were removed *in vacuo*. The residue was extracted into Et_2O (10 cm^3) and the resulting solution cooled to –30 °C to yield a mixture of **21** as dark green crystals (0.37, 32 %) and **22** as red crystals (0.06 g, 4 % based on Bu^t-DAB) which were manually separated.

Data for **21**: m. p. 126 – 131 °C; IR ν/cm^{-1} (Nujol): 1634 m, 1527 s, 1260 s, 1204 m, 779 m; MS(APCI) m/z (%): 492 [Bu^t-DABGaI_2^+, 27], 169 [Bu^t-DABH$^+$, 100]; $C_{20}H_{40}N_4Ga_2I_2$ requires C 32.91, H 5.52, N 7.68 %; found C 33.43, H 5.64, N 7.74 %.

Data for **22**: m. p. 85 – 92 °C; IR ν/cm^{-1} (Nujol): 1634 m, 1265 s, 1199 m, 1015 m, 799 m; MS(APCI) m/z (%): 492 [M$^+$, 5], 169 [Bu^t-DABH$^+$, 100]; $C_{10}H_{20}N_2GaI_2$ requires C 24.42, H 4.10, N 5.70 %; found C 24.66, H 4.14, N 5.48 %.

[(Ar-DAB$^{\bullet}$)AlI$_2$] (23)

To a suspension of Al powder (0.073 g, 2.70 mmol) in toluene (15 cm^3) was added I_2 (0.342 g, 0.135 mmol) at 25 °C. The resulting suspension was sonicated for 4 hours to yield an AlI_3/Al mixture. A solution of Ar-DAB (1.0 g, 2.7 mmol) in toluene (15 cm^3) was added to this over 5 min at 25 °C to give an intermediate deep red colour to the suspension. This was stirred overnight during which time a proportion of the Al powder was seen to dissolve. Volatiles were removed *in vacuo* and the residue extracted into Et_2O (20 cm^3). Cooling to –30 °C yielded red crystals of **23** overnight (0.70 g, 40 % based upon Ar-DAB); m. p. 224 – 227 °C; IR ν/cm^{-1} (Nujol): 1516 s, 1219 s, 1055 s, 886 m, 789 m; MS(APCI) m/z (%): 531 [M$^+$-I, 61], 377 [Ar-DABH$^+$, 100]; $C_{26}H_{36}N_2AlI_2$ requires C 47.50, H 5.52, N 4.26 %; found C 47.16, H 5.57, N 4.10 %.

[(Ar-DAB)AlI$_2$]I (24)

To a suspension of AlI_3 (0.54 g, 1.33 mmol) in toluene (15 cm^3) was added a solution of Ar-DAB (0.50 g, 1.33 mmol) in toluene (15 cm^3) over 5 min at 25 °C. The solution immediately became a deep red colour and was stirred for 5 hours whereupon volatiles were removed *in vacuo* and the residue extracted into Et_2O (20 cm^3) and the resulting solution placed at –30 °C to yield red crystals of **24** overnight (0.69, 66 %); m. p. 163 – 176 °C (dec.); ^{1}H NMR (400 MHz, C_6D_6, 298 K) δ 0.95 (br, 24 H, CH_3), 2.98 (br, 4 H, CH), 7.02 (br, 6 H, ArH), 8.05 (br, 2 H, NCH); IR ν/cm^{-1} (Nujol): 1532 s, 1276 s, 1255 m, 1107 s, 799 m; MS(EI) m/z (%): 531 [M$^+$-2I, 10], 332 [Ar-DAB$^+$, 100]. Reproducible microanalyses on the compound could not be obtained as samples were contaminated with traces of **23**.

[{(THF)KGa(Ar-DAB)}$_2$] (25)

A solution of **20** (0.70 g, 1.00 mmol) in THF (15 cm^3) was stirred over a potassium mirror (0.80 g, 20 mmol) at 25 °C for 8 hours after which the yellow-orange solution was filtered and volatiles removed *in vacuo*. The residue was extracted into hexane (20 cm^3) and the resulting solution was concentrated to *ca.* 10 cm^3 and cooled to –30 °C overnight to yield **25** as red crystals (0.45 g, 80 %). m. p. 189 °C (dec.); ^{1}H NMR (400 MHz, C_6D_6, 298 K) δ 1.37 (d, 24 H, $^3J_{HH}$ = 6.9 Hz, CH_3), 1.39 (d, 24 H, $^3J_{HH}$ = 6.8 Hz, CH_3), 1.49 (q, 8 H, $^3J_{HH}$ = 6.8 Hz, THF/CH_2), 3.57 (sept, 8 H, $^3J_{HH}$ = 6.9 Hz, CH), 3.63 (t, 8 H, $^3J_{HH}$ = 6.9 Hz, THF/OCH_2), 6.42 (s, 4 H, NCH), 7.20 (t, 4 H, $^3J_{HH}$ = 7.7 Hz, p-ArH), 7.30 (d, 8 H, $^3J_{HH}$ = 7.5 Hz, m-ArH); ^{13}C

NMR (100.6 MHz, C_6D_6, 298 K) δ 23.0 ($CHCH_3$), 24.5 ($CHCH_3$), 26.1 (THF/CH_2), 28.6 (CH), 68.2 (THF/OCH_2), 117.6 (CN), 123.4 (m-ArC), 124.3 (p-ArC), 143.1 (o-ArC), 146.4 (ipso-ArC); IR ν/cm^{-1} (Nujol): 1583 s, 1547 s, 1245 s, 1097 s, 754 s; MS(EI) m/z (%): 377 [Ar-DAB^+, 100], 189 [$ArNCH^+$, 12]. Reproducible microanalyses on the compound could not be obtained due to its extreme air sensitivity.

[{(Et_2O)KGa(Ar-DAB)}$_2$] (26)

A solution of **20** (0.75 g, 1.07 mmol) in THF (15 cm^3) was stirred over a potassium mirror (0.80 g, 20 mmol) at 25 °C for 8 hours after which the yellow-orange solution was filtered and volatiles removed *in vacuo*. The residue was extracted into Et_2O (20 cm^3) and the resulting solution was concentrated to *ca.* 10 cm^3 and cooled to –30°C overnight to yield **26** as red crystals (0.45 g, 75 %); m. p. 180 - 187 °C (dec.); ^1H NMR (400 MHz, C_6D_6, 298 K) δ 1.28 (t, 12 H, $^3J_{HH}$ = 6.4 Hz, CH_3), 1.46 (d, 48 H, $^3J_{HH}$ = 6.8 Hz, CH_3), 3.44 (q, 8 H, $^3J_{HH}$ = 6.4 Hz, CH_2), 3.83 (sept, 8 H, $^3J_{HH}$ = 6.8 Hz, CH), 6.48 (s, 4 H, NCH), 7.23 (t, 4 H, $^3J_{HH}$ = 7.4 Hz, p-ArH), 7.37 (d, 8 H, $^3J_{HH}$ = 7.4 Hz, m-ArH); ^{13}C NMR (100.6 MHz, C_6D_6, 298 K) δ 15.3 (CH_2CH_3), 25.3 ($CHCH_3$), 28.0 (CH), 65.6 (CH_2), 122.5 (CN), 122.8 (m-ArC), 123.7 (p-ArC), 145.8 (o-ArC), 150.2 (ipso-ArC); IR ν/cm^{-1} (Nujol): 1583 s, 1557 m, 1255 s, 1096 s, 927 m; MS(EI) m/z (%): 377 [Ar-DAB^+, 5], 189 [$ArNCH^+$, 100]. Reproducible microanalyses on the compound could not be obtained due to its extreme air sensitivity.

[{(TMEDA)KGa(Ar-DAB)}$_2$] (27)

To a solution of **26** (0.40 g, 0.35 mmol) in Et_2O (25 cm^3) at –78 °C was added TMEDA (0.40 g, 3.50 mmol) and the resulting solution warmed to room temperature and stirred for 4 hours after which time volatiles were removed in *vacuo* and the residue extracted into Et_2O (10 cm^3). The resulting solution was cooled to –30 °C overnight to yield **27** as red crystals (0.30 g, 68 %); m. p. 163 – 166 °C (dec.); ^1H NMR (400 MHz, C_6D_6, 298 K) δ 1.41 (d, 24 H, $^3J_{HH}$ = 6.9 Hz, CH_3), 1.43 (d, 24 H, $^3J_{HH}$ = 6.9 Hz, CH_3), 2.05 (s, 24 H, NCH_3), 2.20 (s, 8 H, NCH_2), 3.82 (sept, 8 H, $^3J_{HH}$ = 6.9 Hz, CH), 6.42 (s, 4 H, NCH), 7.23 (t, 4 H, $^3J_{HH}$ = 7.5 Hz, p-ArH), 7.32 (d, 8 H, $^3J_{HH}$ = 7.5 Hz, m-ArH); ^{13}C NMR (100.6 MHz, C_6D_6, 298 K) 26.0 ($CHCH_3$), 28.7 (CH), 46.2 (NCH_3), 58.2 (NCH_2), 123.1 (CN), 123.4 (m-ArC), 124.3 (p-ArC), 146.3 (o-ArC), 151.0 (ipso-ArC); IR ν/cm^{-1} (Nujol): 1588 s, 1562 m, 1245 s, 1096 s, 1081 m; MS(EI)

m/z (%): 189 [$ArNCH^+$, 12], 115 [$TMEDAH^+$, 100]. Reproducible microanalyses on the compound could not be obtained due to its extreme air sensitivity.

[:Ga(Ar-DAB)]$_2$[(18-crown-6)K(μ-18-crown-6)K(18-crown-6)] (28)

To a solution of **26** (0.29 g, 0.26 mmol) in THF (15 cm^3) at –50 °C was added a solution of 18-crown-6 (0.30 g, 1.14 mmol) in THF (15 cm^3). The resulting orange solution was allowed to warm to 25 °C and was stirred for 2 hours whereupon volatiles were removed *in vacuo*. The residue was extracted into Et_2O (10 cm^3) and the resulting solution cooled to –30 °C to yield **28** as orange needles (0.27 g, 59 %); m. p. 134 – 139 °C ; ^1H NMR (400 MHz, C_6D_6, 298 K) δ 1.58 (d, 24 H, $^3J_{HH}$ = 6.9 Hz, CH_3), 1.64 (d, 24 H, $^3J_{HH}$ = 6.9 Hz, CH_3), 3.27 (s, 72 H, OCH_2), 3.45 (sept, 8 H, $^3J_{HH}$ = 6.9 Hz, CH), 6.82 (s, 4 H, NCH), 7.28 (t, 4 H, $^3J_{HH}$ = 7.5 Hz, p-ArH), 7.43 (d, 8 H, $^3J_{HH}$ = 7.5 Hz, m-ArH); ^{13}C NMR (100.6 MHz, C_6D_6, 298 K) δ 26.0 (CH_3), 26.7 (CH_3), 28.6 (CH), 70.7 (CH_2), 122.2 (CN), 122.4 (m-ArC), 122.7 (p-ArC), 146.5 (o-ArC), 152.6 (ipso-ArC); IR ν/cm^{-1} (Nujol): 1573 s, 1552 m, 1255 s, 1112 s, 794 s; MS(EI) m/z (%): 443 [$Ga(Ar\text{-}DAB)^+$, 17], 377 [$Ar\text{-}DAB^+$, 31]; $C_{88}H_{144}O_{18}N_4Ga_2K_2$ requires C 59.93, H 8.23, N 3.18 %; found C 58.92, C 8.25, N 3.10 %.

3.8 References

1. A. Schnepf, H. Schnöckel, *Angew. Chem., Int. Ed.*, 2002, **41**, 3532.
2. G. Linti, H. Schnöckel, *Coord. Chem. Revs.*, 2000, **206-207**, 285.
3. R.A. Fischer, J. Weiss, *Angew. Chem., Int. Ed. Engl.*, 1999, **38**, 2830.
4. J. Su, X.W. Li, R.C. Crittendon, C.F. Campana, G.H. Robinson, *Organometallics*, 1997, **16**, 4511.
5. F.A. Cotton, X. Feng, *Organometallics*, 1998, **17**, 128.
6. C. Boehme, J. Uddin, G. Frenking, *Coord. Chem. Revs.*, 2000, **197**, 249.
7. G. Frenking, N. Fröhlich, *Chem. Rev.*, 2000, **100**, 717.
8. W. Uhl, M. Benter, S. Melle, W. Saak, G. Frenking, J. Uddin, *Organometallics*, 1999, **18**, 3778.
9. D. Bourissou, O. Guerret, F.P. Gabbai, G. Bertrand, *Chem. Rev.*, 2000, **100**, 39.
10. C.J. Carmalt, A.H. Cowley, *Adv. Inorg. Chem.*, 2000, **50**, 1.
11. W.A. Herrmann, *Angew. Chem., Int. Ed.*, 2002, **41**, 1290.
12. M. Haaf, T.A. Schmedake, R. West, *Acc. Chem. Res.*, 2000, **33**, 704.
13. O. Kühl, *Coord. Chem. Revs.*, 2004, **248**, 411.
14. C.J. Carmalt, V. Lomeli, B.G. McBurnett, A.H. Cowley, *Chem. Commun.*, 1997, 2095.
15. M.K. Denk, S. Gupta, A.J. Lough, *Eur. J. Inorg. Chem.*, 1999, 41.
16. D. Gudat, A. Haghverdi, M. Nieger, *J. Organomet. Chem.*, 2001, **617-618**, 383.
17. N.J. Hardman, M.B. Abrams, M.A. Pribisko, T.M. Gilbert, R.L. Martin, G.J. Kubas, R.T. Baker, *Angew. Chem., Int. Ed.*, 2004, **43**, 1955.
18. E.S. Schmidt, A. Jockisch, H. Schmidbaur, *J. Am. Chem. Soc.*, 1999, **121**, 9758.
19. A. Sundermann, M. Reiher, W.W. Schoeller, *Eur. J. Inorg. Chem.*, 1998, 305.
20. N. Metzler-Nolte, *New. J. Chem.*, 1998, 793.
21. W.W. Schoeller, D. Eisner, *Inorg. Chem.*, 2004, **43**, 2585.
22. M. Reiher, A. Sundermann, *Eur. J. Inorg. Chem.*, 2002, 1854.
23. M. Stender, A.D. Phillips, P.P. Power, *Inorg. Chem.*, 2001, **40**, 5314.
24. E.S. Schmidt, A. Schier, H. Schmidbaur, *J. Chem. Soc., Dalton Trans.*, 2001, 505.
25. C. Cui, H.W. Roesky, H.G. Schmidt, M. Noltemeyer, H. Hao, F. Cimpoesu, *Angew. Chem., Int. Ed.*, 2000, **39**, 4274.
26. N.J. Hardman, B.E. Eichler, P.P. Power, *Chem. Commun.*, 2000, 1991.

27. M.S. Hill, P.B. Hitchcock, *Chem. Commun.*, 2004, 1818.
28. M. Stender, P.P. Power, *Polyhedron*, 2002, **21**, 525.
29. N.J. Hardman, A.D. Phillips, P.P. Power, *ACS Symp. Ser.*, 2002, **822**, 2.
30. N.J. Hardman, R.J. Wright, A.D. Phillips, P.P. Power, *J. Am. Chem. Soc.*, 2003, **125**, 2667.
31. N.J. Hardman, P.P. Power, J.D. Gorden, C.L.B. Macdonald, A.H. Cowley, *Chem. Commun.*, 2001, 1866.
32. N. Metzler, M. Denk, *Chem. Commun.*, 1996, 2657.
33. C. Cui, S. Köpke, R. Herbst-Irmer, H.W. Roesky, M. Noltemayer, H.G. Schmidt, B. Wrackmeyer, *J. Am. Chem. Soc.*, 2001, **123**, 9091.
34. C. Cui, H.W. Roesky, H.G. Schmidt, M. Noltemeyer, *Angew. Chem., Int. Ed.*, 2000, **39**, 4531.
35. N.J. Hardman, P.P. Power, *Chem. Commun.*, 2001, 1184.
36. N.J. Hardman, C. Cui, H.W. Roesky, W.H. Fink, P.P. Power, *Angew. Chem., Int. Ed.*, 2001, **40**, 2172.
37. M. Denk, R. Hayashi, R. West, *J. Am. Chem. Soc.*, 1994, **116**, 10813.
38. B. Gehrhus, M.F. Lappert, *Polyhedron*, 1998, **17**, 999.
39. N. Burford, P.J. Ragogna, K.N. Robertson, T.S. Cameron, N.J. Hardman, P.P. Power, *J. Am. Chem. Soc.*, 2002, **124**, 382.
40. H. Zhu, J. Chai, V. Chandrasekhar, H.W. Roesky, J. Magull, D. Vidovic, H.G. Schmidt, M. Noltemeyer, P.P. Power, W.A. Merrill, *J. Am. Chem. Soc.*, 2004, **126**, 9472.
41. N.J. Hardman, P.P. Power, *Inorg. Chem.*, 2001, **40**, 2474.
42. T. Pott, P. Jutzi, B. Neumann, H.G. Stammler, *Organometallics*, 2001, **20**, 1965.
43. T. Pott, P. Jutzi, W. Kaim, W.W. Schoeller, B. Neumann, A. Stammler, H.G. Stammler, M. Wanner, *Organometallics*, 2002, **21**, 3169.
44. M.J. Taylor, D.G. Tuck, L. Victoriano, *Can. J. Chem.*, 1982, **60**, 690.
45. M.G. Gardiner, G.R. Hanson, M.J. Henderson, F.C. Lee, C.L. Raston, *Inorg. Chem.*, 1994, **33**, 2456.
46. S.M. Godfrey, K.J. Kelly, P. Kramkowski, C.A. McAuliffe, R.G. Pritchard, *Chem. Commun.*, 1997, 1001.
47. W.W. Schoeller, S. Grigoleit, *Dalton Trans.*, 2002, 405.

48. J.A.C. Clyburne, R.D. Culp, S. Kamepalli, A.H. Cowley, A. Decken, *Inorg. Chem.*, 1996, **35**, 6651.
49. F.S. Mair, R. Manning, R.G. Pritchard, J.E. Warren, *Chem. Commun.*, 2001, 1136.
50. J. Emsley, *"The Elements"*, Oxford University Press, Oxford, 1989.
51. G. Linti, R. Frey, M. Schmidt, *Z. Naturforsch., Teil B*, 1994, **49**, 958.
52. M.L.H. Green, P. Mountford, G.J. Smout, S.R. Speel, *Polyhedron*, 1990, **9**, 2763.
53. L. Jafarpour, E.D. Stevens, S.P. Nolan, *J. Organomet. Chem.*, 2000, **606**, 49.
54. J.M. Kliegman, R.K. Barnes, *Tetrahedron*, 1970, **26**, 2555.
55. WINEPR SIMFONIA Version 1.25, Bruker Analytische Messtechnick GmbH, 1996.

Chapter 4

Reactivity of a New Gallium(I) Carbene Analogue Towards Main Group Halide Complexes

4.1 Introduction

This chapter explores the reactivity of a novel anionic gallium(I) carbene heterocycle and its analogies with isoelectronic N-heterocyclic carbenes. The synthesis and characterisation of this gallium(I) heterocycle is described in Chapter 3. The first section (**4.2**) provides an overview of complexes resulting from its reactivity towards transition metal precursors. These novel and exciting complexes have only recently been prepared and investigated in the Jones research group.

Section **4.4** details the reactions of the gallium(I) heterocycle towards main group metal precursors. Particular emphasis is placed upon some decomposition products which are paramagnetic and have been studied crystallographically and by EPR spectroscopy. These reactivity studies culminate in a oxidative coupling reaction of this anionic gallium(I) heterocycle, which has led to the first example of a symmetrically bridged Cyclopentadienyl-digallane complex which exhibits the only known π-interaction to a Ga(II) center.

4.2 Reactions of a New Anionic Gallium(I) Carbene Analogue with Transition Metal Precursors

Jones *et al*, have embarked on a comprehensive survey of the reactivity of [{(TMEDA)KGa(Ar-DAB)}$_2$], **1** towards transition metals to ascertain how the reactivity of this carbene analogue compares to that of N-heterocyclic carbenes (NHCs), as there are now numerous NHC complexes of transition metals known.[1] The reactions of NHCs with metallocenes have recently been reported and products of the type [$Cp_2M(NHC)_{1\ or\ 2}$] may be isolated which contain varying degrees of Cp ring slippage or even complete Cp^- ring dissociation, as in the formation of $[CpNi(IMe)_2]^+[Cp]^-$ (IMe = :C{N(Me)C(Me)}$_2$).[2, 3] In comparison, treatment of Cp_2M (M = Ni, Co) with **1** under any stoichiometry results in the

formation of $[(\{(H)CN(Ar)\}_2Ga)_2M(\mu\text{-}Cp)K(TMEDA)(\mu\text{-}Cp)K(\mu\text{-}PhMe)_{0.5}]_\infty$, **2**,[4] in moderate yields (*ca.* 46 %) (Scheme 1).

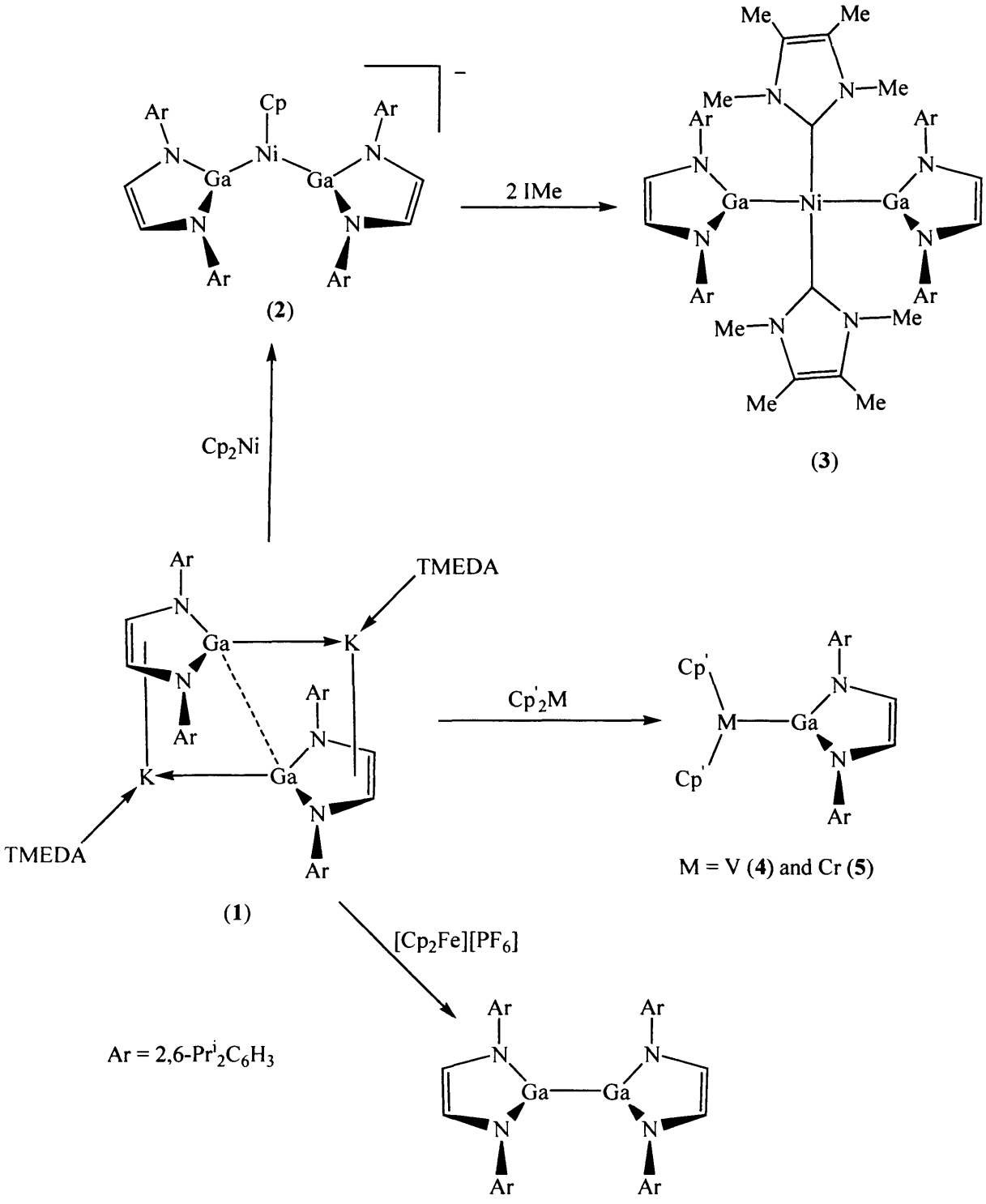

Scheme 1

This complex arises from the displacement of a Cp^- ligand, which unusually is incorporated in the product. Dissolution of the complex in Et_2O leads to the monomeric contact ion pair, $[(TMEDA)(Et_2O)K(\mu\text{-}\eta^5\text{-}Cp)Ni\{:Ga[N(Ar)C(H)]_2\}_2]$, Scheme 1. This is an anionic analogue of the NHC complex, $[CpNi(NHC)_2]^+$.[2] The structure of **2** shows a short Ni—Ga bond length (2.2175 Å average); the only shorter Ni—Ga bond is that in $[Ni\{GaC(SiMe_3)_3\}_4]$ (2.1700(4) Å)[5] for which significant Ni—Ga back bonding has been suggested. The reaction of **2** with excess $[:C\{N(Me)C(Me)\}_2]$ was also investigated and the complex $[Ni\{C[N(Me)C(Me)]_2\}_2\{Ga[N(Ar)C(H)]_2\}_2]$, **3**,[4] could be isolated in a 42 % yield. The Ni—C bond lengths in this are typical for other NHC complexes of nickel but the Ni—Ga bond lengths are approximately 0.11 Å longer than in **2**. This is presumably due to the *trans* disposition of the gallium heterocycles but also suggests that there may be back bonding in **2**. Preliminary DFT calculations on a model of **3** shows that there is a significant increase in the positive charge (+0.803 average) on the gallium centres compared to that in the free heterocycle (+0.263), whilst the nickel centre is almost neutral (+0.079).

Somewhat surprisingly, **1** does not react with ferrocene but does with $[Cp_2Fe][PF_6]$. This gives rise to the known digallane, $[\{(Ar\text{-}DAB)Ga\}_2]$,[6] *via* an oxidative coupling of two anionic fragments of **1** with the elimination of KPF_6 and formation of ferrocene.[7] A different reactivity pattern was again observed when **1** was reacted with Cp'_2M ($Cp' = C_5H_4Me$; M = V, Cr). These reactions afforded complexes of the type $[Cp'_2M\{Ga[N(Ar)C(H)]_2\}]$ (M = V (**4**); Cr (**5**)) in low yields (~10 %), *i.e.* M(III) compounds (Scheme 1). This can be rationalised by the oxidative coupling of two anionic fragments of **1** to give the digallane, which then oxidatively adds to excess metallocene. Indeed, the reactions of Cp'_2M with the digallane give the same products in much enhanced yields. As yet it is not known what causes the oxidation of **1** in its reactions with Cp'_2M.

These complexes, **4** and **5**, are paramagnetic and have magnetic moments expected for d^2 and d^3 metal centres. The solid-state structures of both compounds have been measured. Compound **4** contains the first example of a structurally characterised V—Ga bond (V—Ga = 2.5303 Å) so no conclusions can be drawn as to any back-bonding into the empty *p* orbital on the gallium centre. Compound **5** does show a short Ga—Cr bond length of 2.4231(11) Å which could suggest Cr—Ga back bonding in this complex.[8] With this in mind DFT calculations are being carried out.

Jones *et al* have also examined the reactivity of **1** towards metal carbonyl compounds (Scheme 2). Compound **1** reacts smoothly with $Fe(CO)_5$ to give the compound [K(TMEDA)] $[(CO)_5Fe\{Ga[N(Ar)C(H)]_2\}]$, **6**, in moderate yield (54 %).[9] The facile nature of the CO displacement reaction is consistent with the strong σ-donor nature of the gallium carbene analogue. The crystal structure reveals this compound to be polymeric, through bridging potassium centres co-ordinated by a molecule of TMEDA, 2 equatorial carbonyl oxygens and an η^2-interaction to one of the heterocycle's arene substituents. The Ga—Fe bond length (2.3068(8) Å) is significantly longer than that in $[(Ar^*Ga)Fe(CO)_4]$ [Ar* = $C_6H_3(C_6H_2Pr^i_3$-2,4,6)$_2$-2,6)] (2.248(7) Å)[10] or $[Fe(CO)_4\{Ga[N(Ar)C(Me)]_2CH\}]$ (2.2851 Å).[11] Additionally the CO stretching frequencies in the infrared spectrum are at significantly lower frequencies (*ca.* 20 - 30 cm^{-1}) than in related neutral $[Fe(CO)_4(NHC)]$ compounds. These two features suggest that there is little back-bonding into the *p*-orbital of the gallium, which is associated with the LUMO of the free ligand. This parallels the chemistry of NHC's.[12, 13]

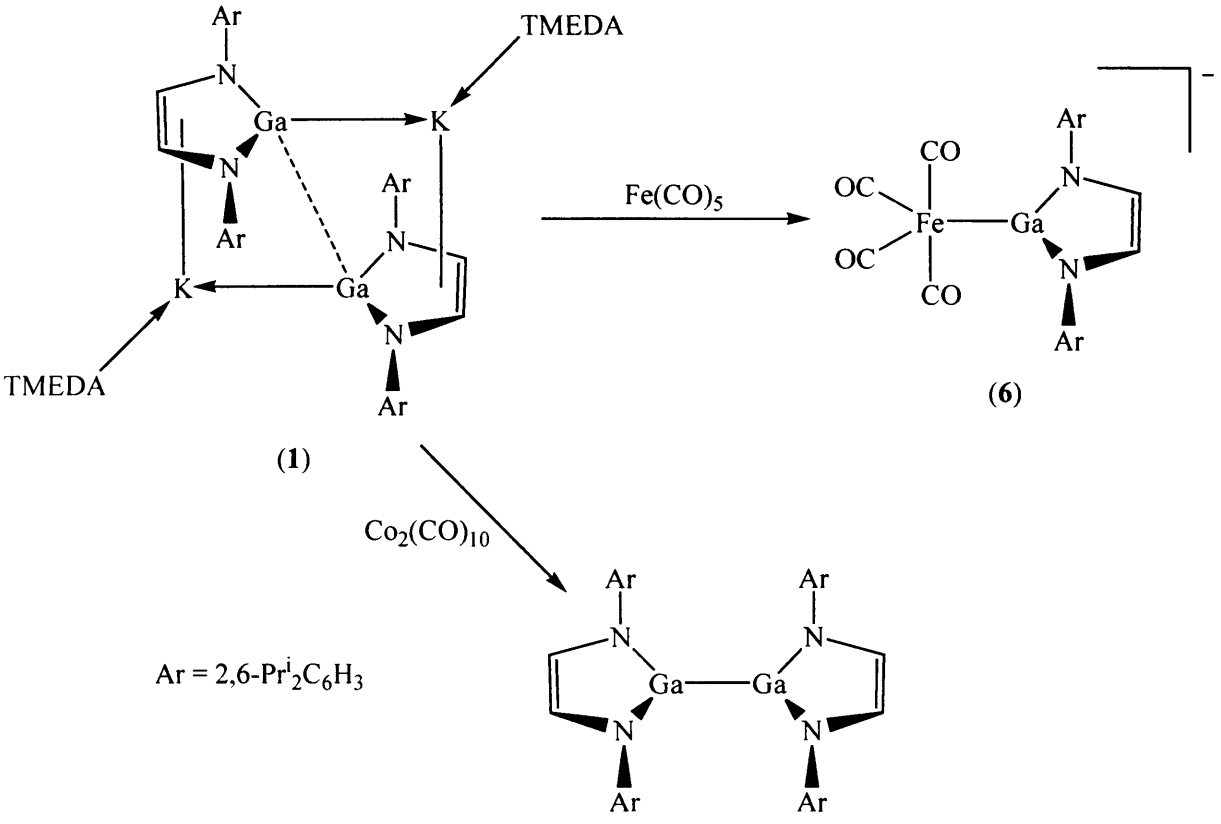

Scheme 2

Compound **6** has also been the subject of a theoretical study to determine the amount of Fe—Ga back bonding it exhibits. A CDA analysis gave a dative/back-bonding ratio (d/b) of 3.40 for the model complex, $[Fe(CO)_4\{Ga[N(H)C(H)]_2\}]^-$, which is close to that in the neutral NHC complex $[Fe(CO)_4\{C[N(H)C(H)]_2\}]$ (d/b = 3.39) and indicates negligible back bonding in either of these compounds (*c.f.* d/b = 1.75 for the Fe—C_{axial} in $Fe(CO_5)$). Natural population analysis showed a significant development of positive charge at the gallium centre relative to the free heterocycle, whilst there was a build up of negative charge at the iron centre relative to $Fe(CO)_5$ and the NHC compound. Finally, the Fe—Ga bond dissociation energy, D_e (94.0 kcal mol^{-1}) was found to be higher than D_e for the Fe—C bonds in the NHC complex (D_e = 64.9 kcal mol^{-1}) and $Fe(CO)_5$ (D_e = 52.2 kcal mol^{-1}). This observation is consistent with facile CO displacement in the formation of **6**.[14]

Reaction of **1** with $Co_2(CO)_8$ gives rise to the digallane, $[\{(Ar\text{-}DAB)Ga\}_2]$, in good yield (95 %). In this reaction, **1** reduces $Co_2(CO)_8$ to $[K][Co(CO)_4]$ whilst two anionic fragments undergo an oxidative coupling reaction to give the digallane. This is a much easier synthetic pathway to the digallane and investigations of its reactivity in relation to diboranes are currently being undertaken.[7] This is perhaps not unsurprising as it has been reported that electron rich alkenes such as $(Me_2N)_2C{=}C(NMe_2)_2$ will also reduce $Co_2(CO)_8$ to give the salt $[(Me_2N)_2C\text{-}C(NMe_2)_2]^{2+}[Co(CO)_4]_2$.[15] In comparison, the first example of an NHC complex of cobalt carbonyl has very recently been reported,[16] and it was also found that treatment of $Co_2(CO)_8$ with the NHC ligand gave the salt $[Co(CO)_3(IMes)_2][Co(CO)_4]$, which is in equilibrium with the neutral complex, $[Co_2(CO)_6(IMes)_2]$.

4.3 Research Proposal

Reduction of [GaI_2(Ar-DAB)] leads to the isolation of a novel valence isoelectronic gallium N-heterocyclic carbene analogue, as described in Chapter 3. There has been intense interest in N-heterocyclic carbene (NHC) ligands forming complexes spanning the whole range of the periodic table,[1] including a considerable number of *p*-block complexes.

The aim of this work was the study of the reactivity of the gallium carbene analogue, **1**, towards main group metal precursors and to compare the chemistry and properties of formed complexes with related NHC and group 13 diyl main group complexes.

4.4 Results and Discussion

4.4.1 Decomposition products derived from reactions of an anionic gallium(I) carbene analogue

In an attempt to prepare a gallium-hydride compound from the reaction of nucleophilic **1** with HBF_4 in a 1:2 stoichiometry in diethyl ethyl ether, only the amino-imine decomposition product, **7**, could be isolated in low yield (Scheme 3).

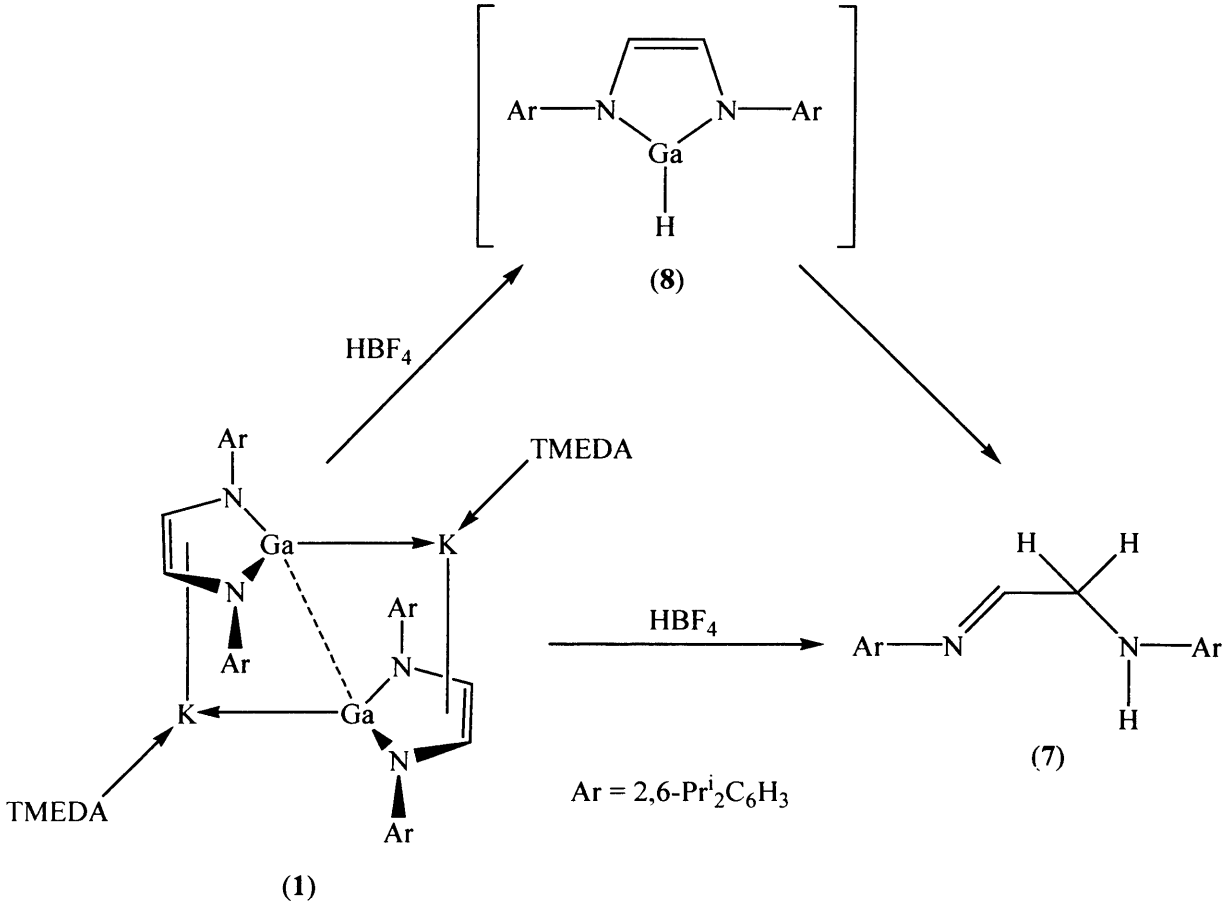

Scheme 3

The mechanism of formation of **7** is presumably *via* an intramolecular hydro-metallation reaction of the diazabutadiene backbone of the gallium hydride intermediate, **8**. The fate of the gallium in this reaction is not known. Compound **7** has been fully characterised and the spectroscopic data are consistent with its structure. For instance, the NH and CH_2 groups may be identified in the ^{1}H-NMR spectrum at δ 5.07 and δ 3.84 ppm, respectively, and the

^{13}C-NMR spectrum shows the CH_2 group at δ 54.3 ppm. IR spectroscopy indicates a strong, broad N—H stretch at 3450 cm^{-1}. To confirm this, X-ray crystallographically studies have been carried out and the molecular structure of **7** is shown in Figure 1.

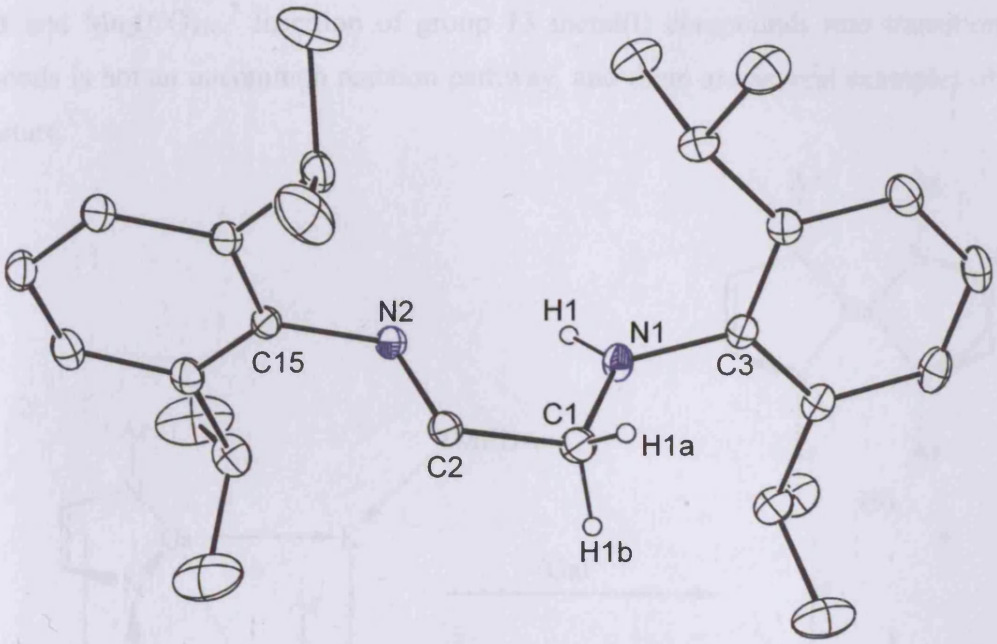

Figure 1 Molecular structure of [ArN=CHCH$_2$N(H)Ar] (**7**)

Selected bond lengths (Å) and angles (°): C(1)—N(1) 1.443(24), C(2)—N(2) 1.259(22), N(1)—C(3) 1.424(51), N(2)—C(15) 1.430(14), C(1)—C(2) 1.489(47), C(2)—C(1)—N(1) 110.58(7), C(1)—C(2)—N(2) 120.44(3), C(2)—N(2)—C(15) 120.92(7), C(1)—N(1)—C(3) 117.49(5).

The C—N bond lengths in compound **7** differ significantly [C(1)—N(1) 1.443(24) Å and C(2)—N(2) 1.259(22) Å] and therefore indicate the amino-imine nature of the compound.

The reaction of 'GaI' with the carbene analogue, **1**, in toluene was hoped to give a sub-valent gallium cluster compound incorporating the gallium heterocycle. Instead, it gave two products, **9** and **10** in low yield (Scheme 4). The mechanism of formation for **9** and **10** is unknown at present but presumably involves a combination of salt elimination and disproportionation reactions. Although not a main group metal precursor, the reaction of

$[Mo(CO)_2Br_2(PPh_3)_2]$ with **1** similarly affords **11** (Scheme 4). In this case, the formation of **11** probably involves an initial insertion of gallium centre into the M—Br bond, to give an intermediate with an unstable Ga—M bond, which undergoes homolytic cleavage and subsequently **11**. This reaction has precedent[17] in the reaction of $Mn(CO)_5Br$ with **1** which gives **11** and $Mn_2(CO)_{10}$.[7] Insertion of group 13 metal(I) compounds into transition metal halide bonds is not an uncommon reaction pathway, and there are several examples of this in the literature.[17]

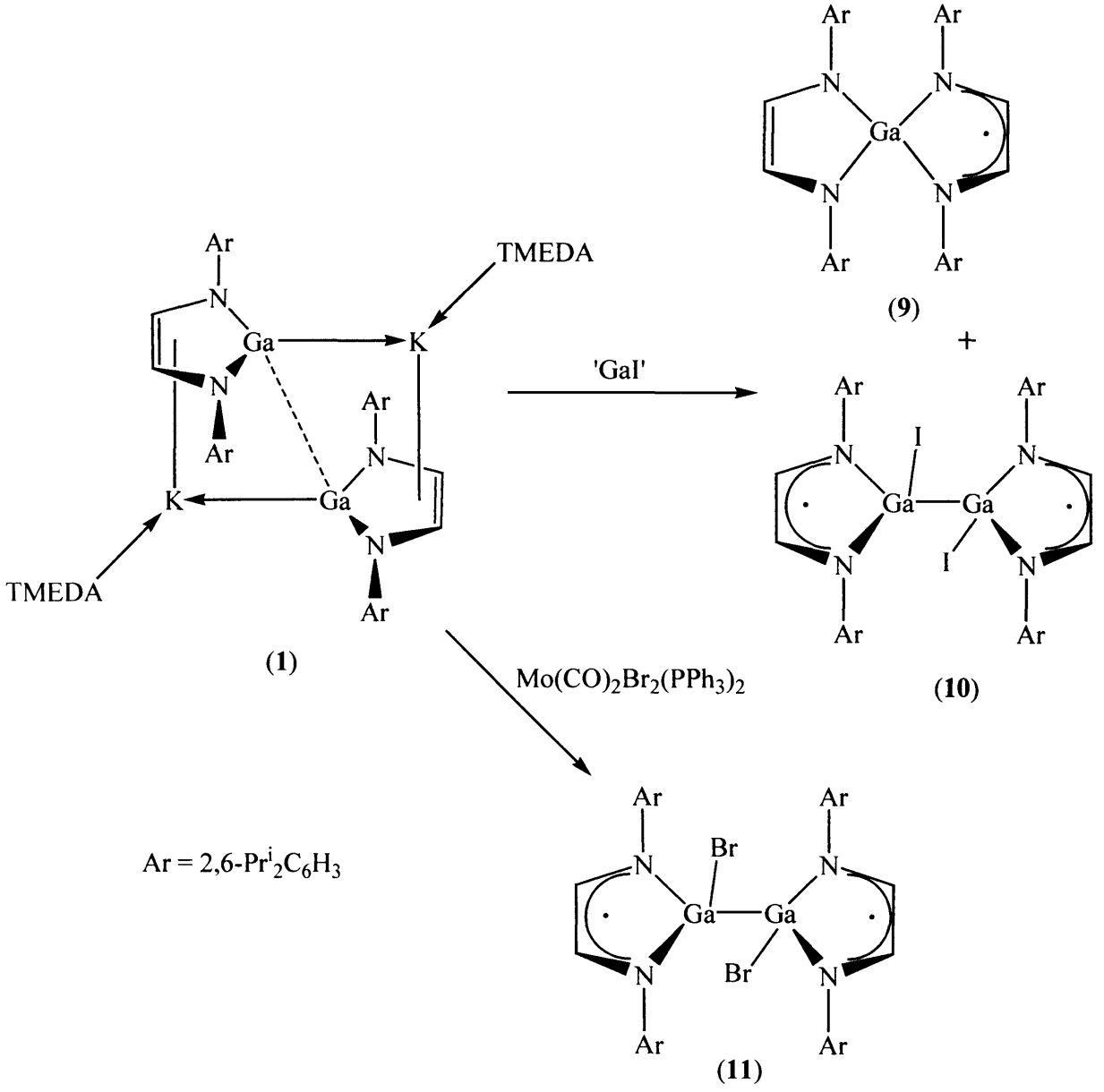

Scheme 4

Compounds **9-11** are paramagnetic, so no meaningful NMR spectroscopy could be obtained. Therefore their identities have been elucidated by X-ray crystallography and the molecular structures are shown in Figures 2-4, respectively.

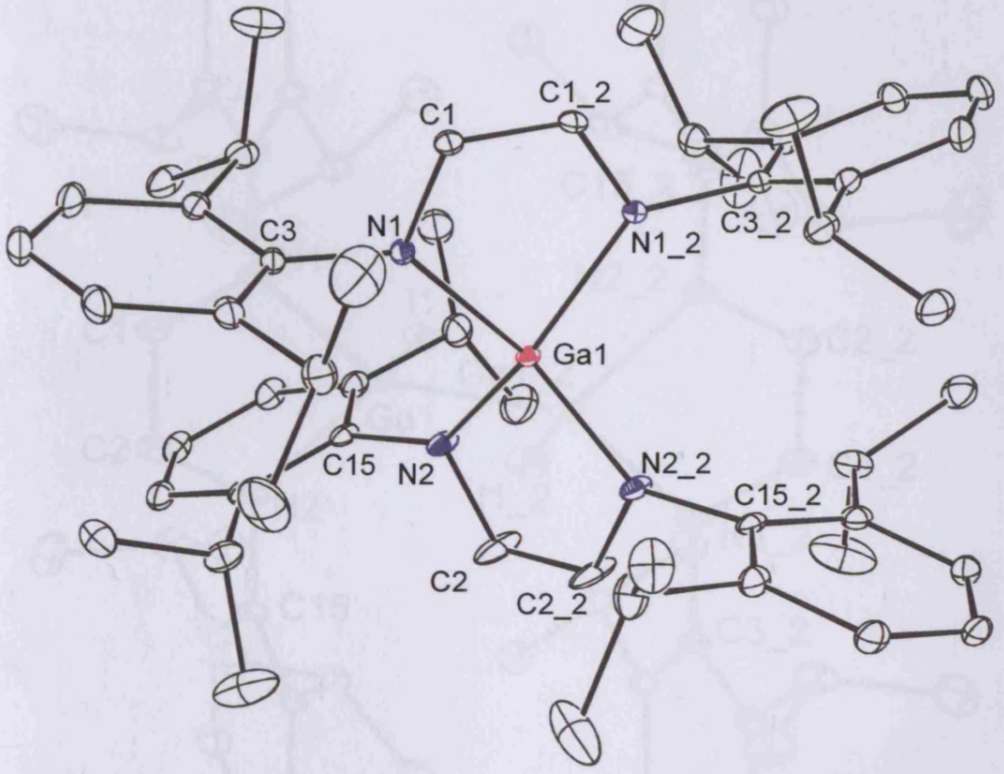

Figure 2 Molecular structure of [(Ar-DAB)Ga(Ar-DAB$^{\bullet}$)] (**9**)

Selected bond lengths (Å) and angles (°): Ga(1)—N(1) 2.007(13), Ga(1)—N(2) 1.901(43), N(1)—C(1) 1.332(4), C(1)—C(1_2) 1.386(15), N(2)—C(2) 1.392(33), C(2)—C(2_2) 1.338(2), N(2)—C(15) 1.438(32), N(1)—Ga(1)—N(1_2) 82.07(3), Ga(1)—N(1)—C(1) 110.99(5), N(1)—C(1)—C(1_2) 117.96(7), N(2)—Ga(1)—N(2_2) 88.33(4), Ga(1)—N(2)—C(2) 107.72(3), N(2)—C(2)—C(2_2) 188.09(4).

The bond lengths within the two diazabutadiene ligands of **9** are significantly different, indicating that one ligand has been doubly reduced whilst the other has an unpaired electron

delocalised over the ligand. The bond lengths in both ligands are very similar to that in the known complex [Ga(Bu^t-DAB)$_2$],[18] as would be expected.

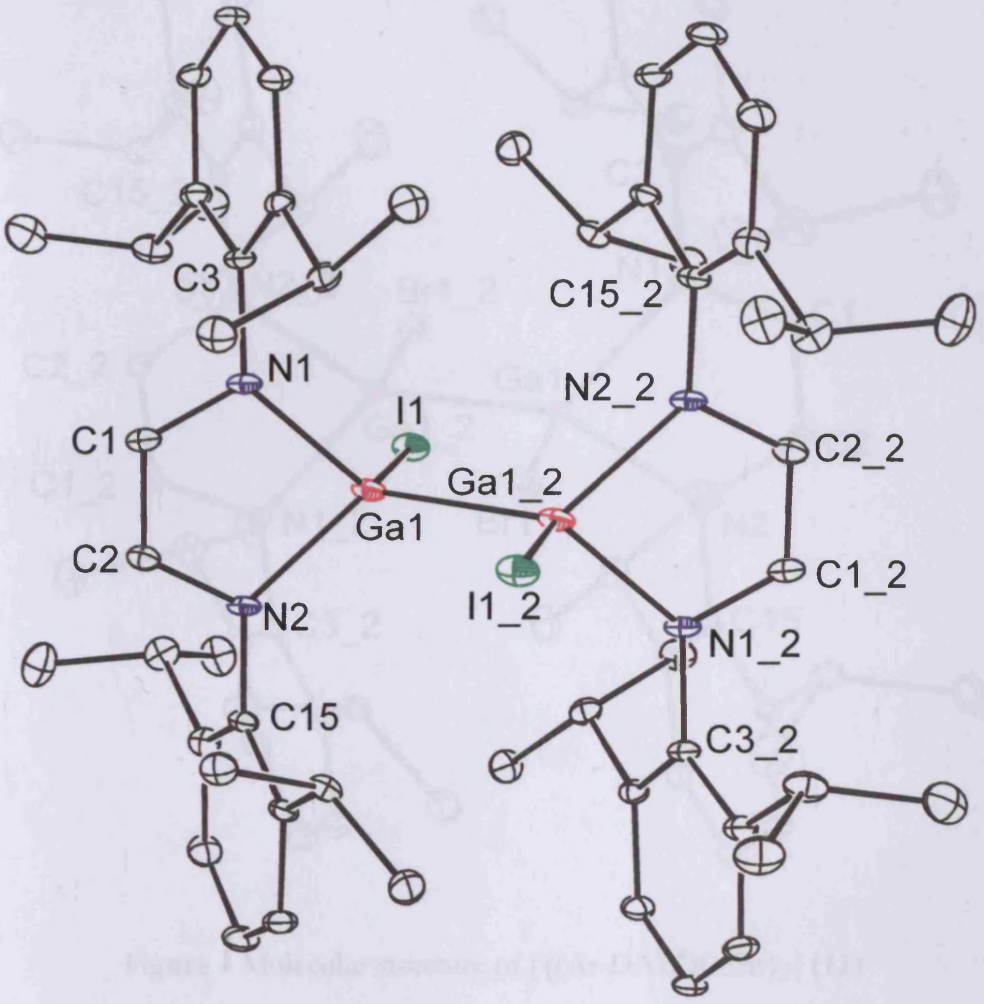

Figure 3 Molecular structure of [{(Ar-DAB$^{\bullet}$)GaI}$_2$] (**10**)

Selected bond lengths (Å) and angles (°): Ga(1)—N(1) 1.984(2), Ga(1)—N(2) 1.996(3), Ga(1)—I(1) 2.586(9), Ga(1)—Ga(1_2) 2.575(9), N(1)—C(1) 1.339(4), N(1)—C(3) 1.445(4), N(2)—C(2) 1.332(4), N(2)—C(15) 1.443(3), N(1)—Ga(1)—N(2) 83.96(9), N(1)—Ga(1)—I(1) 106.17(7), N(2)—Ga(1)—I(1) 104.85(7), N(1)—Ga(1)—Ga(1_2) 121.84(7), N(2)—Ga(1)—Ga(1_2) 121.78(7), I(1)—Ga(1)—Ga(1_2) 113.75(3), C(1)—N(1)—Ga(1) 109.83(19), C(2)—N(2)—Ga(1) 110.24(19), N(1)—C(1)—C(2) 118.45(3), N(2)—C(2)—C(1) 117.46(3).

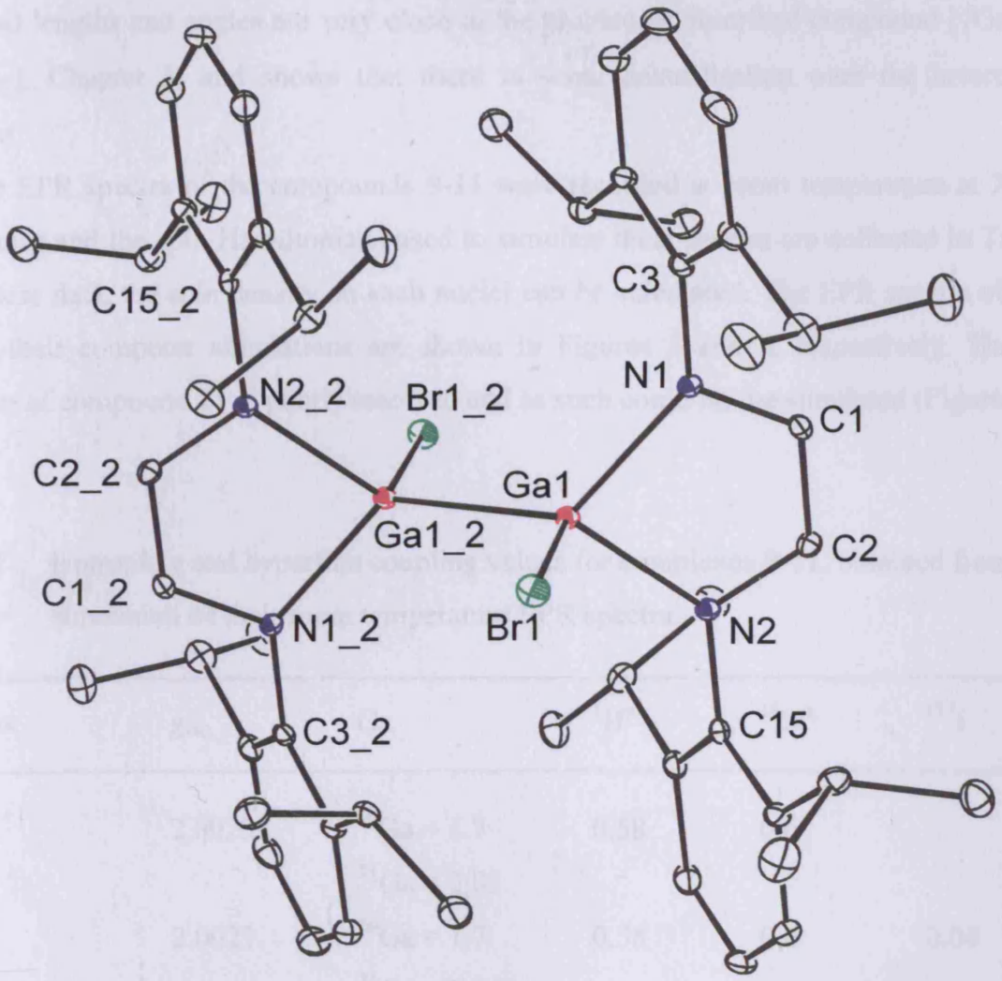

Figure 4 Molecular structure of [{(Ar-DAB$^{\bullet}$)GaBr}$_2$] (**11**)

Selected bond lengths (Å) and angles (°): Ga(1)—N(1) 1.983(1), Ga(1)—N(2) 1.981(4), Ga(1)—Br(1) 2.374(8), Ga(1)—Ga(1_2) 2.466(7), N(1)—C(1) 1.346(2), N(1)—C(3) 1.433(2), N(2)—C(2) 1.340(1), N(2)—C(15) 1.433(2), N(1)—Ga(1)—N(2) 83.91(7), N(1)—Ga(1)—Br(1) 104.25(5), N(2)—Ga(1)—Br(1) 104.44(5), N(1)—Ga(1)—Ga(1_2) 123.37(8), N(2)—Ga(1)—Ga(1_2) 122.90(5), Br(1)—Ga(1)—Ga(1_2) 113.22(3), C(1)—N(1)—Ga(1) 109.64(25), C(2)—N(2)—Ga(1) 110.03(21), N(1)—C(1)—C(2) 118.22(2), N(2)—C(2)—C(1) 118.05(4).

In compounds **10** and **11** the gallium(II) centres sit in distorted tetrahedral environments. The bond lengths and angles are very close to the previously described compound [{GaI(Bu^t-DAB$^\bullet$)}$_2$], Chapter 3, and shows that there is some delocalisation over the heterocyclic fragment.

The EPR spectra of the compounds **9-11** were recorded at room temperature at X-band frequencies and the spin Hamiltonians used to simulate their spectra are collected in Table 1. From these data, the spin density on each nuclei can be calculated. The EPR spectra of **9** and **10** and their computer simulations are shown in Figures 5 and 6, respectively. The EPR spectrum of compound **11** is poorly resolved and as such could not be simulated (Figure 7).

Table 1 Isotropic *g* and hyperfine coupling values for complexes **9-11**, obtained from simulation of their room temperature EPR spectra.

Complex	g_{iso}	Ga	$^1H^a$	$^{14}N^a$	^{127}I
9	2.0023	^{69}Ga = 1.7 ^{71}Ga = 2.05	0.58	0.6	
10	2.0023	^{69}Ga = 1.7 ^{71}Ga = 2.05	0.58	0.6	0.04
11	2.0034				

All isotropic hyperfine couplings in mT. [a] ^{1}H refers to two equivalent imine protons and ^{14}N refers to the two equivalent nitrogen nuclei.

The EPR spectra of **9** and **10** are very similar and both have been satisfactorily simulated using an isotropic *g* value of g_{iso} = 2.0023, and hyperfine splittings to two equivalent protons (a_{iso} = 0.58 mT) and nitrogen (a_{iso} = 0.6 mT) centres. In addition, a splitting arising from an electron interaction with the gallium nucleus was also observed. These $^{69, 71}$Ga couplings indicate that the unpaired isotropic spin density on the gallium nuclei in **9** and **10** remains very small (0.37 %), with only a very small interaction to the iodine nucleus in **10** (0.04 mT).

In all complexes **9-11**, the *g* values are close to free spin, indicating the organic nature of the radical.

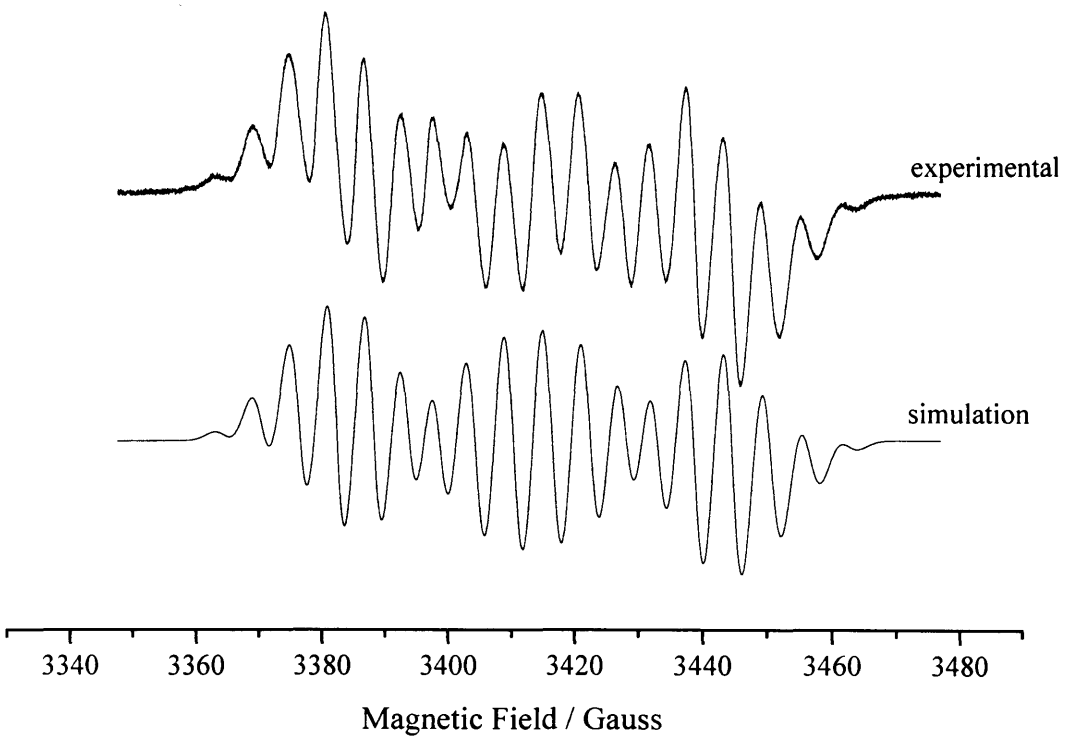

Figure 5 X-band EPR spectrum and computer simulation of [(Ar-DAB)Ga(Ar-DAB$^{\bullet}$)] (**9**) in CD_2Cl_2/C_7D_8 (50 : 50) at 298 K.

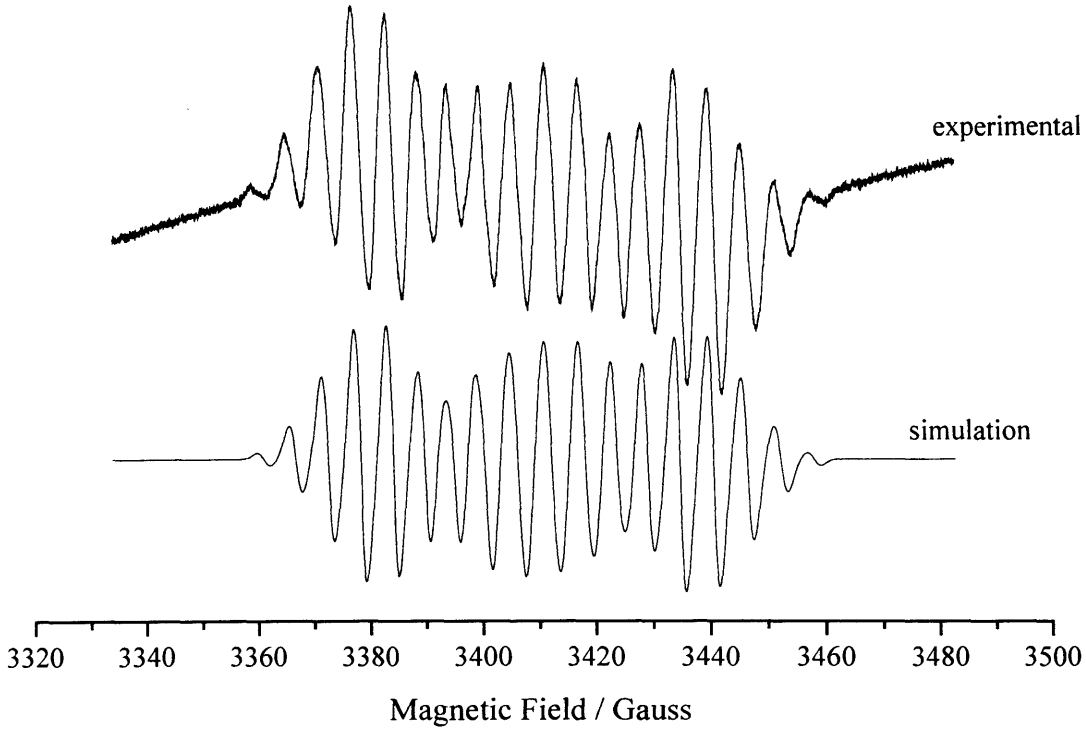

Figure 6 X-band EPR spectrum and computer simulation of [{(Ar-DAB$^{\bullet}$)GaI}$_2$] (**10**) in CD_2Cl_2/C_7D_8 (50 : 50) at 298 K.

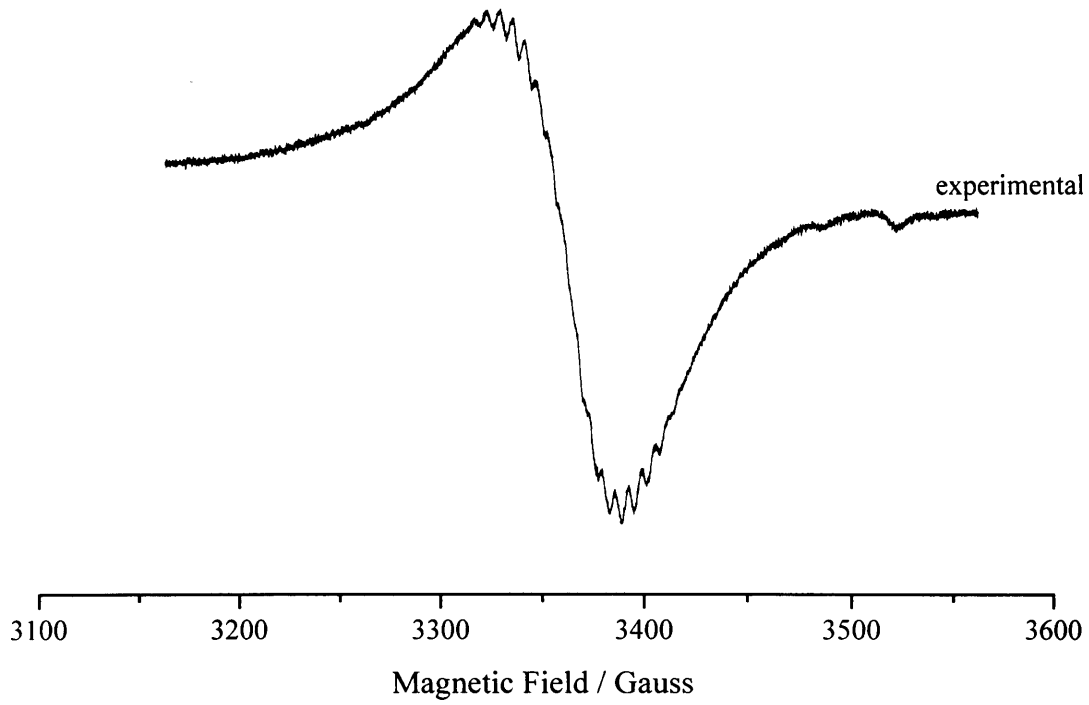

Figure 7 X-band EPR spectrum of [{(Ar-DAB$^{\bullet}$)GaBr}$_2$] (**11**) in CD_2Cl_2/C_7D_8 (50 : 50) at 298 K.

Several other reactions of the gallium carbene analogue, **1**, towards main group precursors have been carried out. The reactions with InCl, InBr, $InBr_3$, $GaCl_3$, $MesBBr_2$ [Mes = mesityl (2,4,6-trimethylphenyl)] and $(CH_3)_2S{\cdot}BH_3$ in 1:1 and 2:1 stoichiometries did not form discrete complexes, instead ligand and metal (Ga, In) formation has been observed. The reaction of Ph_2PCl towards **1** yielded the known digallane complex, [{(Ar-DAB)Ga}$_2$][19] and PPh_2H. In this reaction the product, PPh_2H was identified by ^{31}P-NMR spectroscopy, δ –40 ppm.[20] An explanation for the formation of these products cannot be given at this stage, but presumably, they involve complex mechanisms. Finally, the 1:1 reaction of $GaCp_3$ with **1**, also gave the known compound [{(Ar-DAB)Ga}$_2$],[19] whilst Cy_2GaCl (Cy = cyclohexyl) reacted with **1** to give **9**.

4.4.2 Reactivity of a gallium(I) carbene analogue with group 16 complexes

Organometallic group 13 oxide compounds have gained prominence since the discovery that partially hydrolysed Me_3Al is a highly effective co-catalyst in olefin polymerisation.[21] Whilst there are many examples of alumoxanes, $(RAlO)_n$ (n typically 4 – 8), the analogous galloxane chemistry is less well developed and there are only few structurally characterised examples, *e.g.* $[(Bu^t)_3SiGaO]_4$[22] and $[\{HC[(Me)C(Dipp)N]_2\}GaO]_2$ (Dipp = diisopropyl-phenyl).[23] Therefore it was thought of sufficient interest to examine the reactivity of the anionic gallium carbene analogue, **1**, towards oxygen sources. Exposure of **1** to either dry air or O_2 results in complete oxidation and the diazabutadiene ligand is the only isolable compound. However, treatment of THF solutions of **1** with stoichiometric amounts of N_2O gives rise to $[K(TMEDA)]_2[(Ar\text{-}DAB)_2GaO)_2]$, **12**, in low yield (Scheme 5). The NMR spectra of this compound are almost indistinguishable from that of **1** so X-ray crystallography was used to prove its identity, and the molecular structure of **12** is shown in Figure 8. The molecule is dimeric and sits on a centre of inversion. The dimer is held together by (μ-O) bridges and also by η^5-interactions between the heterocycles and potassium centres. The Ga—O bond lengths are different with one short [1.814(3) Å] and one longer [1.905(3) Å]. There are no known examples of compounds containing a dianionic Ga_2O_2 core, however the bond lengths compare favourably with other Ga—O examples in the literature, *e.g.* $[\{HC[(Me)C(Dipp)N]_2\}GaO]_2$ [1.851(3) Å average] or $[Mes_2GaOLi]_2$ [1.897 Å average].[24] The asymmetry observed may be due to partial multiple bonding in the Ga—O fragment, as p-p overlap may be favoured. The Ga_2O_2 core forms almost a perfect rectangle (Ga—O—Ga = 89.00(14)°; O—Ga—O = 91.00(14)°). The Ga—Ga separation is 2.608 Å, which is shorter than observed in **1** [2.8745(15) Å], and close to typical Ga—Ga bonds. However, there is probably little Ga—Ga interaction in **12** due to the smaller ionic radii of Ga(III) compared to Ga(I) in **1**. In addition, co-ordination of electronegative oxygen atoms would make the gallium centres more ionic in **12**, and would subsequently lead to a smaller effective radius. Moreover, the Ga—K distance in **12** is shorter than in **1** [3.1383(16) Å and 3.5318(18) Å, respectively] whilst the K—C and K—N bonds are longer [3.2355 Å and 3.013 Å average; 3.1145 Å and 3.030 Å]. Furthermore, the angle between the K-heterocycle centroid-Ga is more acute in **12** than compared to **1** [84.24° and 97.88°, respectively] indicating that the

potassium centre has moved from the heterocycle towards the Ga—O fragment with which it appears to have an interaction.

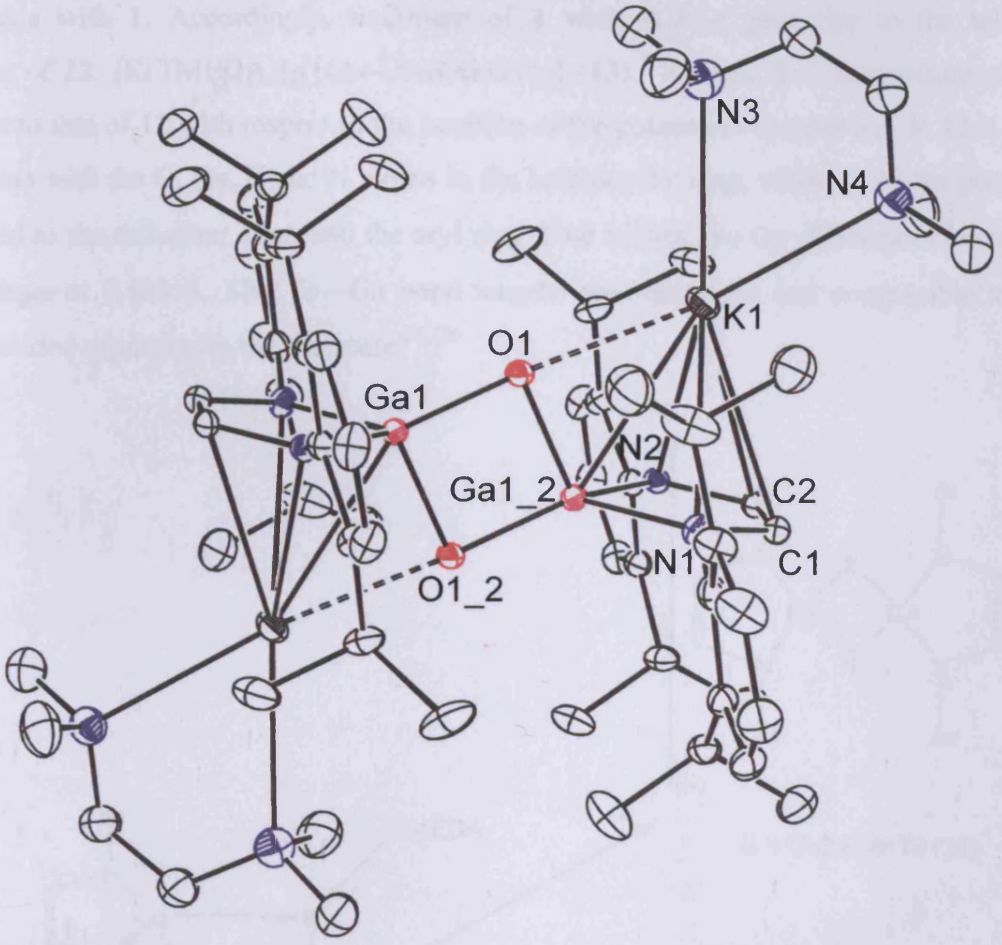

Figure 8 Molecular structure of $[K(TMEDA)]_2[\{(Ar\text{-}DAB)GaO\}_2]$ (**12**)

Selected bond lengths (Å) and angles (°): Ga(1)—O(1) 1.814(3), Ga(1)—O(1_2) 1.905(3), Ga(1_2)—N(1) 1.924(4), Ga(1_2)—N(2) 1.923(4), Ga(1_2)—K(1) 3.1383(16), K(1)—O(1) 2.584(3), K(1)—N(4) 2.883(5), K(1)—N(3) 2.987(6), K(1)—N(1) 3.088(4), K(1)—N(2) 3.140(4), K(1)—C(1) 3.226(5), K(1)—C(2) 3.245(5), N(1)—C(1) 1.408(6), N(2)—C(2) 1.403(6), C(1)—C(2) 1.3467(7), O(1)—Ga(1)—O(1_2) 91.00(14), O(1)—Ga(1_2)—N(2) 129.19(15), O(1_2)—Ga(1_2)—N(2) 111.07(15), O(1)—Ga(1_2)—N(1) 128.02(16), O(1_2)—Ga(1_2)—N(1) 110.00(16), N(2)—Ga(1_2)—N(1) 87.67(16), O(1)—Ga(1_2)—K(1) 146.30(10), N(2)—Ga(1_2)—K(1) 72.23(12), N(1)—Ga(1_2)—K(1) 70.59(13), O(1)—K(1)—N(4) 169.46(14), O(1)—K(1)—N(3) 111.21, N(4)—K(1)—N(3) 61.90(16).

Given that NHC ligands react readily with elemental S, Se and Te, parallel efforts in the Jones group (carried out by Dr. R.J. Baker) have been directed to extending these reactions of chalcogens with **1**. Accordingly, treatment of **1** with Et_3PTe gave rise to the tellurium analogue of **12**, $[K(TMEDA)]_2[\{(Ar\text{-}DAB)GaTe\}_2]$ (**13**),[7] Scheme 5. The structure of **13** is different to that of **12** with respect to the position of the potassium counter ion. In **12** it has an interaction with the O, Ga, C and N atoms in the heterocyclic ring, whilst in **13** the potassium is bonded to the tellurium atom and the aryl ring. Due to this, the Ga···Ga separation in **13** is much larger at 3.408 Å. The Te—Ga bond lengths are equivalent and comparable to other single bonded examples in the literature.[25, 26]

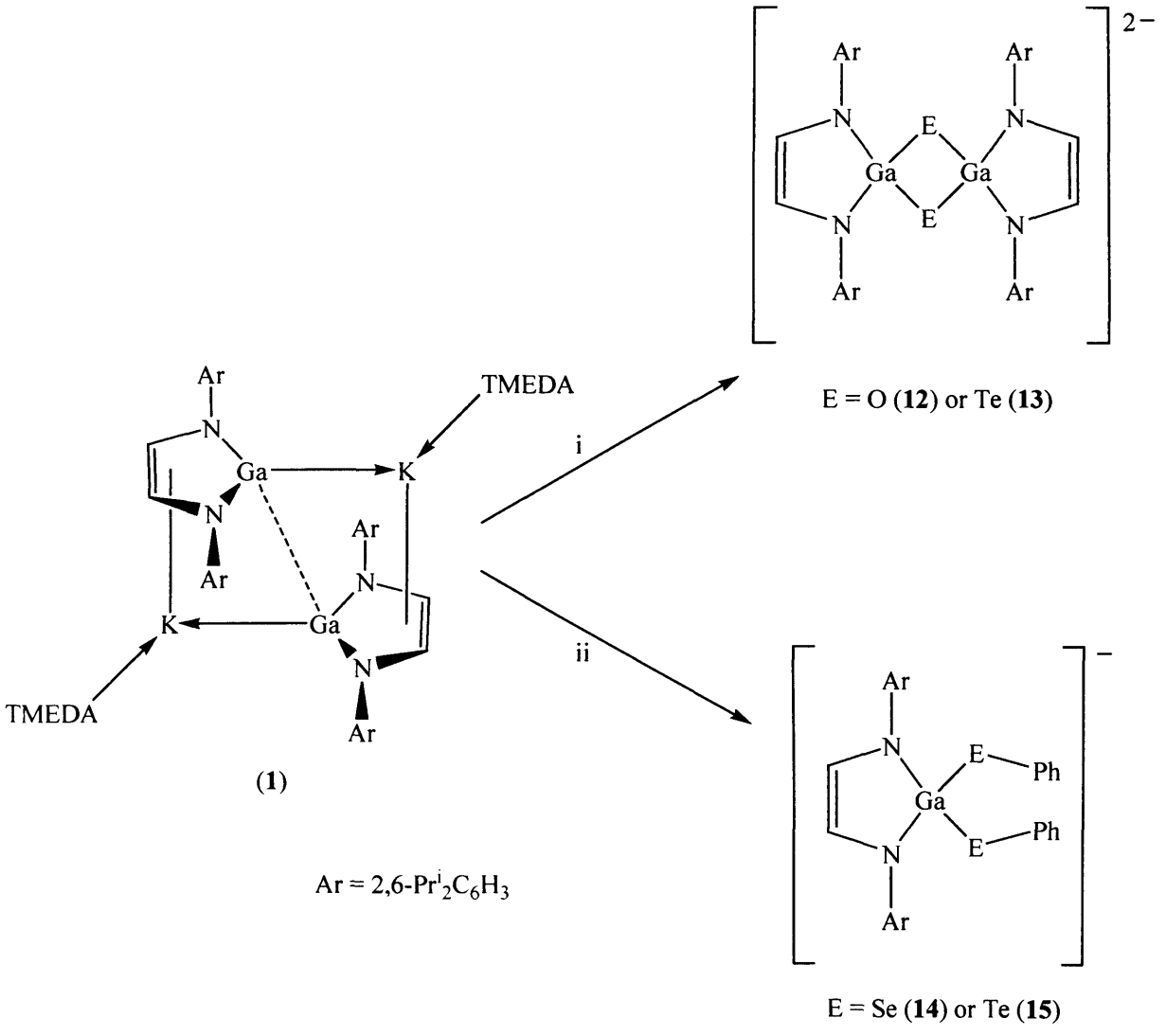

Scheme 5 Reagents and conditions: i, N_2O or Et_3PTe, Et_2O; ii, Ph_2E_2, Et_2O.

Also investigated by other members of the Jones group, have been the reactions of Ph_2E_2 (E = Se, Te) with **1** (Scheme 5). As expected, the E—E bond is cleaved and compounds of the type $[(Ar\text{-}DAB)Ga(EPh)_2]^-$ (E = Se (**14**); Te (**15**)) may be isolated *via* oxidative insertion mechanisms.[7] Both structures differ in the interaction of the anion with the potassium cation. In **14** the structure is polymeric with potassium-selenium and further K-arene interactions, whilst **15** is monomeric with the potassium chelated by two tellurium atoms. Additionally, the E—Ga bond lengths are asymmetric in both examples and **15** could perhaps be described as an '-ate' complex of KTePh.

4.4.3 Reactivity of *p*-block cyclopentadienyl complexes towards a gallium(I) carbene analogue

Given the success of transition metal metallocene reactions with **1**, and the evolving area of main group NHC co-ordination chemistry,[27, 28] investigations of the reactivity of main group Cp compounds with **1** have been carried out.

Treatment of **1** with one equivalent of TlCp led to thallium metal deposition and the formation of the cyclopentadienyl bridged digallane complex, **16**, in moderate yield (46 %) (Scheme 6). The mechanism of this reaction seemingly involves an oxidative coupling of anionic **1** to form the digallane, $[\{Ga(Ar\text{-}DAB)\}_2]$, **17**,which complexes half the generated KCp to give **16**. It is noteworthy that the digallane, **17**, has been reported by Jutzi *et al*,[6] to be formed by photolysis of the galladiazole, $[(\eta^1\text{-}Cp^*)Ga(Ar\text{-}DAB)]$. It has also been shown that **17** can alternatively be prepared in high yield *via* oxidative coupling of **1** with $[FeCp_2]^+$ or $[Co_2(CO)_8]$.[7] This result is comparable to the recently reported ferrocenium induced oxidative coupling of NHCs.[29] The proposed mechanism of formation of **16** seems feasible when it is considered that the direct reaction of **17** with KCp in the presence of excess TMEDA also leads to **16** in good yield (56 %).

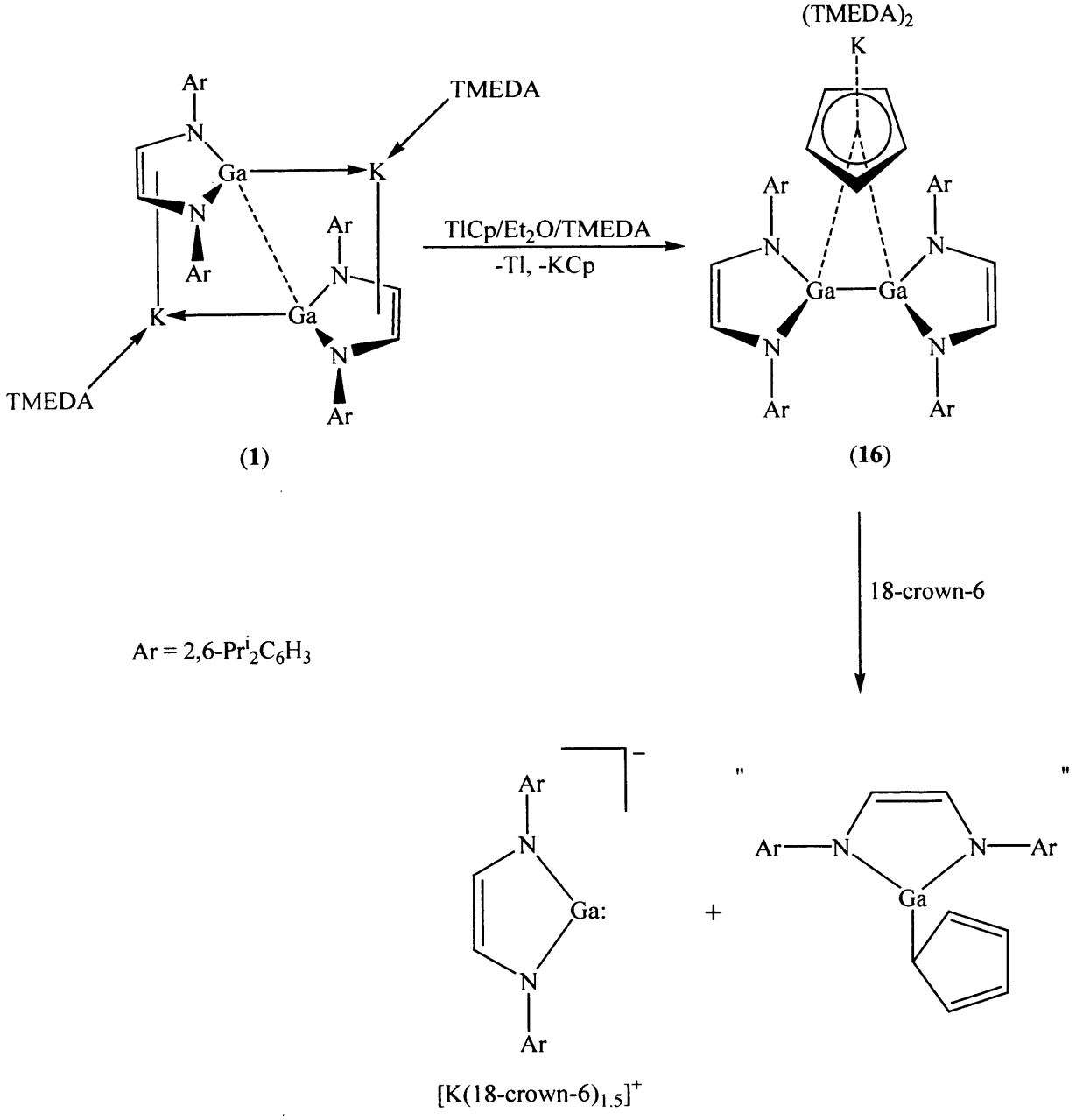
(TMEDA)2
K
Ar
TMEDA
N
Ga
K
N
Ar
Ar
N
Ga
K
TMEDA
N
Ar
TlCp/Et2O/TMEDA
-Tl, -KCp
Ar
Ar
N
N
Ga
Ga
N
N
Ar
Ar
(1)
(16)
18-crown-6
Ar = 2,6-Pri2C6H3
Ar
N
Ga:
N
Ar
−
+
Ar
N
N
Ar
Ga
[K(18-crown-6)1.5]+

Scheme 6

This reaction may be compared to that of lithium alkyls with tetraorganyl digallanes which can lead to nucleophilic attack at one gallium center to give anions of the type $[R_2R'GaGaR_2]^-$, *e.g.* R = $CH(SiMe_3)_2$, R' = C≡CPh,[30] with retention of the Ga—Ga bond. In this respect **16** can be considered as an isolated intermediate in the attack of the Cp^- anion at one of its Ga centres. To test this hypothesis, decomplexation of the K center from the Cp^- anion of **16** by treating it with 18-crown-6 led to a known potassium salt of **1**, (Chapter 3) and presumably [(η^1-Cp)Ga(Ar-DAB)], though this could not be identified in the reaction mixture. This result probably stems from an increase in the nucleophilicity of the Cp^- anion upon potassium decomplexation which leads to its attack at one Ga center and subsequent Ga—Ga bond cleavage.

The spectroscopic data for **16** are largely consistent with its formualtion though resonances corresponding to the Cp^- anion were not observed in its ^1H- or $^{13}C\{^1H\}$-NMR spectra at ambient temperature, or cooling D_8-toluene solutions of **16** to –65 °C. Cooling below this temperature led to significant precipitation of the complex whilst decomposition of the complex commenced above 30 °C. These observations obviously arise from an, as yet unknown, fluxional process which is unusually slow compared to fluxional process in Ga(I) and Ga(III) cyclopentadienyl complexes.[31, 32] These are generally rapid on the NMR timescale at ambient temperature. In **16**, fluxional processes may be slowed by the bridging nature of the Cp ligand and conceivably could involve sigmatropic, haptotropic and/or 1,2-gallium shifts of the Cp ligand.

The molecular structure of **16** is depicted in Figure 9 and shows it to sit on a two-fold rotation axis which necessitates its Cp ligand to be disordered. To the best of our knowledge this represents the first structural characterization of a complex in which a Cp ligand symmetrically bridges two *p*-block metals α- to each other, and thus is related to the Cp bridged α-bimetallic transition metal systems widely explored by Werner's group.[33] It should be noted that Uhl *et al*, have recently detailed a series of related digallane complexes with bridging anionic σ-donor ligands, *e.g.* carboxylates.[34, 35] In addition, **16** can be compared to a complex incorporating a η^1: η^1-Cp ligand bridging two β-Sn centers, *viz.* $[CpNi\{SnN(Bu^t)Si(Me)_2N(Bu^t)\}_2(\mu\text{-}\eta^1\text{:}\eta^1\text{-Cp})]$.[36]

Complex **16** displays the first structurally characterized π-interaction with a Ga(II) center. In comparison, π-complexes of Ga(I) are widely known[31, 32] but those of Ga(III) are very rare and their chemistry is currently evolving.[37, 38] The Cp ligand in **16** is largely delocalised

[C—C distances 1.398(10) - 1.423(10) Å] and sits above the Ga—Ga bond with Ga—C distances [2.515(4) - 3.106(4) Å] markedly longer than normal σ-Ga—C bond lengths (approximately 2.0 - 2.2 Å).[31, 32, 39] Its mode of attachment to the digallane fragment can perhaps be best described as η^1:η^1-π- bridging as the Ga(1)—C(35) and Ga(1_2)—C(33_2) bond lengths are appreciably shorter than the other Ga—C interactions. Compared to the Ga—Ga bond in the free digallane, **17** [2.3482(2) Å],[6] that in **16** is significantly longer at 2.4461(5) Å. Moreover, the Ga centers in **16** are more pyramidal (Σ angles at Ga 346.6°) than those in **17** (Σ angles at Ga 359.6° average) which would be expected if there is partial donation of Cp π-electron density into the empty Ga *p*-orbitals of the digallane fragment in **16**.

An indication of the nature of the observed fluxionality of **16** in solution comes from an isomeric crystalline form of this compound, obtained by parallel work of Dr. R.J. Baker. Although of poor quality, the structure shows significant differences from the aforementioned described isomer in that the Cp ligand has moved considerably toward being localized.

To obtain a preliminary indication of the nature of the interaction between the Cp ligand and the fragment in **16**, DFT calculations were carried out in collaboration with Dr. Jamie Platts at Cardiff University, on the model complex, $[\{Ga[N(Me)C(H)]_2\}_2\{\mu\text{-}CpK(NH_3)_4\}]$ at the BP86/6-31G(d) level of theory. The fully optimised geometry of this complex is similar to that of the symmetrical isomer of **16** but appears to show a weaker interaction between the Cp^- anion and the digallane fragment, as evidenced by longer Ga—C distances [2.733 – 3.330 Å] and less pyramidalised gallium centres (Σ angles at Ga 353.9° average). The theoretical study also indicates a charge transfer of 0.209 electrons between the $CpK(NH_3)_4$ and digallane fragments which is consistent with small overall energy required (28.7 kJ mol^{-1}) to dissociate and fully relax these fragments.

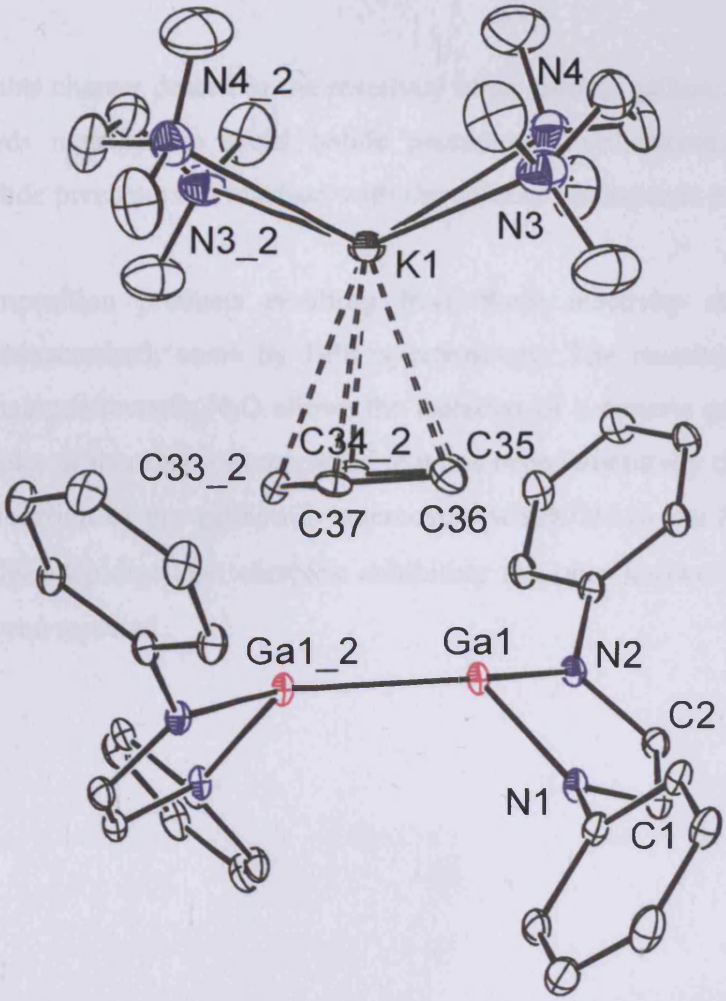

Figure 9 Molecular structure of $[K(TMEDA)_2Cp][\{Ga(Ar\text{-}DAB)\}_2]$ (**16**) (isopropyl groups omitted for clarity)

Selected bond lengths (Å) and angles (°): Ga(1)—N(1) 1.907(3), Ga(1)—N(2) 1.924(3), Ga(1)—Ga(1_2) 2.4461(8), Ga(1)—C(35) 2.630(3), Ga(1)—C(36) 2.811(4), Ga(1)—C(34_2) 3.055(3), Ga(1_2)—C(33_2) 2.515(4), Ga(1_2)—C(37) 2.830(3), Ga(1_2)—C(34_2) 3.106(4), N(1)—Ga(1)—N(2) 86.66(11), N(1)—Ga(1)—Ga(1_2) 119.27(8), N(2)—Ga(1)—Ga(1_2) 140.63(8).

4.5 Conclusions

In conclusion this chapter describes the reactivity of an anionic gallium carbene analogue (Chapter 3) towards main group metal halide precursors. Furthermore, an overview of transition metal halide precursors in reaction with the carbene analogue is provided in section **4.2**.

Several decomposition products resulting from these reactivity studies have been investigated and characterised, some by EPR spectroscopy. The reactivity of the anionic gallium carbene analogue towards N_2O allows the isolation of a dimeric galloxane, which is one of a few examples of this class of compound that has been structurally characterised. Also a novel coupling reaction of the gallium(I) heterocycle which led to the first example of a symmetrically bridged Cp-digallane complex exhibiting the only known π-interaction to a Ga(II) center, has been reported.

4.6 Experimental

For general experimental procedures, refer to appendix 1. 'GaI' was synthesised by a modification of the literature method,[40] and the anionic gallium carbene analogue, **1**, was prepared by the method described in Chapter 3. All other reagents were purchased commercially and purified before use. Meaningful NMR spectra for **9-11** could not be obtained due to their paramagnetic nature. The EPR spectra were recorded at room temperature on an X-band Bruker ESP 300e series spectrometer operating at 12.5 kHz field modulation in a Bruker EN801 cavity. The spectra were obtained with a 2.5 mW power source. The *g* values were obtained using a Bruker ER035 gaussmeter calibrated using the perylene radical cation in concentrated H_2SO_4 (g = 2.002569). Computer simulations were performed using the SIMFONIA Bruker software.[41]

[ArN=CHCH$_2$N(H)Ar] (7)

To a solution of **1** (0.25 g, 0.21 mmol) in Et_2O (15 cm^3) at –78 °C was added HBF_4 (0.037 g, 0.42 mmol) and the resulting solution was warmed to room temperature and stirred overnight. Afterwards the solution was filtered, volatiles removed *in vacuo* and the residue extracted into hexane *ca.* 10 cm^3. Cooling to -30 °C yielded **7** as colourless crystals (0.04 g, 25 %); m. p. 94°C; ^{1}H NMR (400 MHz, C_6D_6, 298 K) δ 1.28 (d, 12 H, $^3J_{HH}$ = 6.9 Hz, CH_3), 1.38 (d, 12 H, $^3J_{HH}$ = 6.9 Hz, CH_3), 3.22 (sept, 2 H, $^3J_{HH}$ = 6.9 Hz, CH), 3.67 (sept, 2 H, $^3J_{HH}$ = 6.9 Hz, CH), 3.84 (dd, 2 H, $^3J_{HH}$ = 5.0 Hz, $^3J_{HH}$ = 5.0 Hz, CH_2), 5.07 (t, 1 H, $^3J_{HH}$ = 5.0 Hz, CNH), 7.25 (m, 6 H, ArH), 7.47 (s, 1 H, NCH); ^{13}C NMR (100.6 MHz, C_6D_6, 298 K) δ 22.2 (CH_3), 22.9 (CH_3), 26.7 (CH), 26.9 (CH), 54.3 (NCH_2), 122.0, 122.6, 136.3, 140.9 (ArC), 146.4 (NCH); IR ν/cm^{-1} (Nujol): 3450 br, s, 1660 s, 1586 s, 1260 s, 1040 s, 930 s; MS(APCI) m/z (%): 379 [M$^+$, 100].

[(Ar-DAB)Ga(Ar-DAB$^\bullet$)] (9) and [{(Ar-DAB$^\bullet$)GaI}$_2$] (10)

To a solution of 'GaI' (1.18 mmol) in toluene (15 cm^3) held at –78 °C was added a solution of **1** (0.71 g, 0.59 mmol) in toluene (15 cm^3). This was warmed to room temperature and stirred overnight to give a red solution. The solvent was removed *in vacuo* and the residue extracted with Et_2O. Concentrating and placement at –35 °C yielded red crystals of **9** (0.08 g, 12 %).

The reaction residue was extracted in toluene, concentrated and placed at –30 °C to yield red crystals of **10** (0.12 g, 25 %).

Data for **9**: m. p. 161 – 164 °C (dec.); IR ν/cm^{-1} (Nujol): 1661 s, 1361 s, 1224 s, 1098 s, 753 s; MS(APCI) m/z (%): 377 [Ar-DAB$^+$, 100]. Reproducible elemental analyses of the compound could not be obtained due to the highly moisture sensitive nature of this compound.

Data for **10**: m. p. 176 – 179 °C; IR ν/cm^{-1} (Nujol): 1360 s, 1250 s, 1201 s, 1110 s, 933 s; MS(APCI) m/z (%): 377 [Ar-DAB$^+$, 100]; $C_{52}H_{72}N_4Ga$ requires C 75.90, H 8.82, N 6.81 %; found C 73.32, H 8.67, N 6.61 %.

[{(Ar-DAB$^•$)GaBr}$_2$] (11)

To a solution of [$MoBr_2(CO)_2(PPh_3)_2$] (0.50 g, 0.41 mmol) in Et_2O (10 cm^3)/ DME (5 cm^3) at –78 °C was added a solution of **1** (0.69 g, 0.82 mmol) in Et_2O (15 cm^3). This was warmed to room temperature and stirred for 3 hours to give a red solution. The solvent was removed *in vacuo* and the residue extracted with DME. Concentrating and placement at –30 °C yielded red crystals of **11** (0.16 g, 36 %); m. p. 152 – 154 °C (dec.); IR ν/cm^{-1} (Nujol): 1945 s, 1890 s, 1845 s, 1097 s, 937 s; MS(APCI) m/z (%): 377 [Ar-DAB$^+$, 100]. Reproducible elemental analyses of the compound could not be obtained due to the highly moisture sensitive nature of this compound.

[K(TMEDA)]$_2$[{(Ar-DAB)GaO}$_2$] (12)

To a solution of **1** (0.40 g, 0.34 mmol) in Et_2O (25 cm^3) at –78 °C was added N_2O (0.68 mmol). The reaction mixture was stirred for 2 hours to give a colourless solution. Concentrating and placement at –30 °C overnight yielded colourless crystals of **12** (*ca.* 0.05 g, < 5 %); m. p. 174 – 176 °C (dec.); ^{1}H NMR (400 MHz, C_6D_6, 298 K) δ 1.16 (d, 24 H, $^3J_{HH}$ = 6.9 Hz, CH_3), 1.33 (d, 24 H, $^3J_{HH}$ = 6.9 Hz, CH_3), 2.11 (s, 24 H, NCH_3), 2.32 (s, 8 H, NCH_2), 3.85 (sept, 8 H, $^3J_{HH}$ = 6.9 Hz, CH), 5.73 (s, 4 H, NCH), 7.19 (t, 4 H, $^3J_{HH}$ = 7.5 Hz, p-ArH), 7.36 (d, 8 H, $^3J_{HH}$ = 7.5 Hz, m-ArH); ^{13}C NMR (100.6 MHz, C_6D_6, 298 K) δ 23.6 (CH_3), 25.0 (CH_3), 27.7 (CH), 57.9 (NCH_3), 65.6 (NCH_2), 122.6 (CN), 122.9 (m-ArC), 123.4 (p-ArC), 142.7 (o-ArC), 146.4 (ipso-ArC); IR ν/cm^{-1} (Nujol): 1619 m, 1571 s, 1323 s, 1202 s, 1099 s, 1021 s, 874 m; MS(EI) m/z (%): 377 [Ar-DAB$^+$, 18], 116 [TMEDAH$^+$, 100]. Reproducible microanalyses on the compound could not be obtained due to the extreme moisture sensitive nature of this compound.

[K(TMEDA)$_2$Cp][{Ga(Ar-DAB)}$_2$] (16)

To a suspension of TlCp (0.22 g, 0.82 mmol) in Et_2O (20 cm^3) was added a solution of **1** (0.50 g, 0.82 mmol) in Et_2O (20 cm^3) / TMDEA (1 cm^3) at -78 °C. This was allowed to warm to room temperature and stirred for 18 hours. The solvent was removed *in vacuo* and the orange residue washed with hexane (2 x 10 cm^3) then extracted into Et_2O (30 cm^3). Filtration, concentration and placement at -30 °C gave yellow-orange crystals of **16** (0.23 g, 46 %), m. p. 75-78 °C (dec); ^{1}H NMR (C_7D_8, 300 MHz, 208 K) δ 0.80 (d, 24 H, $^3J_{HH}$ = 6.5 Hz, CH_3), 0.88 (d, 24 H, $^3J_{HH}$ = 6.6 Hz, CH_3), 1.73 (s, 24H, NCH_3), 2.08 (s, 8H, NCH_2), 2.85 (sept, 4 H, $^3J_{HH}$ = 6.6 Hz, CH), 6.27 (s, 4H, NCH), 6.98 – 7.3 (m, 12H, ArH); ^{13}C NMR (C_7D_8, 75 MHz, 298 K) δ 24.2 (CH_3), 24.7 (CH_3), 28.2 (CH), 45.6 (NCH_3), 58.1 (NCH_2), 116.9 (ArC), 123.0 (ArC), 125.8 (ArC), 144.1 (ArC), 144.8 (C=C); IR ν/cm^{-1} (Nujol): 1659 m, 1624 w, 1352 m, 1256 s, 1066 w, 1056 s, 801 m, 760 s; MS(APCI) m/z (%): 377 [{N(Ar)C(H)}$_2^+$, 100]. A reproducible microanalysis could not be obtained for the compound due to its high air sensitivity and the fact that it slowly decomposes at room temperature.

4.7 References

1. W.A. Herrmann, *Angew. Chem., Int. Ed.*, 2002, **41**, 1290.
2. C.D. Abernethy, J.A. Clyburne, A.H. Cowley, R.A. Jones, *J. Am. Chem. Soc.*, 1999, **121**, 2329.
3. C.D. Abernethy, A.H. Cowley, R.A. Jones, C.L.B. Macdonald, P. Shukla, L.K. Thompson, *Organometallics*, 2001, **20**, 3629.
4. R.J. Baker, C. Jones, J.A. Platts, *J. Am. Chem. Soc.*, 2003, **125**, 10534.
5. W. Uhl, M. Benter, S. Melle, W. Saak, G. Frenking, J. Uddin, *Organometallics*, 1999, **18**, 3778.
6. T. Pott, P. Jutzi, W.W. Schoeller, A. Stammler, H.G. Stammler, *Organometallics*, 2001, **20**, 5492.
7. C. Jones, unpublished results.
8. R.A. Fischer, M.M. Schulte, J. Weiss, L. Zsolnai, A. Jacobi, G. Huttner, G. Frenking, C. Boehme, S.F. Vyboishchikov, *J. Am. Chem. Soc.*, 1998, **120**, 1237.
9. R.J. Baker, C. Jones, J.A. Platts, *Dalton Trans.*, 2003, 3673.
10. F.A. Cotton, X. Feng, *Organometallics*, 1998, **17**, 128.
11. N.J. Hardman, R.J. Wright, A.D. Phillips, P.P. Power, *J. Am. Chem. Soc.*, 2003, **125**, 2667.
12. D. Bourissou, O. Guerret, F.P. Gabbai, G. Bertrand, *Chem. Rev.*, 2000, **100**, 39.
13. C.J. Carmalt, A.H. Cowley, *Adv. Inorg. Chem.*, 2000, **50**, 1.
14. R. West, M. Denk, *Pure Appl. Chem.*, 1996, **68**, 785.
15. R.B. King, *Inorg. Chem.*, 1965, **4**, 1518.
16. H. v. Rensburg, R.P. Tooze, D.F. Foster, A.M.Z. Slawin, *Inorg. Chem.*, 2004, **43**, 2468.
17. T. Steinke, C. Gemel, M. Cokoja, M. Winter, R.A. Fischer, *Chem. Commun.*, 2003, 1066.
18. F.G.N. Cloke, G.R. Hanson, M.J. Henderson, P.B. Hitchcock, C.L. Raston, *J. Chem. Soc., Chem. Commun.*, 1989, 1002.
19. T. Pott, P. Jutzi, W. Kaim, W.W. Schoeller, B. Neumann, A. Stammler, H.G. Stammler, M. Wanner, *Organometallics*, 2002, **21**, 3169.
20. J.L. Bookham, W. McFarlane, M.T. Pett, S. Jones, *J. Chem. Soc., Dalton Trans.*, 1990, 3621.

21. H. Sinn, W. Kaminsky, *Adv. Organomet. Chem.*, 1980, **18**, 99.
22. N. Wiberg, K. Amelunxen, H.W. Lerner, H. Nöth, W. Ponikwar, H. Schwenk, *J. Organomet. Chem.*, 1999, **574**, 246.
23. N.J. Hardman, P.P. Power, *Inorg. Chem.*, 2001, **40**, 2474.
24. J. Storre, C. Schnitter, H.W. Roesky, H.G. Schmidt, M. Noltemeyer, R. Fleischer, D. Stalke, *J. Am. Chem. Soc.*, 1997, **119**, 7505.
25. W. Uhl, U. Schütz, W. Hiller, M. Heckel, *Organometallics*, 1995, **14**, 1073.
26. K.S. Klimek, J. Prust, H.W. Roesky, M. Noltemeyer, H.G. Schmidt, *Organometallics*, 2001, **20**, 2047.
27. A.J. Arduengo III, F. Davidson, R. Krafczyk, W.J. Marshall, M. Tamm, *Organometallics*, 1998, **17**, 3375.
28. H. Schumann, J. Gottfriedsen, M. Glanz, S. Dechert, J. Demtschuk, *J. Organomet. Chem.*, 2001, **617-618**, 588.
29. T. Ramnial, I. McKenzie, B. Gorodetsky, E.M.W. Tsang, J.A.C. Clyburne, *Chem. Commun.*, 2004, 1054.
30. W. Uhl, T. Spies, *Z. Anorg. Allg. Chem.*, 2000, **626**, 1059.
31. P. Jutzi, N. Burford, *Chem. Rev.*, 1999, **99**, 969.
32. P. Jutzi, G.J. Reumann, *J. Chem. Soc., Dalton Trans.*, 2000, 2237.
33. H. Werner, *Adv. Organomet. Chem.*, 1981, **19**, 155.
34. W. Uhl, *Chem. Soc. Rev.*, 2000, **29**, 259.
35. W. Uhl, A. El-Hamdan, *Eur. J. Inorg. Chem.*, 2004, 969.
36. M. Veith, L. Stahl, *Angew. Chem., Int. Ed. Engl.*, 1993, **32**, 106.
37. R.J. Baker, C. Jones, *Chem. Commun.*, 2003, 390.
38. J.M. Pietryga, J.N. Jones, L.A. Mullins, R.J. Wiacek, A.H. Cowley, *Chem. Commun.*, 2003, 2072.
39. J.D. Gorden, C.L.B. Macdonald, A.H. Cowley, *J. Organomet. Chem.*, 2002, **643-644**, 487.
40. M.L.H. Green, P. Mountford, G.J. Smout, S.R. Speel, *Polyhedron*, 1990, **9**, 2763.
41. WINEPR SIMFONIA Version 1.25, Bruker Analytische Messtechnick GmbH, 1996.

Chapter 5

Synthesis and Characterisation of Novel Group 13 Hydride Complexes

5.1 Introduction

This chapter describes the synthesis and characterisation of a range of heavier group 13 metal hydride complexes. Furthermore, the investigation of the reactivity of the prepared complexes is described. Particular emphasis is placed on the synthetic aspects of group 13 trihydride chemistry, highlighting methods used for the spectroscopic and structural characterisation of metal trihydride species which are frequently of low thermal stability. Finally, the chapter culminates in the synthesis of several indium hydride compounds and a low valent In_5 cluster compound.

5.2 General Introduction to Lewis Base Adducts of Alane (AlH_3) and Gallane (GaH_3)

A large amount of research was carried out in the 1990's on the synthesis, structure and reactivity of Lewis base adduct complexes of both alane (AlH_3) and gallane (GaH_3).[1-3] By comparison, indane (InH_3) complexes are relatively unknown. Those structurally authenticated InH_3 complexes have leant heavily on knowledge accrued from the chemistry of lighter group 13 species to identify ligands (Lewis bases) that might stabilise the InH_3 moiety.[4, 5] This introduction broadly reviews the chemistry of the known adducts of alane and gallane, and is to be used as a basis of the work described in this chapter.

The nature of alane and gallane complexes shows one major feature; both entities can display different co-ordination modes given the same ligand.[1, 2] These structural nuances owe their existence to the characteristics of the metal involved. As mentioned earlier in Chapter 1 (**1.5**), the greater Lewis acidity of alane arises from the lesser electronegativity of aluminium relative to gallium.[6, 7] This manifests itself in the normal co-ordination numbers of each metal trihydride; *i.e.* whilst an aluminium centre in a 1:1 alane complex may form intermolecular bridges to be satisfied electronically (5 co-ordinate Al), gallium trihydride species will often complex only one ligand and not show any intermolecular interactions (4 co-ordinate Ga).

5.2.1 General preparative methods for group 13 metal trihydride complexes

Several synthetic routes are commonly used to access metal trihydride complexes. An example and description of each is summarised below.

i) Direct synthesis

Adducts of alane and gallane can be formed from the direct reaction of hydrogen, a chosen ligand and the desired finely divided metal (Equation 1).[8] A drawback of this methodology is its dependence on both temperature and pressure. Often satisfactory yields can only be attained when using extremes of both. Another disadvantage is the required expensive autoclave apparatus, which also impairs monitoring of the reaction.

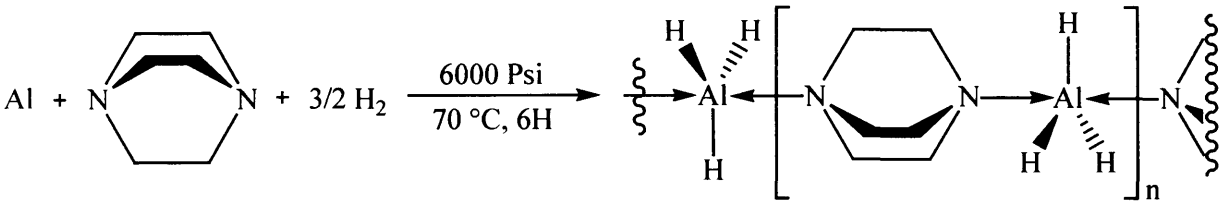

Equation 1

The conditions employed make the stoichiometry of reaction hard to define, whilst ligands lacking thermal stability cannot be used.

ii) Ligand displacement

Ligand displacement is the most common method of preparing clean alane and gallane complexes because only one by-product is produced, the displaced ligand. Often the displaced ligand will be volatile and render the product alone and pure in solution (Equation 2).[9, 10] A disadvantage of this method is the requirement of a donor of greater strength than the nominated leaving group. By employing a large excess of the new ligand this drawback can sometimes be overcome.

The popular precursors for this type of reaction are the diethyl ether adduct of alane and the trimethylamine adducts of both alane and gallane.[9, 11] The labile donation of these Lewis

bases leads to facile displacement, as in the example in Equation 2, where the volatility of the NMe_3 ligand leads to the reaction equilibrium moving to the right.

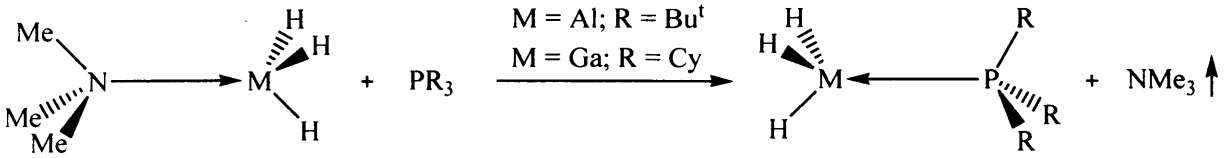

Equation 2

If ligand displacement is attempted with a ligand of similar donor strength to the ligand in the starting complex (Equation 3),[12] five co-ordinate mixed-donor complexes can often result, whereby the donor intended for displacement remains. Usually this only occurs with alane species, given that gallane prefers to exist generally in four co-ordinate complexes.[1]

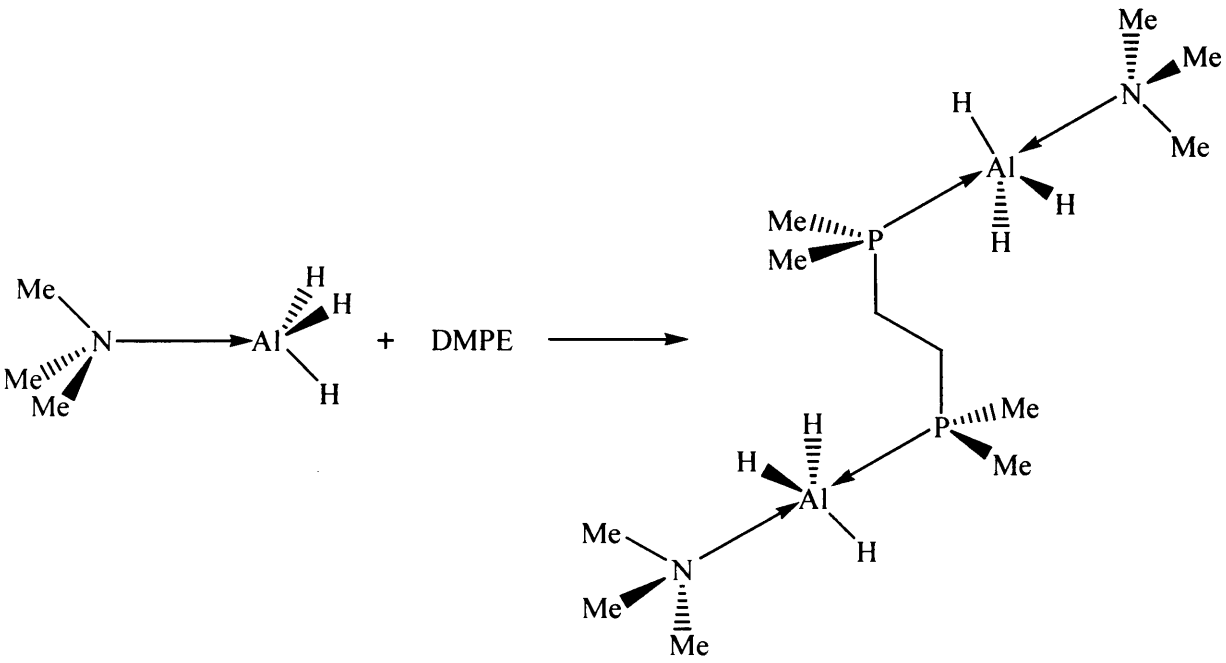

Equation 3

iii) Reaction of $Li[MH_4]$ with a tertiary ammonium halide

The elimination of LiX (X = halide) occurs when lithium tetrahydridoaluminate or -gallate is reacted with an salt (Equation 4). The stoichiometry of the reactants must be carefully controlled to permit the formation of only the $[MH_3(NR_3)]$ complex.[13-15] The stoichiometry of reaction is critical to the final product as an imbalance may permit the synthesis of more than one species, *e.g.* $[MH_2X(NR_3)]$. Trimethylamine adducts of alane and gallane are conveniently prepared by this route,[13, 14] which is advantageous for the introduction of weak donors, especially as the preparation of such species may not be allowed by ligand displacement.[16]

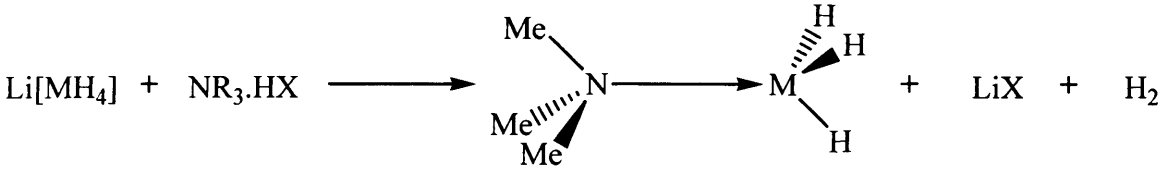

M = Al/Ga, NR_3 = NMe_3, quinuclidine; M = Al, NR_3 = $N(CH_2Ph)Me_2$, N-methylmorpholine
X = Cl, Br

Equation 4

iv) Reduction of a group 13 halide with a hydride source

One technique which is successfully used to prepare mono- and dichloro gallane species is to reduce a stable group 13 halide complex using a metal hydride such as a LiH or Na-/KH (Equation 5),[17, 1-3] or a potent hydride source like Me_3SiH or $Bu^n{}_3SnH$.[18, 19] For the former, usually a larger excess of the reagent has to be used due to a lack of solubility in ethereal solvents.[17] A disadvantage of these syntheses is the extended reaction times needed to ensure complete trihydride complex formation.

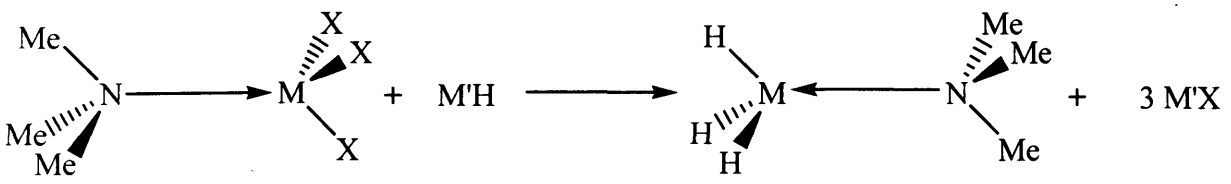

M = Al/Ga, M' = Li/Na/K, X = Cl/Br

Equation 5

v) Reaction of tertiary amines with $Li[AlH_4]$

Reaction of $Li[AlH_4]$ with a tertiary amine can often effect the formation of the desired alane-amine complex, sometimes in high yield (Equation 6).[20] This method is not suitable for all tertiary amines, as the alkyl substituent of the amine can affect the reaction. For example trimethyl amine will form a bis(amine) adduct, but no reaction is observed with triethyl amine.[20]

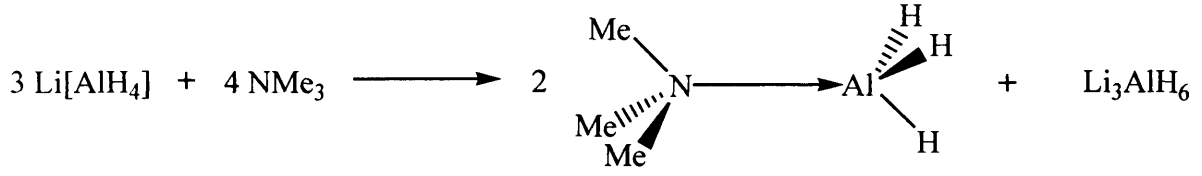

Equation 6

5.2.2 Structural trends of alane and gallane Lewis base adducts

Alane and gallane will often form differing structures when complexed to the same ligand. This section summarises the different types of ligands which form complexes with alane and gallane, and describes their different complexation modes.

i) Monofunctional tertiary amines and phosphines

Monofunctional ligands such as trimethylamine and quinuclidine have been shown to form both four and five co-ordinate complexes of alane,[21, 12] but only four co-ordinate complexes of gallane.[22, 15] Whilst chlorinated gallane species are known to form bis(quinuclidine) adducts which exist happily at elevated temperatures,[23] the lower Lewis acidity of gallium trihydride forbids bis(adduct) formation under ambient conditions.[1] Using the trimethylamine adducts of alane and gallane as an example; $[GaH_3(NMe_3)]$ is monomeric in the solid-state[22] and shows no evidence of intermolecular hydride bridging (**1**). By comparison, the alane complex forms a dimeric species enabling the central metal to assume a five co-ordinate geometry *via* hydride bridging.[14] Given an excess of NMe_3, $[AlH_3(NMe_3)]$ freely forms the 2:1 complex $[AlH_3(NMe_3)_2]$ (**2**).[20] Under the same conditions the gallane analogue, $[GaH_3(NMe_3)_2]$, forms in solution, but eliminates an amine above temperatures of -20 °C.[1] Bulky phosphines such as PCy_3 (Cy = cyclohexyl) form 1:1 complexes with alane and gallane,[9, 10] but do not form 2:1 bis(adduct) species upon addition of another equivalent of ligand. This probably is due to the steric bulk of the phosphine ligand and the small covalent radii of the metal concerned (1.25 Å),[6] which prevents a second ligand co-ordinating to the metal centre.

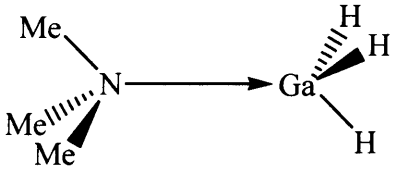

(**1**)

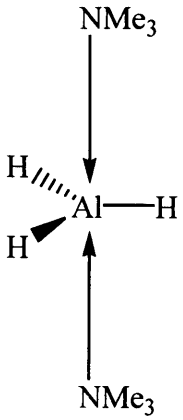

(**2**)

ii) Bifunctional tertiary amines and phosphines

Bifunctional ligands often form five co-ordinate complexes with alane that originate from the interaction of two donor centres with the co-ordinated metal centre. In many cases polymeric species result from such interactions, *e.g.* $[\{AlH_3(TMEDA)\}_\infty]$,[24] $[\{AlH_3(DABCO)\}_\infty]$[8] and $[\{AlH_3[(Pr^i_2PCH_2)_2]\}_\infty]$ (**3**).[11]

When bifunctional ligands react with gallane the general outcome is the formation of bis(gallane)-ligand species such as $[(H_3Ga)_2\{(R_2PCH_2)_2\}]$ (R = Me, Pr^i (**4**), Ph)[9, 10] where, irrespective of excess ligand, solely the 2:1 complexes are formed. Again, this results from the electronic satisfaction of gallane from singular base donation. The reaction of $[GaH_3(NMe_3)]$ with one equivalent of TMEDA in diethyl ether yields an unusual 1:1 gallane / bifunctional ligand adduct which can be isolated as a solid.[15] It is likely that this species contains five co-ordinate gallium centres, however, upon placing the compound *in vacuo* it readily loses one molecule of TMEDA to yield the gallane rich species $[(GaH_3)_2(TMEDA)]$,[15] which contains one attached GaH_3 fragment upon each amine functionality.

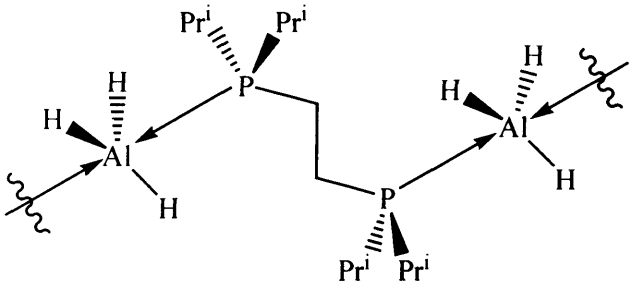

(**3**)

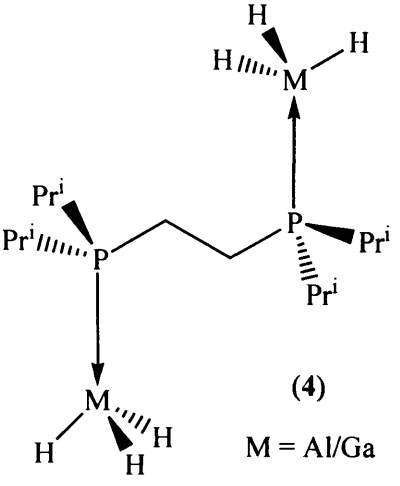

(**4**)

M = Al/Ga

The related 2:1 compound, **4**, M = Al, can be prepared *via* the reaction of two equivalents of $Li[AlH_4]$ with the bis(hydrochloride) salt of $(Pr^i_2PCH_2)_2$.[10] The LiCl elimination method described here ensures that only the alane rich complex results. Interestingly, reaction of alane with (-)-sparteine also yields an alane rich species (**5**).[25] This is believed to result from the steric hindrance of the (-)-sparteine ligand, frustrating polymeric 1:1 alane/ligand chain

propagation. In spite of these examples, when using bidentate ligands, it is rare that polymeric alane species do not result.

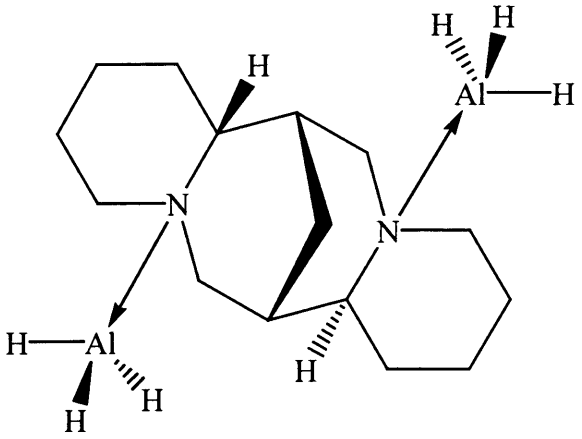

(**5**)

iii) Polyfunctional tertiary amine complexes

Polydentate tertiary amines form neutral, five co-ordinate species, or cationic aluminium hydride complexes. For example, CYCLAM (N,N',N''N'''-tetramethylcyclam) when reacted with $[AlH_3(NMe_3)]$, forms a cationic species from the chelation of all four nitrogens of the ligand to an aluminium centre to form a salt, $[AlH_2(CYCLAM)][AlH_4]$, (**6**).[26] The reaction of $[GaH_3(NMe_3)]$ with CYCLAM does not produce an ionic species, but a neutral complex $[(GaH_3)_2(CYCLAM)]$ (**7**), in which the ligand does not chelate the metal and each GaH_3 fragment is bonded to one nitrogen.[25, 1]

Neutral five co-ordinate adducts such as polymeric $[AlH_3(TRIAZ)]_\infty$ (TRIAZ = 1,3,5-trimethylhexahydro-1,3,5-triazine) (**8**) arise from the reaction of TRIAZ with $[AlH_3(NMe_3)]$.[26] When two equivalents of TRIAZ are reacted with $[AlH_3(NMe_3)]$, a 2:1 complex is formed, $[AlH_3(TRIAZ)_2]$ (**9**).[27]

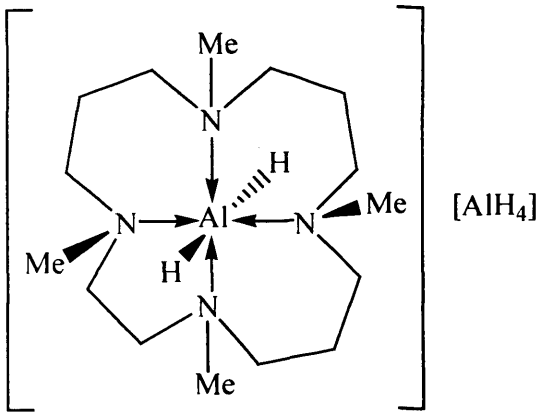

(6)

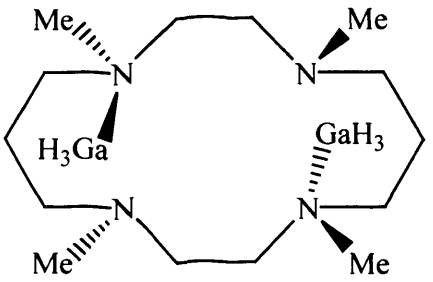

(7)

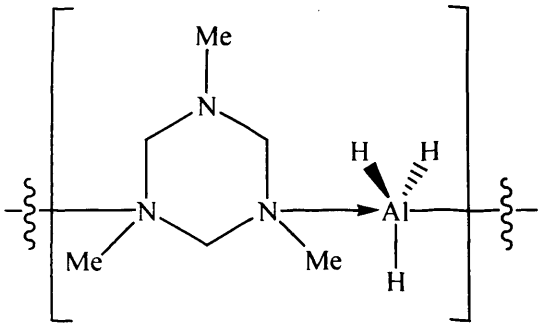

(8)

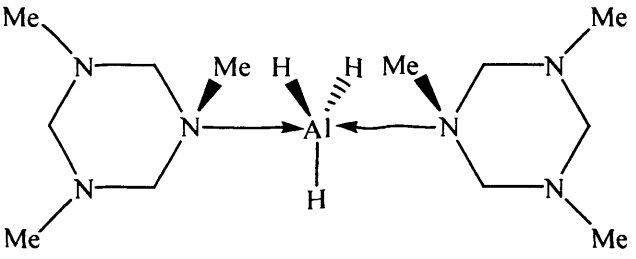

(9)

iv) Mixed donor adducts of alane

Complexation of two different ligands to alane can result in the formation of five co-ordinate adducts, if the strength of the donors are similar. However, if the donor is much stronger than that to be replaced, ligand displacement is usually favoured and a single donor complex will be formed. Examples of mixed donor complexes are $[AlH_3(PMe_3)(NMe_3)]$ and $[AlH_3(PBu^t_3)(NMe_3)]$ (**10**).[10] Complex (**10**) contradicts the above trend in that placing it *in vacuo* renders the four co-ordinate phosphine-alane complex $[AlH_3(PBu^t_3)]$. An explanation for this behaviour is the large steric demand of the phosphine, combined with the volatility of the amine, which changes the reaction equilibrium position towards a preference for $[AlH_3(PBu^t_3)]$.[10]

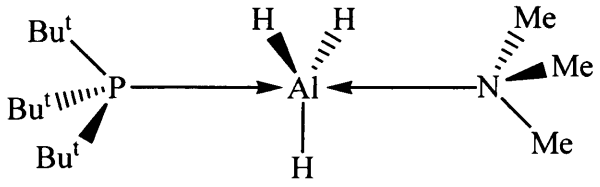

(10)

Mixed donor alane species may be prepared intentionally by the use of ligands that encompass mixed donor sets. The reaction of the bifunctional ligand N-ethylmorphiline with $[AlH_3(NMe_3)]$ yields complex (**11**), which contains two types of five co-ordinate metal centres. One five co-ordinate centre forms from the co-ordination of one oxygen and one nitrogen atom from two independent N-ethylmorpholine molecules, and the second from intermolecular hydride bridges.[28]

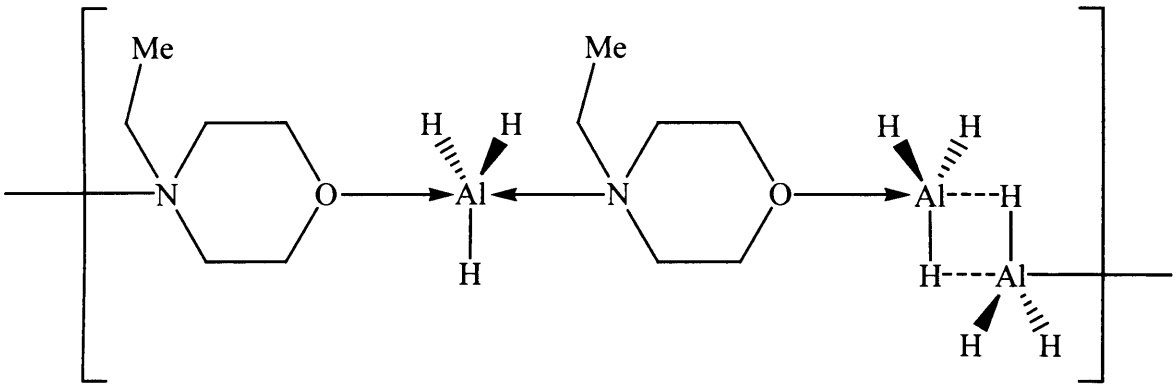

(11)

5.2.3 Reactions of Lewis base adducts of alane and gallane

Alane and gallane adducts are highly reactive species and as such have been used in a wide range of inorganic and organic reactions, some of which are summarised below.

i) Functional group reduction

Alane and gallane complexes have been shown to reduce a wide range of organic functional groups, as well as phosphine oxides.

Wyatt *et al*,[29] have shown that $[AlH_3(THF)]$ will reduce phosphine oxides to the corresponding phosphine (Scheme 1). The $[AlH_3(THF)]$ adduct was synthesised *in situ* from the addition of concentrated H_2SO_4 to $LiAlH_4$ in THF solution. Between one and two equivalents were then added to a series of alkyldiphenylphosphine oxides where the alkyl group varied in size from methyl to pentyl. Quenching the reaction mixture with methanol and filtration through Celite allowed isolation of the phosphine. This process is a convenient synthetic route to phosphines as the need for aqueous work up is avoided. In each reduction, the yield was high (> 96 %).

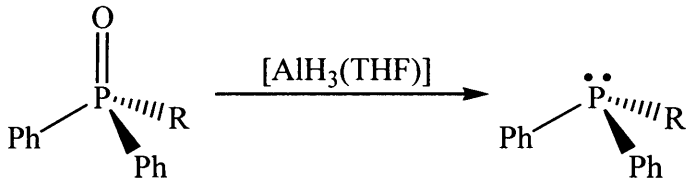

Scheme 1

Lewis base adducts of alane and gallane of the type $[L{\cdot}MH_3]$ (M = Al, Ga; L = Me_3N, quinuclidine, PCy_3) have been shown to reduce several organic functional groups.[30] 4-*tert*-butylcyclohexanone was reduced to the corresponding alcohol, 4-*tert*-butylcyclohexanol by quinuclidine(alane), quinuclidine(gallane) and tricyclohexylphosphine(alane). The reductions occurred in a quantitative manner, in which the *trans* isomer is the dominant product (83 % *trans*, 17 % *cis*) (Scheme 2). A decrease in the molar equivalents of metal hydride used in the reduction to 0.33 gave the same isomeric distribution, but the reduction did not proceed to completion (72 % yield).

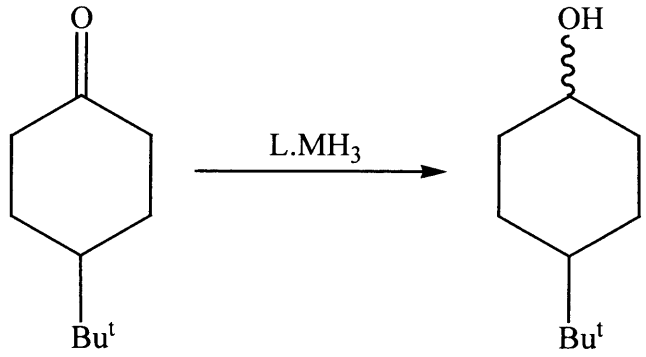

Scheme 2

Ethyl benzoate can be reduced to benzyl alcohol in 80 % yield by $[AlH_3(NMe_3)]$, but not by $[GaH_3(NMe_3)]$.[30] Phenylepoxide can be reduced by $[AlH_3(PCy_3)]$, and forms a 1.7/1 ratio of 2-phenylethanol and 2-hydroxyphenylethanol. When phenylepoxide is reduced by $[GaH_3(PCy_3)]$, the secondary alcohol is formed in a high yield (> 99 %).

Overall, these results show that gallane adducts are softer reducing agents than the corresponding alane adducts, which can be explained by examining the electronegativities of aluminium and gallium. The increased electronegativity of gallium over aluminium results in a less polar M—H bond, resulting in a weaker reducing agent.

ii) Displacement reactions of Lewis base adducts of alane or gallane

The displacement of weaker donors such as trimethylamine can be used to synthesise new complexes of alane or gallane using ligands of greater basicity. For example the highly nucleophilic carbene 1,3-bis(2,4,6-trimethylphenyl)4,5-dihydroimidazol-2-ylidene (IMes)[31] will displace NMe_3 from $[AlH_3(NMe_3)]$ to form the very stable carbene-alane adduct (**12**) (Scheme 3).[32] The thermal stability of this adduct still exceeds any aluminium trihydride complex reported in the literature (m. p. 246 °C, no decomposition temperature listed).[32]

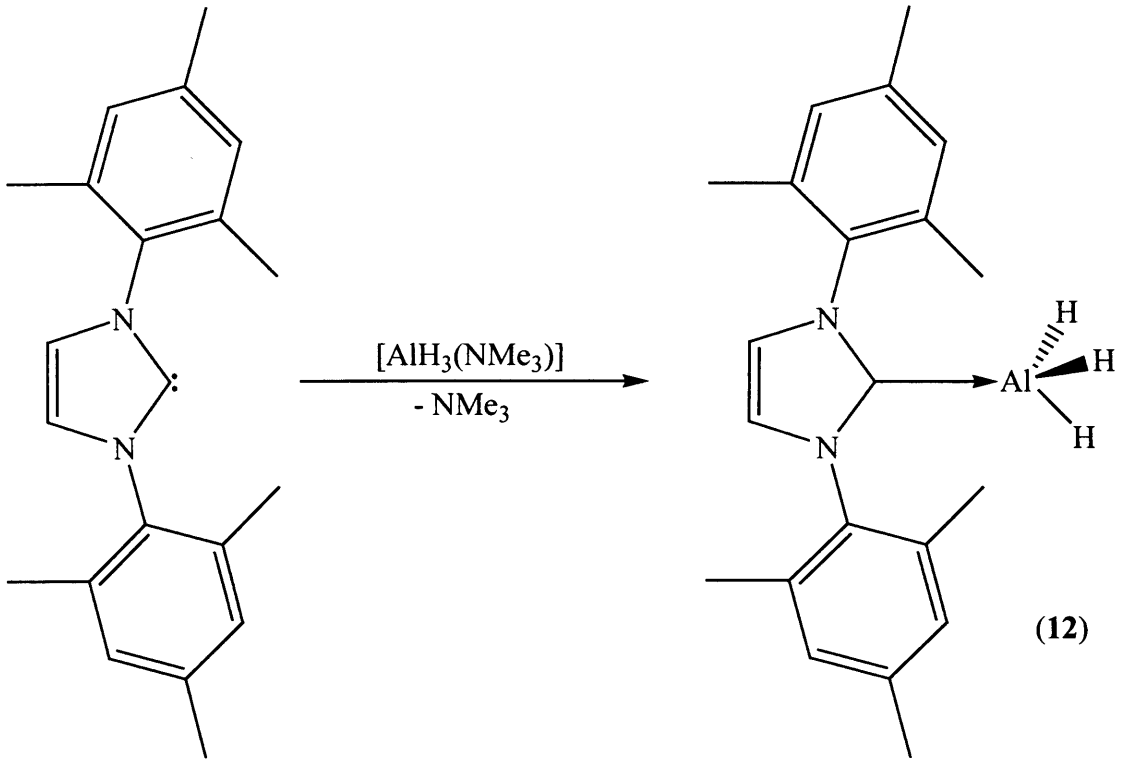

(12)

Scheme 3

Relatively more basic primary and secondary amines usually displace tertiary amines from amine-alane complexes such as $[AlH_3(NMe_3)]$. The products formed are normally unstable with respect to hydrogen elimination leading to amide formation. The hydride ligand is also a stronger donor than a tertiary amine, and therefore will displace NMe_3 from $[AlH_3(NMe_3)]$ to yield $LiAlH_4$ (Scheme 4).[33]

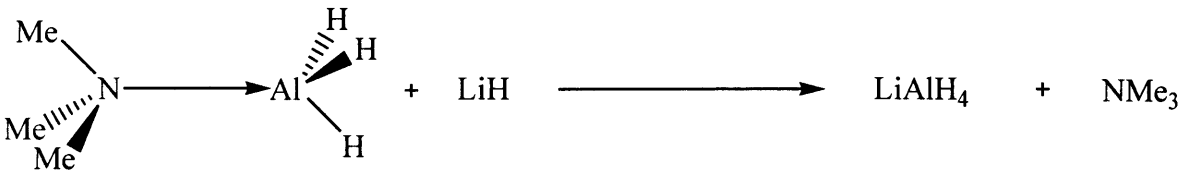

Scheme 4

iii) Surface reactions

In recent years volatile Lewis base adducts of alane have gained considerable attention for their proposed application in chemical vapour deposition (CVD) technology.[34] Likewise, gallane complexes are now drawing attention for similar applications within the microelectronics industry.[35] The adsorption of alane and gallane complexes onto solid substrate surfaces has particular relevance. The implications of adsorption upon reactivity and structure were investigated by Raston *et al*, using $[MH_3(NMe_3)]$ (M = Al or Ga) absorbed upon an oxidised silicon surface/support under UHV conditions.[36, 37] It was shown that $[GaH_3(NMe_3)]$ adsorbs *via* a dissociative mechanism below –30 °C to leave GaH_3 fragments adducted to surface oxygen atoms (Scheme 5) whilst some amines remain trapped as donors to the support's silicon component (a). This is consistent with gallane's preference for singular base donation, although the primary process is likely to be formation of a transient five co-ordinate mixed donor adsorbate.[36] For $[AlH_3(NMe_3)]$ adsorbed pressures less than 5.0 x 10^{-2} mbar molecular adsorption prevails (b). High XPS X-ray flux (> 240 W) results in migration of the NMe_3 to silicon centres, as for gallane.

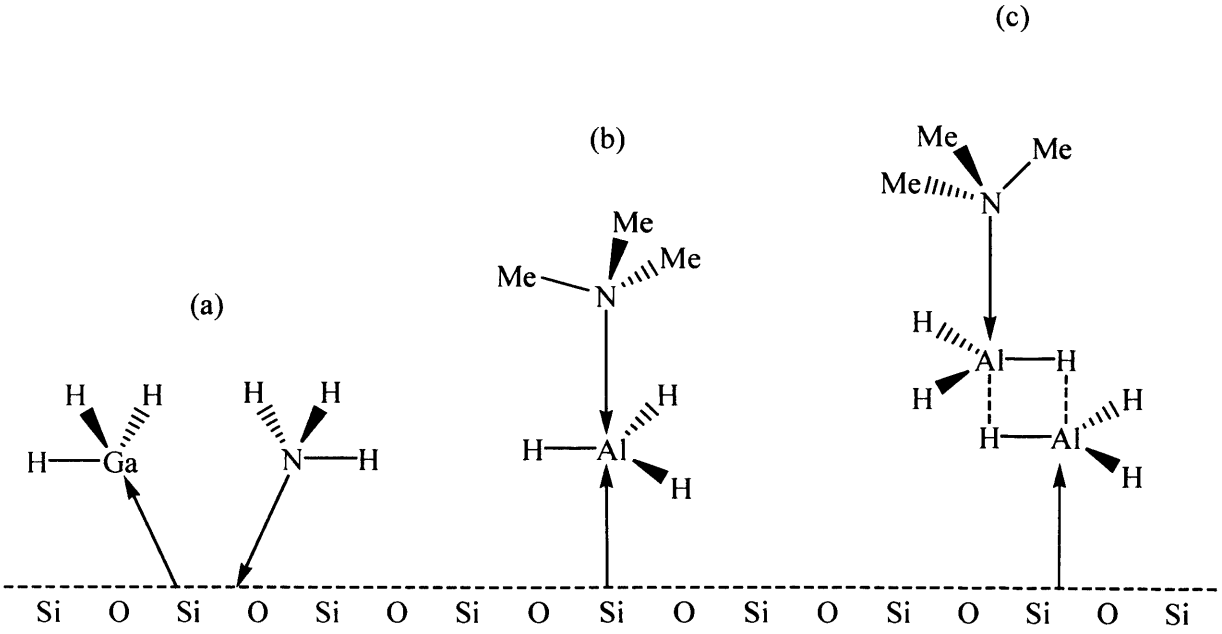

Scheme 5

Increasing the dosing above 5.0 x 10^{-7} mbar results in greater Al to N ratios, possibly by the formation of metal-hydride bridges (c).[37] Interestingly, ultraviolet irradiation initiates the loss of surface amine donors, whilst the provision of a bifunctional amine at the surface, *e.g.* DABCO, effectively dissociates alane from the surface to form conventional [{$AlH_3(NRN)$}$_\infty$] complexes. This latter process also initiates amine loss from the surface, probably due to loss of electrostatic neutrality.

iv) Halo- and alkylalane formation employing [$AlH_3(NMe_3)$]

The hydride ligands of trimethylamine alane may be displaced selectively by the action of alkyl lithiums or mercurial halides and alkyls to form halo- and alkylalane species. Some of these are illustrated in Scheme 6.[33, 38]

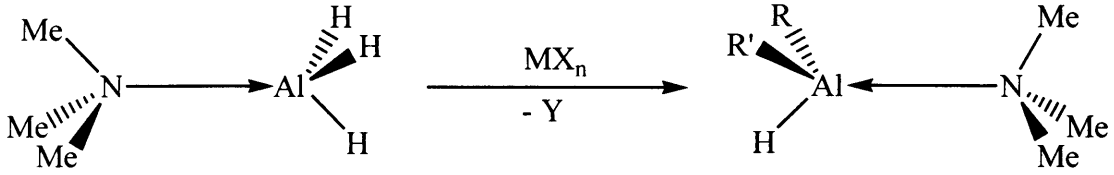

M = Hg, n = 2, X = Me; R/R' = Me, Y = Hg, H_2
M = Hg, n = 2, X = Cl; R/R' = Cl, Y = Hg, H_2
M = Li, n = 1, X = Bu^n; R = H, R' = Bu^n, Y = LiH

Scheme 6

v) Hydrometallation

Alane and gallane complexes have been used as hydride sources in many hydrometallation reactions. For example, the ligand N,N-1,4-*tert*-butyldiazabutadiene reacts with [$AlH_3(NMe_3)$][39] affording a partially hydrometallated paramagnetic species (**13**). When the ligand is added to [$GaH_3(NMe_3)$], complete metallation occurs and the result is a gallane rich complex (**14**) (Scheme 7).

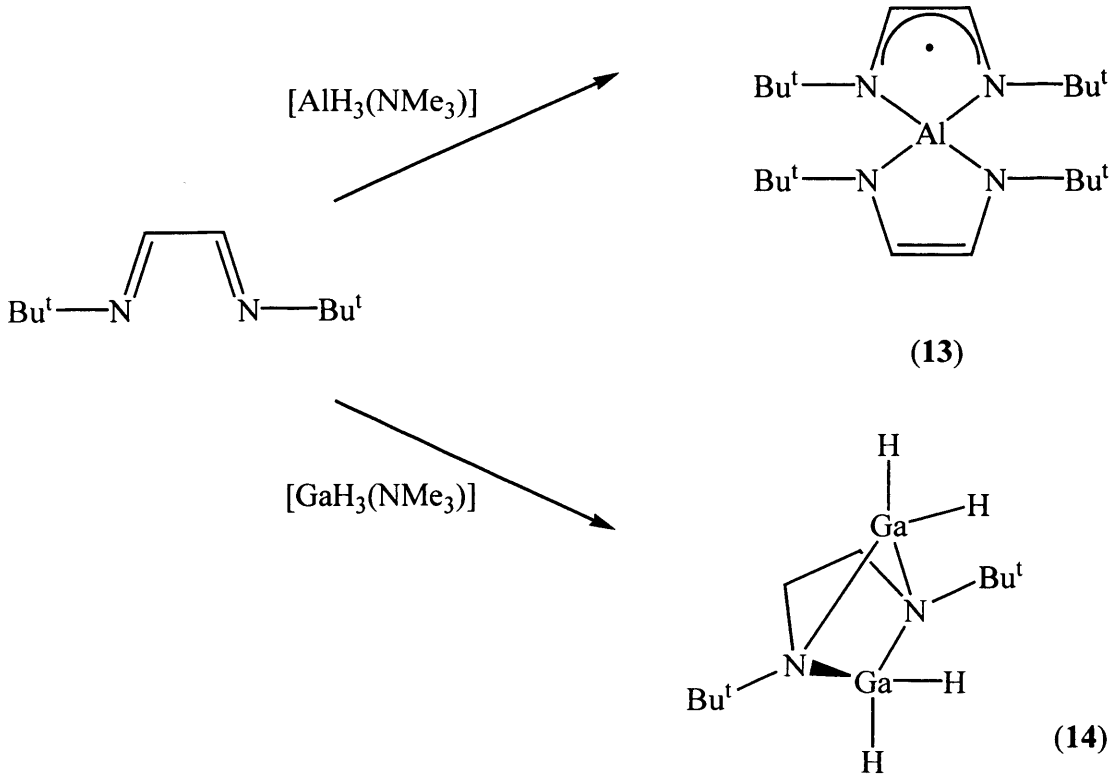

Scheme 7

vi) Redistribution reactions

Often the formation of mono or dihalo gallane complexes may be useful as these compounds give access to reactions involving a broad range of metathesis reagents (*e.g.* alkyllithium and Grignard reagents). The use of stoichiometric amounts of trihalo and trihydride aluminium or gallium species can be used to effect redistribution, thereby forming specific mixed species given the correct solvent medium. Such an example is disclosed below (Scheme 8).[40]

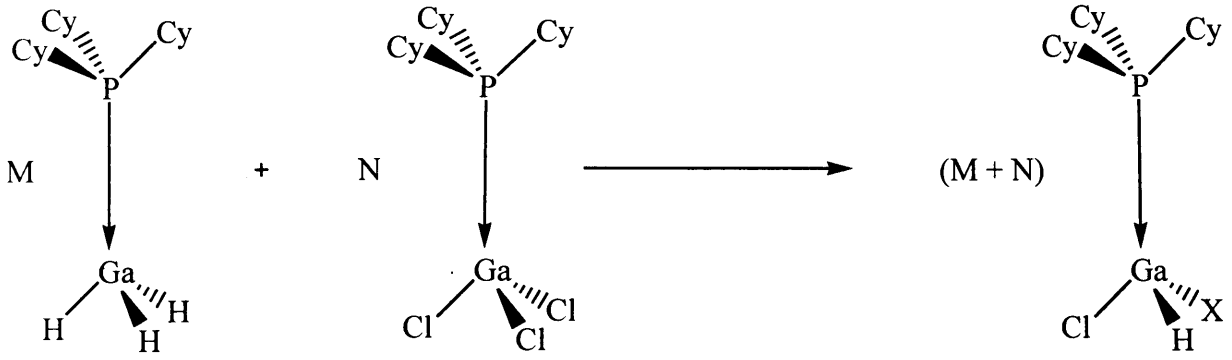

X = H; M = 2, N = 1. X = Cl; M = 1, N = 2

Scheme 8

vii) Reactions of alane and gallane with chalcogenide sources

The chalcogens selenium and tellurium are reduced by $[AlH_3(NMe_3)]$ *via* hydrogen elimination to give products of the type *trans*-$[\{(Me_3N)(H)Al(\mu\text{-}E)\}_2]$ (E = Se, Te)[41] **(15)** (Scheme 9). These exhibit high melting points (215 °C and 256 °C) and are extremely sensitive to moisture.

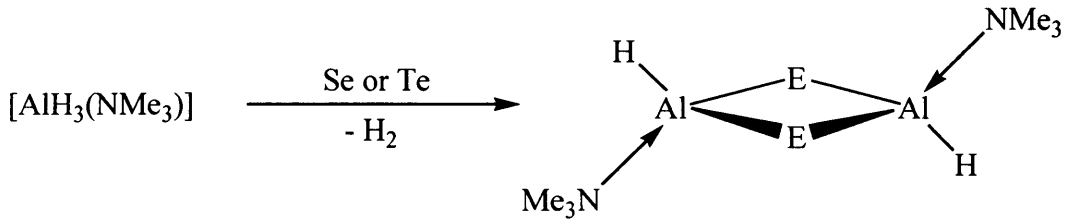

(15)

Scheme 9

When diphenyldiselenide or diphenylditelluride, are added to $[AlH_3(NMe_3)]$, elimination of hydrogen occurs and tri-substituted species of the type $[Al(PhE)_3(NMe_3)]$ (E = Se, Te) can be isolated.[42] These complexes are monomeric in the solid state, and contain four co-ordinate aluminium centres. $[GaH_3(NMe_3)]$ reacts with diphenyldiselenide under identical conditions

and the isostructural gallane species can be isolated.[42] $[GaH_3(PCy_3)]$ has also been reacted with Te_2Ph_2 to give $[Ga(TePh)_3(PCy_3)]$, which is an air and thermally stable complex.

viii) Halide-hydride exchange

Given two distinct group 13 species that differ in-terms of the central element, interesting reactions may take place. These usually proceed according to the respective thermodynamics of the hydride bonds involved. Scheme 10 illustrates how the simple exchange of a ligand from a weaker Lewis acid to a stronger acid may be complicated by hydride-halide exchange.[43]

Scheme 10

5.2.4 Application of alane and gallane complexes to chemical vapour deposition

Over the last decade there has been a growing interest in the potential use of group 13 metal hydrides as precursors to metal films in chemical vapour deposition (CVD) processes, see also **5.2.3** (surface reactions). Until recently, precursors for group 13 metal deposition predominantly relied upon metal alkyls such as MMe_3 (M = Al, Ga, In) and the combined use with EH_3 sources (E = N, P, As) to form III/V semiconductor materials. These were, and still are heavily used because of their widespread availability. However, the use of alkylated precursors does present problems overcome by hydride sources. Aluminium alkyls contain Al—C bonds that ordinarily result in a high degree of aluminium carbide deposition in Al films. These carbonaceous contaminants interfere with the electronic properties of the material by providing a 'negative' hole to purely group 13 films, and a 'positive' hole to III/V semiconductors (negative and positive as in npn and pnp transistors). This restricts the working characteristics of the resultant material. Furthermore, the inclusion of carbon can lead to reflectivity problems in deposited metals.

Metal trihydrides such as $[AlH_3(NMe_3)]$[44] and $[AlH_3(NMe_2Et)]$,[45] have been shown to be excellent alternatives to metal alkyls in CVD processes. During thermolysis, the Al—N bond of $[AlH_3(NMe_3)]$ is cleaved in preference to N—C bonds, resulting in low levels of carbon contaminants. Additionally, alane and gallane sources are less pyrophoric than metal alkyl alternatives, which is a significant advantage in their manipulation.

Passing a stream of precursor over a surface in a reactor at an elevated temperature (130 – 350 °C) initiates a series of decomposition reactions (Scheme 11).[45] This stepwise decomposition forms an aluminium film upon the surface that can be grown at a rate proportional to the vapour pressure of the system. This assists in controlling the thickness of the film, thereby yielding a uniform surface. The level of carbonaceous contaminant using this method was comparable to that from device quality sputtered films ($< 10^{-3}$ %). Another advantage of alane CVD processes is their independence of hot and cold reactors. This means they can be deposited onto a multitude of surfaces including Al_2O_3 or SiO_2. Furthermore, LICVD (Laser Inducted CVD) is possible using metal hydride sources.[46] This allows precise masking of surfaces to facilitate the deposition of aluminium and gallium in submicron width lines and circuit paths. It can be concluded that the exponentially increasing application of group 13 hydride species as CVD precursors ensures that group 13 trihydride chemistry will become an even more fruitful area of research in the future.

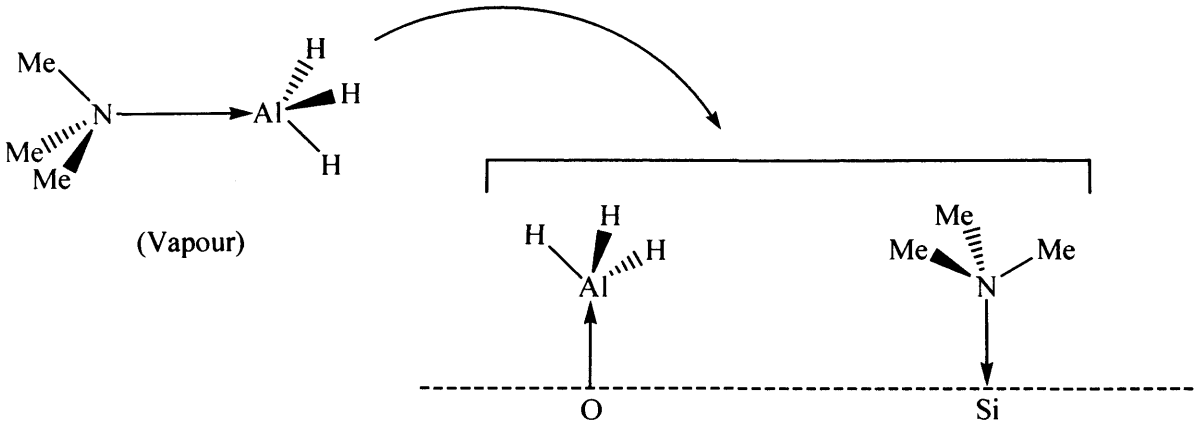

Step 1 - adsorption and dissociation

Step 2 - desorption of NMe_3

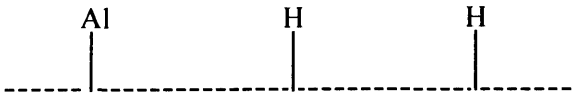

Step 3 - dissociation of AlH_3 fragment

Step 4 - reaction of adsorbed hydrogen and loss of H_2 gas

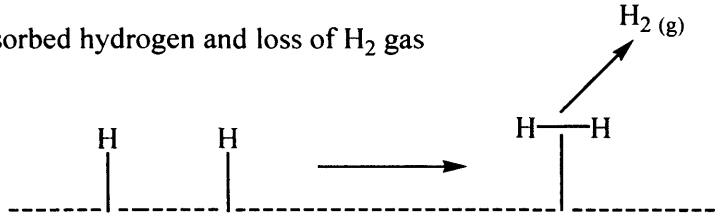

Scheme 11

5.3 Introduction to Theoretical and Synthetic Studies of Indium Hydrides and Their Complexes

In comparison to the amount of work describing the synthesis of alane and gallane complexes, InH_3 compounds have been virtually ignored.[1-4] Until recently the structural archive contained only a handful structurally defined compounds containing In—H bonds.[47-52]

In many cases the hydride ligand could not be structurally refined and was inferred from corroborative spectroscopic data.[47, 49] None of these complexes contained an InH_3 fragment.

The challenge of synthesising stable indium trihydride species was taken by a number of groups worldwide. Indeed, such was the level of synthetic difficulty involved in their synthesis that one review deemed that uncoordinated InH_3 would be impossible to prepare.[46] The intrinsic instability of indane (InH_3) can be attributed to its kinetically facile decomposition as well as its inherent thermodynamic frailty. Early reports of indium hydride compounds failed to detail any characterisation,[53, 17] consequently their syntheses, which included lithium tetrahydridoindate and polymeric indane, must be treated with a degree of scepticism. The first successful preparation of polymeric indane and its spectroscopic characterisation has very recently been reported.[54]

Since 1998, studies undertaken in the Jones laboratory led to reports of the first examples of structurally characterised Lewis base indane complexes.[4, 5, 55]

5.3.1 Known indium hydride complexes

Indium trihydride complexes were unknown prior to 1998. Only a handful of structurally characterised examples of complexes containing bridging or terminal hydrides (non-trihydride) were reported prior to 1998 and are highlighted below. An overview of Lewis base adducts of indium trihydride prepared in the last 6 years is also given in this section.

i) Indium hydride complexes prior to 1998

Smith *et al*,[47] were successful in isolating complex $[Li(THF)_2][In_2H_5\{C(SiMe_3)_3\}_2]$ (**16**) from the reaction of $[Li(THF)_3(\mu\text{-}Cl)In\{C(SiMe_3)_3\}Cl_2]$ and excess lithium tetrahydridoaluminate at low temperatures in THF.

No hydride ligands were located in the crystal structure of (**16**), but the presence of In—H bonds were inferred from IR and NMR spectra. Three absorptions at 1635, 1695 and 1725 cm^{-1} were reasonably assigned as those of In—H stretches, whilst the ^{1}H-NMR spectrum showed signals attributable to the tris(trimethylsilyl)methyl group of (**16**) and the tetrahydrofuran ligands. The quadrupolar nature of the indium centres (^{115}In (*I* 9/2)) and possible intermolecular exchange of hydride ligands purportedly made the In—H signals

broad, weak and difficult to observe. However, irradiation of the ^{1}H region at 180 Hz intervals gave a strong nuclear Overhauser effect in the $^{6}Li\{^{1}H\}$ spectrum of (**16**).[56] This was apparently generated by a broad signal centred at 4.75 ppm (half height width 900 Hz) that was identified as originating from proximal In—H—Li bridging hydrides. It was therefore surmised that hydride bridges between the lithium and indium persisted in solution, and hence, although the application of solution data to solid-state structure could not be taken as definite, it seemed likely that the solid-state nature of (**16**) was that defined below.

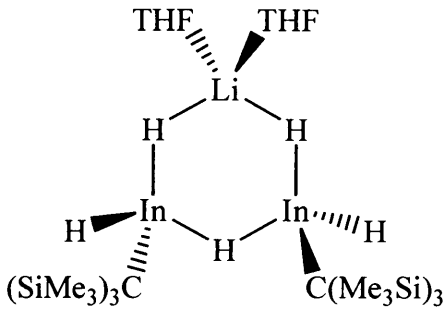

(**16**)

Churchill *et al*,[48] produced two organoindium hydride complexes and performed full characterisation of each. $K^{+}[HIn(CH_2CMe_3)_3]^{-}$ resulted from the treatment of $In(CH_2CMe_3)_3$ with excess KH at room temperature. The subsequent reaction of $K^{+}[HIn(CH_2CMe_3)_3]^{-}$ with further $[In(CH_2CMe_3)_3]$ produced $K^{+}[H\{In(CH_2CMe_3)_3\}_2]^{-}$ (**17**) (Scheme 12).

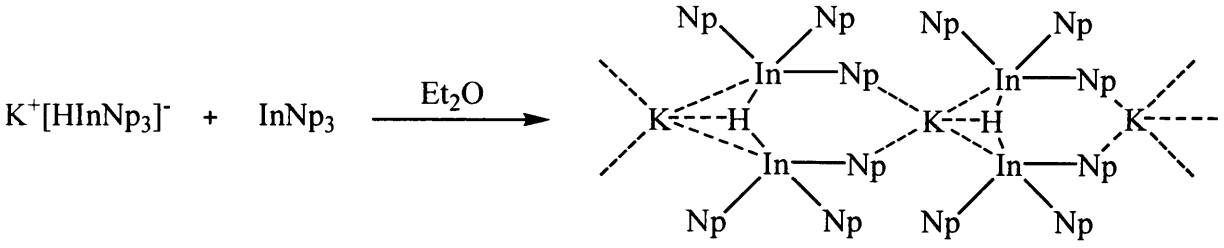

$Np = CH_2CMe_3$

(**17**)

Scheme 12

Both complexes are thermally robust, not decomposing until temperatures greater than 110 °C. Their ^{1}H-NMR spectra showed In—H hydride resonances at 3.41 and 3.09 ppm for $K^+[HIn(CH_2CMe_3)_3]^-$ and (**17**) respectively. The crystal structure of (**17**) is best described as an ordered array of potassium cations and $[(Me_3CCH_2)_3In—H—In—(CH_2CMe_3)]^-$ anions in a 1:1 ratio. In solution, (**17**) is thought to adopt a dimeric structure with two $[\{In(CH_2CH_3)_3\}_2H]^-$ anions bridged by two potassium cations.

Whilst attempting to grow crystals of $K^+[HIn(CH_2CMe_3)_3]^-$ from a pentane solution, the indium hydride complex (**18**) was formed.[49] Compound (**18**) was crystallographically characterised and shown to involve the co-ordination of a planar heptametric cyclopolysiloxane, *c*-$(Me_2SiO)_7$, acting as a *pseudo*-14-crown-7 ligand towards a potassium cation.[49] This arose from the adventitious inclusion of high vacuum grease in the crystallisation procedure. The use of grease was invited in-order to prevent the repeated loss of solvent observed upon isolation of $K^+[HIn(CH_2CMe_3)_3]^-$ crystals.

$K_3[K(Me_2SiO)_7]$ 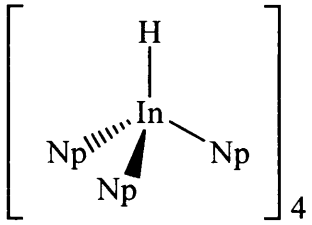

Np = (CH_2CMe_3)

(**18**)

In 1996 the volatile indium hydride, $[Me_2InB_3H_8]$ (**19**) was prepared by Aldridge *et al.*[50] This was achieved by the reaction of trimethylindium with tetraborane, (Scheme 13). The product is relatively unstable, decomposing over several days *in vacuo* at room temperature. The solid state structure of (**19**) may be thought of as ionic, $[Me_2In][B_3H_8]$, where the primary indium co-ordination sphere is augmented by secondary interactions with B_3H_8 terminal hydrides. The hydrides were located in the crystal structure from difference maps, and the In—H bond length reported to be very long at 2.53 Å.

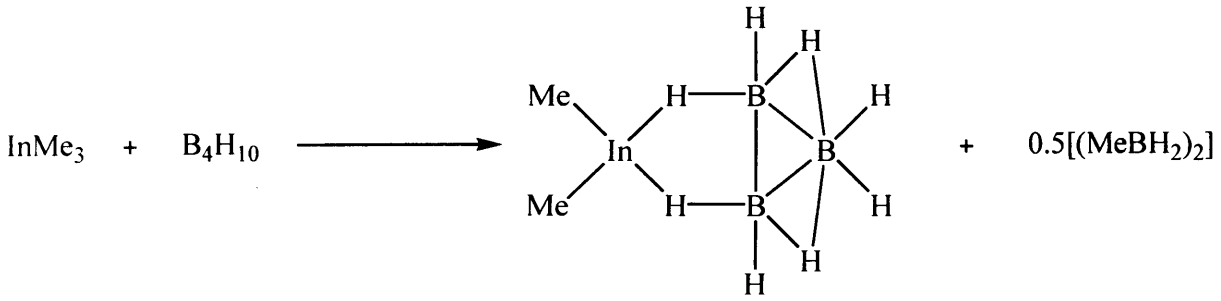

(19)

Scheme 13

Also in 1996 the potential isolation of non-ionic indium hydride species was effected by the preparation of a neutral indium hydride species by Meller *et al.*[51] Addition of bis-{2-(dimethylaminomethyl)phenyl}indium bromide to a solution of $Li[InH_4]$ afforded crystals of $[\{(C_6H_4)CH_2NMe_2\}_2InH]$ (**20**), of sufficient stability for an X-ray crystal structure to be obtained. Surprisingly (**20**) is relatively thermally stable, decomposing at +90 °C.[51] The IR spectrum shows the In—H stretch at 1677 cm^{-1}. Compound (**20**) displays the first structurally located terminal In—H bond, possessing a length of 1.691(33) Å.

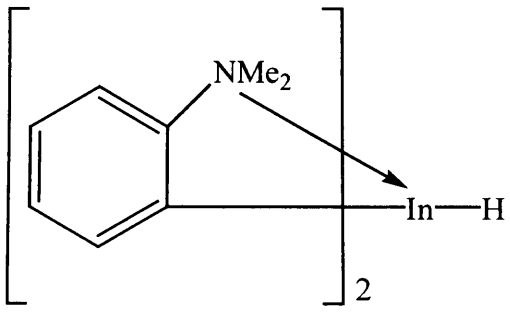

(20)

The sixth and final indium hydride (non-trihydride) complex structurally characterised prior 1998 was the sterically unhindered compound $[Li(TMEDA)_2][H(InMe_3)_2]$, (**21**).[52] Compound (**21**) was prepared by Jones *et al*, *via* the low temperature treatment of $InMe_3.Et_2O$ or $InMe_2Cl$ with a large quantity of lithium hydride in diethyl ether. In the solid state the

In—H—In bridge of (**21**) was found to be bent. This contrasted with the linear Al—H—Al unit of the related complex $[Na][H(AlMe_3)_2]$.[57]

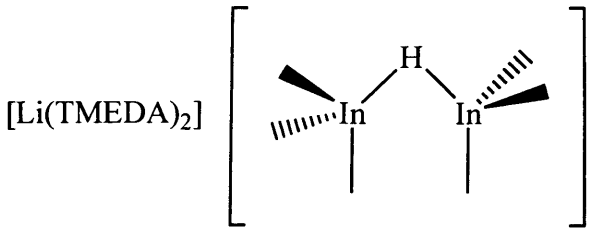

(**21**)

Compound (**21**) is a colourless crystalline solid that remained stable indefinitely in solution and as a solid at 0 °C, but decomposed at room temperature (dec. +5 °C). The average In—H distance of (**21**), 1.87 Å, is unsurprisingly longer than that of the terminal hydride of (**20**), 1.691(33) Å.[51]

ii) Lewis base adducts of indium trihydride

As described above, the trimethylamine adducts of alane and gallane are frequently used as precursors in the 'clean' substitution preparations of many other alane and gallane Lewis base adducts.[1-3] These tertiary amine complexes are commonly synthesised *via* the addition of an amine hydrochloride or –bromide salt to a solution of lithium tetrahydridometallate. Given the apparently successful synthesis of $Li[InH_4]$ from $InBr_3$ reported in the synthesis of (**20**),[51] Jones *et al*, reported the successful synthesis of $[InH_3(NMe_3)]$ by the above means in 1998.[4]

The preparation of $Li[InH_4]$ used a modification of that published by Wiberg in 1957.[53] This was the high dilution reaction of thirty equivalents of lithium hydride with one equivalent of doubly sublimed indium tribromide in diethyl ether at –78 °C. The resulting solution was warmed to –30 °C over a period of four hours with subsequent filtration. Reaction with 0.9 molar equivalents of solid NMe_3.HCl yielded the trimethylamine adduct, $[InH_3(NMe_3)]$, as a highly temperature sensitive diethyl ether solution (stability < -30 °C) (Scheme 14).

Removal of volatiles *in vacuo* highlighted the concentration dependence of the stability of this system. Immediate deposition of an indium mirror with concomitant hydrogen evolution was observed, even when conducted at –50 °C. Similarly, the concentration

dependence of $Li[InH_4]$ was illustrated by congruent deposition of indium upon removal of volatiles *in vacuo*, in-spite of its superior thermal stability (in solution dec. *ca.* 0 °C).[58] An intriguing aspect of this study was the realisation that once decomposition began it could not be halted. It was proposed that indium metal itself acts as a catalyst to the decomposition pathway, creating a cascade effect once indium metal appeared. This behaviour also suggested that the co-ordinating solvent, diethyl ether, was a significant contributor to the stability of both species. Similar reactions employing tetrahydrofuran and dimethoxyethane as the solvent were successful but resulted in decomposition as $Li[InH_4]$ was generated. Meanwhile non co-ordinating solvents did not facilitate any reaction. The $InCl_3$ methodology of Wiberg, used in the preparation of $Li[InH_4]$, was also applied,[53, 17] however, the low solubility of $InCl_3$ precluded reaction with large excesses of LiH in Et_2O, whilst use of tetrahydrofuran was successful but led to immediate decomposition upon formation of $Li[InH_4]$.

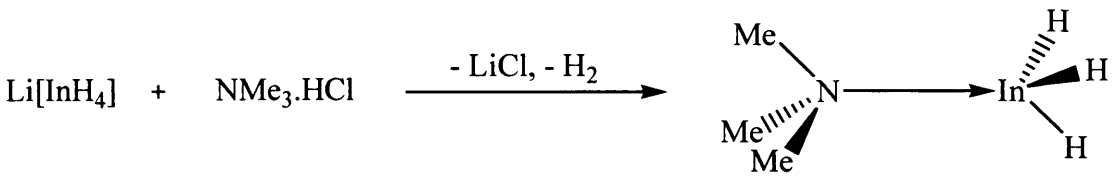

Scheme 14

The thermal instability of both species frustrated spectroscopic characterisation, thus, conclusive proof of their synthesis was not immediately available. To prove their formation indirectly, ligands that intrinsically stabilised the trihydride moieties of alane and gallane were sought. The ligand types nominated were the highly nucleophilic Arduengo type carbenes (an example of which had stabilised alane to a melting point of 246 °C)[31] and bulky tertiary phosphines such as PCy_3 (which had stabilised gallane to temperatures in excess of 130 °C).[9] These, it was postulated, would frustrate the facile decomposition of indium hydrides by limiting aggregate formation *via* their steric bulk.[46] Furthermore, as for alane and gallane, both ligands would inherently stabilise the indane fragment *via* their high nucleophilicity and /or Lewis basicity.[9, 11]

The first indium trihydride complex $[InH_3\{CN(Pr^i)C_2Me_2N(Pr^i)\}]$, (**22**), was reported in 1998 by Jones *et al.*[4] This is thermally stabile up to –20 °C in solution and –5 °C in the solid

state. Treatment of an ethereal solution of either $[InH_3(NMe_3)]$ or $Li[InH_4]$ with excess of the imidazol-2-ylidene, $:CN(Pr^i)C_2Me_2N(Pr^i)$, afforded (**22**) in moderate yields (42 and 38 % respectively) (Scheme 15).

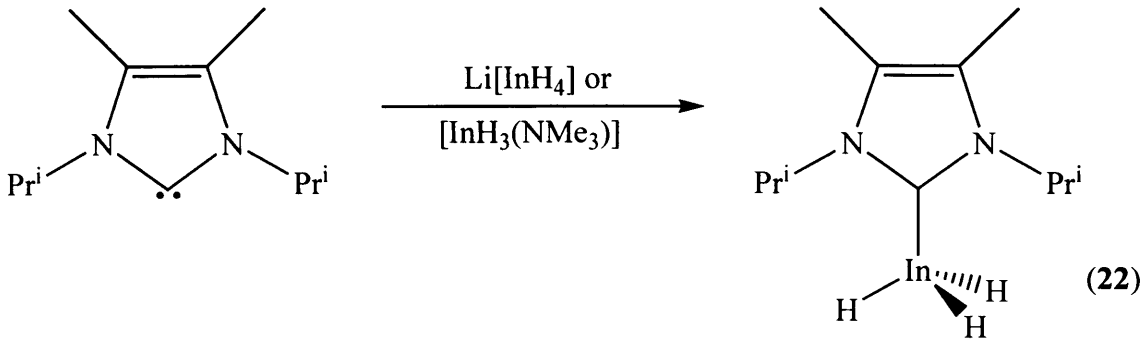

(**22**)

Scheme 15

Unfortunately, the structure determination of (**22**) failed to locate the hydride ligands. Their presence was confirmed by spectroscopic data; IR: In—H stretch of 1640 cm^{-1}, ^{1}H-NMR: broad resonance at δ 5.58 ppm, integrating to three hydrogens.[4] However, one anomaly that plagued the synthesis of (**22**) was its limited thermal stability. Compared to the alane and gallane analogues, which display melting points far in excess of those normally observed for Lewis base adducts at 160 °C (dec. 250 °C) and 180 °C (dec.)[58] respectively, there was no obvious explanation for this discrepancy. However, the decomposition products did not include the free carbene, but a complex mixture of products that contained organoindium species. Therefore, it was thought in this case decomposition proceeded *via* metallation of the carbene isopropyl substituents by the InH_3 unit.[58]

Accordingly the mesityl substituted carbene, IMes, was employed in identical reactions as it was thought that it would be sterically less likely for any formed adduct to decompose *via* metallation of the N-substituents. This indeed proved to be the case and the reaction depicted in Scheme 16 yielded **23** in up to an 86 % yield.[59] Complex **23** proved to be remarkably stable in that it remained intact in the solid state up to 115 °C (*cf.* $[AlH_3(IMes)]$ m. p. 246 °C,[32] $[GaH_3(IMes)]$ 214 °C decompositon[59]) and could be heated as a toluene solution to 110 °C for up to 2.5 hours before decomposition was complete.

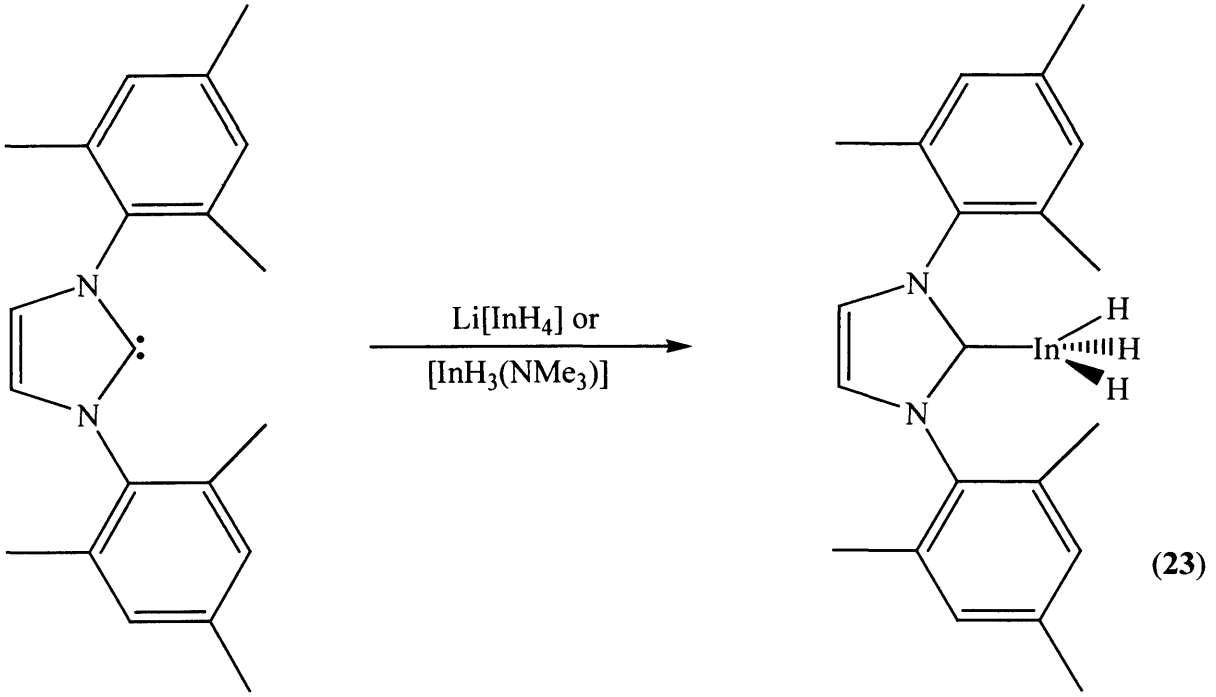

(23)

Scheme 16

The crystal structure determination of **(23)** failed to locate the hydride ligands. Its NMR and IR data confirmed the presence of the hydride ligands and the latter revealed the In—H stretching absorption (1640 cm^{-1}) to be at the low end of the normal range.[59]

This work has been extended to an investigation of the interaction of bidentate carbenes with indane. The rationale here was that alane forms very stable ionic species of the type $[AlH_2(L)][AlH_4]$ with polydentate donors[26] and it was believed a similar outcome might result with indane. However, the reaction of **24** with either $[InH_3(NMe_3)]$ or $Li[InH_4]$ gave the indane rich 2:1 adduct, **25** (Scheme 17) under any stoichiometry of reactants.[60]

Unfortunately, **25** did not prove to be very thermally stable as it decomposes slowly above 0 °C. However, in its crystal structure the hydride ligands were located for the first time in a carbene-indane complex.

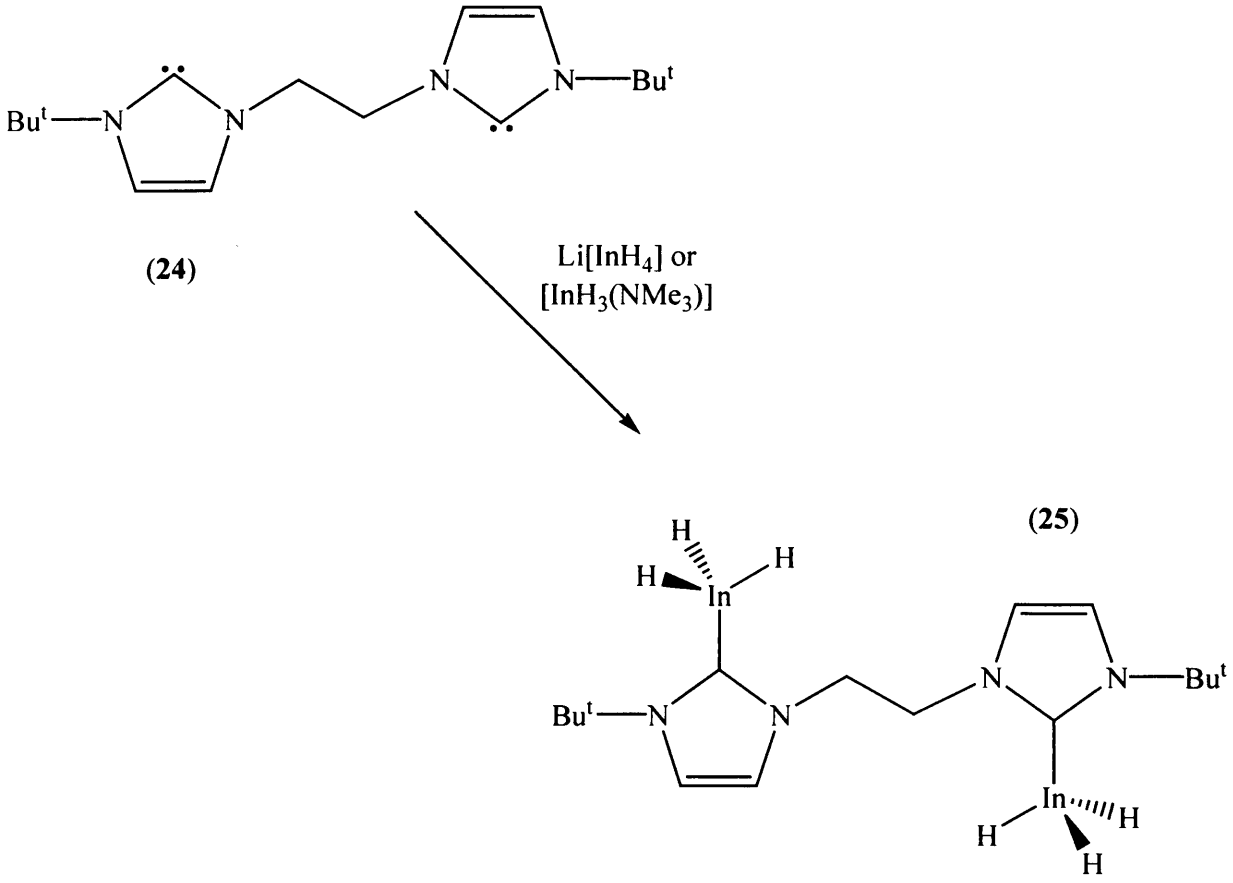

Scheme 17

Although tertiary phosphines are much poorer donors than tertiary amines towards alane, both ligand types have similar donor ability towards gallane. Despite theoretical studies which have predicted that tertiary phosphines would be poorer donors than amines towards indane,[61] the preparation of a series of phosphino-indane complexes was attempted (Scheme 18). It was found that both 1:1 and 2:1 complexes could be prepared using a ligand displacement route but reactions of PR_3/HCl with Li[InH_4] proved fruitless even though a similar route can be used to form gallane complexes.[9]

In general, the phosphine-indane complexes possessed remarkable thermal stability that increases with the σ-donating and steric properties of the phosphine ligand. The 1:1 and 2:1 PCy_3 adducts were the most stable in the solid state (**26** decomposition 50 °C and **29** decomposition 37 °C) though all complexes decomposed to indium, $H_{2(g)}$ and the free phosphine.[5, 62] Remarkably, crystalline samples of **26** proved to be completely stable to the atmosphere at room temperature over a 24 hour period.

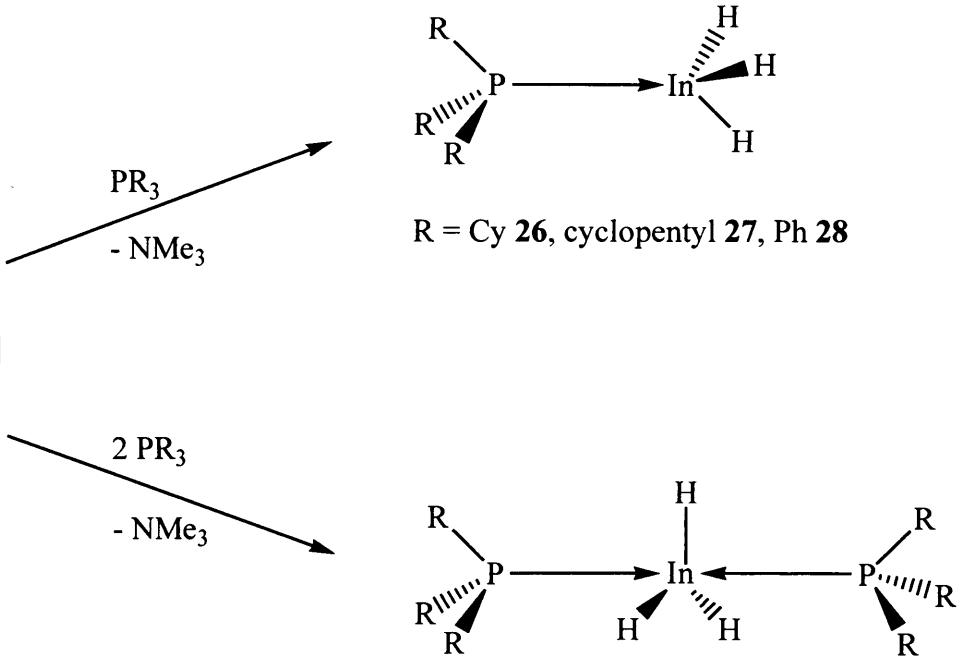

Scheme 18

Both **26** and **29** have been crystallographically characterised and in the case of **26** the hydride ligands were located. All the phosphine-indane complexes mentioned, displayed strong In—H stretching absorptions in their IR spectra (*ca.* 1630 – 1690 cm^{-1}).[5, 62]

The fact that the 5 co-ordinate complex **29** forms, whereas alane and gallane form only 1:1 4 co-ordinate complexes with the bulky phosphine, PCy_3, suggests that the InH_3 unit prefers a higher co-ordination number than either AlH_3 or GaH_3. This probably arises from the relatively high covalent radius of In as it has an electronegativity intermediate between that of Al and Ga. As a result, the InH_3 unit should have a Lewis acidity intermediate between the AlH_3 and GaH_3 units.

5.3.2 Reactivity of indium hydride complexes in organic synthesis

Three independent research groups from Japan have employed organoindium hydride complexes as reductants in organic synthesis. A report in 1995 by Butsugan *et al*,[63] detailed the use of $Li[InH_4]$, formed *via* Wiberg's synthesis,[53] to reduce a variety of organic

functionalities such as aldehydes (*e.g.* n-$C_7H_{15}CHO$), ketones (*e.g.* acetophenone), acid chlorides (*e.g.* p-BrC_6H_4COCl) and esters (*e.g.* p-Br_6H_4COOEt). The results indicated that aldehydes and acid chlorides were reduced quantitatively by lithium tetrahydridoindate, whilst ketones and esters were reduced to a lesser extent. This contrasted with the behaviour of common reducing agents like $Li[AlH_4]$ and $Na[BH_4]$. Each reduction was repeated with LiH alone as a control, which displayed complete inactivity.[63]

The species $Li[InPhH_3]$ and $Li[InPh_2H_2]$ were also synthesised from the stoichiometric 1:1 and 2:1 treatments of $InCl_3$ with LiPh, followed by treatment with lithium hydride.[63] Both species were used *in situ* and found to possess greater reductive capability than $Li[InH_4]$. Both were reported to have stabilities in solution exceeding room temperature, and therefore that of $Li[InH_4]$ (solution decomposition *ca.* 0 °C). However, given that the synthesis of the described compound (**21**),[52] it seems unlikely that these reagents were the only reductively active species in solution. Discounting this, esters were reduced in greater yields using the phenylated reactants, whilst ketone reduction was more efficient by $Li[InPhH_3]$, but not $Li[InPh_2H_2]$.[63]

In 1997, the group of Araki used lithium tetrahydridoindate to reduce acyclic alpha and beta hydroxyketones and diketones.[64] This reagent was found to reduce bi(functional) substrates with a degree of diastereoselectivity that was superior to that of lighter group 13 hydride reagents. To confirm this, substrates such as benzoin (PhCOCH(OH)Ph) and benzil (PhCOCOPh) were reduced employing $Li[InH_4]$, $Na[BH_4]$ and $Li[AlH_4]$, and their reductive character compared. Whilst $Li[AlH_4]$ gave similar results, the extent of diastereoselectivity given by $Li[InH_4]$ was far greater. In contrast, $Na[BH_4]$ reacted sporadically, giving almost random diastereoselectivities without any tangible pattern. The extent of diastereoselectivity seen for $Li[InH_4]$ was rationalised by the formation of a cyclic transition state after metallation, which allowed a directed hydride delivery to one side of the bi(functional) substrate.[64] However, no theoretical or solid-state structure determinations were offered to add credit to this rationale.

The nature of these first two reports, which utilised low stability reagents lacking conclusive characterisation, was joined in 1998 by report of a solvent stabilised $[InCl_2H]$ reagent.[65] $[InCl_2H(THF)]$ was putatively formed from the reaction of $InCl_3$ and one equivalent of Bu^nSnH in tetrahydrofuran. This formed the aforementioned complex, which could be used *in situ* for a multitude of organic reductions at room temperature. Subsequent reactions were undertaken upon a enormous array of alkyl and aryl-aldehydes, as well as ketones, alpha-beta

unsaturated ketones, esters and alkyl bromides. All displayed the high yielding reductions typical of previously studied indium hydride reagents.

Jones *et al*, reported the use of indane complexes as reducing agents in organic synthesis; some of these complexes are described in **5.3.1**. Indium has an electronegativity between that of Al and Ga. Therefore it might be expected that the In—H bond has a polarity between that of Al—H and Ga—H bonds. As a result, indane complexes could display a degree of chemoselectivity in the reduction of organic functionalities. This proved to be the case as both **23** and **26** readily reduce ketones but showed no activity towards a variety of ester functionalities that are readily reduced by alane complexes.[66] In addition, the debromination qualities of **26** towards 2,4'-dibromoacetophenone (57 % C—Br cleavage) are mid way between those of alane complexes, which quantitatively effect α C—Br cleavage, and gallane complexes which show only minimal activity towards alkyl bromides. It is noteworthy that $[BH_3(NMe_3)]$ is completely inactive towards this substrate. In addition, the reduction of styrene oxide by **26** highlights an intermediate regioselectivity of this reductant (reduction product mixture: 56 % 1-phenylethanol, 44 % 2-phenylethanol) over $[GaH_3(PCy_3)]$ which gives 99 % of the secondary alcohol and [AlH$_3$(quinuclidine)] which yields 37 % of the primary alcohol as a reduction product.

Indium has a greater covalent radius (1.50 Å) than either aluminium or gallium (1.25 Å) which means that like alane but unlike gallane, indane should form hypervalent complexes as has been demonstrated with the preparation of **29**. It was thought this preference could lead to indane complexes showing diastereoselectivity in the reduction of potentially chelating bifunctional substrates. This has been confirmed with the reductions of benzoin, benzil and benzoin methyl ether by **26**, all of which occur with > 99 % diastereoselectivity. These results suggest a chelation of the substrate to the indium centre of the complex which allows a direct hydride delivery leading to the observed result.[66]

5.4 Introduction to Group 13 Metalloid Cluster Complexes

Recently there has been a great deal of interest in the chemistry of metastable aluminium(I) and gallium(I) halide complexes, which are turning out to be very useful as precursors to a wide range of novel low oxidation state metal complexes and cluster compounds, see Chapter 1 (**1.2**).

In general these aluminium and gallium clusters, which contain both ligand-bearing and naked metal atoms that are only bonded to other metal atoms are called metalloid clusters.[67] Such metalloid clusters contain more direct metal-metal contacts than metal-ligand contacts. Until a few years ago, metalloid clusters were known exclusively for the noble transition metals, such as the $[Au_{55}(PPh_3)_{12}Cl_6]$ cluster[68] which is the prototype of this family but has not been structurally characterised. A common method used to synthesise low valent aluminium and gallium cluster compounds is the controlled disproportionation of MX solutions, M = Al or Ga; X = halide, with or without concomitant treatment with lithium amides, alkyls or silyls. Prominent examples of such cluster compounds are; $[Al_{22}Br_{20}(THF)_{12}]$, $[Ga_{84}\{N(SiMe_3)_2\}_{20}]^{4-}$, $[Ga_{19}\{C(SiMe_3)_3\}_6]^-$ and $[Ga_{26}\{Si(SiMe_3)_3\}_8]^{2-}$.[69]

Indium analogues of such metal rich metalloid cluster compounds, however, are unknown and it seems these cannot be prepared *via* disproportionation of indium(I) halide solutions.

5.5 Research Proposal

The use of aluminium and gallium hydrides as molecular precursors has been an important development in the field of materials science. Alane and gallane complexes have been used in a variety of techniques, such as chemical vapour deposition and solution based methodologies, to synthesise materials ranging from aluminium films to nanocrystalline III/V materials.[70] Given that this is an area of exceptional growth and development, the potential rewards of indane-based substrates remain invitingly untapped.

As mentioned in **5.4**, there has recently been a great deal of interest in the chemistry of metastable aluminium(I) and gallium(I) halide complexes, which are turning out to be very useful as precursors to a wide range of novel low oxidation state metal complexes and cluster compounds.[69] Indium analogues of such cluster compounds are unknown and cannot be synthesised by the aforementioned method.

The aim of this work was to expand the limited archive of indane and indium hydride species and discover compounds that possess thermal stabilities in excess of those previously reported. In doing so, it is thought that indane complexes may viably participate in studies such as those listed above. Furthermore it was intended to investigate the decomposition pathways of indium hydride complexes and isolate intermediate compounds which may form in the decomposition process. It is possible these intermediates could include sub-valent indium cluster compounds.

5.6 Results and Discussion

5.6.1 Amido group 13 hydride complexes

Bulky amide ligands have been widely used to stabilise aluminium and gallium hydride complexes,[71, 72] though amido-indium hydride complexes are unknown, except for several matrix-isolated examples, for example, $[H_2InNH_2]$.[73] It was proposed to prepare such complexes and the amidinate class of ligand, $[RNC(R')NR]^-$, seemed appropriate to this cause. The stabilising features this class of ligand offers include an ability to chelate metal centres and the potential to incorporate bulky substituents on the nitrogen atom and on the carbon backbone of the ligand. Both stabilising features have been previously exploited in a range of group 13 halide and alkyl complexes.[74-76] In this preliminary study, the bulky formamidinate ligand, $[ArNC(H)NAr]^-$ (Ar = 2,6-$Pr^i_2C_6H_3$ (Fiso)),[77] has been chosen.

Treatment of an ethereal solution of $Li[InH_4]$ with two equivalents of HFiso led to H_2 and LiH elimination and a moderate yield of **31** after re-crystallisation from diethyl ether (Scheme 19). In the solid state, **31** does not show any decomposition in air after one week and under argon does not begin to decompose until 160 °C. In toluene solutions it can be heated in a sealed tube at 125 °C for 3 hours before complete decomposition occurs. This does not afford indium metal but HFiso and an insoluble, brown organo-indium material, the exact identity of which could not be determined. The decomposition process is presumably intramolecular and involves hydrogen transfer to one Fiso ligand and metallation of the other (compare with NHC metallation in the decomposition of $[InH_3\{C[N(Pr^i)CH]_2\}]$).[55] The ^{1}H-NMR spectrum of **31** does not exhibit an observable In—H resonance, which can be explained by quadrupolar broadening of this signal by the ^{113}In and ^{115}In isotopes (I = 9/2). Its infrared spectrum does, however, show a sharp In—H stretching absorption, as would be expected for a terminal hydride ligand. This occurs at significantly higher frequency (1748 cm^{-1}) than the In—H stretching modes for InH_3 complexes (1640 – 1660 cm^{-1})[55] due to a negative inductive effect from the two anionic Fiso ligands, which decreases the relative polarity of the In—H bond. Consequently, this decrease should lead to a decrease in the predisposition of the indium hydride fragment to be involved in intermolecular hydride bridges. The deuteride analogue of **31**, namely, **31**-D (decomposition 165 – 170 °C), was prepared from $Li[InD_4]$ and HFiso and its infrared spectrum is essentially identical to that of **31**, though no absorption at

1748 cm^{-1} is present. A corresponding In—D stretch was not discernable at the expected wavenumber (*ca.* 1240 cm^{-1}) due to strong masking from the fingerprint region.

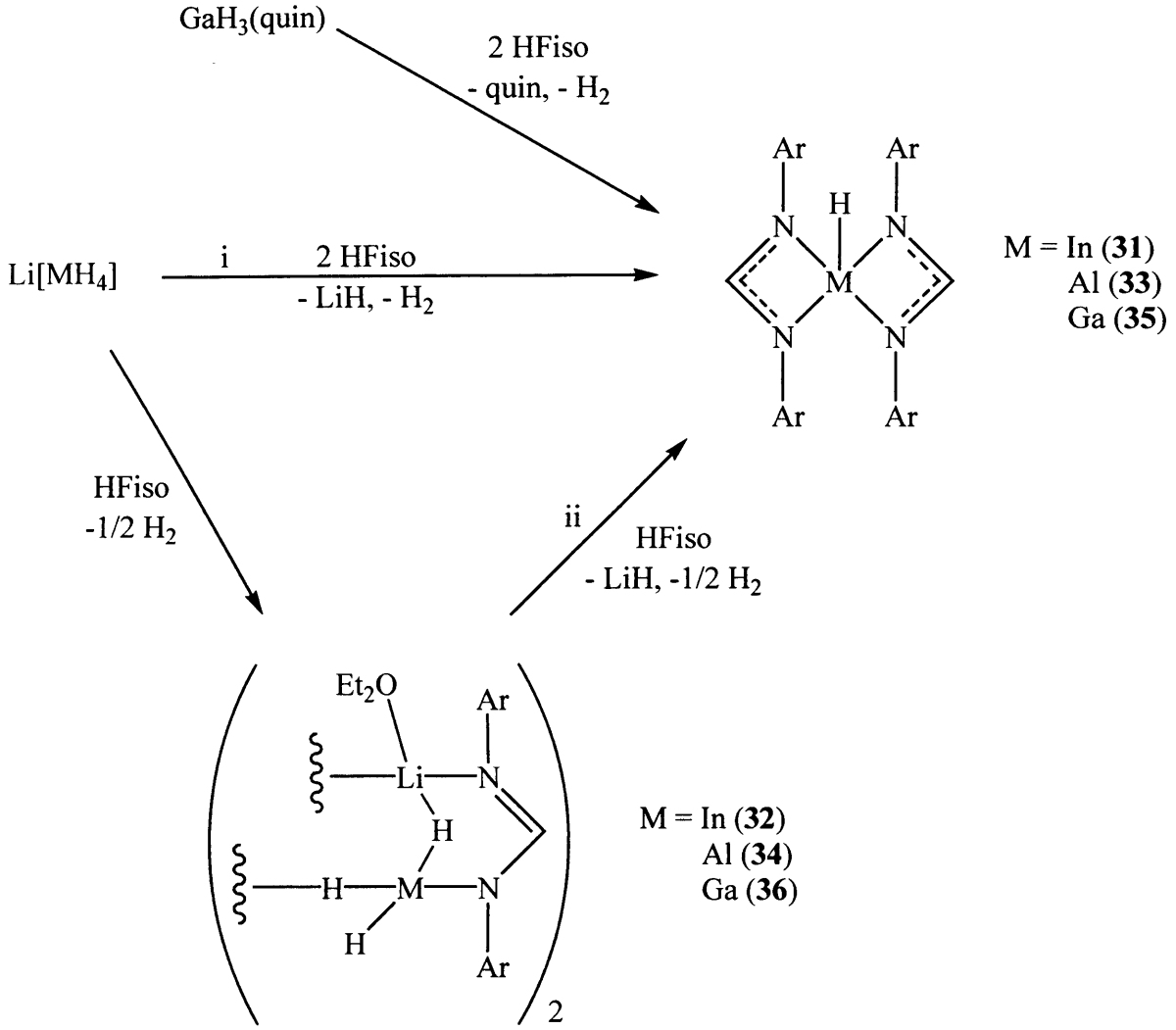

Scheme 19 Reagents and conditions: i, M = In and Al; ii, M = In and Al; quin = quinuclidine.

The molecular structure of **31** (Figure 1 a) shows that the complex is monomeric and has a heavily distorted trigonal bipyramidal indium co-ordination environment with N(2) and N(4) in axial positions. The hydride ligand was located from difference maps and refined isotropically to give an In—H bond length of 1.71(6) Å (*cf.* 1.68 Å average in $[InH_3(PCy_3)]$, Cy = cyclohexyl).[55] The geometry of **31** is similar to that of the related indium chloride complex, $[InCl\{CyNC(Bu^t)NCy\}_2]$,[78] and the only other example of a structurally

characterised amidinate group 13 hydride complex, $[AlH\{(Me_3\text{-}Si)NC(Ph)N(SiMe_3)\}_2]$,[79] though the bulk of the Ar substituents in **31** cause it to be significantly more distorted. Presumably, these groups also lead to the remarkable thermal stability of the complex by forming a heavily protected 'pocket' in which the hydride ligand sits (Figure 1 b). This pocket prevents the formation of intermolecular In—H—In bridges, which are thought to accelerate indium hydride complex decomposition.[55] In addition, the pocket hinders chemical attack of the InH moiety.

a)

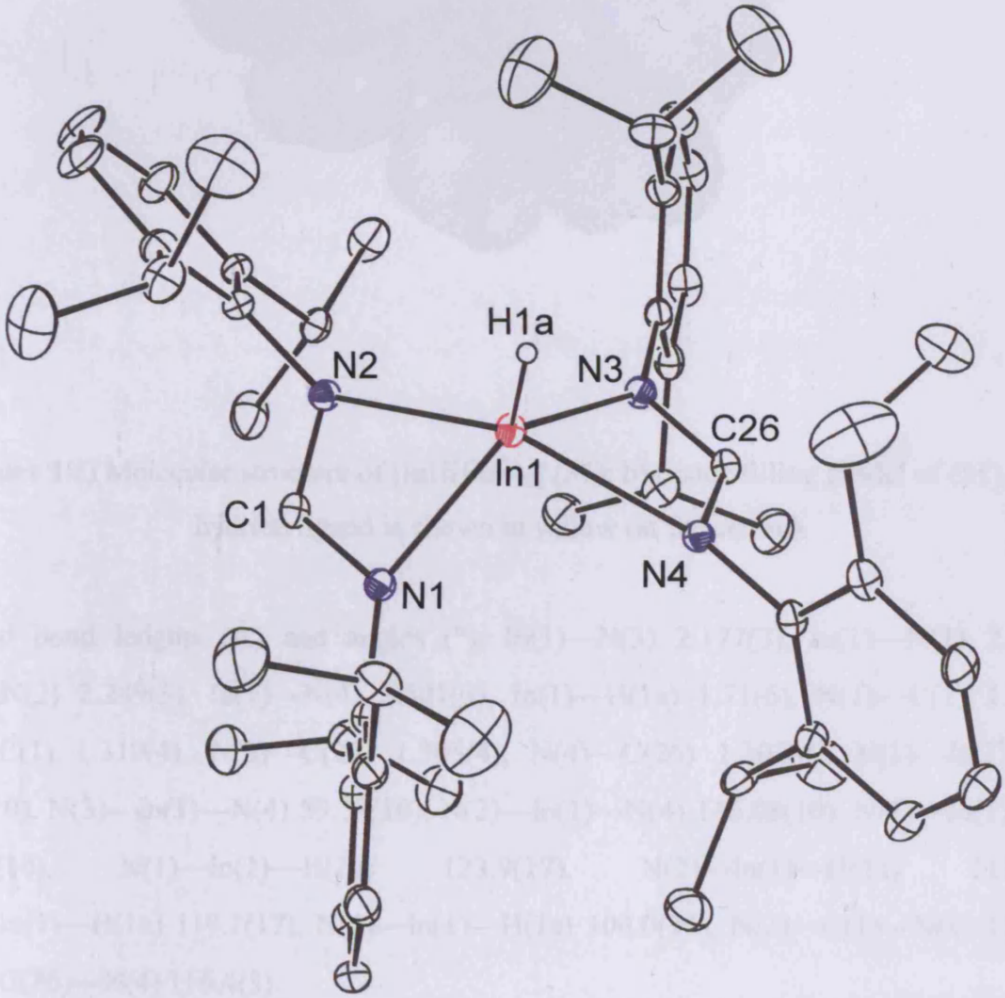

b)

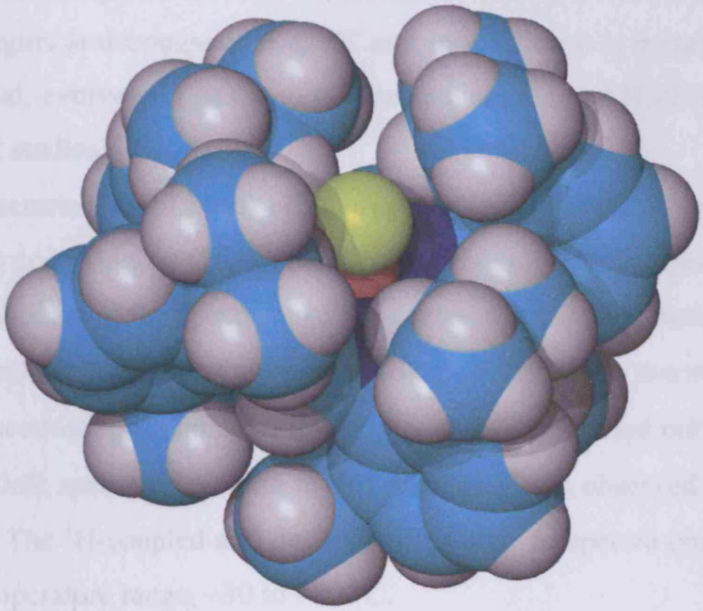

Figure 1 a) Molecular structure of [InH(Fiso)$_2$] (**31**); b) Space filling model of (**31**), the hydride ligand is shown in yellow (at the centre).

Selected bond lengths (Å) and angles (°): In(1)—N(3) 2.177(3), In(1)—N(1) 2.196(3), In(1)—N(2) 2.289(3), In(1)—N(4) 2.301(3), In(1)—H(1a) 1.71(6), N(1)—C(1) 1.320(4), N(2)—C(1) 1.310(4), N(3)—C(26) 1.305(4), N(4)—C(26) 1.307(4), N(1)—In(1)—N(2) 59.64(10), N(3)—In(1)—N(4) 59.38(10), N(2)—In(1)—N(4) 146.08(10), N(1)—In(1)—N(3) 116.26(10), N(1)—In(1)—H(1a) 123.9(17), N(2)—In(1)—H(1a) 113.8(19), N(3)—In(1)—H(1a) 119.1(17), N(4)—In(1)—H(1a) 100.0(19), N(2)—C(1)—N(1) 116.1(3), N(3)—C(26)—N(4) 116.4(3).

To examine the mechanism of formation of **31**, the reaction of $Li[InH_4]$ with HFiso was carried out in a 1:1 stoichiometry, which led to the formation of the amidotrihydrido indate complex, **32**, in moderate yield. Further treatment of **32** with HFiso led to the formation of **31**, H_2, and LiH, thus confirming that **32** is an intermediate in the aforementioned 2:1 reaction. In the solid state, **32** begins to decompose at 42 °C and in solution it is unstable above 0 °C and deposits indium metal, evolves H_2 gas, and generates a solution of [Li(Fiso)], as determined by ^{7}Li- and ^{1}H-NMR studies.

The infrared spectrum (Nujol mull) of **32** displays In—H stretching absorptions for the terminal (1719 cm^{-1}) and bridging (1632 cm^{-1}) hydride ligands, the assignment of which was confirmed by their absence in the spectrum of the corresponding trideuteride complex, **32**-D_3 (1161 cm^{-1} In—D bridging, In—D terminal-masked). Because of the thermal instability of **32** in solution, NMR spectroscopic studies of this compound were carried out at ≤ -30 °C and in the case of the ^{1}H-NMR spectrum, a broad In—H resonance was observed at δ = 6.02 ppm in the normal region.[55] The ^{1}H-coupled and decoupled ^{6}Li and ^{7}Li spectra comprise only singlet resonances in the temperature range, –30 to –80 °C.

The solid-state structure of **32** is depicted in Figure 2 and represents the first structural characterisation of an amido-trihydrido indate complex. The location and isotropic refinement of the hydride ligands confirmed that the complex dimerises through intermolecular hydride bridges to give a $\{Li_2In_2H_4\}$ ring, which adopts what could be described as a boat conformation with the intramolecular hydride bridges, H(2a) and H(2a_2), *cis* to each other.

For reasons of comparison, this work has been extended to aluminium and gallium chemistry. Accordingly, solutions of $Li[MH_4]$ (M = Al and Ga) were reacted with HFiso in 1:1 and 2:1 stoichiometries (Scheme 19). The 1:1 reactions of $Li[AlH_4]$ and $Li[GaH_4]$ with HFiso led in both cases to the formation of the amidotrihydrido alanate, **34**, and gallate, **36**, complexes, in moderate yields (compare formation of **32**). Treatment of a solution of $Li[AlH_4]$ in THF with two equivalents of HFiso led to H_2 and LiH elimination and a moderate yield of **33** after re-crystallisation from toluene (compare formation of **31**). Treatment of $Li[GaH_4]$ with two equivalents of HFiso did not give the expected analogous Ga-complex, but instead only the 1:1 complex, **36**. This behaviour can be explained by the less hydridic nature of Ga—H bonds compared with Al—H and In—H bonds[3, 55] and the fact that gallium hydride complexes disfavour co-ordination numbers greater than 4.[3] The 2:1 reaction of $[GaH_3(quin)]$ (quin = quinuclidine) with HFiso, however, led to H_2 and quinuclidine elimination and

complex **35**, a gallium analogue of compounds **31** and **33**. The formation of **35** is unusual, considering the fact that gallium hydrides disfavour co-ordination numbers greater than 4.[3]

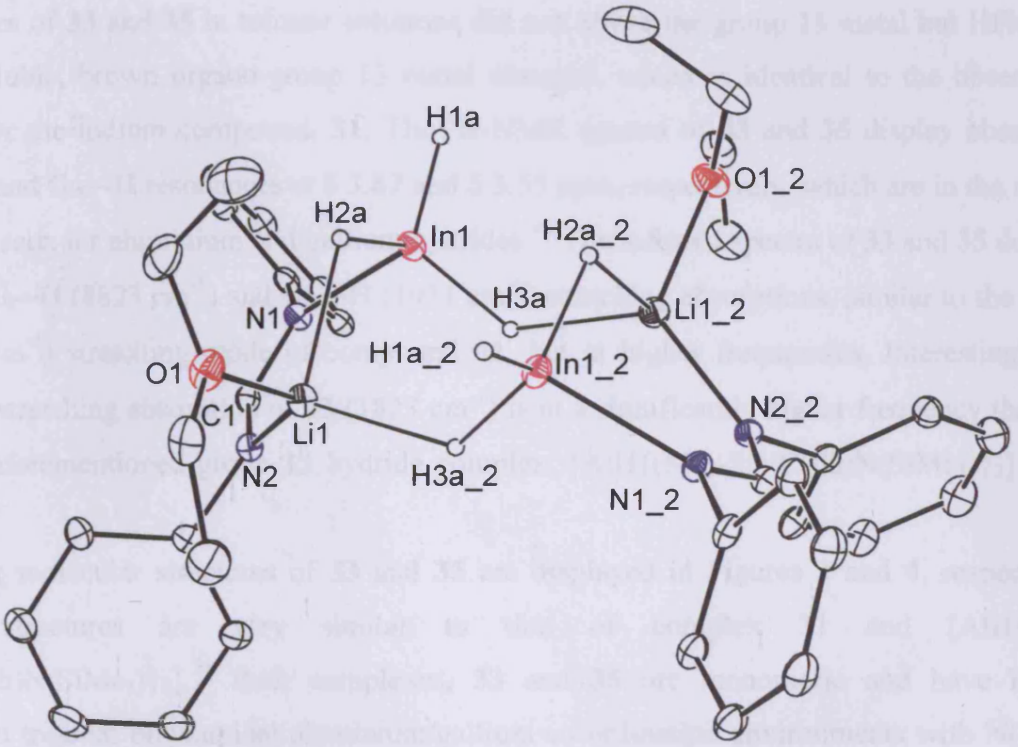

Figure 2 Molecular structure of [{InH_3(Fiso)Li(Et_2O)}$_2$] (**32**)
(isopropyl groups omitted for clarity)

Selected bond lengths (Å) and angles (°): In(1)—N(1) 2.178(3), In(1)—H(1a) 1.64(4), In(1)—H(2a) 1.71(4), In(1)—H(3a) 1.66(4), Li(1)—H(2a) 2.14(5), Li(1)—H(3a_2) 2.10(5), N(2)—Li(1) 2.002(6), N(1)—C(1) 1.329(4), N(2)—C(1) 1.308(4), N(1)—In(1)—H(1a) 106.9(15), N(1)—In(1)—H(2a) 99.7(15), N(1)—In(1)—H(3a) 104.8(13), H(1a)—In(1)—H(2a) 114.6(19), H(1a)—In(1)—H(3a) 115.3(19), H(2a)—In(1)—H(3a) 113.3(2), In(1)—H(2a)—Li(1) 106.5(2), Li(1_2)—H(2a_2)—In(1_2) 124.2(4), N(1)—C(1)—N(2) 124.8(3).

Both compounds, **33** and **35** are remarkably air stable. They are also very thermally stable and decompose under argon at, 231 – 233 °C (**33**) and 211 °C (**35**), (*cf.* **31**, (160 °C)). As expected, the decomposition temperature of the gallium compound **35** is slightly lower compared to its congruent aluminium compound, **33**. Investigations of the decomposition processes of **33** and **35** in toluene solutions did not afford the group 13 metal but HFiso and an insoluble, brown organo-group 13 metal material, which is identical to the observation made for the indium compound, **31**. The ^{1}H-NMR spectra of **33** and **35** display observable Al—H and Ga—H resonances at δ 3.87 and δ 3.55 ppm, respectively, which are in the normal regions seen for aluminium and gallium hydrides.[10] The infrared spectra of **33** and **35** do show sharp Al—H (1823 cm^{-1}) and Ga—H (1911 cm^{-1}) stretching absorptions, similar to the In—H (1748 cm^{-1}) stretching mode of compound **31**, but at higher frequencies. Interestingly, the Al—H stretching absorption of **33** (1823 cm^{-1}) is at a significantly higher frequency than that in the aforementioned group 13 hydride complex, [AlH{(Me$_3$-SiNC(Ph)N(SiMe$_3$)}$_2$] (1773 cm^{-1}).[79]

The molecular structures of **33** and **35** are displayed in Figures 3 and 4, respectively. Their structures are very similar to that of complex **31** and [AlH{(Me$_3$-SiNC(Ph)N(SiMe$_3$)}$_2$].[79] Both complexes, **33** and **35** are monomeric and have heavily distorted trigonal bipyramidal aluminium/gallium co-ordination environments with N(1) and N(4) in axial positions. The Al—H bond length is 1.83(2) Å (*cf.* 1.55(2) Å in [AlH{(Me$_3$-SiNC(Ph)N(SiMe$_3$)}$_2$])[79] and the Ga—H bond length is 1.64(8) Å (*cf.* average 1.59 Å in [(H$_3$Ga)$_2${(PPr$^{i}_2$CH$_2$)$_2$}]).[10] The M—N distances in both complexes are in the normal range.

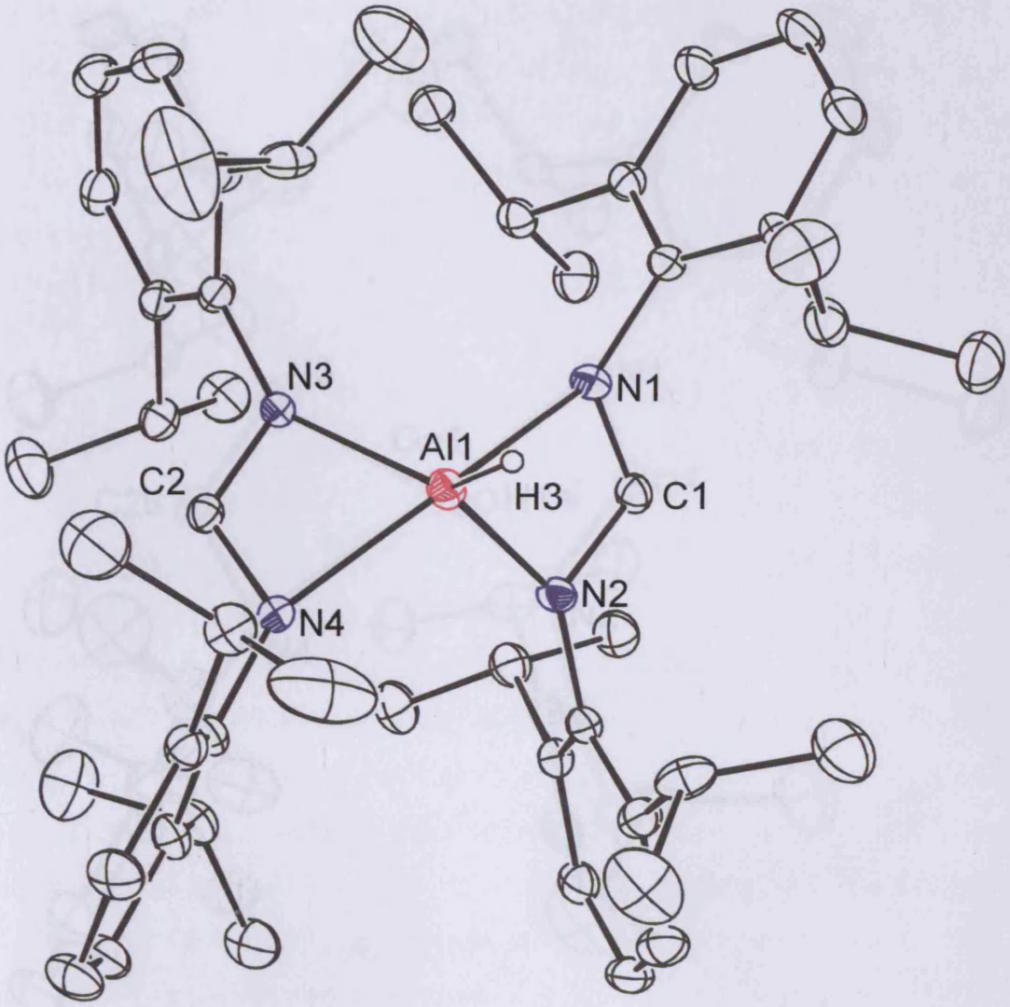

Figure 3 Molecular structure of $[AlH(Fiso)_2]$ (**33**)

Selected bond lengths (Å) and angles (°): Al(1)—N(3) 1.929(2), Al(1)—N(1) 2.059(2), Al(1)—N(2) 1.911(2), Al(1)—N(4) 2.079(2), Al(1)—H(3) 1.832(5), N(1)—C(1) 1.298(3), N(2)—C(1) 1.332(3), N(3)—C(2) 1.332(4), N(4)—C(2) 1.296(3), N(1)—Al(1)—N(2) 66.68(09), N(3)—Al(1)—N(4) 66.61(09), N(1)—Al(1)—N(4) 158.10(09), N(2)—Al(1)—N(3) 123.21(09), N(1)—Al(1)—H(3) 100.54(15), N(2)—Al(1)—H(3) 117.1(39), N(3)—Al(1)—H(3) 119.6(67), N(4)—Al(1)—H(3) 101.3(67), N(2)—C(1)—N(1) 112.3(8), N(3)—C(2)—N(4) 114.0(3).

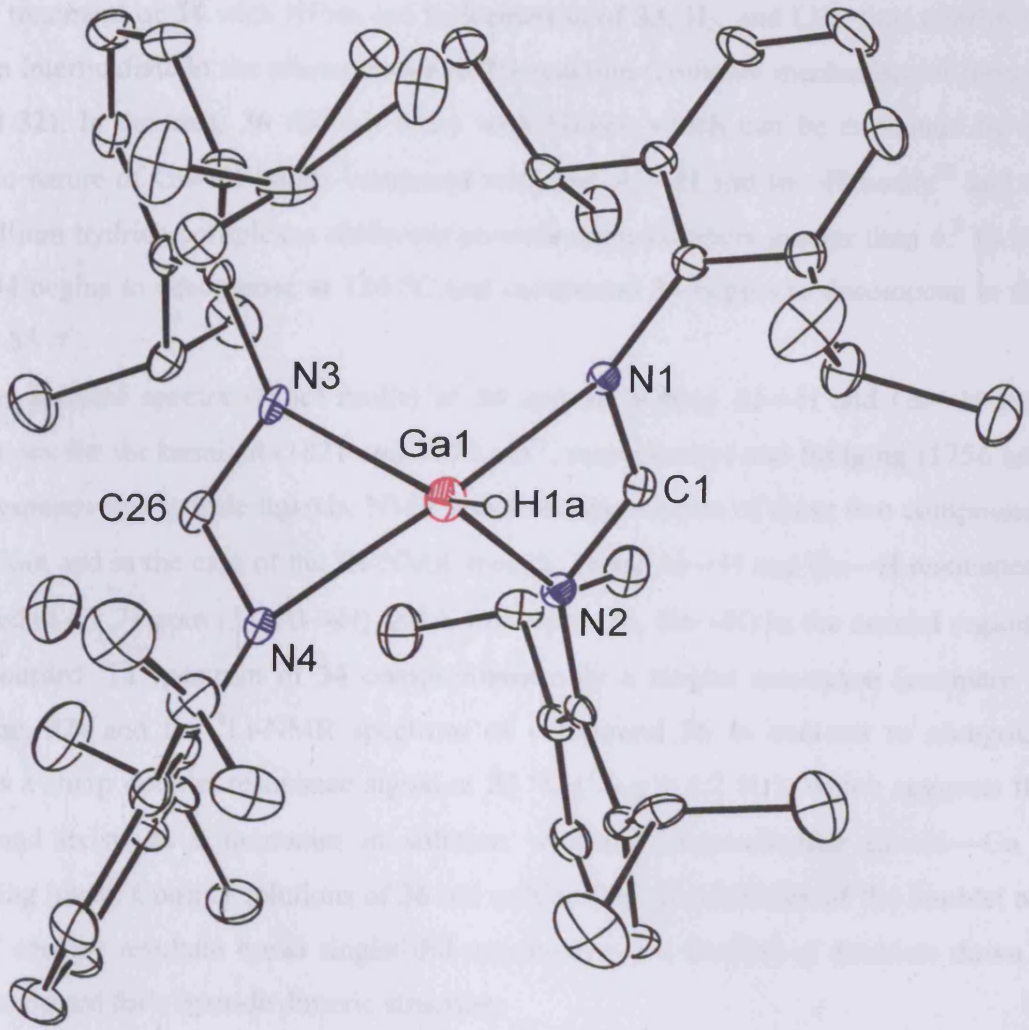

Figure 4 Molecular structure of [GaH(Fiso)$_2$] (**35**)

Selected bond lengths (Å) and angles (°): Ga(1)—N(3) 1.977(4), Ga(1)—N(1) 2.137(4), Ga(1)—N(2) 2.001(4), Ga(1)—N(4) 2.173(4), Ga(1)—H(1a) 1.648(5), N(1)—C(1) 1.297(4), N(2)—C(1) 1.312(5), N(3)—C(26) 1.314(5), N(4)—C(26) 1.302(3), N(1)—Al(1)—N(2) 64.68(11), N(3)—Ga(1)—N(4) 64.55(11), N(1)—Ga(1)—N(4) 152.68(11), N(2)—Ga(1)—N(3) 119.61(12), N(1)—Ga(1)—H(1a) 103.86(13), N(2)—Ga(1)—H(1a) 120.3(04), N(3)—Ga(1)—H(1a) 120.0(76), N(4)—Ga(1)—H(1a) 103.4(36), N(2)—C(1)—N(1) 116.3(2), N(3)—C(26)—N(4) 116.3(6).

Compounds **34** and **36** are closely related to their indium analogue, **32**. It was found that further treatment of **34** with HFiso led to formation of **33**, H_2, and LiH, thus confirming that **34** is an intermediate in the aforementioned 2:1 reaction (compare mechanism of formation of **31** and **32**). In contrast, **36** did not react with HFiso, which can be explained by the less hydridic nature of Ga—H bonds compared with and Al—H and In—H bonds[55] and the fact that gallium hydride complexes disfavour co-ordination numbers greater than 4.[3] In the solid state, **34** begins to decompose at 126 °C and compound **36** begins to decompose in the solid state at 85 °C.

The infrared spectra (Nujol mulls) of **34** and **36** display Al—H and Ga—H stretching absorptions for the terminal (1821 and 1879 cm^{-1}, respectively) and bridging (1756 and 1769 cm^{-1}, respectively) hydride ligands. NMR spectroscopic studies of these two compounds were carried out and in the case of the ^{1}H-NMR spectra, broad Al—H and Ga—H resonances were observed at δ 3.74 ppm (**34**, Al—H) and δ 4.68 ppm (**36**, Ga—H) in the normal region.[10] The ^{1}H-decoupled ^{7}Li spectrum of **34** compromises only a singlet resonance (compare indium analogue, **32**) and the ^{6}Li-NMR spectrum of compound **36** in contrast to compound **32**, exhibits a sharp doublet resonance signal at 25 °C ($^1J_{LiH}$ = 1.2 Hz), which suggests that this compound exists as a monomer in solution with the intramolecular Li—H—Ga bridge remaining intact. Cooling solutions of **36** led only to loss of resolution of the doublet at about –15 °C and the resultant broad singlet did not resolve to a doublet of doublets down to –80 °C, as expected for a hydride dimeric structure.

The solid state structures of **34** and **36** are depicted in Figures 5 and 6, respectively. As seen for the indium compound, **32**, the location and isotropic refinement of the hydride ligands confirmed that the complexes dimerise through intermolecular hydride bridges to give $\{Li_2M_2H_4\}$ (M = Al and Ga) rings, which adopt what could be described as chair conformations with the intramolecular hydride bridges, H(2a) and H(2a_2), *trans* to each other (compare **32**, H(2a) and H(2a_2), *cis* to each other, giving a *pseudo* boat conformation). The bridging formamidinate ligand backbones in **34** and **36** are more open [N(1)—C(1)—N(2) 122.8(7)° and 123.4(4)°, respectively] and significantly more localised than the chelating ligands in **33** and **35** [average N—C—N 113.2° and 116.3°, respectively].

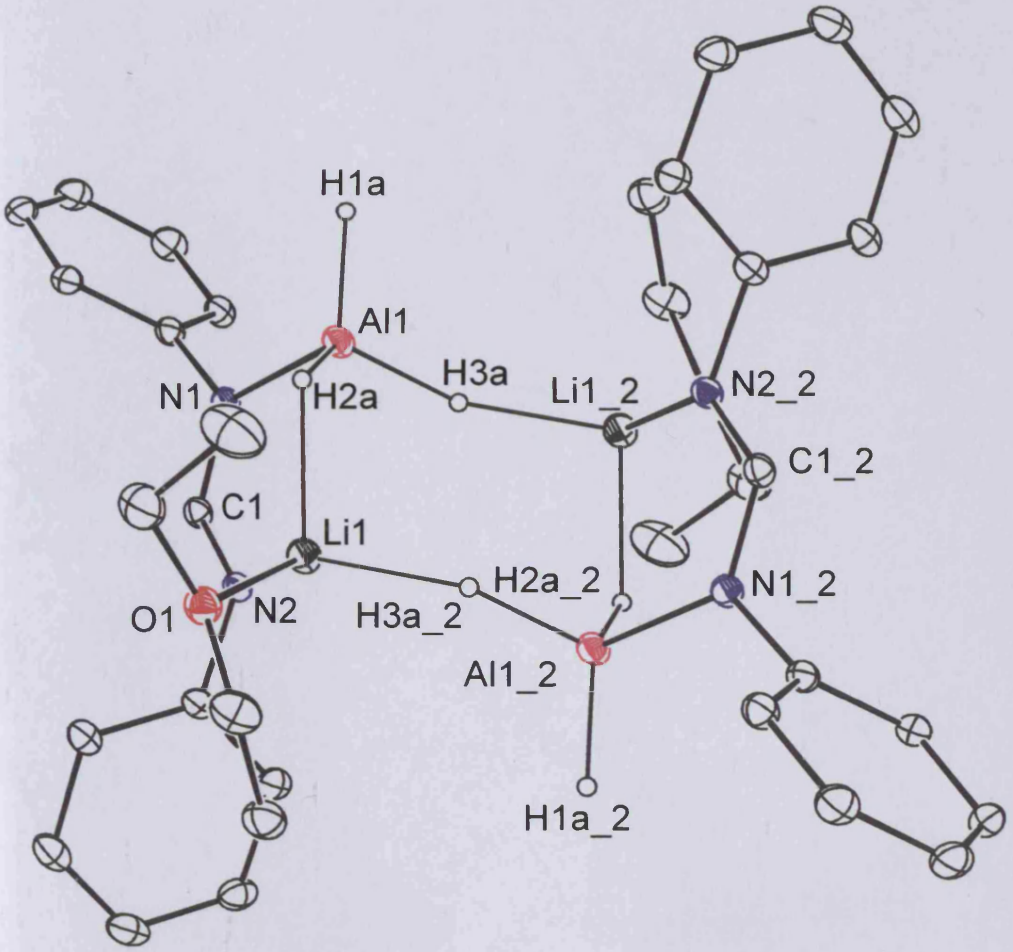

Figure 5 Molecular structure of [{AlH_3(Fiso)Li(Et_2O)}$_2$] (**34**)
(isopropyl groups omitted for clarity)

Selected bond lengths (Å) and angles (°): Al(1)—N(1) 1.892(2), Al(1)—H(1a) 1.52(3), Al(1)—H(2a) 1.50(6), Al(1)—H(3a) 1.55(7), Li(1)—H(2a) 1.96(7), Li(1)—H(3a_2) 1.92(7), N(2)—Li(1) 2.038(5), N(1)—C(1) 1.343(3), N(2)—C(1) 1.297(3), N(1)—Al(1)—H(1a) 108.6(6), N(1)—Al(1)—H(2a) 105.5(23), N(1)—Al(1)—H(3a) 108.7(38), H(1a)—Al(1)—H(2a) 114.8(29), H(1a)—Al(1)—H(3a) 112.0(51), H(2a)—Al(1)—H(3a) 106.6(7), Al(1)—H(2a)—Li(1) 111.5(3), Li(1_2)—H(2a_2)—Al(1_2) 97.4(4), N(1)—C(1)—N(2) 122.8(7).

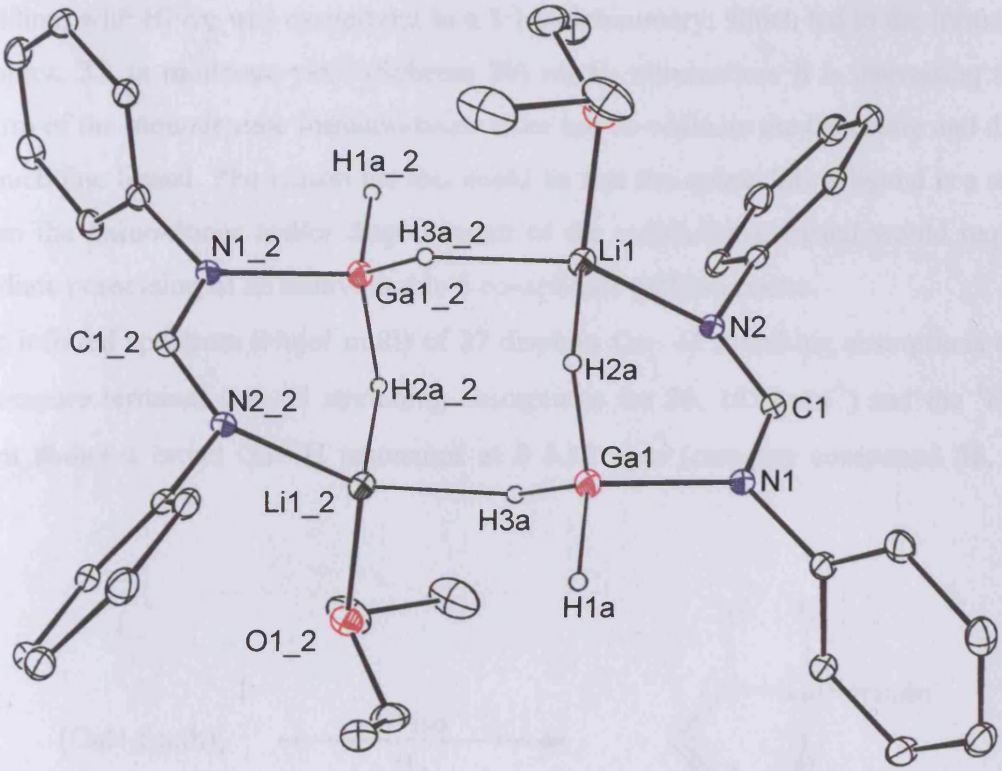

Figure 6 Molecular structure of [{GaH_3(Fiso)Li(Et_2O)}$_2$] (**36**)
(isopropyl groups omitted for clarity)

Selected bond lengths (Å) and angles (°): Ga(1)—N(1) 1.955(5), Ga(1)—H(1a) 1.48(0), Ga(1)—H(2a) 1.54(4), Ga(1)—H(3a) 1.51(0), Li(1)—H(2a) 2.01(8), Li(1)—H(3a_2) 1.97(0), N(2)—Li(1) 2.003(2), N(1)—C(1) 1.336(5), N(2)—C(1) 1.298(7), N(1)—Ga(1)—H(1a) 106.2(1), N(1)—Ga(1)—H(2a) 103.6(13), N(1)—Ga(1)—H(3a) 106.1(93), H(1a)—Ga(1)—H(2a) 115.9(92), H(1a)—Ga(1)—H(3a) 114.5(21), H(2a)—Ga(1)—H(3a) 109.2(2), Ga(1)—H(2a)—Li(1) 105.8(8), Li(1_2)—H(2a_2)—Ga(1_2) 96.6(9), N(1)—C(1)—N(2) 123.4(4).

To examine the mechanism of formation of **35**, the reaction of $[GaH_3(quin)]$ (quin = quinuclidine) with HFiso was carried out in a 1:1 stoichiometry, which led to the formation of the complex, **37**, in moderate yield (Scheme 20) *via* H_2 elimination. It is interesting that the imino-arm of the monodentate formamidinate does not co-ordinate the Ga centre and displace the quinuclidine ligand. The reason for this could be that the quinuclidine ligand is a stronger base than the imino-donor and/or displacement of the quinuclidine ligand would require an intermediate possessing of an unfavourable 5 co-ordinate gallium centre.

The infrared spectrum (Nujol mull) of **37** displays Ga—H stretching absorptions at 1872 cm^{-1} (compare terminal Ga—H stretching absorptions for **36**, 1879 cm^{-1}) and the ^{1}H-NMR spectrum shows a broad Ga—H resonance at δ 5.12 ppm (compare compound **36**, δ 4.68 ppm).

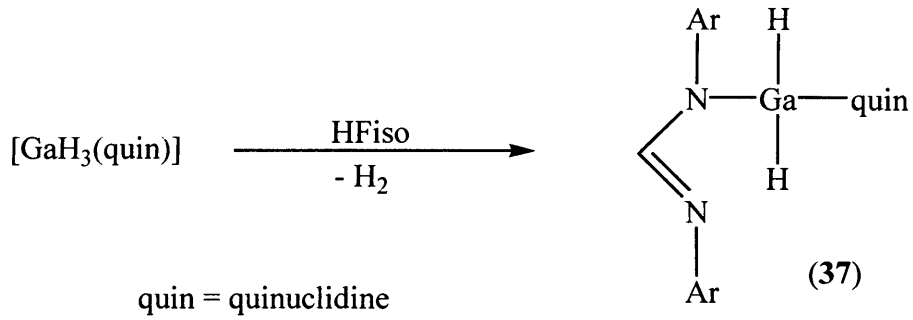

Scheme 20

The solid state structure of **37** is shown in Figure 7. The gallium centre has a distorted tetrahedral co-ordination environment and the Ga—N bond length for the quinuclidine ligand is slightly longer than that for the Fiso fragment [Ga(1)—N(3) 2.063(3) Å and Ga(1)—N(1) 1.948(7) Å] but similar to the Ga—N bond lengths seen in other N-donor ligand gallium complexes (*e.g.* $[GaCl_2H(quin)]$[23] 2.017(3) Å and $[GaCl_3(HFiso)]$ 1.941(5) Å, see Chapter 2). The Ga—H distances (1.52 Å average) are comparable to the Ga—H distances observed in $[GaClH_2(quin)_2]$ (1.51 Å average).[23] An examination of the N—C distances of the backbone of the Fiso ligand shows it to be largely localised with a C(1)—N(2) double bond and a C(1)—N(1) single bond.

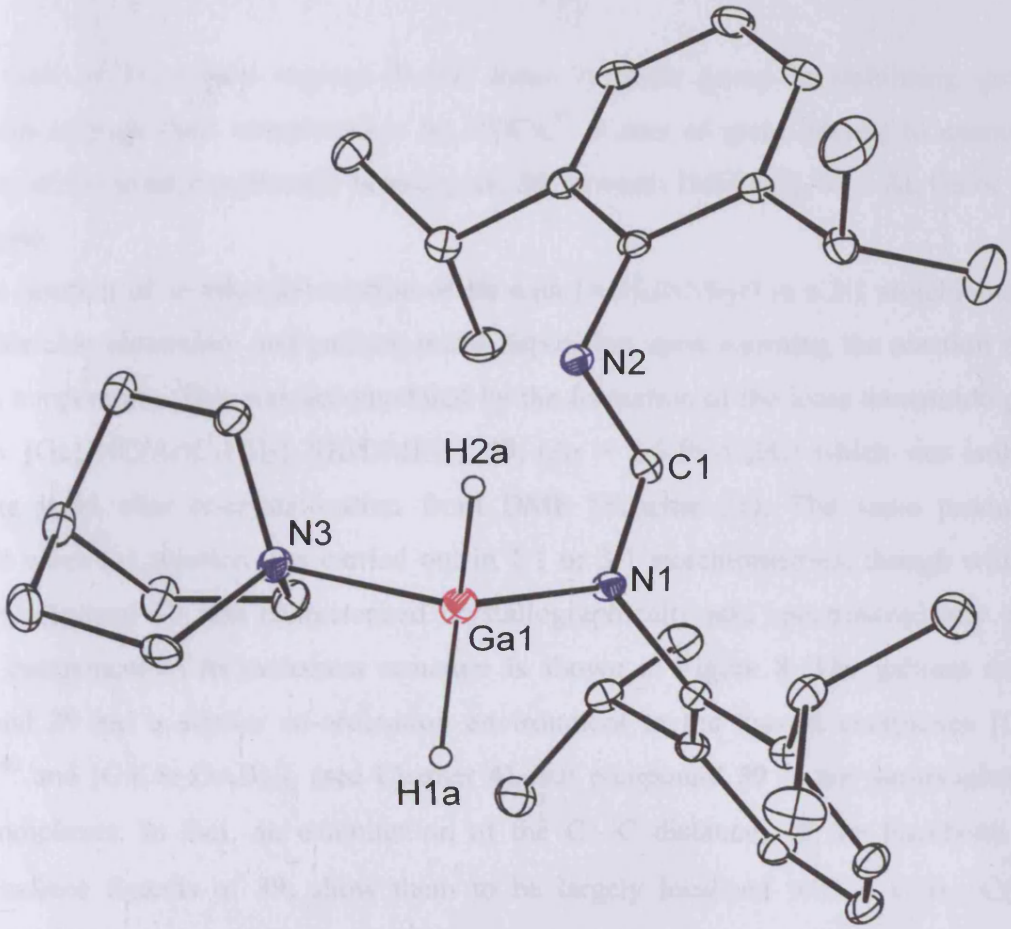

Figure 7 Molecular structure of [(Fiso)GaH_2(quin)] (**37**)

Selected bond lengths (Å) and angles (°): Ga(1)—N(1) 1.948(7), Ga(1)—N(3) 2.063(3), Ga(1)—H(1a) 1.505(4), Ga(1)—H(2a) 1.529(3), N(1)—C(1) 1.354(7), N(2)—C(1) 1.285(5), N(1)—Ga(1)—N(3) 108.41(5), N(1)—C(1)—N(2) 123.31(4), N(1)—Ga(1)—H(1a) 111.29(3), N(1)—Ga(1)—H(2a) 108.26(4), N(3)—Ga(1)—H(1a) 103.23(7), N(3)—Ga(1)—H(2a) 104.26(5).

5.6.2 Group 13 hydride complexes derived from a gallium(I) carbene analogue

In view of the recent success in the Jones research group in stabilising group 13 trihydrides through their complexation by NHCs,[55] it was of great interest to examine the reactivity of the anionic gallium(I) heterocycle, **38**, towards $[MH_3(L)]$, M = Al, Ga or In, L = Lewis base.

The reaction of an ethereal solution of **38** with $[AlH_3(NMe_3)]$ in a 2:1 stoichiometry led to considerable aluminium and gallium metal deposition upon warming the reaction mixture to room temperature. This was accompanied by the formation of the ionic tetraamido gallium complex $[Ga\{[NC(Ar)C(H)]_2\}_2][K(DME)_4]$, **39**, (Ar = 2,6-$Pr^i_2C_6H_3$) which was isolated in moderate yield after re-crystallisation from DME (Scheme 21). The same product was obtained when the reaction was carried out in 1:1 or 3:1 stoichiometries, though with lower yields. Compound **39** was characterised crystallographically and spectroscopically and the anionic component of its molecular structure is shown in Figure 8. The gallium centre of compound **39** has a similar co-ordination environment to the known complexes $[Ga(Bu^t\text{-}DAB)_2]$[80] and $[Ga(Ar\text{-}DAB)_2]$, (see Chapter 4), but compound **39** is not paramagnetic like those complexes. In fact, an examination of the C—C distances of the backbone of the diazabutadiene ligands of **39**, show them to be largely localised with a C(1)—C(2) and C(27)—C(28) double bonds. Complex **39** presumably forms *via* an unknown intermediate which is unstable at room temperature. It was originally thought this decomposition process involved the generation of the free diazabutadiene, $(ArN{=}C(H))_2$, which was doubly reduced by an excess of **38** to give the observed product. However, this was discounted as intentionally treating $(ArN{=}C(H))_2$ with **38** led to no reaction.

An indication of the nature of the intermediate in the decomposition process that affords **39** might come from the analogous reactions of **38** with tertiary amine adducts of GaH_3 and InH_3 in 2:1 stoichiometries (Scheme 21). These reactions gave high yields of the novel trimetallic group 13 hydride complexes, **40** and **41**. When these reactions were carried out in 1:1 or 3:1 stoichiometries, the same products were formed but with reduced yields. It is noteworthy that the lithium counterion in **41** originates from LiBr, which is generated as an inseparable by-product in the *in situ* preparation of $[InH_3(NMe_3)]$.

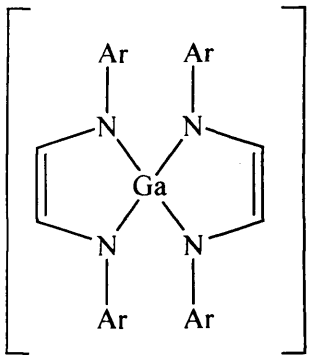

(39)

$[K(DME)_4]$

$[AlH_3(NMe_3)]$
Et_2O / DME

$[GaH_3(quin)]$

Et_2O

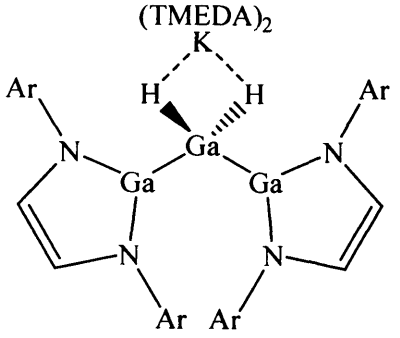

(40)

2

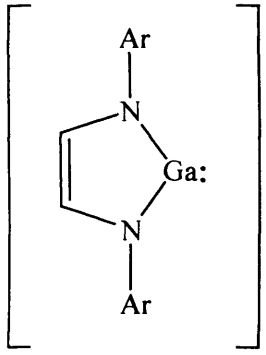

$[K(TMEDA)]$

(38)

$[InH_3(NMe_3)]$, LiBr

Et_2O

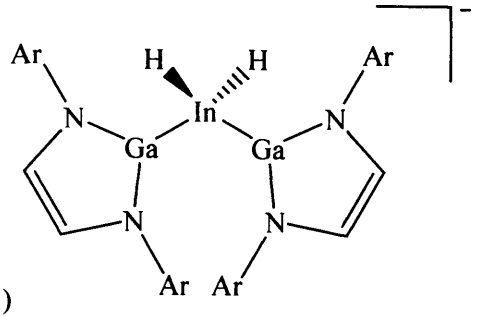

(41)

$[Li(TMEDA)_2]^+$

Ar = 2,6-$Pr^i_2C_6H_3$
quin = quinuclidine

Scheme 21

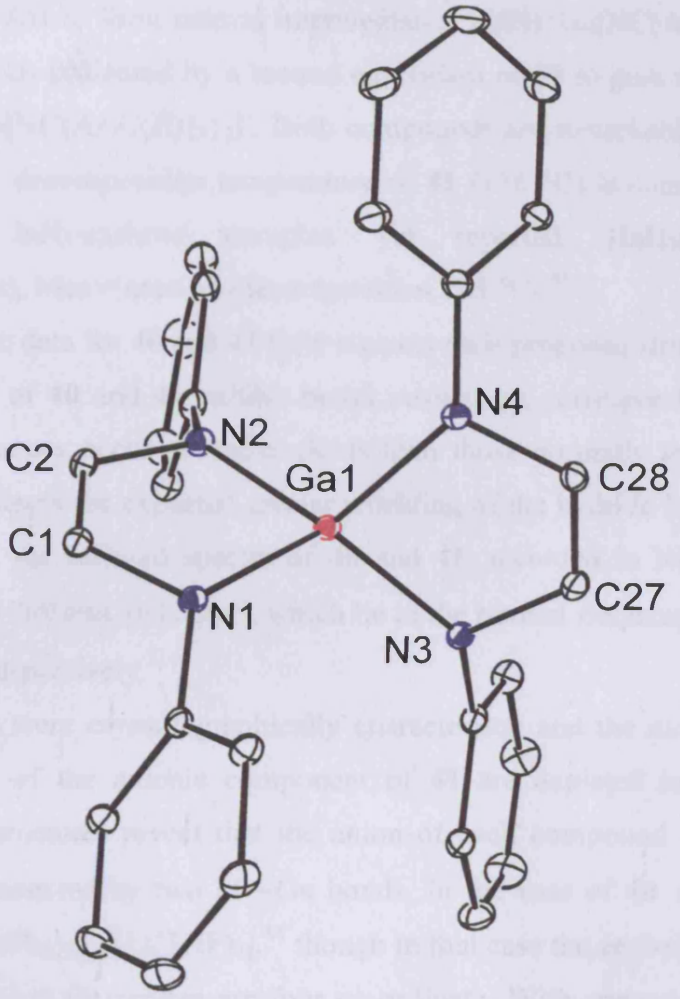

Figure 8 Structure of the anionic component of $[Ga(Ar\text{-}DAB)_2][K(DME)_4]$ (**39**) (isopropyl groups omitted for clarity)

Selected bond lengths (Å) and angles (°): Ga(1)—N(1) 1.940(5), Ga(1)—N(2) 1.928(3), Ga(1)—N(3) 1.926(7), Ga(1)—N(4) 1.941(2), C(1)—C(2) 1.336(9), C(27)—C(28) 1.333(5), N(1)—C(1) 1.416(2), N(2)—C(2) 1.410(1), N(3)—C(27) 1.410(4), N(4)—C(28) 1.404(3), N(1)—Ga(1)—N(2) 88.93(5), N(3)—Ga(1)—N(4) 88.15(3), Ga(1)—N(1)—C(1) 105.95(2), Ga(1)—N(2)—C(2) 106.63(5), Ga(1)—N(3)—C(27) 106.92(7), Ga(1)—N(4)—C(28) 106.99(3), N(1)—C(1)—C(2) 119.21(5), N(3)—C(27)—C(28) 119.15(7), N(1)—Ga(1)—N(3) 115.01(6), N(2)—Ga(1)—N(4) 111.76(3).

The mechanisms of formation of **40** and **41** are unknown but presumably involve an initial elimination of KH to form neutral intermediates, $[MH_2\{Ga[NC(Ar)C(H)]_2\}]$, M = Ga or In, which are then co-ordinated by a second equivalent of **38** to give the observed anionic complexes, $[MH_2\{Ga[NC(Ar)C(H)]_2\}_2]^-$. Both compounds are remarkably stable in the solid state and, indeed, the decomposition temperature of **41** (116 °C) is comparable with that of the most stable InH_3-carbene complex yet reported, $[InH_3(IMes)]$, IMes = $:CN(Mes)C_2H_2N(Mes)$, Mes = mesityl (decomposition 115 °C).[55]

The spectroscopic data for **40** and **41** fully support their proposed structures. In particular, the ^{1}H-NMR spectra of **40** and **41** exhibit broad resonances corresponding to their hydride ligands. These resonances occur at higher fields than those normally seen for neutral MH_3 complexes, which reflects the expected greater shielding of the hydride ligands in the anionic systems. In addition, the infrared spectra of **40** and **41**, recorded in Nujol, display strong, broad absorptions at 1769 and 1632 cm^{-1}, which lie in the normal frequency ranges for Ga—H and In—H stretches respectively.[1, 55]

Both compounds were crystallographically characterised and the molecular structure of **40** and the structure of the anionic component of **41** are depicted in Figures 9 and 10 respectively. These structures reveal that the anion of each compound contains a chain of three metal atoms connected by two M—Ga bonds. In the case of **40**, comparisons can be made with $[Ga\{Ga(GePh_3)_3\}_2][Li(THF)_4]$,[81] though in that case the central Ga atom is two co-ordinate and the terminal Ga centres are four co-ordinate. With respect to **41**, there are no previously reported compounds containing Ga_2In chains but In_3 chains are relatively common, as in, for example, $[In\{C(SiMe_3)_3\}\{\mu\text{-Br-Li}(THF)_4\}\{In[C(SiMe_3)_3](\mu\text{-Br})\}_2]$.[82]

The hydride ligands of **40** and **41** were located from difference maps and refined isotropically. Those in **40** bridge the Ga and K centres to effectively from a contact ion pair. The central group 13 metal atom in each complex has a distorted tetrahedral environment whilst the gallium heterocycles are essentially planar and contain trigonal planar metal centers.

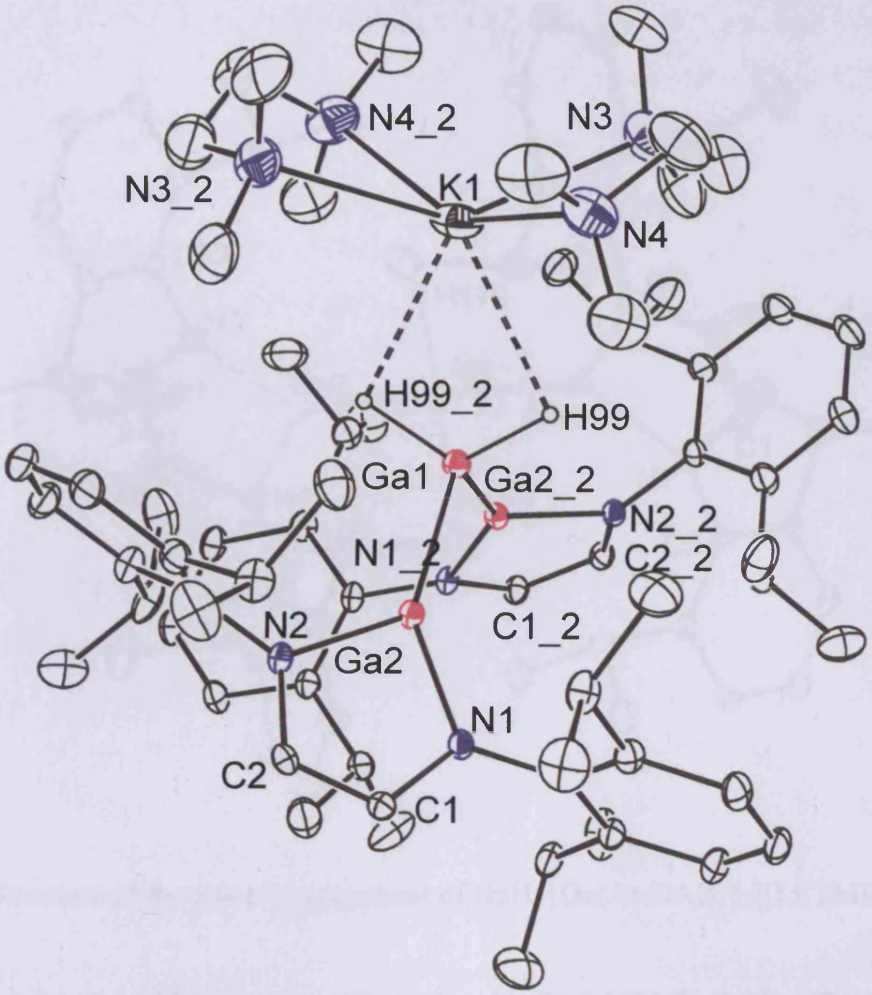

Figure 9 Molecular structure of $[GaH_2\{Ga(Ar\text{-}DAB)\}_2][K(TMEDA)_2]$ (**40**)

Selected bond lengths (Å) and angles (°): Ga(1)—Ga(2) 2.4071(9), Ga(1)—H(99) 1.49(6), Ga(2)—N(1) 1.877(4), Ga(2)—N(2) 1.886(4), C(1)—C(2) 1.357(7), N(1)—C(1) 1.399(6), N(2)—C(2) 1.381(6), K(1)—H(99) 2.87(6), K(1)—N(3) 2.760(7), K(1)—N(4) 2.920(9), Ga(2)—Ga(1)—Ga(2_2) 107.24(4), Ga(2)—Ga(1)—H(99) 111.(2), Ga(2_2)—Ga(1)—H(99) 106.(2), H(99)—Ga(1)—H(99_2) 116.(2), N(1)—Ga(2)—N(2) 86.98(16), N(1)—Ga(2)—Ga(1) 142.88(12), N(2)—Ga(2)—Ga(1) 129.68(11), C(1)—N(1)—Ga(2) 110.4(3), C(2)—N(2)—Ga(2) 110.0(3).

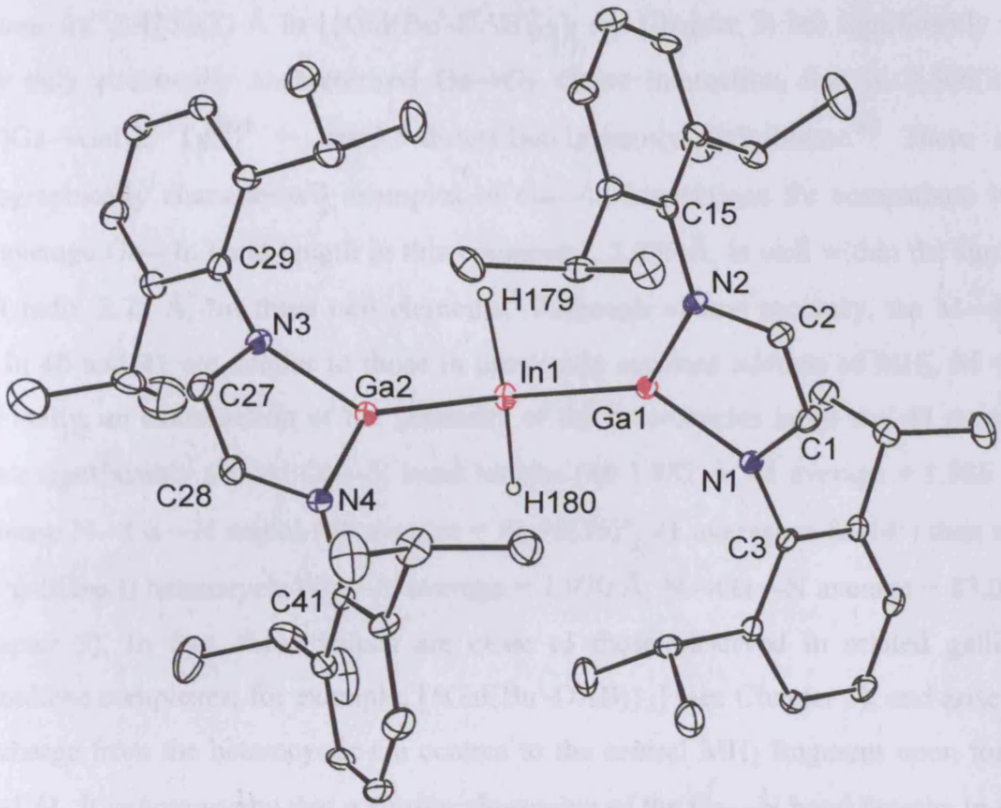

Figure 10 Structure of the anionic component of $[InH_2\{Ga(Ar\text{-}DAB)\}_2][Li(TMEDA)_2]$ (**41**)

Selected bond lengths (Å) and angles (°): In(1)—Ga(2) 2.5921(8), In(1)—Ga(1) 2.5983(8), In(1)—H(179) 1.72(2), In(1)—H(180) 1.73(2), Ga(1)—N(1) 1.896(4), Ga(1)—N(2) 1.883(4), Ga(2)—N(3) 1.885(5), Ga(2)—N(4) 1.880(5), N(1)—C(1) 1.400(7), N(2)—C(2) 1.383(7), N(3)—C(27) 1.405(7), N(4)—C(28) 1.394(7), C(1)—C(2) 1.331(7), C(27)—C(28) 1.336(8), Ga(1)—In(1)—Ga(2) 103.19(3), Ga(2)—In(1)—H(179) 101.0(2), Ga(1)—In(1)—H(179) 108.0(2), Ga(2)—In(1)—H(180) 110.0(2), Ga(1)—In(1)—H(180) 110.0(2), H(179)—In(1)—H(180) 123.0(3), N(2)—Ga(1)—N(1) 86.09(18), N(3)—Ga(2)—N(4) 86.8(2), N(2)—Ga(1)—In(1) 136.44(13), N(1)—Ga(1)—In(1) 137.39(13), N(3)—Ga(2)—In(1) 135.11(14), N(4)—Ga(2)—In(1) 138.08(14).

The Ga—Ga bonds in **40** (2.4071(9) Å) are normal for single, covalent Ga—Ga interactions (*cf.* 2.4232(7) Å in [{GaI(Bu^t-DAB)}$_2$], see Chapter 3) but significantly shorter than the only structurally characterised Ga→Ga dative interaction, that is, 2.506(3) Å in [(Tp^{tBu2})Ga→GaI$_3$], Tp^{tBu2} = tris(3,5-di-tert-butylpyrazolyl)hydroborate.[83] There are no crystallographically characterised examples of Ga—In interactions for comparison with **41** but the average Ga—In bond length in this compound, 2.595 Å, is well within the sum of the covalent radii, 2.75 Å, for these two elements.[6] Although of low accuracy, the M—H bond lengths in **40** and **41** are similar to those in previously reported adducts of MH$_3$, M = Ga or In.[1, 55] Finally, an examination of the geometry of the heterocycles in **40** and **41** reveals that they have significantly shorter Ga—N bond lengths (**40** 1.882 Å, **41** average = 1.886 Å) and more obtuse N—Ga—N angles (**40** average = 86.98(16)°, **41** average = 86.44°) than those in the free gallium(I) heterocycle (Ga—N average = 1.970 Å, N—Ga—N average = 83.02(11)°, see Chapter 3). In fact, these values are close to those observed in related gallium(II)-diazabutadiene complexes, for example, [{GaI(Bu^t-DAB)}$_2$] (see Chapter 3), and arise from a loss of charge from the heterocyclic Ga centres to the central MH$_2$ fragment upon formation of **40** and **41**. It is noteworthy that a similar shortening of the Ga—N bond lengths in gallium donor ligand of [(Tp^{tBu2})Ga→GaI$_3$] occurs upon complex formation.

This effect in **40** and **41** has been examined by preliminary Density Functional calculations which have been carried out on the model anions, [MH$_2${Ga[NC(H)C(H)]$_2$}$_2$]$^-$, M = Ga (**42**) or In (**43**). The fully optimised geometries of these compounds are similar to those of the anions in **40** and **41** taking into account the steric differences between the theoretical and experimental situations. Significantly, the Ga—N distances (**42** average = 1.900 Å, **43** average = 1.900 Å) and the N—Ga—N angles (**42** average = 85.66°, **43** average = 85.74°) are comparable with those in **40**, **41** and Ga^{II} diazabutadiene complexes. In addition, there is a significant development of negative charge on the central metal atoms and MH$_2$ fragments (**42** Ga –0.35, MH$_2$ –0.77; **43** In –0.09, MH$_2$ –0.63) relative to the gallium atoms of the heterocycles (**42** average = +1.04, **43** average = +0.96).

5.6.3 Tertiary amine adducts of indium trihydride

Tertiary amine adducts of alane and gallane are often synthesised from the addition of an ammonium halide salt to a solution of either $Li[AlH_4]$ or $Li[GaH_4]$.[1-3] Alternatively, when using stronger primary (NH_2R) and secondary (NHR_2) amine donors or bi- / polydentate amines, the use of an $[MH_3(NMe_3)]$ (M = Al or Ga) reagent can be employed in direct ligand substitutions.[26, 27] In order to synthesise stable amine complexes of indane, the chosen ligand was quinuclidine.

The addition of quinuclidine or quinuclidine hydrochloride to solutions of $[GaH_3(NMe_3)]$ and $Li[AlH_4]$ respectively yields the stable complexes $[GaH_3(quin)]$[15] and $[AlH_3(quin)]$.[12] The analogous reaction of quinuclidine hydrochloride with $Li[InH_4]$ was undertaken by Jones *et al.*, and the complex $[InH_3(quin)]$, **44**, could be isolated (Scheme 22).[60] Due to the limited thermal tolerance of **44**, its molecular structure could not be confirmed by crystallographic studies, but all other spectroscopic data point towards its molecular structure, *e.g.* a broad In—H stretch in the infrared spectrum at 1639 cm^{-1}.

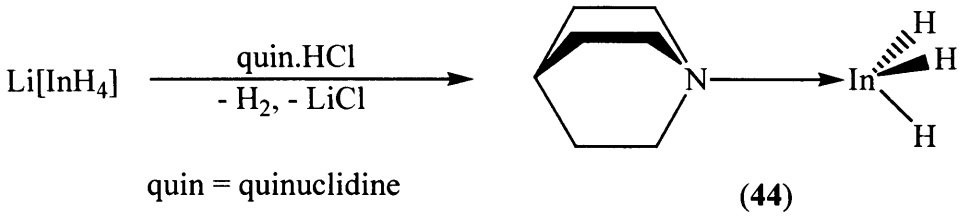

quin = quinuclidine

(44)

Scheme 22

Considering the thermal sensitivity of compound **44** and in view of complex, $[GaClH_2(quin)_2]$,[23] and its remarkable thermal stability (165 °C), the synthesis of the indium analogue compound $[InBrH_2(quin)_2]$, **45**, was attempted *via* the 2:1 reaction of quinuclidine hydrochloride with an ethereal solution of $Li[InH_4]$ (Scheme 23). Crystalline samples of **45** were obtained from the concentrated reaction mother liquor as colourless prisms that decompose at temperatures greater than 72 °C and in solution above 0 °C. It is noteworthy that the bromide in **45** originates from LiBr, which is generated as an inseparable by-product in the *in situ* preparation of $Li[InH_4]$.[55] The mechanism of formation of **45** presumably involves an initial elimination of H_2 and LiCl to form an intermediate, **44**, which is then

co-ordinated by a second equivalent of quinuclidine, which involves again elimination of H_2 and LiCl.

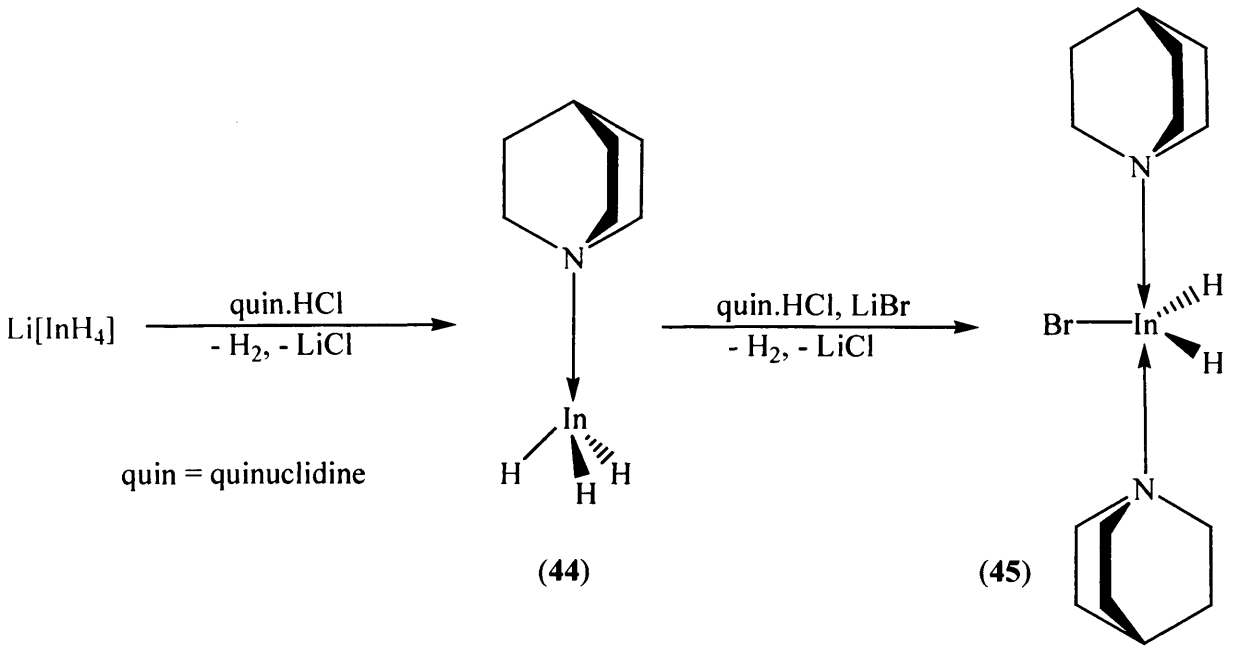

Scheme 23

The crystal structure of **45** was determined and can be seen in Figure 11. Compound **45** is monomeric in the solid state with a slightly distorted trigonal bipyramidal geometry about the metal centre (Br—In—N 89.02(34)°), which bears the quinuclidine ligands in the axial positions. This is comparable to the geometry of $[GaClH_2(quin)_2]$ (H—Ga—H 127(2)°, H—Ga—Cl 116.6(9)°, Cl—Ga—N 90.88(4)°), and likewise concurs with Bent's rule,[23] (compare **45**; H—In—H 132.58(3)°, H—In—Br 113.71(56)°, Br—In—N 89.02(34)°). The In—N bond lengths (average 2.42 Å) of **45** are comparable to those observed in $[InBr_3(quin)_2]$ (average 2.36 Å) and also the In—Br bond length of 2.593 Å is comparable to those seen in $[InBr_3(quin)_2]$, (In—Br bond lengths average 2.53 Å) (Chapter 2). The symmetry related hydride ligands were located, and their positions and isotropic thermal parameters were refined. The In—H bond length of 1.601(3) Å is similar to those in previously reported adducts of indium hydrides.[55]

Because of the thermal instability of **45** in solution, NMR spectroscopic studies of this compound were carried out at –30 °C and in the case of the ^{1}H-NMR spectrum, a broad

resonance was observed at δ = 3.56 ppm in the normal region for indium hydrides.[55] The infrared spectrum (Nujol mull) of **45** displays In—H stretching absorptions at 1707 cm^{-1}, which lies just in the normal frequency range for In—H stretches.[55]

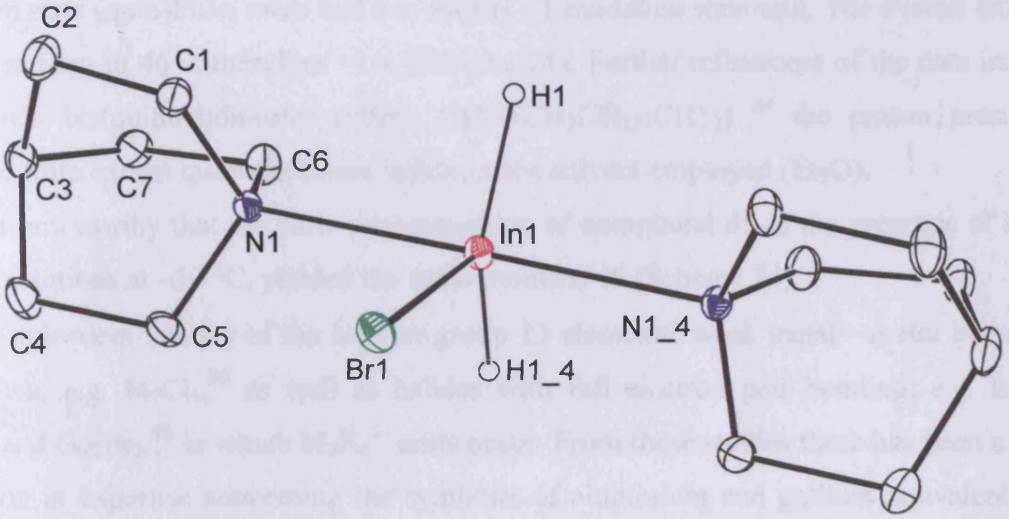

Figure 11 Molecular structure of $[InBrH_2(quinuclidine)_2]$ (**45**)

Selected bond lengths (Å) and angles (°): In(1)—Br(1) 2.593(4), In(1)—H(1) 1.601(3), In(1)—N(1) 2.429(2), N(1)—C(1) 1.478(1), N(1)—C(5) 1.486(2), N(1)—C(6) 1.481(7), N(1)—In(1)—Br(1) 89.02(34), N(1)—In(1)—H(1) 89.97(2), Br(1)—In(1)—H(1) 113.71(56), H(1)—In(1)—H(1_4) 132.58(3).

It is noteworthy that in an attempted synthesis of **45**, as laid out in Scheme 23, the total reaction mixture was left at –30 °C for a period of 5 days over which a colour change from colourless to orange occurred. After that time, volatiles were removed from the coloured solution to render a deep orange oily solid, **46**, which decomposed instantaneously at +5 °C yielding indium metal and behaved pyrophorically in air to yield a dark grey material that gave an indigo flame when combusted.

Subsequent re-crystallisation of **46** from toluene (-30 °C) yielded dark orange triangular prisms after placement at –50 °C for several days. The ^{1}H-NMR spectrum of the compound merely indicated the presence of equivalent quinuclidine ligands. The X-ray crystal structure of **46** was determined and is illustrated in Figure 12. This compound was first prepared and

characterised by Dr. M. Cole in the Jones research group but the X-ray data obtained was of insufficient quality to define bond lengths and angles accurately.[60]

The structure revealed an anionic 'In_5Br_8' subvalent indium cluster possessing an indium of formal oxidation state zero, at the tetrahedral pentaindium centre, three peripheral +2 oxidation state (quin)$InBr_2$ units and one formal +1 oxidation state unit. The overall oxidation state of indium in **46** is therefore +1.4 (Scheme 24). Further refinement of the data indicated the known bis(quinuclidinium) cation, $[H\{N(CH_2CH_2)_3CH\}_2]^+$,[84] the proton presumably procured from excess quinuclidinium halide or the solvent employed (Et_2O).

It is noteworthy that the slow decomposition of compound **45** in the presence of LiBr in toluene solutions at –30 °C, yielded the same product, **46** (Scheme 24).

For subvalent halides of the heavier group 13 elements, weak metal—metal interactions are known, *e.g.* In_7Cl_9,[85] as well as halides with full electron pair bonding, *e.g.* In_5Br_7,[86] Ga_2I_3[87] and Ga_2Br_3,[88] in which $M_2X_6^{2-}$ units occur. From these studies there has been a radical expansion in expertise concerning the synthesis of aluminium and gallium subvalent halide compounds. One such compound is the thermally sensitive, yellow coloured gallium cluster $[\{(Et_2O)_2ClGa\}Ga\{GaCl_2(Et_2O)\}_3]$, which disproportionates above 0 °C and bares a remarkable similarity to the anion of **46**.[89] This, analogously tetrahedral Ga_5 complex was prepared from the slow crystallisation of 'metastable' gallium(I) chloride from diethyl ether / toluene. The different oxidation states of the gallium in this compound (one of 0, one of +1 and three of +2, average oxidation state of gallium +1.4) are believed to result from disproportionation reactions, *e.g.* 2 Ga(I) → Ga(0) + Ga(I), and the comproportionation reaction Ga(III) + Ga(I) → Ga(II), the latter facilitated by the inevitable formation of gallium trichloride that results from the disproportionation of gallium(I) chloride under the conditions employed.[89] Given the +3 oxidation state of **44** and **45**, the formation and isolation of **46** presumably represents a trapped intermediate in the decomposition of such species to indium metal *via* processes such as H_2 elimination, hydride-/bromide exchange, disproportionation and/or HBr reductive elimination.

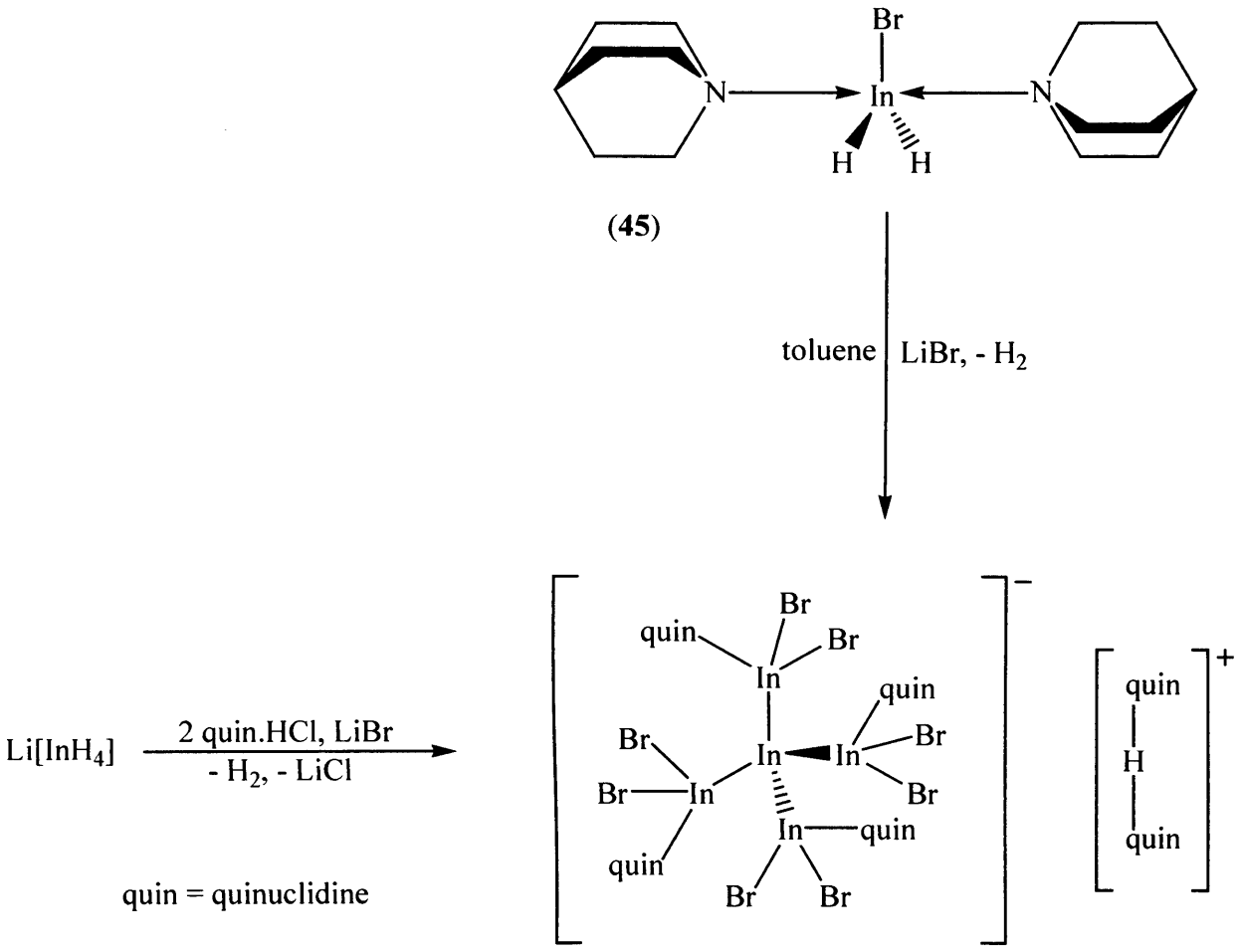
Br
N
In
N
H
H
(45)
toluene
LiBr, - H2
Li[InH4]
2 quin.HCl, LiBr
- H2, - LiCl
quin = quinuclidine
quin
Br
Br
In
quin
Br
In
In
Br
Br
In
Br
In
quin
quin
Br
Br
quin
H
quin
(46)

Scheme 24

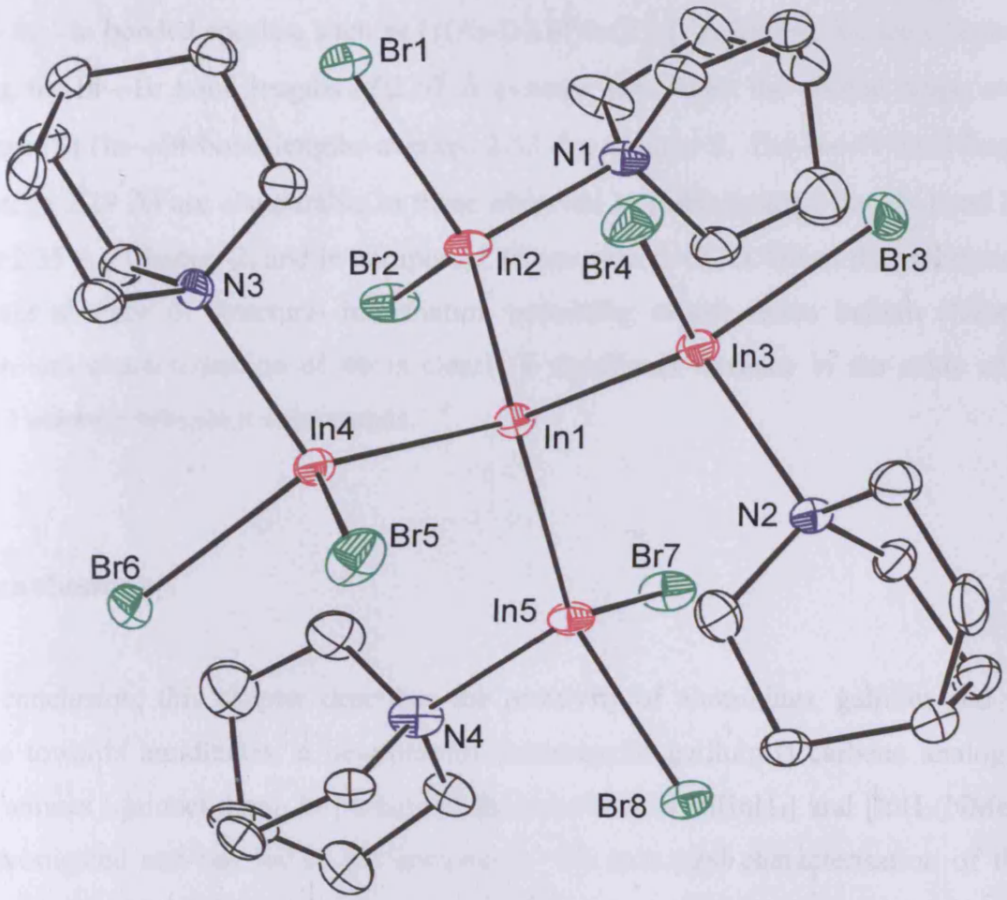

Figure 12 Structure of the anionic component of $[In\{InBr_2(quinuclidine)\}_4][(quinuclidine)_2H]$ (**46**)

Selected bond lengths (Å) and angles (°): In(1)—In(2) 2.746(3), In(1)—In(3) 2.747(5), In(1)—In(4) 2.748(7), In(1)—In(5) 2.745(1), In(2)—N(1) 2.260(1), In(3)—N(2) 2.297(3), In(4)—N(3) 2.298(2), In(5)—N(4) 2.268(6), In(2)—Br(1) 2.565(3), In(2)—Br(2) 2.552(5), In(3)—Br(3) 2.588(1), In(3)—Br(4) 2.565(4), In(4)—Br(5) 2.566(7), In(4)—Br(6) 2.586(2), In(5)—Br(7) 2.553(2), In(5)—Br(8) 2.566(8), In(2)—In(1)—In(4) 112.42(36), In(2)—In(1)—In(3) 110.19(53), In(3)—In(1)—In(5) 112.47(43), In(5)—In(1)—In(4) 110.07(03), N(1)—In(2)—Br(1) 95.86(4), N(1)—In(2)—Br(2) 96.88(2), Br(1)—In(2)—Br(2) 99.46(7).

The In—In bond lengths in compound **46** (average 2.74 Å) are comparable to those seen in other In—In bonded species, such as [{(Ar-DAB$^{\bullet}$)InCl}$_2$] (2.7280(9) Å), see Chapter 3. In addition, the In—Br bond lengths of 2.57 Å average, are within the normal range, compare [$InBr_3(quin)_2$] (In—Br bond lengths average 2.53 Å), Chapter 2. The In—N bond lengths of **46** (average 2.29 Å) are comparable to those observed in [$InBr_3(quin)_2$] (In—N bond lengths average 2.35 Å), Chapter 2, and in compound **45** (average 2.42 Å). Given the unfortunate and significant absence of structural information pertaining to sub-valent indium clusters, the isolation and characterisation of **46** is clearly a significant advance in the study of heavy group 13 element subvalent compounds.

5.7 Conclusions

In conclusion, this chapter describes the reactivity of aluminium, gallium and indium hydrides towards amidinates, a new anionic heterocyclic gallium(I) carbene analogue and tertiary amines (quinuclidine). In particular, the reactivity of Li[InH_4] and [$InH_3(NMe_3)$] has been investigated and has led to the preparation and structural characterisation of the first examples of amido indium hydride complexes, **31** and **32**, one of which, **31**, has an unprecedented thermal stability. Furthermore these studies yielded the first covalently bonded metal complexes derived from an anionic gallium carbene analogue, one of which, **41**, contains the first example of a structurally authenticated In—Ga bond. Finally, this chapter culminated in the preparation of a subvalent indium-5 cluster compound, **46**, which forms *via* the controlled decomposition of indane complexes.

5.8 Experimental

For general experimental procedures, refer to appendix 1. $Li[InH_4]$ was prepared *via* the literature procedure,[55] and the ligand HFiso was synthesised by a modification of the literature method.[90] The anionic gallium carbene analogue, **38**, was prepared by the method described in Chapter 3. Quinuclidine hydrochloride and NMe_3.HCl were purchased from Aldrich and dried prior to use by heating (150 °C) under vacuum for several hours. All other used reagents were purchased commercially and purified before use. Geometries of **42** and **43** were optimised in Gaussian 98 using the mPW91 functional with the 6-311 + G(d) basis set on Ga, C, N and H atoms and LANL2DZ basis set and core potential for In. Atomic charge, orbital population, and bonding analyses were carried out by the NBO scheme.

[InH(Fiso)$_2$] (31)

To an *in situ* generated solution of $Li[InH_4]$ (1.41 mmol) in Et_2O (50 cm^3) at -78 °C was added a solution of HFiso (1.03 g, 2.82 mmol) in Et_2O (40 cm^3) over 5 min. The resulting suspension was allowed to warm up to 25 °C after which it was concentrated to *ca.* 35 cm^3 and filtered. Slow cooling to –35 °C yielded colourless crystals of **31** (0.34 g, 29 %); m. p. 160 – 170 °C (dec.); ^{1}H NMR (250 MHz, C_6D_6, 298 K) δ 1.18 (d, 24 H, $^3J_{HH}$ = 6.8 Hz, CH_3), 1.26 (d, 24 H, $^3J_{HH}$ = 6.7 Hz, CH_3), 3.55 (sept, 8 H, $^3J_{HH}$ = 6.7 Hz, CH), 7.22 (m, 12 H, Ar-H), 7.77 (s, 2 H, NC(H)N); ^{13}C NMR (100.6 MHz, C_6D_6, 298 K) δ 23.7 (CH_3), 24.4 (CH_3), 28.5 (CH), 123.6 (p-ArC), 125.4 (m-ArC), 140.9 (o-ArC), 143.7 (ipso-ArC), 164.3 (NCN); IR ν/cm^{-1} (Nujol): 1748 (sh s, In-H); MS(APCI) m/z (%): 366 [$HFiso^+$, 100], 844 [M^+, 18]; $C_{50}H_{71}InN_4$ requires C 71.24, H 8.49, N 6.64 %; found C 71.12, C 8.57, N 6.94 %.

[{InH$_3$(Fiso)Li(Et$_2$O)}$_2$] (32)

To an *in situ* generated solution of $Li[InH_4]$ (1.41 mmol) in Et_2O (50 cm^3) at - 78°C was added a solution of HFiso (0.51 g, 1.41 mmol) in Et_2O (20 cm^3) over 5 min. The resulting suspension was allowed to warm to -20 °C and solvents were removed under vacuum. The residue was extracted into hexane (20 cm^3) and slow cooling to –35 °C yielded colourless crystals of **32** (0.43 g, 27 %); m. p. 42 °C (dec.); ^{1}H NMR (300 MHz, toluene-d_3, 243 K) δ 0.79 (br, 12 H, CH_3), 1.21 – 1.46 (br overlapping m, 48 H, CH_3), 2.91 (br, 8 H, CH_2), 3.54

(br, 8 H, CH), 6.02 (br, 6 H, InH_3), 7.10 - 7.25 (br, 12 H, Ar-H), 7.29 (br, 2 H, NC(H)N); ^{13}C NMR (75.57 MHz, toluene-d_3, 243 K) δ 14.3 (CH_3), 23.5 (CH_3), 25.2 (CH_3), 28.1 (CH_3), 32.1 (CH), 34.6 (CH), 65.2 (CH_2), 123.6 (p-ArC), 124.2 (m-ArC), 143.0 (o-ArC), 147.4 (ipso-ArC), 167.9 (NCN), all signals broad; $^{7}Li\{^{1}H\}$NMR (116.79 MHz, toluene-d_3, 243 K) δ 1.45; $^{6}Li\{^{1}H\}$NMR (44.22 MHz, toluene-d_3, 243 K) δ 1.51; IR ν/cm^{-1} (Nujol): 1719 (shp s, terminal In-H), 1632 (br. s, bridging In-H); MS(APCI) m/z (%): 366 [$HFiso^+$, 100]. Reproducible elemental analyses of the compound could not be obtained due to the highly air and moisture sensitive nature of this compound.

[AlH(Fiso)$_2$] (33)

To a solution of $Li[AlH_4]$ (0.052 g, 1.37 mmol) in THF (10 cm^3) at –78 °C was added a solution of HFiso (1.00 g, 2.74 mmol) in THF (10 cm^3) over 5 min. The resulting suspension was allowed to warm to 25 °C, filtered and solvents were removed under vacuum. The residue was extracted into toluene (5 cm^3) and slow cooling to –35 °C yielded colourless crystals of **33** (0.31 g, 60 %); m. p. 231 – 233 °C (dec.); ^{1}H NMR (300 MHz, C_6D_6, 298 K) δ 1.14 (d, 24 H, $^{3}J_{HH}$ = 6.6 Hz, CH_3), 1.20 (d, 24 H, $^{3}J_{HH}$ = 6.7 Hz, CH_3), 3.40 (sept, 8 H, $^{3}J_{HH}$ = 7.1 Hz, CH), 3.87 (br s, 1 H, Al-H), 7.19 – 7.34 (m, 12 H, Ar-H), 7.62 (s, 2 H, NC(H)N); ^{13}C NMR (100.6 MHz, C_6D_6, 298 K) δ 24.1 (CH_3), 24.7 (CH_3), 27.3 (CH), 122.5 (p-ArC), 124.6 (m-ArC), 138.0 (o-ArC), 143.4 (ipso-ArC), 166.4 (NCN); IR ν/cm^{-1} (Nujol): 1823 (sh s, Al-H); MS(APCI) m/z (%): 366 [$HFiso^+$, 100], 756 [M^+, 24]; $C_{50}H_{71}AlN_4$ requires C 79.53, H 9.48, N 7.42 %; found C 78.69, C 9.42, N 7.66 %.

[{AlH$_3$(Fiso)Li(Et$_2$O)}$_2$] (34)

To a solution of $Li[AlH_4]$ (0.20 g, 5.27 mmol) in Et_2O (10 cm^3) at -78 °C was added a solution of HFiso (1.92 g, 5.72 mmol) in Et_2O (40 cm^3) over 5 min. The resulting suspension was allowed to warm to 25 °C and solvents were removed under vacuum. The residue was extracted into hexane (25 cm^3) and slow cooling to –35 °C yielded colourless crystals of **34** (1.91 g, 77 %); m. p. 126 °C; ^{1}H NMR (400 MHz, C_6D_6, 298 K) δ 0.86 (t, 12 H, $^{3}J_{HH}$ = 7.0 Hz, CH_3), 1.19 (d, 24 H, $^{3}J_{HH}$ = 6.9 Hz, CH_3), 1.35 (d, 12 H, $^{3}J_{HH}$ = 6.9 Hz, CH_3), 1.60 (d, 12 H, $^{3}J_{HH}$ = 6.9 Hz, CH_3), 3.06 (q, 8 H, $^{3}J_{HH}$ = 7.0 Hz, CH_2), 3.74 (br s, 14 H, CH, AlH_3), 7.23 – 7.38 (m, 12 H, Ar-H), 7.40 (s, 2 H, NC(H)N); ^{13}C NMR (100.6 MHz, C_6D_6, 298 K) δ 14.3 (CH_3), 24.2 (CH_3), 24.9 (CH_3), 25.3 (CH_3), 28.1 (CH), 65.8 (CH_2), 123.3 (p-ArC), 124.0 (m-

ArC), 144.4 (o-ArC), 165.1 (ipso-ArC), 166.8 (NCN); $^{7}Li\{^{1}H\}$NMR (116.79 MHz, C_6D_6, 298 K) δ 0.72; IR ν/cm^{-1} (Nujol): 1821 (sh s, terminal Al-H), 1756 (br s, bridging Al-H); MS(APCI) m/z (%): 366 [HFiso^{+}, 100]; $C_{58}H_{96}Al_2Li_2N_4O_2$ requires C 73.39, H 10.19, N 5.90 %; found C 72.94, C 10.27, N 6.12 %.

[GaH(Fiso)$_2$] (35)

To a solution of [(quinuclidine)GaH_3] (0.25 g, 1.36 mmol) in Et_2O (10 cm^3) at -78 °C was added a solution of HFiso (0.99 g, 2.72 mmol) in Et_2O (40 cm^3) over 5 min. The resulting suspension was allowed to warm to 25 °C after which solvents were removed under vacuum. The residue was extracted into hexane (15 cm^3) and slow cooling to –35 °C yielded colourless crystals of **35** (0.22 g, 21 %); m. p. 211 °C (dec.); ^{1}H NMR (250 MHz, C_6D_6, 298 K) δ 1.19 (d, 24 H, $^{3}J_{HH}$ = 7.9 Hz, CH_3), 1.32 (d, 24 H, $^{3}J_{HH}$ = 7.8 Hz, CH_3), 3.55 (br s, 9 H, CH, Ga-H), 7.28 – 7.43 (m, 12 H, Ar-H), 7.55 (s, 2 H, NC(H)N); ^{13}C NMR (100.6 MHz, C_6D_6, 298 K) δ 23.6 (CH_3), 23.9 (CH_3), 28.3 (CH), 123.2 (p-ArC), 125.4 (m-ArC), 140.2 (o-ArC), 143.8 (ipso-ArC), 163.8 (NCN); IR ν/cm^{-1} (Nujol): 1911 (sh s, Ga-H); MS(APCI) m/z (%): 366 [HFiso^{+}, 100]; $C_{50}H_{71}GaN_4$ requires C 75.27, H 8.97, N 7.02 %; found C 74.31, C 8.78, N 7.36 %.

[{GaH_3(Fiso)Li(Et_2O)}$_2$] (36)

To an *in situ* generated solution of Li[GaH_4] (1.38 mmol) in Et_2O (40 cm^3) at –78 °C was added a solution of HFiso (0.50 g, 1.38 mmol) in Et_2O (20 cm^3) over 5 min. The resulting suspension was allowed to warm to 25 °C and solvents were removed under vacuum. The residue was extracted into hexane (20 cm^3) and slow cooling to –35 °C yielded colourless crystals of **36** (0.45 g, 31 %); m. p. 84 – 86 °C; ^{1}H NMR (400 MHz, C_6D_6, 298 K) δ 0.81 (t, 12 H, $^{3}J_{HH}$ = 7.1 Hz, CH_3), 1.32 (d, 24 H, $^{3}J_{HH}$ = 6.9 Hz, CH_3), 1.38 (d, 12 H, $^{3}J_{HH}$ = 6.9 Hz, CH_3), 1.56 (d, 12 H, $^{3}J_{HH}$ = 6.9 Hz, CH_3), 2.97 (q, 8 H, $^{3}J_{HH}$ = 7.0 Hz, CH_2), 3.68 (sept, 4 H, $^{3}J_{HH}$ = 6.9 Hz, CH), 3.87 (sept, 4 H, $^{3}J_{HH}$ = 6.8 Hz, CH), 4.68 (br, 6 H, GaH_3), 7.32 – 7.47 (m, 12 H, Ar-H), 7.43 (s, 2 H, NC(H)N); ^{13}C NMR (100.6 MHz, C_6D_6, 298 K) δ 14.7 (CH_3), 24.0 (CH_3), 24.8 (CH_3), 25.5 (CH_3), 28.5 (CH), 28.7 (CH), 66.5 (CH_2), 123.7 (p-ArC), 124.0 (p-ArC), 124.7 (m-ArC), 126.6 (m-ArC), 143.2 (o-ArC), 145.1 (ipso-ArC), 146.5 (o-ArC), 147.6 (ipso-ArC), 164.7 (NCN); $^{7}Li\{^{1}H\}$NMR (116.79 MHz, C_6D_6, 298 K) δ 1.01; $^{6}Li\{^{1}H\}$NMR (44.22 MHz, C_6D_6, 298 K) δ 1.02; ^{6}Li NMR (44.22 MHz, C_6D_6, 298 K) δ 1.04 (d, 4 H, $^{1}J_{LiH}$ =

1.2 Hz, LiH); IR ν/cm^{-1} (Nujol): 1879 (sh s, terminal Ga-H), 1769 (br s, bridging Ga-H); MS(APCI) m/z (%): 366 [HFiso$^+$, 100]; $C_{58}H_{96}Ga_2Li_2N_4O_2$ requires C 67.24, H 9.50, N 5.22 %; found C 67.05, C 9.51, N 5.50 %.

[(Fiso)GaH$_2$(quin)] (37)

To a solution of [(quinuclidine)GaH$_3$] (0.32 g, 1.74 mmol) in Et$_2$O (10 cm^3) at –78 °C was added a solution of HFiso (0.63 g, 1.74 mmol) in Et$_2$O (40 cm^3) over 5 min. The resulting suspension was allowed to warm to 25 °C after which solvents were removed *in vacuo*. The residue was extracted into hexane (15 cm^3) and slow cooling to –35 °C yielded colourless crystals of **37** (0.36 g, 38 %); m. p. 148 °C (dec.); ^{1}H NMR (250 MHz, C_6D_6, 298 K) δ 1.16 (br s, 6 H, CH_2), 1.43 (br s, 25 H, CH, CH_3), 3.06 (br s, 6 H, CH_2N), 3.85 (br s, 4 H, CH), 5.12 (br s, 2 H, GaH_2), 7.26 – 7.41 (m, 6 H, Ar-H), 7.55 (s, 1 H, NC(H)N); ^{13}C NMR (100.6 MHz, C_6D_6, 298 K) δ 20.1 (CH), 24.4 (CH_3), 25.6 (CH_2), 28.2 (CH), 48.1 (NCH_2), 123.2 (p-ArC), 125.3 (m-ArC), 143.8 (o-ArC), 145.9 (ipso-ArC), 163.7 (NCN); IR ν/cm^{-1} (Nujol): 1872 (br s, Ga-H_2); MS(APCI) m/z (%): 366 [HFiso$^+$, 100], 547 [M$^+$, 7]; $C_{32}H_{50}GaN_3$ requires C 70.33, H 9.22, N 7.69 %; found C 69.10, H 9.26, N 7.80 %.

[Ga(Ar-DAB)$_2$][K(DME)$_4$] (39)

To a solution of [$AlH_3(NMe_3)$] (0.06 g, 0.66 mmol) in Et$_2$O (10 cm^3) at –78 °C was added a solution of **38** (0.80 g, 1.34 mmol) in Et$_2$O (15 cm^3) at –78 °C. The resulting suspension was allowed to warm to 25 °C and stirred for 24 hours after which time volatiles were removed *in vacuo*. The residue was extracted into DME (10 cm^3). Filtration and cooling of the filtrate to –35 °C yielded colourless crystals of **39** overnight (0.55 g, 64 %); m. p. 96 °C (dec.); ^{1}H NMR (400 MHz, D_6-DMSO, 298 K) δ 0.76 (br s, 48 H, CH_3), 3.17 (s, 24 H, OCH_3), 3.36 (s, 16 H, OCH_2), 3.41 (br m, 8 H, CH), 5.14 (s, 4 H, NCH), 6.67 (t, 4 H, $^3J_{HH}$ = 7.8 Hz, p-Ar), 6.74 (d, 8 H, $^3J_{HH}$ = 7.0 Hz, m-Ar); ^{13}C NMR (100.6 MHz, D_6-DMSO, 298 K) δ 23.7 (CH_3), 27.3 (CH), 58.6 (OCH_3), 71.6 (OCH_2), 121.5 (m-ArC), 123.2 (p-ArC), 136.4 (o-ArC), 146.2 (ipso-ArC), 149.9 (CN); IR ν/cm^{-1} (Nujol): 1586 s, 1318 s, 1243 s, 1090 s, 845 s; MS(APCI) m/z (%): 377 [$(ArNC(H))_2^+$, 54], 190 [ArNCH$^+$, 100]. Reproducible elemental analyses of the compound could not be obtained due to the moisture sensitive nature of this compound.

$[GaH_2\{Ga(Ar\text{-}DAB)\}_2][K(TMEDA)_2]$ (40)

To a solution of $[GaH_3(quinuclidine)]$ (0.08 g, 0.43 mmol) in Et_2O (10 cm^3) at –78 °C was added a solution of **38** (0.50 g, 0.84 mmol) in Et_2O (15 cm^3) over 5 min. The resulting suspension was allowed to warm to 25 °C, filtered and the filtrate concentrated to *ca.* 10 cm^3. Slow cooling of the filtrate to –35 °C yielded yellow crystals of **40** (0.39 g, 71 %); m. p. 128 – 131 °C (dec.); ^1H NMR (400 MHz, C_6D_6, 298 K) δ 1.00 (d, 24 H, $^3J_{HH}$ = 6.8 Hz, CH_3), 1.20 (d, 24 H, $^3J_{HH}$ = 6.9 Hz, CH_3), 1.75 (s, 24 H, NCH_3), 1.89 (s, 8 H, NCH_2), 2.17 (br s, 2 H, GaH_2), 3.56 (sept, 8 H, $^3J_{HH}$ = 6.8 Hz, CH), 6.19 (s, 4 H, NCH), 6.96 (t, 4 H, $^3J_{HH}$ = 7.3 Hz, p-Ar), 7.07 (d, 8 H, $^3J_{HH}$ = 7.6 Hz, m-Ar); ^{13}C NMR (100.6 MHz, C_6D_6, 298 K) δ 23.3 (CH_3), 24.2 (CH_3), 26.7 (CH), 44.2 (NCH_3), 56.2 (NCH_2), 120.9 (CN), 121.6 (m-ArC), 123.5 (p-ArC), 145.2 (o-ArC), 146.1 (ipso-ArC); IR ν/cm^{-1} (Nujol): 1769 (br s, Ga-H); MS(APCI) m/z (%): 377 $[(ArNC(H))_2^+$, 100]. Reproducible elemental analyses of the compound could not be obtained due to the highly air and moisture sensitive nature of this compound.

$[InH_2\{Ga(Ar\text{-}DAB)\}_2][Li(TMEDA)_2]$ (41)

To an *in situ* generated solution of $[InH_3(NMe_3)]$ (0.42 mmol) in Et_2O (10 cm^3) at –78 °C was added a solution of **38** (0.50 g, 0.84 mmol) in Et_2O (15 cm^3) over 5 min. The resulting suspension was allowed to warm to –30 °C and kept at this temperature for 24 hours, after which it was filtered, the filtrate warmed to –15 °C and concentrated to *ca.* 10 cm^3. Slow cooling of the filtrate to –35 °C yielded yellow crystals of **41** (0.33 g, 63 %); m. p. 116 – 118 °C (dec.); ^1H NMR (300 MHz, CD_2Cl_2, 243 K) δ 0.85 (d, 24 H, $^3J_{HH}$ = 6.6 Hz, CH_3), 1.08 (d, 24 H, $^3J_{HH}$ = 6.6 Hz, CH_3), 2.18 (s, 24 H, NCH_3), 2.34 (s, 8 H, NCH_2), 2.93 (br s, 2 H, InH_2), 3.27 (sept, 8 H, $^3J_{HH}$ = 6.6 Hz, CH), 5.86 (s, 4 H, NCH), 7.03 – 7.18 (m, 12 H, p-Ar and m-Ar); ^{13}C NMR (75.57 MHz, CD_2Cl_2, 243 K) δ 24.0 (CH_3), 25.4 (CH_3), 27.5 (CH), 46.6 (NCH_3), 57.1 (NCH_2), 121.3 (CN), 122.5 (m-ArC), 123.9 (p-ArC), 145.8 (o-ArC), 146.8 (ipso-ArC); IR ν/cm^{-1} (Nujol): 1632 (br s, In-H); MS(APCI) m/z (%): 377 $[(ArNC(H))_2^+$, 100]. Reproducible elemental analyses of the compound could not be obtained due to the highly air and moisture sensitive nature of this compound.

$[InBrH_2(quinuclidine)_2]$ (45)

To an *in situ* generated solution of $Li[InH_4]$ (1.41 mmol) in Et_2O (60 cm^3) at –78 °C was added quin·HCl (0.42 g, 2.82 mmol) over 5 min. The resulting suspension was allowed to

warm to –30 °C and kept at this temperature for 72 hours, after which the solution became a red colour and colourless crystals of **45** were formed (0.14 g, 24 %); m. p. 72 °C (dec.); ^{1}H NMR (300 MHz, toluene-d_3, 243 K) δ 1.29 (br s, 12 H, CH_2), 1.49 (br m, 2 H, CH), 2.79 (br s, 12 H, CH_2N), 3.56 (br m, 2 H, InH); ^{13}C NMR (75.57 MHz, toluene-d_3, 243 K) δ 26.6 (CH), 30.4 (CH_2), 47.8 (NCH_2); IR ν/cm^{-1} (Nujol): 1707 (br s, In-H); MS(APCI) m/z (%): 112 [quinH^+, 100]. Reproducible elemental analyses of the compound could not be obtained due to the highly air and moisture sensitive nature of this compound.

[In{$InBr_2$(quinuclidine)}$_4$][(quinuclidine)$_2$H] (46)

Compound **45** was extracted into toluene (5 cm^3) at –45 °C. Placement of the colourless solution at –30 °C over 5 days yielded a clear orange solution and deep orange/red triangular prisms of **46** (0.06 g, < 6 %). decomposition +5 °C; ^{1}H NMR (400 MHz, $C_6D_5CD_3$, 243 K) δ 1.89 (br m, 6 H, CH_2), 2.19 (br m, 1 H, CH), 3.26 (br m, 6 H, CH_2N); IR ν/cm^{-1} (Nujol): 1318 m, 1047 s, 981 s, 826 m, 791 m.

5.9 References

1. C. Jones, G.A. Koutsantonis, C.L. Raston, *Polyhedron*, 1993, **12**, 1829.
2. C.L. Raston, *J. Organomet. Chem.*, 1994, **475**, 15.
3. M.G. Gardiner, C.L. Raston, *Coord. Chem. Revs.*, 1997, **166**, 1.
4. D.E. Hibbs, M.B. Hursthouse, C. Jones, N.A. Smithies, *Chem. Commun.*, 1998, 869.
5. D.E. Hibbs, C. Jones, N.A. Smithies, *Chem. Commun.*, 1999, 185.
6. J. Emsley, *"The Elements"*, Oxford University Press, Oxford, 1989.
7. E.A. Keiter J.E. Huheey, R.L. Keiter, *"Inorganic Chemistry, Priciples of Structure and Reactivity"*, fourth edn., Harper Collins College Publishers, New York, 1993.
8. E.C. Ashby, *J. Am. Chem. Soc.*, 1964, **86**, 1882.
9. J.L. Atwood, F.R. Bennett, F.M. Elms, G.A. Koutsantonis, C.L. Raston, K.D. Robinson, D.J. Young, *Inorg. Chem.*, 1992, **31**, 2673.
10. F.M. Elms, M.G. Gardiner, G.A. Koutsantonis, C.L. Raston, J.L. Atwood, K.D. Robinson, *J. Organomet. Chem.*, 1993, **449**, 45.
11. F.R. Bennett, F.M. Elms, M.G. Gardiner, G.A. Koutsantonis, C.L. Raston, N.K. Roberts, *Organometallics*, 1992, **11**, 1457.
12. J.L. Atwood, K.W. Butz, M.G. Gardiner, C. Jones, G.A. Koutsantonis, C.L. Raston, K.D. Robinson, *Inorg. Chem.*, 1993, **32**, 3482.
13. N.N. Greenwood, A. Storr, M.G.H. Wallbridge, *Inorg. Chem.*, 1963, **2**, 1036.
14. J.L. Atwood, F.R. Bennett, F.M. Elms, C. Jones, C.L. Raston, K.D. Robinson, *J. Am. Chem. Soc.*, 1991, **113**, 8183.
15. J.L. Atwood, S.G. Bott, F.M. Elms, C. Jones, C.L. Raston, *Inorg. Chem.*, 1991, **30**, 3792.
16. J.M. Davidson, T. Wartik, *J. Am. Chem. Soc.*, 1960, **82**, 5506.
17. E. Wiberg, E. Amberger, *"Hydrides of the Elements of Main Groups I-IV"*, Elsevier, London, 1971, Chapter 5.
18. H. Schmidbaur, W. Findeiss, E. Gast, *Angew. Chem.*, 1965, **77**, 170.
19. M.J. Goode, A.J. Downs, C.R. Pulham, D.W.H. Rankin, H.E. Robertson, *J. Chem. Soc., Chem. Commun.*, 1988, 768.
20. J.A. Dilts, E.C. Ashby, *Inorg. Chem.*, 1970, **9**, 855.
21. C.W. Heitsch, C.E. Nordman, R.W. Parry, *Inorg. Chem.*, 1963, **2**, 508.
22. D.F. Shriver, C.E. Nordman, *Inorg. Chem.*, 1963, **2**, 1298.

44. W.L. Gladfelter, D.C. Boyd, K.F. Jensen, *Chem. Mater.*, 1989, **1**, 339.
45. M.G. Simmonds, W.L. Gladfelter, N. Rao, W.W. Szymanski, K.A. Ahn, P.H. McMurry, *J. Vac. Sci. Technol. A*, 1991, **9**, 2782.
46. A.J. Downs, C.R. Pulham, *Chem. Soc. Revs.*, 1994, **23**, 175.
47. A.G. Avent, C. Eaborn, P.B. Hitchcock, J.D. Smith, A.C. Sullivan, *J. Chem. Soc., Chem. Commun.*, 1986, 988.
48. O.T. Beachley, S.L. Chao, M.R. Churchill, R.F. See, *Organometallics*, 1992, **11**, 1486.
49. M.R. Churchill, C.H. Lake, S.L. Chao, O.T. Beachley, *J. Chem. Soc., Chem. Commun.*, 1993, 1577.
50. S. Aldridge, A.J. Downs, S. Parsons, *Chem. Commun.*, 1996, 2055.
51. C. Kümmel, A. Meller, M. Noltemeyer, *Z. Naturforsch., Teil B*, 1996, **51**, 209.
52. D.E. Hibbs, M.B. Hursthouse, C. Jones, N.A. Smithies, *Organometallics*, 1998, **17**, 3108.
53. E. Wiberg, O.Z. Dittmann, H. Nöth, M.Z. Schmidt, *Z. Naturforsch. B*, 1957, **12**, 61.
54. L. Andrews, X. Wang, *Angew. Chem., Int. Ed.*, 2004, **43**, 1706.
55. C. Jones, *Chem. Commun.*, 2001, 2293.
56. A.G. Avent, C. Eaborn, M.N.A. El-Kheli, M.E. Molla, J.D. Smith, A.C. Sullivan, *J. Am. Chem. Soc.*, 1986, **108**, 3854.
57. J.L. Atwood, D.C. Hrncir, R.D. Rogers, J.A.K. Howard, *J. Am. Chem. Soc.*, 1981, **103**, 6787.
58. M.D. Francis, D.E. Hibbs, M.B. Hursthouse, C. Jones, N.A. Smithies, *J. Chem. Soc., Dalton Trans.*, 1998, 3249.
59. C.D. Abernathy, M.L. Cole, C. Jones, *Organometallics*, 2000, **19**, 4852.
60. M.L. Cole, 2001, PhD Thesis, Cardiff University, Wales, UK
61. M. Chaillet, A. Dargelos, C.J. Marsden, *New. J. Chem.*, 1994, **18**, 693.
62. M.L. Cole, D.E. Hibbs, C. Jones, N.A. Smithies, *J. Chem. Soc., Dalton Trans.*, 2000, 545.
63. M. Yamada, K. Tanaka, S. Araki, Y. Butsugan, *Tett. Lett.*, 1995, **36**, 3169.
64. M. Yamada, T. Horie, M. Kawai, H. Yamamura, S. Araki, *Tetrahedron*, 1997, **53**, 15685.
65. T. Miyai, K. Inoue, M. Yasuda, I. Shibata, A. Baba, *Tett. Lett.*, 1998, **39**, 1929.
66. C.D. Abernathy, M.L. Cole, A.J. Davies, C. Jones, *Tett. Lett.*, 2000, **41**, 7567.

67. A. Schnepf, H. Schnöckel, G. Stößer, *J. Am. Chem. Soc.*, 2000, **122**, 9178.
68. D.H. Rapoport, W. Vogel, H. Cölfen, R. Schlögl, *J. Phys. Chem. B*, 1997, **101**, 4175.
69. A. Schnepf, H. Schnöckel, *Angew. Chem., Int. Ed.*, 2002, **41**, 3532.
70. B. Luo, M. Pink, W.L. Gladfelter, *Inorg. Chem.*, 2001, **40**, 307.
71. B. Luo, V.G. Young, W.L. Gladfelter, *Inorg. Chem.*, 2000, **39**, 1705.
72. H. Zhu, J. Chai, H.W. Roesky, M. Noltemeyer, H.G. Schmidt, D. Vidovic, J. Magull, *Eur. J. Inorg. Chem.*, 2003, 3113.
73. H.J. Himmel, A.J. Downs, T.M. Greene, *J. Am. Chem. Soc.*, 2000, **122**, 9793.
74. S. Dagorne, I.A. Guzei, M.P. Coles, R.F. Jordan, *J. Am. Chem. Soc.*, 2000, **122**, 274.
75. D. Abeysekera, K.N. Robertson, T.S. Cameron, J.A.C. Clyburne, *Organometallics*, 2001, **20**, 5532.
76. J.A.R. Schmidt, J. Arnold, *Organometallics*, 2002, **21**, 2306.
77. M.L. Cole, P.C. Junk, *J. Organomet. Chem.*, 2003, **666**, 55.
78. Y. Zhou, D.S. Richeson, *Inorg. Chem.*, 1996, **35**, 2448.
79. R. Duchateau, A. Meetsma, J.H. Teuben, *Chem. Commun.*, 1996, 223.
80. F.G.N. Cloke, G.R. Hanson, M.J. Henderson, P.B. Hitchcock, C.L. Raston, *J. Chem. Soc., Chem. Commun.*, 1989, 1002.
81. G. Linti, A. Rodig, W. Köstler, *Z. Anorg. Allg. Chem.*, 2001, **627**, 1465.
82. W. Uhl, F. Schmock, G. Geiseler, *Z. Anorg. Allg. Chem.*, 2002, **628**, 1963.
83. M.C. Kuchta, J.B. Bonanno, G. Parkin, *J. Am. Chem. Soc.*, 1996, **118**, 10914.
84. J. Roziere, C. Belin, M.S. Lehman, *J. Chem. Soc., Chem. Commun.*, 1982, 388.
85. H.P. Beck, D. Wilhelm, *Angew. Chem., Int. Ed.*, 1991, **30**, 824.
86. G. Meyer, *Z. Anorg. Allg. Chem.*, 1990, **582**, 128.
87. G. Gerlach, W. Hönle, A. Simon, *Z. Anorg. Allg. Chem.*, 1982, **426**, 7.
88. W. Hönle, G. Gerlach, W. Weppner, A. Simon, *J. Solid State Chem.*, 1986, **61**, 171.
89. D. Loos, H. Schnöckel, D. Fenske, *Angew. Chem., Int. Ed. Engl.*, 1993, **32**, 1059.
90. R.M. Roberts, *J. Org. Chem.*, 1949, **14**, 277.

Appendix 1

General experimental procedures

All manipulations were performed using conventional Schlenk or glovebox techniques under an atmosphere of high purity argon or dinitrogen (BOC 99.9 %) in flame-dried glassware. All apparatus was cleaned in a solution of potassium hydroxide / isopropyl alcohol followed by rinsing with hydrochloric acid, distilled water and acetone, and placed in an oven at 110 °C.

The solvents diethyl ether, hexane, tetrahydrofuran, DME and toluene were predried by storage over sodium wire, or in the case of dichloromethane and acetonitrile, over granular calcium hydride. Except for dichloromethane and acetonitrile, where calcium hydride was used, all solvents were refluxed under an atmosphere of high purity argon or dinitrogen for 12 hours over either potassium or Na/K alloy prior to collection.

Ambient temperature ^{1}H and ^{13}C NMR spectra were recorded on either a Bruker DPX 400 spectrometer (400 MHz, 100.6 MHz), a Bruker DPX 250 spectrometer (250 MHz, 62.88 MHz) or a Jeol Eclipse 300 spectrometer (300 MHz, 75.57 MHz) in C_6D_6, CD_3CN, $CD_3C_6D_5$, $CDCl_3$, CD_2Cl_2 and referenced to the residual ^{1}H or ^{13}C resonances of the solvent used. Low temperature ^{1}H and ^{13}C were recorded on a Jeol Eclipse 300 spectrometer, in $CD_3C_6D_5$ or CD_2Cl_2. ^{31}P NMR spectra were recorded on a Jeol Eclipse 300 spectrometer (121.5 MHz) and referenced to 85 % H_3PO_4. ^{7}Li and ^{6}Li NMR spectra were recorded on a Jeol Eclipse 300 spectrometer (116.79 MHz, 44.22 MHz) and referenced to 1M LiCl D_2O solution. Infrared spectra were recorded as Nujol mulls using sodium chloride plates on a Perkin-Elmer 4200 series FTIR spectrometer, between 4000 an 400 cm^{-1}.

Mass Spectra were recorded using a VG Fison Plattform II instrument under EI or APCI conditions. Melting points were determined in sealed glass capillaries under argon, and are uncorrected. The Warwick Analytical Service carried out elemental analyses.

Appendix 2

Publications in support of this thesis

- Robert J. Baker, Robert D. Farley, Cameron Jones, Marc Kloth and Damien M. Murphy. Synthesis and characterisation of the first carbene and diazabutadiene-indium(II) complexes. *Chem. Commun.*, **2002**, 1196 – 1197.

- Robert J. Baker, Aaron J. Davies, Cameron Jones, Marc Kloth. Structural and spectroscopic studies of carbene and N-donor ligand complexes of Group 13 hydrides and halides. *Journal of Organometallic Chemistry*, 656, **2002**, 203 – 210.

- Robert J. Baker, Robert D. Farley, Cameron Jones, Marc Kloth and Damien M. Murphy. The reactivity of diazabutadienes toward low oxidation state Group 13 iodides and the synthesis of a new gallium(I) carbene analogue. *J. Chem. Soc., Dalton Trans.*, **2002**, 3844 – 3850.

- Robert J. Baker, Cameron Jones, Marc Kloth and Jamie A. Platts. Synthesis and Structural Characterization of Thermally Stable Group 13 Hydride Complexes Derived from a Gallium(I) Carbene Analogue. *Angew. Chem. Int. Ed.*, **2003**, 42, 2660 – 2663.

- Robert J. Baker, Cameron Jones, Marc Kloth and David P. Mills. The reactivity of gallium(I) and indium(I) halides towards bipyridines, terpyridines, imino-substituted pyridines and bis(imino)acenaphthenes. *New J. Chem.*, **2004**, 28, 207 - 213.

- Robert J. Baker, Cameron Jones, Peter Junk and Marc Kloth. Kinetic Control over the Thermal Stability of the In—H Bond: Synthesis and Characterization of Amido Indium Hydride Complexes. *Angew. Chem. Int. Ed.*, **2004**, 43, 3852 – 3855.

- Robert J. Baker, Cameron Jones, Marc Kloth and Jamie Platts. Oxidative Coupling of an Anionic Gallium(I) Carbene Analogue: Synthesis and Structural Characterization of an Unprecedented π-Cyclopentadienyl-Bridged Digallane Complex. *Organometallics*, **2004**, 23, 4811 - 4813.